Investigating a novel platform to optimize chronic glucagon agonism in the treatment of NAFLD

Tatiana Raquel Gonçalves Lopes

2023

Department of Metabolism, Digestion and Reproduction

Imperial College London

A thesis submitted for the degree of Doctor of Philosophy

Abstract

NAFLD impacts 30% of Western population, yet FDA-approved treatments remain elusive due to its incomplete understanding. Thus, this PhD sought to generate a minimally invasive platform to track NAFLD longitudinally and explore pre-clinical therapeutic options.

Before doing so, a secondary project was executed to provide technical training, that aimed to establish a platform for tracking tumour vascularization through intravital imaging. For that, renal carcinoma (RCC)-derived cells were transplanted into the anterior chamber of the eye (ACE) of animals with fluorescent blood vessels. This led to a platform yielding consistently sized tumours with trackable growth. However, loss of blood vessel fluorescence within tumours, likely due to Tie2 downregulation, hindered the original goal. Nevertheless, this platform could potentially be used to test anti-angiogenic/Tie2-normalizing drugs.

The platform to track NAFLD longitudinally was explored next. To do so, *in vitro* generated liver tissue with fluorescent lipid droplets would be transplanted into a host animal's ACE, and NAFLD would then be induced via high-fat diet regime. It was hypothesized that changes in fat content could be tracked in the ectopic liver tissue through repeated imaging. Several approaches were investigated to generate liver tissue capable of long-term vascularization upon transplantation, which highlighted the difficulty of generating engraftable tissue. Nevertheless, final experiments showed that so-called liver buds were capable of vascularizing upon transplantation. Further optimization of intra-ocular liver buds' fat accumulation capacity is required.

Research demonstrated that glucagon analogue G108 improves hepatic fat and glycemia in obese animals; however, also leads to lean mass loss. This thesis final aim was to explore G108's NAFLD potential using the aforementioned NAFLD platform, which could not be fully validated. Nevertheless, traditional *in vivo* methods revealed that lowering G108 dosage in the context of a high-protein diet prevented lean mass loss, without compromising the benefits on liver fat or glucose tolerance.

Statement of originality

I hereby declare that this thesis and all work presented within are my own and any contributions or materials sourced from external works are properly acknowledged and referenced.
All collaborations and assistance are listed below:

Chapter II: Renca cells were fluorescently tagged by Dr Alexandra Milona. Eye injections and intravital imaging experiments were carried out with assistance from Dr Victoria Salem.

Chapter III: FoxO1-GFP and stock liver organoids were provided by Dr Alexandra Milona. hESCs were kindly differentiated into hHE cells by Miss Faiza Farhan from Dr Wei Cui's lab. Figure 3.15 was generated by Miss Faiza Farhan. Eye injections and intravital imaging experiments were carried out with assistance from Dr Victoria Salem.

Chapter IV: Grip strength experiments were carried out with aid from Dr David Hope. Ip-GTT experiments were carried out with aid from Dr Bryn Owen and Miss Cecilia Dunsterville. Blind scoring of ORO-stained liver tissue was carried out by Dr Anna Curtis. The macro for the automated quantification of ORO-stained liver tissue was written by Mister Dirk Doorman from MRC-LMS microscopy facility. Culling and tissue collection was carried out with aid from Dr Bryn Owen, Dr Phyllis Phuah, Miss Cecilia Dunsterville and Miss Iona Davis.

Copyright declaration

The copyright of this thesis rests with the author. Unless otherwise indicated, its contents are licensed under a Creative Commons Attribution-NonCommercial 4.0 International Licence (CC BY-NC). Under this licence, you may copy and redistribute the material in any medium or format. You may also create and distribute modified versions of the work. This is on the condition that: you credit the author and do not use it, or any derivative works, for a commercial purpose. When reusing or sharing this work, ensure you make the licence terms clear to others by naming the licence and linking to the licence text. Where a work has been adapted, you should indicate that the work has been changed and describe those changes. Please seek permission from the copyright holder for uses of this work that are not included in this licence or permitted under UK Copyright Law.

Acknowledgements

First, I would like to express my gratitude to my supervisor, Dr Bryn Owen, for all his support, time, and trust throughout these four years.

I would also like to thank my co-supervisor, Dr Victoria Salem, for her support and for always finding the time to help with experiments.

I am also grateful to all the scientist I came across during this journey for their support and for making this experience much more enjoyable. In particular, I would like to thank P.P., M.N., L.M., C.D., J.B.V., K.C., D.H., S.C., C.H., F.B., A.M., G.Z., B.J., K.M., Y.P., A.A., I.D.

Finally, I would like to dedicate my thesis to my mom, dad, sister and partner for their support, patience, and motivation. I could not have done this without you.

Table of contents

Abstract 2
Statement of originality 3
Copyright declaration 4
Acknowledgements 5
Table of contents 6
List of figures 11
List of tables 14
Abbreviations 15
Chapter I - General introduction 19
1.1. The healthy liver 20
1.1.1. Composition and organization 20
1.1.2. Liver roles 21
1.1.2.1. The roles of liver in lipid metabolism 22
1.1.2.2. The roles of liver in glucose metabolism 25
1.1.2.3. The roles of liver in amino acid metabolism 28
1.2. The liver in non-alcoholic fatty liver disease (NAFLD) 30
1.2.1. NAFDL definition and aetiology 30
1.2.2. Pathology of hepatic fat accumulation 31
1.2.2.1. Why hepatic fat accumulation leads to lipotoxicity 31
1.2.2.1.1. Overwhelming of TAG and LD synthesis pathways 31
1.2.2.1.2. Altered levels of non-TAG lipids 32
1.2.2.2. How lipotoxicity is exerted at the cell level 34
1.2.2.2.1. Dysregulation of organelles function 34
1.2.2.2.2. Direct modification of signalling pathways 36
1.2.3. Diagnosing NAFLD 38
1.2.4. Sources of hepatic fat in NAFLD 39
1.2.4.1. Fats derived from NEFA pool 40
1.2.4.2. Fats derived from diet 41
1.2.4.3. Fats derived from *de novo* lipogenesis (DNL) 41
1.2.4.4. Deficient fat handling 42
1.2.5. Risk factors 43
1.2.5.1. Diet 43
1.2.5.2. Obesity 45
1.2.5.3. Metabolic syndrome 46
1.2.5.4. Insulin resistance 46
1.2.5.5. Drug-induced fatty liver disease 47
1.2.5.6. Other underlying diseases 48
1.2.5.7. Genetic predisposition 49
1.2.5.8. Intestinal microbiome composition 49
1.2.5.9. Age 50

1.2.5.10. Maternal influence 50
1.2.5.11. Gender 50
1.2.6. Therapeutic strategies 51
1.2.6.1. Lifestyle change 51
1.2.6.1.1. Weight loss 51
1.2.6.1.2. Diet 52
1.2.6.1.3. Exercise 52
1.2.6.2. Drugs 53
1.2.6.2.1. Glucose lowering drugs 53
1.2.6.2.2. Lipid-lowering drugs 55
1.2.6.2.3. Bile-pathway targeting drugs 56
1.2.6.2.4. Anti-inflammatory drugs 57
1.2.7. Glucagon signalling modulation in NAFLD treatment 58
1.2.7.1. Glucagon 58
1.2.7.2. Glucagon secretion 58
1.2.7.3. Glucagon roles 59
1.2.7.3.1. Glucagon in the liver 59
1.2.7.3.2. Glucagon in other organs 60
1.2.7.4. Glucagon pathophysiology 61
1.2.7.5. Potential of modulating glucagon signalling in NAFLD treatment 63

1.3. *In vitro* and *in vivo* models to study NAFLD 65
1.3.1. *In vitro* models 66
1.3.1.1. 2D monocultures 66
1.3.1.2. 2D co-cultures 67
1.3.1.3. 3D monocultures 67
1.3.1.4. 3D co-cultures 67
1.3.2. *In vivo* models 68
1.3.2.1. Diet induced models 68
1.3.2.2. Chemically induced models 69
1.3.2.3. Genetically induced models 70
1.3.2.4. Platforms to study NAFLD *in vivo* longitudinally 71

1.4. Hypothesis and aims 72

Chapter II: Investigating a platform for the in vivo characterization of tumour vascularization 77

2.1. Introduction 78
2.1.1. Currently available models to study tumour vascularization 78
2.1.2. The potential of ACE as a platform to study tumour vascularization 79
2.1.3. Types of tumour vascularization 83
2.1.3.1. Angiogenesis 85
2.1.3.2. Vasculogenesis/*de novo* vessel formation 86
2.1.3.3. Vessel co-option 87
2.1.3.4. Vasculogenic mimicry (VM) 88
2.1.3.5. Lymphangiogenesis 89
2.1.4. Renal cell carcinoma (RCC) 91

2.2. Hypothesis and aims 92

2.3. Materials and methods 94
2.3.1. Animals 94
2.3.2. Cell line 94
2.3.3. Generating spheroids *in vitro* 94

2.3.4. Tube formation vasculogenic mimicry assay 95
2.3.5. Transplantation into the ACE 95
2.3.6. *In vivo* imaging 95
2.3.7. Post-acquisition image analysis 95
2.3.8. Immunohistochemistry of eye slices 96

2.4. Results 97
2.4.1. Renca cells form spheroids *in vitro* that engraft and grow upon transplantation into the ACE of host mice 97
2.4.2. Intra-spheroid blood vessel fluorescence is lost due to Tie2-GFP down-regulation 104
2.4.3. Cancer cell-lined channels are present in Renca spheroids 108

2.5. Discussion and future studies 112

Chapter III: Investigating a novel in vivo longitudinal platform to study NAFLD 120

3.1. Introduction 121
3.1.1. Sources of hepatocytes to establish *in vitro* models 121
3.1.2. *In vitro* differentiation of stem cells into HLCs 121
3.1.3. Liver spheroids and organoids as *in vitro* NAFLD models 123
3.1.4. Strategies available to generate vascularized *in vitro* grown 3D models 130
3.1.4.1. Co-culture with ECs 130
3.1.4.2. Co-culture with ECs and vessel stabilizing cells 131
3.1.4.3. Co-culture with stromal vascular fraction 132
3.1.4.4. Co-culture with isolated micro vessel fragments 132
3.1.5. The potential of the ACE as a platform to study NAFLD longitudinally *in vivo* 133

3.2. Hypothesis and aims 136

3.3. Materials and methods 137
3.3.1. Animals 137
3.3.2. Cell lines 137
3.3.2.1. Liver organoids 137
3.3.2.2. Hepatic endothelial cells 138
3.3.2.3. Mouse mesenchymal stem cells 138
3.3.2.4. Human embryonic stem cells 138
3.3.3. Assessing fat storing and *de novo* lipogenesis capacity *in vitro* 139
3.3.4. RT-qPCR 139
3.3.5. Generation of engraftable liver model 140
3.3.5.1. Using liver organoids 140
3.3.5.1.1. Seeding 3D differentiated organoids and ECs in ULA plates 140
3.3.5.1.2. Seeding 3D differentiated organoids, ECs and MSCs in ULA plates 141
3.3.5.1.3. Seeding differentiated organoid-derived single cells, ECs and MSCs in ULA plates . 141
3.3.5.1.4. Seeding differentiated organoid-derived single cells, ECs and MSCs on Matrigel 141
3.3.5.2. Using HLCs 142
3.3.5.2.1. Seeding hHE cells, ECs and MSCs on Matrigel 142
3.3.6. Transplantation of *in vitro* models into the ACE 142
3.3.7. *In vivo* imaging 142
3.3.8. Immunocytochemistry 142
3.3.9. Immunohistochemistry of eye slices 143
3.3.10. Albumin ELISA 143
3.3.11. Statistical analysis 143

3.4. Results 144
3.4.1. Attempting to generate liver model capable of vascularizing *in vivo* using liver organoids 144

3.4.1.1. Differentiated liver organoids only 144
3.4.1.1.1. Isolation and validation of hepatic organoids 144
3.4.1.1.2. Transplantation of differentiated liver organoids into ACE 148
3.4.1.2. Differentiated liver organoids enriched with endothelial cells 149
3.4.1.2.1. Isolation and validation of hepatic endothelial cells 149
3.4.1.2.2. Co-culture of differentiated liver organoids and endothelial cells on ULA plates 151
3.4.1.2.3. Transplantation of differentiated liver organoids enriched with ECs into the ACE 153
3.4.1.3. Differentiated liver organoids enriched with endothelial and mesenchymal stem cells 154
3.4.1.3.1. Co-culture of differentiated organoids with endothelial and mesenchymal stem cells on ULA plates 154
3.4.1.3.2. Transplantation of differentiated liver organoids enriched with endothelial and mesenchymal stem cells into the ACE 156
3.4.1.4. Aggregates made from differentiated liver organoid-derived single cells, endothelial and mesenchymal stem cells on ULA plates 158
3.4.1.4.1. Co-culture of single cells from differentiated organoids with endothelial and mesenchymal stem cells on ULA plates 158
3.4.1.4.2. Transplantation of aggregates made from differentiated liver organoid-derived single cells, endothelial and mesenchymal stem cells into the ACE 161
3.4.1.5. Liver buds from differentiated liver organoid-derived single cells, endothelial and mesenchymal stem cells 161
3.4.2. Attempting to generate liver model capable of vascularizing *in vivo* using hepatocyte like cells 163
3.4.2.1. Liver buds from human HLC 164
3.4.2.1.1. Differentiation of hESCs into HLC 165
3.4.2.1.2. Liver bud formation from hHE cells 165
3.4.2.1.3. Transplantation of liver buds from hHE cells into the ACE 167
3.4.2.1.4. Assessing whether intra-ocular liver buds from hHE cells accumulate fat 170
3.5. Discussion and future perspectives 171
Chapter IV – Optimization of chronic GCGR-agonism in the treatment of NAFLD 181
4.1. Introduction 182
4.1.1. A new glucagon analogue, G108, improves glycemia and possibly hepatic steatosis in obese mice 182
4.1.2. Side effects of G108 chronic administration: hypoaminoacidemia, increased energy expenditure, and fat and lean mass loss. 182
4.1.2.1. G108 chronic treatment induces hypoaminoacidemia 182
4.1.2.2. G108-induced hypoaminoacidemia leads to increased energy expenditure and consequentially fat mass loss 183
4.1.2.3. G108-induced hypoaminoacidemia leads to lean mass loss 185
4.1.3. Partial mitigation of G108-induced side-effects does not prevent improved glycemia or hepatic steatosis 187
4.2. Hypothesis and aims 189
4.3. Materials and methods 190
4.3.1. Animals 190
4.3.2. Chronic G108 treatment 190
4.3.3. Body weight and food intake 190
4.3.4. Lean and fat mass MRI measurement 191
4.3.5. Grip strength 191
4.3.6. Plasma amino acid quantification 191
4.3.7. Intra-peritoneal glucose tolerance test (Ip-GTT) 191
4.3.8. Histology: double ORO and haematoxylin staining 192

4.3.9. RT-qPCR 192
4.4. Results 194
4.4.1. Lean mass loss is completely prevented by 2.5nmol/kg G108 dose in the context of high protein supplementation 194
4.4.2. Improved glycemia and hepatic steatosis are still maintained after complete mitigation of lean mass loss 204
4.5. Discussion and future perspectives 208
Chapter V - Concluding remarks 221
References 224

List of figures

Figure 1.1. Schematic of liver microscopic organization. 21
Figure 1.2. Schematic representing the roles of liver in lipid, glucose, and protein metabolism. 22
Figure 1.3. Schematic representing potential progression of NAFLD.. 31
Figure 1.4. Schematic representing different sources of hepatic fat. 40
Figure 1.5. Schematic depicting some of the risk factor associated with NAFLD onset and progression. 43
Figure 1.6. Schematic representing some of the currently available *in vivo* and *in vitro* models to study NAFLD. 66
Figure 1.7. Schematic depicting the initial aims of this thesis 76
Figure 2.1. Schematic depicting structures in the eye. 80
Figure 2.2. Schematic illustrating and describing the different types of tumour vascularization. 85
Figure 2.3. Injecting a Renca cell suspension into ACE of host mice leads to development of multiple tumours that grow over time 97
Figure 2.4. Renca tumours and host mouse blood vessels can be visualized under fluorescent microscopy. 98
Figure 2.5. Single Tie2-GFP cells can be observed around and within some tumours.. 100
Figure 2.6. Renca cells form cohesive spheroids through low-attachment culture upon centrifugation and in the presence of Matrigel. 101
Figure 2.7. *In vitro* generated Renca spheroids engraft and grow overtime upon transplantation into ACE 103
Figure 2.8. Channel-like looking structures developing in Renca spheroids overtime upon transplantation into ACE 105
Figure 2.9. Loss of blood vessel fluorescence within tumours is likely not due to laser penetration issues. 106
Figure 2.10. Loss of blood vessel fluorescence within tumours is likely caused by Tie2-GFP down-regulation. 107
Figure 2.11. Occasionally, a few GFP+ cells could be seen in intra-tumour blood vessels.. 108

Figure 2.12. Presence of channels lined by endothelial cells and channels lined by tumour cells within spheroids. 109
Figure 2.13. Channels lined by tumour cells are positive for PAS and negative for CD31, and do not seem to be perfused with blood.. 110
Figure 2.14. Renca cells do not form tube-like structures when seeded on Matrigel, instead they form spheroids..... 111
Figure 2.15. Schematic representing how this platform was developed and how it can potentially be used. 119
Figure 3.1. Validation of the differentiation of isolated liver organoids.. 147
Figure 3.2. Liver organoids differentiate into functional hepatic organoids capable of fat uptake, and maybe *de novo* lipogenesis.. 148
Figure 3.3. Differentiated liver organoids do not vascularize after transplantation into the anterior chamber or the eye..... 148
Figure 3.4. Validation of endothelial cells isolated from mouse liver. 151
Figure 3.5. EC-rich liver organoid made from co-culturing differentiated liver organoids and endothelial cells (ECs) on ultra-low attachment (ULA) plate. 153
Figure 3.6. Liver organoid made from differentiated liver organoids and endothelial cells (ECs) briefly vascularize after transplantation into the anterior chamber or the eye. 154
Figure 3.7. Mesenchymal stem cells stain positive for CD44. 156
Figure 3.8. Liver organoid made from differentiated organoids, endothelial cells (ECs) and mesenchymal stem cells (MSCs) on ultra-low attachment (ULA) plate. 156
Figure 3.9. Liver organoids made from differentiated liver organoids, endothelial cells (ECs) and mesenchymal stem cells (MSCs) briefly vascularize after transplantation into the anterior chamber or the eye.. 157
Figure 3.10. Blood vessels regress over time from liver organoids transplanted into anterior chamber of the eye. 158
Figure 3.11. Liver spheroids made from co-culturing differentiated liver organoids-derived single cells, endothelial cells (ECs) and mesenchymal stem cells (MSCs) on ultra-low attachment (ULA) plate.. 160
Figure 3.12. Liver spheroids (LS) made from culturing differentiated liver organoids-derived single cells, endothelial cells (ECs) and mesenchymal stem cells (MSCs) on ULA plate do not vascularize after transplantation into the anterior chamber or the eye. 161
Figure 3.13. Liver buds failed to form when co-culturing single cells from differentiated organoids, endothelial cells (ECs) and mesenchymal stem cells (MSCs) on matrigel..... 163

Figure 3.14. Schematic representing Takebe and colleagues' approach to generate liver buds. 164
Figure 3.15. hESCs are successfully differentiated into HLCs. 165
Figure 3.16. Liver buds made from co-culturing parenchymal human and non-parenchymal mouse cells.....167
Figure 3.17. Liver buds transplanted into host ACE vascularize for long term. 169
Figure 3.18. Liver buds remain vascularized two months post-transplantation, but BVs density is lower than in liver tissue. 170
Figure 3.19. Liver buds fail to accumulate fat in response to host being fed an HFD. 170
Figure 4.1. Schematic depicting relevant findings of (Hope et al., 2022).. 188
Figure 4.2. Schematic of study's experimental design.. 195
Figure 4.3. Chronic G108 treatment with 5 nmol/kg, but not 2.5 nmol/kg, leads to body weight loss. 197
Figure 4.4. High protein diet, but not G108, reduces food intake. 198
Figure 4.5. Chronic G108 treatment with 5 nmol/kg, but not 2.5 nmol/kg, leads to fat mass loss.. 199
Figure 4.6. Lean mass loss is completely prevented by high protein supplementation in mice chronically treated with 2.5 nmol/kg, but not 5 nmol/kg G108.....200
Figure 4.7. Expression levels of muscle turnover markers do not reflect lean mass loss.....202
Figure 4.8. G108-chronic treatment with both 2.5 and 5 nmol/kg dose induces hypoaminoacidemia, that is completely rescued by high protein supplementation.....204
Figure 4.9. G108-chronic treatment still improves glycemia after complete mitigation of lean mass loss.. 205
Figure 4.10. G108-chronic treatment still improves hepatic steatosis after complete mitigation of lean mass loss. 207
Figure 4.11. Schematic summarizing study's findings. 220

List of tables

Table 1.1. Some of the currently available techniques to study NAFLD longitudinally *in vivo*. 72

Table 2.1. Examples of *in vivo* platforms to study tumour vascularization longitudinally through intravital fluorescent imaging. 81

Table 3.1. Summary of different strategies to make liver spheroids *in vitro*. 126

Table 3.2. Summary of different strategies to make liver organoids *in vitro* 128

Table 3.3. List of primers used in data from Fig. 3.15. 140

Table 4.1. Animal diets composition. 190

Table 4.2. List of primers used in qPCR experiments. 193

Abbreviations

2D	2-Dimentional
3D	3-Dimentional
4epb1	4E-binding protein 1
ACC1	Acetyl-CoA carboxylase 1
ACE	Anterior chamber of the eye
ACLY	ATP-citrate lyase
ALT	Alanine aminotransferase
Ang	Angiopoietin
ANOVA	Analysis of variance
Arg	Arginase
ASC	Adult stem cells
Asl	Argininosuccinate Lyase
Ass1	Argininosuccinate Synthase 1
AST	Aspartate aminotransferase
ATP	Adenosine triphosphate
AUC	Area under curve
BMP	Bone morphogenetic protein
BSA	Bovine serum albumin
BV	Blood vessel
cAMP	Cyclic adenosine monophosphate
CCl4	Carbon tetrachloride
cGMP	Cyclic guanosine monophosphate
CoA	Coenzyme A
Cps1	Carbamoyl-Phosphate Synthase 1
Cpt1	Carnitine palmitoyltransferase 1
Cpt2	Carnitine palmitoyltransferase 2
DAGs	Diacylglycerols
DIO	Diet-induced obese
DNL	*De novo* lipogenesis
DR5	Death receptor 5
EAA	Essential amino acids
EC	Endothelial cell
ECM	Extracellular matrix
EDTA	Ethylenediamine tetra acetic acid

EGF	Epidermal growth factor
EPCs	Endothelial precursor cells
ER	Endoplasmic reticulum
F-Box Protein 32	F-Box Protein 32
$FADH_2$	Flavin adenine dinucleotide
FASN	Fatty acid synthase
FBS	Foetal serum albumin
FDA	Food and drug administration
FFA	Free fatty acid
FGF21	Fibroblast growth factor 21
FRP2	Formyl peptide receptor 2
FXR	Farnesoid-X-receptors
GCGR	Glucagon receptor
GFP	Green fluorescent protein
GFR	Growth factor reduced
GIP	Glucose-dependent insulinotropic peptide
GLP-1R	Glucagon-like peptide 1 receptor
GLP-2	Glucagon-like peptide 2
Glut2	Glucose transporter 2
GSK-3	Glycogen synthase kinase-3
H&E	Haematoxylin-eosin
HAMECs	Human Adipose Microvascular Endothelial Cells
HbA1c	A haemoglobin A1c
HCC	Hepatocellular carcinoma
HDL	High-density lipoprotein
hESC	Human embryonic stem cell
HFD	High fat diet
hHE	Human hepatic endoderm
HHEX	Haematopoietically Expressed Homeobox
HLC	Hepatic like cell
HMG-CoA	Hydroxy-3-methyl-glutaryl-coenzyme A
HNFs	Hepatocyte nuclear factor
HP	High protein
HPD	High protein diet
HUVEC	Human umbilical vein endothelial cell
ICC	Immunocytochemistry

IHC	Immunohistochemistry
IKK	Inhibitor of NF-kappaB kinase
Ip-GTT	Intra peritoneal glucose tolerance test
iPSC	Induced pluripotent stem cell
IR	Insulin resistance
JNK	Jun N-terminal kinase
KC	Kupfer cell
LB	Liver bud
LCFA	Long chain fatty acid
LD	Lipid droplets
LDL	Low-density lipoprotein
LPS	lipopolysaccharides
LSECs	Liver sinusoidal endothelial cells
MALFD	metabolic dysfunction-associated fatty liver disease
map1lc3b	Microtubule-associated proteins 1A/1B light chain 3B
MCD	Methionine and choline deficient
MCFA	Medium chain fatty acid
mESC	Mouse embryonic stem cell
MPGF	Major proglucagon fragment
MRI	Magnetic resonance imaging
MSC	Mesenchymal stem cell
MUFAs	Monounsaturated fatty acids
MVF	Microvessel fragments
NADH	Nicotinamide Adenine Dinucleotide
NAFL	Non-alcoholic fatty liver
NAFLD	Non-alcoholic fatty liver disease
NAS	NAFLD activity score
NASH	Non-alcoholic steatohepatitis
NEAA	Non-essential amino acids
NEFA	Non-esterified fatty acids
NPC1L1	Niemann-Pick C1-Like 1
NPCs	Non-parenchymal cells
OA	Oleic acid
OCA	Obeticholic acid
ORO	Oil-Red-O
PAS	Periodic acid Schiff

PBS	Phosphate buffer solution
PCNA	Proliferating cell nuclear antigen
PDE	Phosphodiesterase
PFA	Paraformaldehyde
PHH	Primary human hepatocytes
PKCε	Protein kinase C
PNPLA3	Patatin-Like Phospholipase Domain Containing 3
PPAR	Peroxisome proliferator-activated receptors
PSCs	Pluripotent stem cells
PUFAs	Polyunsaturated fatty acids
RCC	Renal cell carcinoma
RFP	Red fluorescent protein
ROS	Reactive oxygen species
RPL22	Ribosomal Protein L22
SCD-1	Stearoyl-CoA desaturase 1
SCFA	Short chain fatty acid
SCID	Severe combined immunodeficiency
SLC1	Solute carrier 1
SP	Standard protein
SREBP1	Sterol regulatory element-binding transcription factor 1
SVF	Stromal vascular fraction
T2DM	Type 2 diabetes mellitus
TAG	Triacylglyceride
TC	Tissue culture
TCA	Tricarboxylic acid cycle
TLR	Toll-like receptor
TME	Tumour microenvironment
TNF	Tumour necrosis factor
UDP	Uridine diphosphate glucose
ULA	Ultra-low attachment
UPR	Unfolded protein response
VEGF	Vascular endothelial growth factor
VEGFR2	VEGF receptor 2
VEGFR3	VEGF receptor 3
VLDL	Very-low density lipoprotein
VM	Vascular mimicry

Chapter I - General introduction

1.1. The healthy liver

1.1.1. Composition and organization

The liver is a complex organ, and its organization and composition are going to be discussed from macroscopic to microscopic detail in the paragraphs below. Macroscopically, the human liver is split into four lobes (Sibulesky, 2013). Microscopically, each lobe consists of numerous hexagonally shaped units called lobules. Each lobule has one central vein and six portal triads, one in each corner of the hexagon, composed of a portal vein, a hepatic artery, and a bile duct (Fig. 1.1). The portal vein carries nutrient-rich blood from the gastrointestinal tract, gallbladder, spleen, and pancreas, whilst the hepatic artery carries oxygenated blood into the liver. Both portal and arterial blood perfuse the liver through low pressure channels called sinusoids, which then drain into the central vein. Thus, the liver receives blood from two sources: the portal vein and the hepatic artery, which corresponds to 80% and 20% of the hepatic blood volume perfusion, respectively. Lastly, the bile ducts collect the bile made in the liver, which helps with digestion of fats in the intestine, to be stored in the gallbladder until needed. Each lobule is organized into 3 zones depending on the hepatocytes distance to the portal triad, and thus, perfusion levels. Zone I is the periportal area where hepatocytes are most exposed to fresh (oxygenated and nutrient rich) blood perfusion, followed by the zone II, which is described as the pericentral region, and finally zone III, where blood perfusion is the weakest. Whilst all hepatocytes can perform liver-specific functions, recent studies suggest that the localization of hepatocytes within distinct zones of the lobule can result in variations in the extent of their functional capacity. For example, hepatocytes from zone I have strong fatty acid b-oxidation, amino acid catabolism and gluconeogenic activity; hepatocytes from zone II, on the other hand, are key in producing new hepatocytes during homeostasis and regeneration; finally, hepatocytes from zone III are more strongly involved in drug metabolization, glycolysis, glycogenesis, and lipogenesis (Kalra et al., 2023; Trefts et al., 2017).

The liver is composed by parenchymal cells - hepatocytes and cholangiocytes -, and non-parenchymal cells - endothelial cells, stellate cells, and the resident macrophages Kupfer cells. Each of these cell types has distinct roles that work together to regulate liver function across multiple levels. The hepatocytes, which account for 70% of all liver mass, are responsible for carrying out many of the previously mentioned liver related functions. The cholangiocytes line the lumen of the bile ducts but are also actively involved in modifying the composition of the hepatocyte-produced bile as it flows through the channels (Tabibian et al., 2013; Trefts et al.,

2017). The hepatic endothelial cells are the building blocks of hepatic blood vessels and are the second biggest cell type in the liver, just after hepatocytes. There are different types of hepatic endothelial cells, and the liver sinusoidal endothelial cells (LSECs) form the biggest subpopulation. These are characterized by being discontinuous, having fenestrations, lacking basement membrane and tight junctions, and having a great endocytic capacity. All the previously mentioned characteristics contribute for the effectiveness of LSECs in transporting molecules from the plasma and into the liver, thus making them key players for the liver normal function (X. Sun & Harris, 2020). The Kupfer cells are the macrophages that reside in the liver and are the first immune cells to contact with pathogens that arrive to the liver via portal vein. Finally, the stellate cells, in healthy conditions, mainly store vitamin A in lipid droplets, but can then be activated, in response to liver damage, into collagen producing cells, leading to tissue scarring (Trefts et al., 2017).

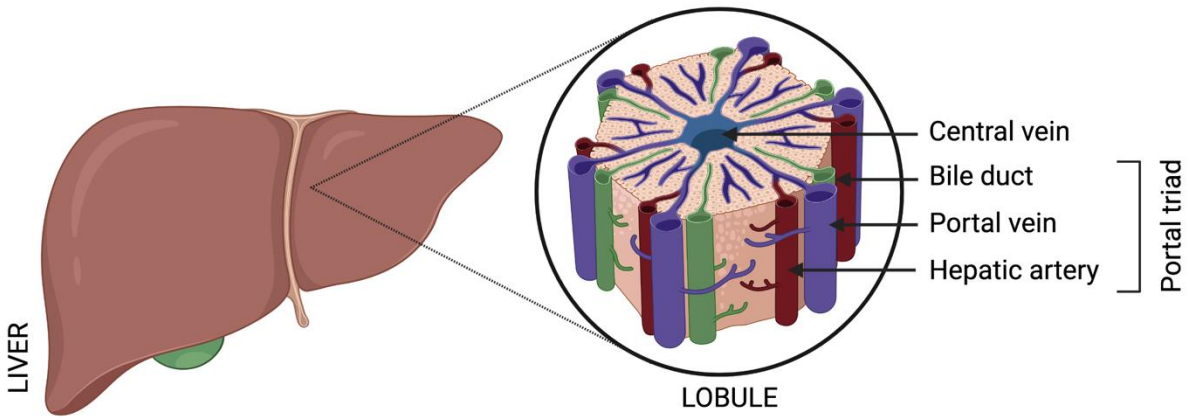


Figure 1.1. Schematic of liver microscopic organization. *Created on BioRender.*

1.1.2. Liver roles

The liver is a very important organ involved in, among other things, digestion, immune response, drug metabolization, protein synthesis, vitamin storage and detoxification. The liver is also key in maintaining energy levels through metabolization of organic fuels (Trefts et al., 2017). There are three types of organic fuels: glucose, fatty acids, and amino acids. The role of the liver in the handling and metabolization of each one of these fuels is further explored below, and a summary can be found in Fig. 1.2.

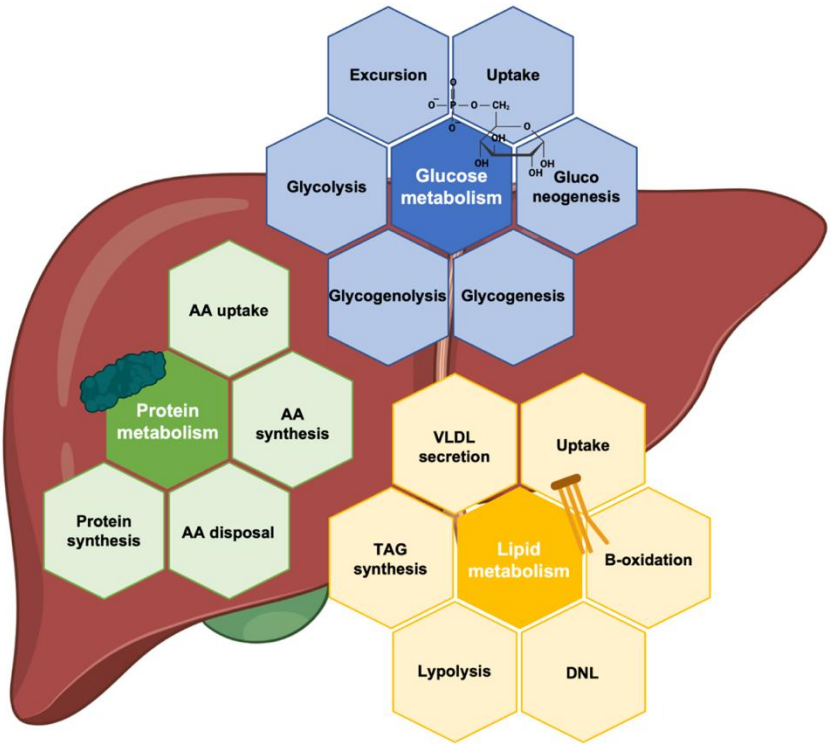


Figure 1.2. Schematic representing the roles of liver in lipid, glucose, and protein metabolism. AA: amino acids; VLDL: very low-density lipoproteins; TAG: triglycerides; DNL: *de novo* lipogenesis; *Created in BioRender*

1.1.2.1. The roles of liver in lipid metabolism

In addition to aiding digestion of dietary fats through bile production, the liver also plays an essential role in the direct handling and metabolism of lipids, and the tasks it performs can be broadly grouped into lipid acquisition, storage and usage (Enjoji et al., 2016).

Lipid acquisition includes 1) uptake of dietary lipids from portal blood (portal vein), 2) up-take of lipids from circulation (hepatic artery), 3) as well as lipids newly made by the liver through *de novo* lipogenesis (DNL).

1) The dietary lipids that make it to the liver via portal vein are a minority, since only short chain fatty acids (SCFA) are small enough to squeeze through the intestinal epithelium. Thus, most dietary lipids need to enter circulation first before reaching the liver.

2) The lipids exist in circulation in two forms: as fatty acids, that together form the pool of circulating non-esterified fatty acids (NEFA), and as part of lipoproteins, like chylomicrons, low-density (LDL) and high-density lipoproteins (HDL). When blood lipid levels are in excess, the liver can uptake them and convert them into triglycerides (TAGs) for storage in hepatocytes cytoplasmic lipid droplets. CD36 is the main receptor involved in hepatic fatty acid uptake and storage.

3) The liver can also make its own fats through *de novo* lipogenesis, which is usually promoted during postprandial conditions and excess energy availability. This pathway is regulated not only by substrate availability, but also by insulin signaling. During DNL, new fatty acids are made from the excess of a substrate molecule that is a product of both carbohydrates and protein catabolism - acetyl-CoA. During carbohydrates catabolism, carbs are broken into glucose molecules that undergo glycolysis, generating two molecules of pyruvate. Pyruvate can then enter the mitochondria where it is converted into acetyl-CoA, that enters the Krebs cycle originating citrate. The citrate, when in excess, can then be transported to the cytoplasm where it is converted into acetyl-CoA by ATP-citrate lyase (ACLY), and then further converted into malonyl-CoA by Acetyl-CoA carboxylase 1 (ACC1). Finally, malonyl CoA is then converted into palmitate by fatty acid synthase (FASN), that can then suffer elongation and desaturation to give rise to other fatty acids (Enjoji et al., 2016). During protein catabolism, proteins are broken down into amino acids which, after deamination, and just like in the carbohydrate's metabolism, can also provide a substrate for DNL by feeding into the Krebs cycle. Different amino acids can feed into the cycle at different points, but it always culminates with citrate exportation into the cytoplasm that will then follow the same pathway previously described for glucose, originating fatty acids (Charidemou et al., 2019a). The resulting fatty acids produced by DNL can then be esterified into TAGs, that can either be secreted as VLDL particles to be distributed to other tissues, or stored in cytoplasmic lipid droplets to be used as substrate for energy producing-b-oxidation when needed (Enjoji et al., 2016).

Lipid storage includes TAG synthesis, as well as the formation of lipid droplets (LD). TAGs are made from combining one glycerol and three fatty acid molecules together. Fatty acids are converted into TAGs for storage as this is a more stable and a less bio reactive/toxic form of energy source. When TAGs are not exported, they are stored into lipid droplets, which are made from TAG molecules surrounded by a phospholipid monolayer that contains other structural proteins. LDs are considered highly metabolically active structures, and, when energy is needed, they can undergo lipolysis, thus liberating TAGs that can be used as substrates in energy-producing pathways (Enjoji et al., 2016).

Lipid usage includes 1) lipolysis, 2) fatty acid b-oxidation, as well as 3) secretion of very low-density lipoproteins (VLDL). The liver is involved in maintaining normal energy levels, and one such substrate to generate energy is lipids. The liver can use lipids locally to generate energy or export them to serve as energy to other tissues.

1) The first step to generate energy from stored lipids is through lipolysis of LD-containing TAGs, which happens not only through the action of cytosolic lipases, but also through lipophagy (Mashek et al., 2020). During LD lipolysis TAGs are broken down into its constituent's glycerol and fatty acids.

2) The free fatty acids can then undergo b-oxidation in the mitochondria (short, medium and long-chain fatty acids) or peroxisomes (very long-chain fatty acids). However, whilst still in the cytoplasm, fatty acids bound for degradation in the mitochondria need to be conjugated with coenzyme A (CoA) originating a molecule called fatty acyl-CoA. Mitochondrial b-oxidation requires, as first step, the shuttle of fatty acyl-CoA molecules from the cytoplasm into the mitochondria. Whilst short and medium-chain fatty acyl-CoAs can simply enter the mitochondria via a transporter, long-chain fatty acyl-CoAs need to exchange their Coenzyme A group for a carnitine first, with this reaction being mediated by carnitine palmitoyltransferase 1 (Cpt1). After entering the mitochondria, that carnitine is replaced back by a Coenzyme A via carnitine palmitoyltransferase 2 (Cpt2). This molecule, derived from a long chain fatty acyl-CoA, is now ready, together with the short and medium-chain fatty acyl-CoAs, to enter a cycle of 4 stages comprised of dehydrogenation, hydration, dehydrogenation and thiolytic cleavage. With each cycle, the bond between the first (alpha) and second (beta) carbons of each fatty acyl-CoA molecule is broken. This releases an acetyl-CoA (which holds two additional carbons), as well as a molecule made of the leftover carbon structure, to which another Coenzyme A is added, generating a (two carbon-) shorter fatty acyl-CoA molecule. Because fatty acyl-CoA molecules bound for degradation have several carbons (2 to 22), and only 2 carbons are removed per cycle, this cycle keeps on going until the fatty acyl-CoA molecule is completely broken down, always releasing acetyl-CoA at the end of each cycle. The acetyl-CoA molecules can then be used to make ketone bodies, or can enter the Krebs (TCA) cycle, ultimately generating NADH and $FADH_2$, which will then be used by the mitochondrial electron transport chain to produce ATP, i.e., energy.

3) TAGs can also be released by the liver as nascent VLDL particles to be used for energy (through b-oxidation) or for storage in other tissues, like skeletal muscle and adipose tissue. Nascent VLDL particles are made from a phospholipid membrane, that contains cholesterols and apolipoproteins, enclosing a load of TAG molecules. Thus, VLDL secretion rate is controlled not only by TAGs and TAGs constituents' availability, but also by apolipoprotein availability. Upon release into the blood stream, these particles further mature by receiving other apolipoproteins from HDL. Then, when they reach the intended organs, they are broken

down by lipolipases and the resulting fatty acids can be up taken by the nearby tissue, whilst the VLDL remnants can go back to the liver for recycling (Enjoji et al., 2016).

1.1.2.2. The roles of liver in glucose metabolism

The liver plays an important role in preserving energy homeostasis, specially under conditions of nutrient scarcity. Glucose is the principal source of energy used by the body, and so it is not surprising that the liver plays a key role in its metabolism. In fact, the liver is responsible for steadily supplying the other organs in the body with glucose during periods of fasting or exercise. Just like with lipid metabolism, glucose handling by the liver can also be split into glucose acquisition, storage, and usage (Adeva-Andany et al., 2016).

Glucose acquisition includes the 1) uptake of dietary sugars from portal blood (portal vein), 2) glucose up taken from blood circulation (hepatic artery), as well as 3) glucose newly made by the liver through gluconeogenesis (Moore et al., 2012).

1) Sugars can be split into mono- (e.g., glucose and fructose), di- (e.g., sucrose), and polysaccharides (e.g., starches). Whilst monosaccharides are ready to be absorbed by the intestinal epithelium, di- and polysaccharides must be digested and broken down into monosaccharides first, whilst travelling through the gastrointestinal tract. Monosaccharides leave the intestinal lumen by entering the intestine enterocytes via SLC1 transporters, and potentially glucose transporter 2 (Glut2), when luminal sugar levels are very high. They can then be exported out of enterocytes and into blood circulation through Glut2 transporters, finally reaching the liver via portal vein. Here, some glucose (depending on peripheral blood glucose levels) and most fructose monosaccharides are removed from the blood before it joins peripheral circulation (Gromova et al., 2021; Southgate, 1995).

2) Whilst the liver can also uptake glucose from the blood that arrives via hepatic artery, the portal vein is the main route through which sugars enter the liver. Nevertheless, glucose is the main sugar found in the blood and, after reaching the liver, it goes into the hepatocytes passively via the bidirectional Glut2 in a process independent of insulin. Because Glut2 works both ways, to prevent its diffusion back out of the cell, intracellular glucose is phosphorylated by glucokinase into glucose-6-phosphate in an ATP-consuming reaction.

3) In addition to acquiring sugars, the liver can also synthesise its own. Gluconeogenesis consists in the formation of glucose from non-hexose precursors that can originate in the liver,

but also in extrahepatic tissues, that are released into blood circulation and eventually up taken by the liver. Examples of such gluconeogenic substrates are lactate, gluconeogenic amino acids, fructose and glycerol, and this process is inhibited by insulin. Depending on the initial substrate, gluconeogenic substrates enter the gluconeogenic pathway, which starts with pyruvate, at different stages. Lactate can be oxidized into pyruvate by lactate dehydrogenase; amino acids, on the other hand, can be converted into a-ketoacids that are later converted into TCA cycle intermediates, including pyruvate and oxaloacetate. In addition, specific amino acids like alanine, can be directly converted into pyruvate through the action of alanine aminotransferase. Pyruvate can then be converted into oxaloacetate, through pyruvate carboxylase, which is then converted into phosphoenolpyruvate via phosphoenolpyruvate carboxykinase. The phosphoenolpyruvate is then sequentially transformed into 2-phosphoglycerate, 3-phosphoglycerate, 1,3-biphosphoglycerate and glyceraldehyde 3-phosphate, which condenses with dihydroxyacetone phosphate to originate fructose 1,6-bisphosphate. It is at this stage that fructose and glycerol substrates can join the gluconeogenic pathway, by first being converted into dihydroxyacetone phosphate. Fructose 1,6-bisphosphate is then dephosphorylated into Fructose 6-phosphate, which in turn is converted into the glucose phosphorylated form of glucose: Glucose 6-phosphate (Moore et al., 2012; L. M. Sanders, 2016).

Regardless of the glucose source, i.e., whether acquired or newly made, hepatic glucose can then be stored or used, depending on energy availability.

Glucose storage is mainly promoted post-prandially, i.e., in conditions of increased energy availability, where around 50% of glucose is converted to glycogen through glycogenesis. Since there are limitations regarding how much glucose can be stored as glycogen, some glucose can also be converted into fats for storage through the DNL pathway mentioned in the previous section. During glycogenesis, which is promoted by hormones like insulin, and inhibited by glucagon, glycogen molecules are made from glucose 6-phophate. Briefly, glucose 6-phosphate is converted into glucose-1-phosphate by phosphoglucomutase, which is in turn converted into UDP-glucose. Glucosyl groups, derived from UDP-glucose molecules, are then added together by glycogen synthase to build a 10 to 20 glucosyl residues-long strand. After that, branching starts to occur via glycogen branching enzyme, an important step that increases, not only glycogen molecules size, but also its solubility (Daghlas & Mohiuddin, 2023).

Under low energy availability, where glucose storage is not being promoted, glucose can then be used by the liver.

Glucose usage includes the pathways of 1) glycogenolysis, 2) glycolysis as well as 3) glucose excursion into circulation to be used by other organs.

1) Given that glucose is stored as glycogen molecules, the first step, to use glucose, is to break glycogen stores through glycogenolysis. The first product of this reaction is glucose 1-phosphate, that is then converted into the common intracellular glucose form: glucose 6-phosphate.

2) Glucose 6-phosphate can then enter the glycolysis pathway where, in the first step, is converted into fructose 6-phosphate, which is then phosphorylated in an ATP-consuming reaction. Finally, the fructose 1,6-biphosphate molecule goes through a series of reactions that release ATP and that culminate with synthesis of two pyruvate molecules. In addition to the ATP released through the glycolysis pathway, the final product, pyruvate, can then be converted into acetyl-CoA and enter the TCA cycle, generating further ATP. As mentioned in section 1.1.2.1., excess glucose can also be used as a substrate for the synthesis of fatty acids through DNL, as excess pyruvate leads to excessive acetyl-CoA thus saturating the TCA cycle and resulting in citrate exportation from the mitochondria into the cytoplasm. Furthermore, hepatic glucose is also used in other non-energy producing, but still important, pathways, like the pentose phosphate pathway, that provides precursors for nucleotide and amino acid biosynthesis.

3) In addition to glucose metabolization to fulfil internal energy requirements, the liver can also export glucose that will provide energy to other organs. Hepatic glucose excursion is inhibited post-prandially, mainly by suppression of glycogenolysis, but also through attenuation of gluconeogenesis. Increased and decreased insulin and glucagon secretion, respectively, drive this inhibition. Thus, in conditions of low blood sugar, where insulin levels are low and glucagon high, the liver increases its glucose export rate. This can happen, during short-term fasting, through breaking of glycogen stores through the previously mentioned pathway of glycogenolysis and, for longer term fasting situations, by synthesising glucose *de novo* through the gluconeogenic pathway. Regardless, since intracellular glucose exists in the phosphorylated form (glucose-6-phosphate), before leaving the cell it needs to be de-phosphorylated through the action of glucose-6-phosphatase (G6Pase). Glucose is then ready to be exported into the blood via Glut2 (Adeva-Andany et al., 2016).

1.1.2.3. The roles of liver in amino acid metabolism

Amino acids are the building blocks of proteins, and the liver is responsible for synthesising a great percentage of circulating protein volume. Thus, it is not surprising that this organ has a key role in amino acids metabolism (Trefts et al., 2017). The liver is involved in amino acid metabolism in several ways: to synthesise amino acids from other amino acids (transamination), to dispose of amino acids (deamination) (urea cycle), to generate energy (TCA cycle), to convert them into glucose or fatty acids through gluconeogenesis and *de novo* lipogenesis, respectively, and to generate nucleotides. Just like with lipid and glucose metabolism, amino acid handling by the liver can also be split into amino acid acquisition, storage, and usage (Paulusma et al., 2022).

Amino acid acquisition includes 1) up-take of amino acids from blood bound to the liver for degradation/recycling, 2) uptake of dietary amino acids and 3) synthesis of non-essential amino acids through transamination.

1) and 2) Given the range of processes in which amino acids are involved, keeping an adequate level of circulating amino acids is essential for the normal function of the body. In fact, and given that the liver is responsible for both protein synthesis and amino acid degradation, the liver is known to be a key player in regulating plasma amino acid levels by up taking them from and releasing them into circulation. Apart from branched chain amino acids, hepatic uptake of amino acids is very efficient. The liver extracts amino acids from the blood arriving from both portal vein and hepatic artery, via transporters located in the hepatocyte's membranes. These transporters belong to the SLC family, and different transporters are present in distinct liver zones, meaning that certain amino acids can be up taken preferentially in certain areas of this organ (Paulusma et al., 2022). AAs can be split into the essential or non-essential categories, depending on whether they must be obtained from diet or can be synthesised by the body, respectively. Thus, the aa up-taken from the blood into the liver can be derived from aa heading to the liver for degradation or recycling and from digestion of dietary proteins.

3) Non-essential amino acids can also be synthesised from other amino acids through a reversible process known as transamination. Structurally, aa consist of an amino group linked to a carbon skeleton. The process of transamination involves both processes of deamination and amination. Briefly, during this process, which is mediated by transaminases (aminotransferases) and pyridoxal phosphate, the amino group of an existent amino acid is transferred (deamination) to an acceptor keto-acid molecule (amination) (which provides the

carbon skeleton), transforming the latter into a new amino acid, and the original amino acid into a keto acid. Which non-essential aa will be newly generated depends on both the original amino acid that provides the amino group, as well as the acceptor keto acid. For example, when the amino acid L-Glutamate donates its amino group to the keto acid pyruvate, the new amino acid L-Alanine is generated, together with the new keto acid a-ketoglutarate (Bhagavan & Ha, 2015).

Amino acid storage includes 1) deamination, 2) DNL and 3) gluconeogenesis.
1) In situations of amino acid excess, aa are up taken from blood by the liver. Unlike sugars and lipids that can be stored as glycogen and TAGs, respectively, amino acids cannot be stored as amino acids or protein in the liver. Instead, they need to be deaminated first and then converted into the two others previously mentioned organic fuels: glucose or fatty acids.
2) and 3) Thus, following the first step of deamination, the resulting carbon structure is then further degraded, and, under high energy availability conditions, degradation products can then feed into the *de novo* lipogenic and gluconeogenic pathways, as has been explained in the previous two sections (Paulusma et al., 2022).

Amino acid usage by the liver includes 1) amino acid disposal, 2) energy production and 3) protein synthesis.
1) The liver is one of the main organs where amino acids go to be disposed, with the first step being deamination, where the amino group is separated from the carbon skeleton. The resulting amino group gives rise to ammonium, a highly toxic compound that needs to be converted into urea, through the urea cycle, before leaving the liver to be safely excreted it in urine.
2) Under low energy availability, the products of amino acid degradation can enter the TCA cycle which, just like as explained before for the products of glucose and fatty acid degradation, leads to NADH and $FADH_2$ generation, that can then enter the oxidative phosphorylation pathway, thus generating ATP.
3) In addition to being a source of energy, amino acids are also used by the liver to synthesise 85–90% of all circulating plasma proteins (with albumin being the most abundant of those). Furthermore, the ammonia released through amino acid deamination can also be used to synthesise nitrogen-containing compounds like nucleotide bases (Chandel, 2021; Trefts et al., 2017).

1.2. The liver in non-alcoholic fatty liver disease (NAFLD)

1.2.1. NAFDL definition and aetiology

As explained earlier in this chapter, the liver plays an essential role in maintaining energy levels within physiological ranges, especially in situations of low energy availability. These processes are tightly regulated in healthy individuals but, in some situations, they might get dysregulated and lead to excessive hepatic fat accumulation.

Non-alcoholic fatty liver disease (NAFLD) is a rapidly growing disease in western countries affecting around 30% of its population. Its prevalence is growing not only in developed, but also developing countries, where it is becoming the primary cause of end-stage liver disease, and thus the main indicator for liver transplantation. Recently, given the new insights into this disease etiology, a panel of experts proposed updating NAFLD's nomenclature to metabolic dysfunction-associated fatty liver disease (MALFD). Nevertheless, given that the majority of studies referenced in this dissertation retained the original terminology, the term NAFLD was consistently employed throughout this thesis (Eslam et al., 2020). As the name suggests, NAFLD consists in hepatic fat accumulation, mainly in the form of triglycerides (TAGs), and is relatively harmless in early stages. However, the continuous excessive hepatic fat accumulation can lead to lipotoxicity which sensitizes the liver to further insults that injure the hepatocytes, which can lead to the disease progressing into hepatitis, fibrosis, and cirrhosis. Hence, depending on the degree of injury caused to the liver, NAFLD can be divided into non-alcoholic fatty liver (NAFL), characterized by the harmless simple accumulation of fat in more than 5% of the parenchyma (also known as steatosis), and non-alcoholic steatohepatitis (NASH), where the hepatocytes sustain injury (Fig. 1.3). Around 20-30% of NAFL patients progress into NASH, and, of these, between 3-15% progress into cirrhosis. From those, 4-27% end up developing HCC (Dhamija et al., 2019; Fernando et al., 2019).

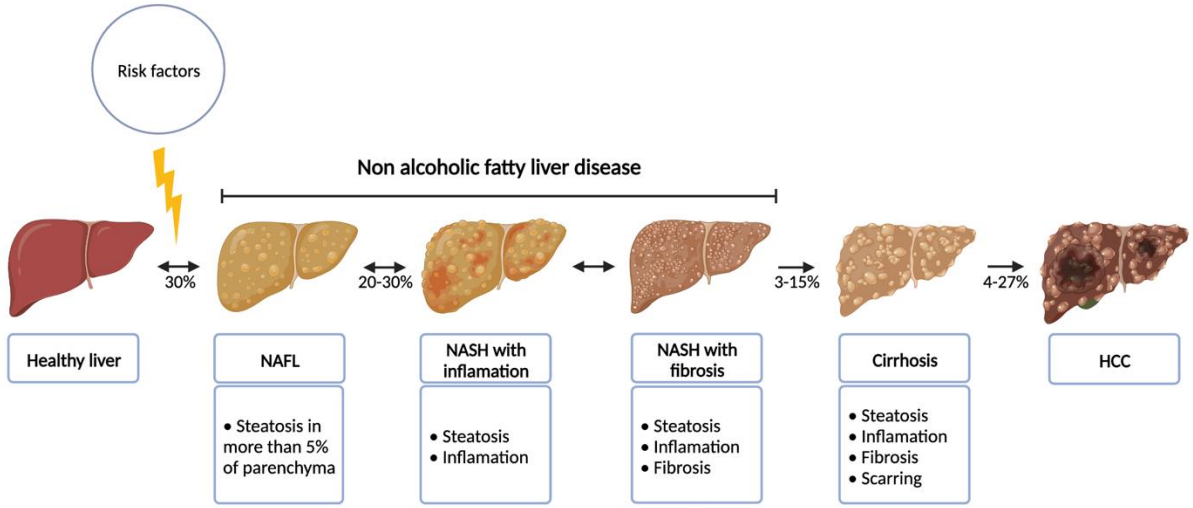


Figure 1.3. Schematic representing potential progression of NAFLD. NAFLD: non-alcoholic fatty liver disease; NASH: non-alcoholic steatohepatitis; HCC: hepatocellular carcinoma. *Created in BioRender*.

1.2.2. Pathology of hepatic fat accumulation

NAFLD starts as harmless accumulation of fat in the liver due to an imbalance between lipid uptake/synthesis and usage. But how does lipid accumulation in the liver ends up leading to liver disease?

1.2.2.1. Why hepatic fat accumulation leads to lipotoxicity

Although, as the name suggests, lipotoxicity is caused by lipids, these can exert such toxicity through several ways. Lipotoxicity has been shown to be caused, not only by excessive hepatic fat accumulation, but also by the presence of certain lipid species.

1.2.2.1.1. Overwhelming of TAG and LD synthesis pathways

In early stage NAFLD, fat accumulation, also known as simple steatosis, does not harm the hepatocytes that simply store the fats (mainly) as TAGs in their cytoplasmic lipid droplets (LD). However, the continuous high level of fat getting stored in the liver eventually overwhelms the TAG synthesis pathway, as well as the lipid droplets storage capacity, meaning that hepatocytes are no longer capable of properly accommodating additional fats. TAGs are inert non-toxic molecules that are packed into lipid droplets for storage. As previously

mentioned, most fats are stored as TAGs which are made of one glycerol and three fatty acid molecules. Those fatty acids can be saturated, monounsaturated, or polyunsaturated, depending on the number of double bonds between their carbon atoms, and studies have shown that some free fatty acids are more toxic than others. For example, polyunsaturated fatty acids (PUFAs) and monounsaturated fatty acids (MUFAs) have been shown to be beneficial in NAFLD, as they reduce hepatic lipid deposition, oxidative stress, and inflammation. Saturated fatty acids, on the other hand, have been shown to have a detrimental effect on hepatocytes, causing cell damage and death. The mechanisms through which this happens are not fully known, but Jun N-terminal kinase (JNK)-induced ER stress is thought to play a role. Nevertheless, fatty acids are only toxic under their free form, which means that they are not toxic when they are packed into TAG molecules. Indeed, incorporating saturated fatty acids into TAG molecules is a way of reducing lipotoxicity (Wasilewska & Lebensztejn, 2021). Thus, when the hepatocytes capacity of packing free fatty acids into TAG molecules and LDs is overwhelmed, the cells can be exposed to lipotoxic fatty acids and, therefore, to a lipotoxic environment, which leads to a series of occurrences that can ultimately result in cell damage and death.

1.2.2.1.2. Altered levels of non-TAG lipids

Lipotoxicity is not caused only due to the excessive absolute level of fats, but also due to an imbalance in the relative levels of the various classes of fats that accumulate in the liver. TAGs are not directly lipotoxic, but altered levels of other lipids, like cholesterol, sphingolipids and glycerophospholipids can be.

- Cholesterol: Cholesterol is an important lipid and plays key roles in cell membrane structure, vitamin and steroid hormone synthesis, among other things. There are several studies showing that cholesterol homeostasis is altered in NAFLD, and it is influenced by cholesterol absorption, *de novo* synthesis, usage, and excretion. Cholesterol can be obtained from diet or synthesised *de novo*. Regarding excessive cholesterol absorption, this can be due to excess dietary intake coupled with diets richer in fats, both common in NAFLD patients, which contributes to increased levels of ingested cholesterol. Cholesterol synthesised *de novo* has also been shown to be upregulated in NAFLD patients due to upregulation of transcription factors and increased substrate availability. This lipid is used in a plethora of processes, and so, a decrease in cholesterol usage can also result in increased availability of free cholesterol. For

example, cholesterol is used for LD, VLDL and bile synthesis, thus, when storage of fats in LD particles is overwhelmed, and VLDL secretion and bile synthesis are reduced, also often found in NAFLD patients, less hepatic cholesterol will be used, and more free cholesterol is available. Research has shown that excessive free cholesterol causes lipotoxicity and is involved in promoting the progression of NAFL to NASH. Exactly how excess free cholesterol leads to lipotoxicity is not fully understood, but its pathology might be exerted in different liver cell types. For example, studies suggest that excess free cholesterol in the hepatocytes precipitates into crystals that then promote Kupffer cells-mediated inflammation, but direct accumulation of cholesterol in Kupfer cells lysosomes and hepatic stellate cells have also been suggested to trigger inflammation pathways and fibrosis. Additionally, other studies suggest that excessive free cholesterol might also lead to mitochondrial glutathione depletion, which makes hepatocytes more sensitive to apoptosis. Indeed cholesterol-lowering drugs have shown positive results in improving NAFLD symptoms (Arguello et al., 2015; Malhotra et al., 2020).

- Sphingolipids: Sphingolipids are important structural constituents of cell membranes. They include ceramides, whose hepatic levels have been shown to be altered in NAFLD. Ceramides synthesis is promoted by increased availability of free fatty acids. Thus, excess of free fatty acids that are not packed into lipid droplet-TAGs, often found in NALFD patients, increase ceramides synthesis. Exactly how ceramides lead to lipotoxicity is still an area of active research, but studies have shown that higher levels of hepatic ceramides were associated with worsened hepatic insulin resistance, activation of inflammatory pathways, cytokine release, as well as increased mitochondrial reactive oxygen species (ROS). Indeed, studies carried out in NAFLD animal models where ceramide synthesis was inhibited led to significantly improvement of steatosis and fibrosis (Wasilewska & Lebensztejn, 2021).

- Glycerophospholipids: Glycerophospholipids are also key constituents of cell membranes. Phosphatidylcholine is one of the most abundant lipids of this type and, in addition to having a cell membrane structural role, it also has functions in regulating VLDL synthesis and secretion. Decreased phosphatidylcholine hepatic levels have been found in NAFLD patients and a causal role in disease onset and progression has been proposed. Phosphatidylcholine can be synthesised *de novo* from diet-derived choline or converted from phosphatidylethanolamine. Both poor intake of choline, as well as low phosphatidylethanolamine levels, have been shown to result in decreased levels of

phosphatidylcholine in NAFLD patients. How low levels of phosphatidylcholine influence NAFLD is not fully understood, but decreased levels of this lipid have been shown to impair VLDL secretion, thus promoting hepatic fat accumulation. Furthermore, low phosphatidylcholine levels have also been shown to promote *de novo* lipogenesis through up-regulation of SREBP1, which results in further hepatic steatosis. Given the role of phosphatidylcholine as a structural component of cell membranes, low levels of this lipid are also though to result in a compromised cell membrane integrity that can be more permeable to pro-inflammatory factors, thus contributing to disease progression. Indeed, increasing phosphatidylcholine intake has been shown to improve steatosis (Kartsoli et al., 2020; Osipova et al., 2022; Sherriff et al., 2016).

1.2.2.2. How lipotoxicity is exerted at the cell level

The exact means through which lipids can exert toxicity in the hepatocytes are still an area of active research. Nevertheless, studies showed that lipotoxicity can be exerted at a cellular level through 1) dysregulation of cellular organelles function, as well as through 2) direct modification of intracellular signalling pathways. Both can lead to detrimental effects to the cell including insulin resistance, inflammation, and apoptosis, which can result in impaired cell function leading to cell damage and potentially cell death. Although it is not completely known what leads harmless NAFL to progress into harmful NASH in some patients, the previously mentioned lipotoxicity-induced events are thought to play an important role (Geng et al., 2021; Marra & Svegliati-Baroni, 2018).

1.2.2.2.1. Dysregulation of organelles function

In addition to directly affecting specific pathways that lead to detrimental effects in the cell, toxic lipids can also promote the dysregulation of normal cell function by affecting its organelles. Among those dysregulated organelles, endoplasmic reticulum (ER) stress and mitochondrial dysfunction are the most explored ones, and they can both lead to negative effects in the cell like oxidative stress, inflammation, injury and death.

- ER stress: The endoplasmic reticulum is an important organelle involved in, among other things, protein folding and assembly, *de novo* lipogenesis, lipid synthesis (e.g., TAGs,

cholesterol, phospholipids), storage (LD synthesis) and b-oxidation, as well as VLDL assembly and maturation. Given the key roles that the ER plays in lipid metabolism, increased intracellular levels of lipids result in increased levels of lipids in the ER. Thus, the continuous excessive levels of fats that enter the ER lumen might overwhelm it and interfere with its normal function. This might lead to altered membrane composition, disrupted ER-to-Golgi protein trafficking, impaired lipid storage, b-oxidation and assembly of VLDL (promoting further steatosis), as well as to protein misfolding. Accumulation of misfolded or unfolded proteins then induces ER stress which, in an attempt to attenuate cellular strain, triggers the activation of the unfolded protein response (UPR). The initial activation of the UPR pathway aims to restore ER homeostasis by increasing protein folding, as well as clearance capacity through autophagy and ER-associated degradation, whilst also reducing secretory protein load and promoting antioxidant response. However, if the insults continue and the ER stress persists, the UPR pathway might not be capable of fixing ER function anymore. When this happens, the UPR pathway switches to a terminal fate where pathways leading to up-regulation of pro-apoptotic genes, ROS production, calcium release, and pro-inflammatory cytokines production are induced. Such events will then result in oxidative stress, inflammation and eventually cell death, and have been linked to NAFLD onset and progression. UPR activation is a common finding in NAFLD patients, and the degree of its activation varies depending on the stage of the disease (Akazawa & Nakao, 2018; Geng et al., 2021; Lebeaupin et al., 2018; Rada et al., 2020).

- Mitochondrial dysfunction: Mitochondria play important functions in cells in general, like energy and reactive oxygen species production (which have important roles in cell signalling), and it is involved in the urea cycle. In lipid metabolism, in particular, it is involved in, among other things, b-oxidation of fatty acids, ketogenesis (where ketone bodies, an alternative energy source, are synthesized from fatty acids) as well as TAG synthesis. Given the roles that mitochondria play in lipid metabolism, increased intra-cellular fat accumulation results in increased levels of fat (and fat metabolism) in this organelle. As previously explained in section 1.1.2.1., b-oxidation of fatty acids is carried out preferentially in the mitochondria in a process that leads to ROS production. In situations of excess fats, the mitochondria antioxidative capacity can be overwhelmed, which can result in the accumulation of ROS within the organelle. This accumulation can be toxic and lead to the dysregulation of mitochondrial normal functions (Rada et al., 2020; Sunny et al., 2016). One of those compromised functions is the b-oxidation pathway, which, can be incomplete and lead to the

formation of toxic intermediates. Furthermore, when the capacity of fatty acid b-oxidation is impaired in the mitochondria, fatty acids b-oxidation can be promoted in peroxisomes and the ER, which results in the formation of ROS. On the contrary of mitochondrial oxidation, where, under normal conditions, ROS levels are tightly controlled, ROS production in extra-mitochondrial organelles is not regulated. This leads to an accumulation of ROS in the cell, leading to oxidative stress, that has detrimental effects in the mitochondria and in the cell in general. This can ultimately lead to production of pro-inflammatory cytokines, activation of Kupfer cells and apoptosis. Another mitochondrial function that can be impaired by lipotoxicity is the electron transport chain through which, as previously mentioned, energy is generated in the form of ATP. Impaired energy levels can compromise mitochondria function in particular, and the whole cell in general, resulting in worsening of mitochondrial dysfunction. Thus, mitochondrial dysfunction has been regarded as one of the contributors for NAFLD severity, and it is a common finding in patients with NAFLD. In fact, mitigating cellular mitochondria dysfunction through drugs targeting oxidative stress, as well as through intravascular infusion of healthy mitochondria, has been shown to improve NAFLD symptoms (Ramanathan et al., 2022; Simões et al., 2018).

1.2.2.2.2. Direct modification of signalling pathways

Impacting intracellular signalling directly is another way through which lipids can exert lipotoxicity and thus impair normal cell function. Different lipids play key roles in intracellular signal transduction. Thus, when they are in excess, and/or there is an imbalance in the relative amount of each lipid, both often found in NAFDL patients, normal intracellular signalling can get dysregulated and lead to negative effects on cells. Indeed, several pathways can be directly triggered by lipids, such as inflammatory, cell death and insulin pathways (Pei et al., 2020).

- Inflammation pathways: Dysregulated inflammation pathways are a common finding in patients with more advanced NAFLD. Indeed, studies have showed that some lipids can directly promote inflammation in liver cells. For example, the PUFA arachidonic acid plays a key role in promoting hepatic inflammation in NAFLD. Arachidonic acid is a precursor of eicosanoids which are bioactive lipids that have a potent inflammatory effect. These eicosanoids can then leave the cells and bind and activate receptors on immune cells (like macrophages) resulting in the upregulation of inflammatory signalling pathways, which will

lead to inflammation. Thus, increased hepatic levels of this particular PUFA can increase the intracellular levels of eicosanoids which in turn induces lipotoxicity through direct influence in pro-inflammatory signalling pathways (Pei et al., 2020). Saturated fatty acids have also been shown to trigger inflammation through direct binding to the toll-like receptor (TLR), an important mediator of inflammatory pathways, which is located on the hepatocyte's membrane. The binding results in the activation of the downstream JNK and IKK pathways which are key players involved in inflammation (Liangpunsakul & Chalasani, 2019). Additionally, lysophosphatidylcholine, ceramides and free fatty acids can also promote the release of inflammatory extracellular vesicles carrying inflammatory mediators from the hepatocytes, that can activate macrophages and thus promote inflammation. In addition, the vesicles can also be internalized by hepatic stellate cells resulting in its activation. Activated hepatic stellate cells are known to dysregulate ECM production and can then lead to fibrosis. Thus, dysregulated lipid quantity and quality can promote inflammation through direct modulation of cellular inflammatory signalling pathways (Akazawa & Nakao, 2018; Liangpunsakul & Chalasani, 2019).

- Cell death pathways: Programmed cell death in the context of NAFLD can occur through apoptosis, necrosis and pyroptosis. Apoptosis is by far the best understood one and it will be explored next (Hirsova & Gores, 2015). Hepatocytes can undergo apoptosis through extrinsic and intrinsic pathways. Whilst the intrinsic pathways are secondary to other things happening in the cell (like ER stress and mitochondrial dysfunction), the extrinsic ones are promoted by direct action of lipids that alone can trigger death pathways. Despite the distinct triggers, the process of apoptosis is always mediated by the mitochondria, meaning that both extrinsic and intrinsic apoptotic pathways converge in this organelle (Ibrahim et al., 2011). The examples given bellow refer to the lipid-triggered extrinsic pathway. Given that apoptosis in NAFLD is a secondary consequence of altered hepatic fat accumulation, it is often referred to as lipoapoptosis. Several lipids have been shown to directly promote lipoapoptosis. For example, saturated free fatty acids have been shown to trigger the extrinsic death pathway by promoting GSK-3 mediated phosphorylation of JNK, thus triggering cell death (Akazawa & Nakao, 2016). Additionally, the extrinsic pathway can also be activated by death receptors like death receptor 5 (DR5), whose expression is often found to be upregulated in NAFLD patients' livers. Excess free fatty acids have been shown to upregulate and promote DR5 self-aggregation on the cell membrane which then triggers apoptosis, thus also leading to cell death (Akazawa & Nakao, 2018).

- Insulin pathways: Another way through which lipotoxicity is induced is by promoting hepatic insulin resistance. For example, the previously mentioned ceramides can promote, in addition to inflammation, hepatic insulin resistance, which has a detrimental effect on cells, through both activation of protein kinase C, IKK and JNK pathways, and through dephosphorylation of Akt (Liangpunsakul & Chalasani, 2019). In addition to ceramides, diacylglycerols (DAGs) have also been shown to promote hepatic insulin resistance through promoting PKCε activation and translocation into the membrane, which in turn inhibits insulin receptor kinase, and consequently, insulin signalling pathway. Thus, increased DAG levels impair the normal response of hepatocytes to insulin, which leads to hepatic insulin resistance (Birkenfeld & Shulman, 2014).

- Autophagy pathways: Another key player in NAFLD is autophagy, which is key in keeping cellular homeostasis as it is responsible for intracellular organelle turnover, i.e., it promotes degradation of old/compromised organelles. Lipotoxicity can often damage mitochondria, which, if not sorted, might lead to/worsen oxidative stress, which plays a key role in NAFLD pathophysiology. Here, autophagy plays a key role in degrading compromised mitochondria in a process termed mitophagy, so that they can be replaced by healthy ones. Research has shown that accumulation of certain fats, such as saturated fatty acids, can directly inhibit autophagy through Rubicon upregulation, which in turn suppresses one of the final autophagy steps, the autophagosome formation. Indeed, autophagy has been shown to be downregulated in the livers of NAFLD patients. Furthermore, together with *in vitro* experiments, the downregulation of autophagy has been shown to promote NAFLD progression. Besides, promoting autophagy in fatty liver has been shown to improve NASH symptoms. Thus, saturated fatty acids can directly modulate autophagy via Rubicon upregulation, which has detrimental effects for the hepatocytes (Khambu et al., 2018).

1.2.3. Diagnosing NAFLD

There are several tools available that can aid NAFLD diagnostic, from blood tests and imaging techniques to the gold standard biopsy. Each has its own advantages and disadvantages so, employing a combination of techniques, together with the patient medical record, is often the chosen approach to investigate a potential NAFLD diagnosis.

Blood tests can be performed to assess blood lipid levels, which are often altered in NAFLD patients, as well as to assess liver function through quantification of liver enzymes, like alanine aminotransferase (ALT) and aspartate aminotransferase (AST). However, liver enzymes are often only altered in more advanced stages.

Imaging techniques can provide additional information about the state of the liver, and the most common ones employed in NAFLD diagnostic are abdominal ultrasound, magnetic resonance imaging (MRI) and transient elastography. Whilst ultrasound can detect hepatic fat accumulation and is, therefore, the go to option for an initial imaging test, it is not very accurate, since quantification of the level of hepatic steatosis (key information for NAFL diagnosis) is not precise. MRI, on the other hand, can accurately quantify hepatic fat accumulation, whilst also providing some information regarding the level of fibrosis. Transient elastography is mostly used to assess presence of fibrosis through assessment of liver stiffness.

Despite the previously mentioned tests all providing information that can guide NAFLD diagnostic, liver biopsy is still the golden standard for NAFLD diagnosis and staging (Cataldo et al., 2021; Juo & Livingston, 2019). Liver biopsies consists in the excision of small pieces of liver tissue for posterior histologic preparation, where the presence and extent of steatosis, inflammation, hepatocyte ballooning and fibrosis can all be assessed, and a NAFLD activity score produced. Steatosis can be visualized and quantified in liver samples stained with hematoxylin-eosin (H&E) or Oil-Red-O (ORO) stain, and it can present as macrovesicular or microvesicular (less common and more damaging), depending on the size of the fat vacuoles. As previously explained in section 1.2.1., NASH consists in the presence of hepatic inflammation, hepatocyte ballooning and (sometimes) fibrosis in the context of steatosis. Thus, in addition to H&E, which can also be used to assess hepatocytes shape and highlight the presence of immune cells, collagen staining dyes, like Sirius red and Masson trichrome, can be used to assess fibrosis (Leow et al., 2022).

1.2.4. Sources of hepatic fat in NAFLD

As explored earlier in section 1.2.2.1., the pathological effects of NAFLD are caused by excessive and altered fat accumulation in the liver, but where does that fat come from? A study by Donnelly and colleagues using multiple-stable-isotopes has identified the contributions of the different sources of the TAGs that accumulate in the liver of NAFLD patients. They reported that, in the post-absorptive state, 60% of hepatic fats are derived from the circulating

plasma pool of non-esterified fatty acids (NEFA), less than 15% come directly from diet, and 26% originate from *de novo* lipogenesis (DNL) within the liver (Fig. 1.4) (Donnelly et al., 2005a).

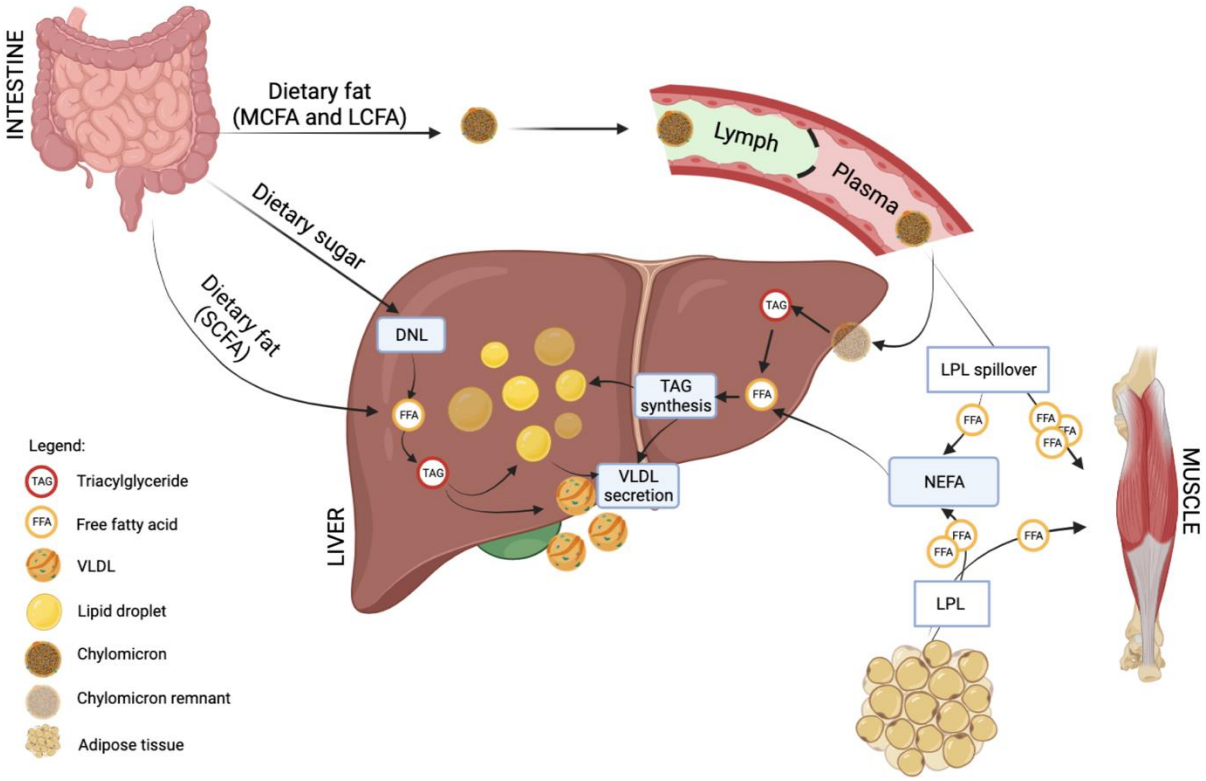


Figure 1.4. Schematic representing different sources of hepatic fat. TAG: triacylglyceride; VLDL: very low-density lipoprotein; SCFA: short chain fatty acid; MCFA: medium chain fatty acid; LSFA: long chain fatty acid; LPL: lipoprotein lipase; NEFA: non esterified fatty acid; DNL: *de novo* lipogenesis. Schematic inspired on (Donnelly et al., 2005a). *Created on BioRender.*

1.2.4.1. Fats derived from NEFA pool

The free fatty acids (FFAs, i.e., non-esterified with glycerol) found in circulation are commonly referred to as the pool of non-esterified fatty acids (NEFA). The main source of free fatty acids that form the NEFA pool is from adipose tissue lipolysis, which, in a normal/healthy situation, serves to hydrolyze stored TAG into glycerol and fatty acids to be used as energy substrates by peripheral organs. The circulating FFAs that are not used by the peripheral tissues for energy are then up taken by the liver, that cannot regulate the amount of FFAs that takes in. This means that, in a situation of increased levels of NEFA pool (like often reported in NAFLD patients), the liver will up-take excess FFAs, thus increasing hepatic fat content (Donnelly et al., 2005b; Duncan et al., 2007).

1.2.4.2. Fats derived from diet

Dietary fats can enter the liver in 3 ways: 1) the short chain fatty acids can go directly to the liver via portal vein. However, the medium and long chain fatty acids are too big to be able to squeeze through the intestinal epithelium. Thus, they must enter the lymphatic system (via lacteals that eventually drain into the thoracic duct) as part of chylomicrons first, before entering the blood circulation when the thoracic duct drains into the left subclavian vein. After that, the blood from the left (and right) subclavian vein drains into the superior vena cava, finally reaching the heart that pumps it to the lungs, returning to the heart via pulmonary veins after. The oxygenated blood carrying the dietary chylomicrons is then pumped to the whole body. When chylomicrons reach organs like the adipose tissue, and cardiac and skeletal muscle, the lipid components of the chylomicrons are hydrolyzed by lipoprotein lipases, so that the released free fatty acids can be absorbed by these tissues. 2) During this process, some fatty acids might escape absorption by those tissues and enter the blood circulation instead, contributing to the fats that build the NEFA pool, thus ending up being up taken by the liver as well. 3) After being hydrolyzed by lipoprotein lipase, the chylomicron remnants, which can still carry some fats, join the blood circulation and are then up taken by the liver to be recycled. Thus, the leftover fats in the chylomicron remnants also contribute for the hepatic fat content (Cooper, 1997; Goldberg et al., 2009; Null & Agarwal, 2022; *Subclavian Vein: Location, Anatomy and Function*, n.d.). Those 15% of fats stored in the liver of NAFLD patients derived from diet reported by Donnelly and colleagues includes these three routes.

1.2.4.3. Fats derived from *de novo* lipogenesis (DNL)

Whilst *de novo* lipogenesis (DNL) can be seen as a natural process to convert excessive precursor substances into stored energy, persistent activation of DNL is a key contributor for the abnormal build-up of triglycerides within hepatocytes. DNL consist in fatty acids synthesis, mainly in the form of palmitate, from excessive non-lipid precursors like sugars and amino acids, and it is stimulated by substrate availability and insulin. Carbohydrates are the most well studied substrates for DNL, with fructose being the most potent DNL-inducing one. When sugar availability exceeds the body's needs, which is usually coupled with hyperinsulinemia, sugar Is up taken primarily by the liver to be converted and stored as glycogen for later use.

There is a limited amount of sugars that can be stored as glycogen, and so, in situations of high sugar levels, these can also induce DNL which ends up leading to production of fatty acids that can subsequently be esterified and stored as triglycerides, thus increasing hepatic fat content. Therefore, excessive over nutrition that results in increased carbohydrates intake (commonly found in NAFLD patients), and of fructose in particular, leads to hepatic steatosis (Belew & Jones, 2022).

1.2.4.4. Deficient fat handling

Even though NAFLD is caused by fat accumulation in the liver, it is not only excessive fat-storage (prevenient from NEFA, DNL and diet) that contributes to the disease, but also a defective fat handling. The liver can reduce its fat storage in two ways 1) through fat exportation in VLDL particles and 2) through fatty acid oxidation. Thus, dysregulation of any of these (often found in NAFLD patients) can also contribute to increased hepatic steatosis. 1) As explained in section 1.1.2.1., the liver can export lipids to be used in energy-generating pathways or to be stored by other organs, as VLDL particles. In NAFLD patients, VLDL export is increased in earlier stages of the disease, as a measure to try to counteract the excessive hepatic fat accumulation, but this then plateaus, or can even decrease, as the disease progresses. This is likely due to the increasingly compromised function of the hepatocytes due to organ damage caused by lipotoxicity induced-NAFLD advancement, which ultimately also contributes to hepatic fat accumulation (Ipsen et al., 2018). 2) As mentioned earlier in this chapter, in situations of low glucose, b-oxidation of fatty acids occurs to generate energy for hepatocytes and ketone bodies, that are exported into circulation to be used as metabolic fuel by other organs. In normal conditions, fatty acids oxidation occurs mainly in the mitochondria, apart from very long chain fatty acids that must be oxidized in the peroxisome due to their size, this is known as mitochondrial and peroxisomal b-oxidation, respectively. In situations of excess lipid, like in NAFLD, fatty acids oxidation can also occur in the cytochrome or endoplasmic reticulum in a process known as omega-oxidation, however this results in production of reactive oxygen species and oxidative stress. There are conflictive results about fatty acid b-oxidation levels in NAFLD patients, where studies have showed increased, unchanged, and even decreased levels with disease progression. However, the main finding is that the omega-oxidation is often abnormally increased in these patients, which leads to

hepatocyte damage further impairing liver function, promoting further hepatic steatosis, and driving disease progression (Ipsen et al., 2018).

1.2.5. Risk factors

NAFLD is widely accepted as a multifactorial disease, but the mechanisms that lead to it are not fully understood. There have been, however, several risk factors identified in playing a role in the disease onset and progression (Fig. 1.5). Most of them have some form of metabolic imbalance, like metabolic syndrome or insulin resistance, but genetics, intestinal microbiome composition, diet, age and even gender have also been associated with increased NAFLD predisposition (Huh et al., 2022).

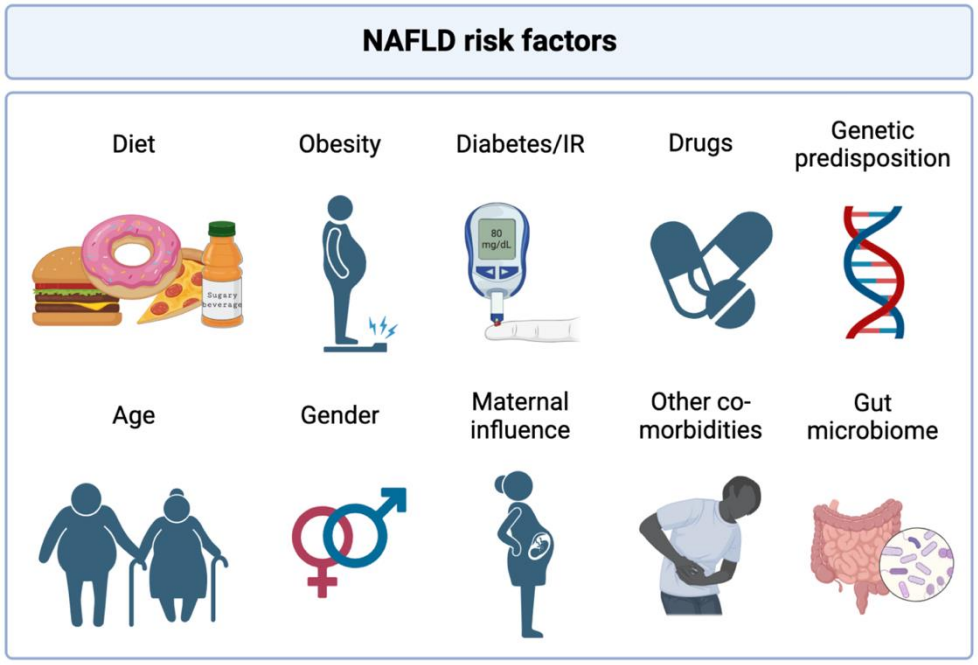


Figure 1.5. Schematic depicting some of the risk factor associated with NAFLD onset and progression. IR: insulin resistance. *Created on BioRender.*

1.2.5.1. Diet

Given NAFLD aetiology, as well as the role of the liver in the metabolism of dietary energy sources, it comes to no surprise that certain dietary behaviours can pose a risk for disease onset and progression. The role that diets play in the risk of NAFLD development has been traditionally associated with increased energy intake, which is a fact. However, and despite being hard to detangle the effects of diet from obesity in risk of NAFLD, studies have shown

that diets composed of certain nutrients can be beneficial to NAFLD compared to other iso-caloric diets, and even in the absence of body weight changes. Thus, the association between diet and NAFLD is way more complex than just a matter of increased total energy intake. Balanced diets are composed of healthy levels of macronutrients, like fats, carbs and proteins, and micronutrients, like minerals and vitamins. Dietary patterns where consistent derangement of any of these nutrient levels are adopted can negatively impact NAFLD. Simultaneously, upscaling the intake of specific nutrients over others seems to have a favourable impact in NAFLD prevention and progression (Berná & Romero-Gomez, 2020; S. M. B. Duarte et al., 2019). A brief summary of the effects of some of those nutrients in the risk of/protectiveness against NAFLD can be found bellow.

- Fats: Despite the undeniable association between high dietary fat levels and NAFDL onset and progression, not all types of fat impact NAFLD equally. Fats can be grouped into saturated, monounsaturated, and polyunsaturated. Indeed, and despite being somewhat controversial, it has been shown that whilst diets rich in trans (found in e.g., processed foods and oils) and saturated fats (e.g., meat and butter) can promote NAFLD, diets rich in monounsaturated (e.g., avocado and olive oil) and polyunsaturated (e.g., fish and nuts) fats have been established has having a positive impact in NAFLD risk and progression (Berná & Romero-Gomez, 2020; S. M. B. Duarte et al., 2019).

- Carbohydrates: it is well established that diets rich in carbohydrates can increase the risk of NAFLD, however, just like with fats, distinct types of sugars can affect NAFLD differently. Sugars can be transformed into fats through *de novo* lipogenesis, and it has been shown that fructose (commonly present in sugary beverages and snacks) is the most potent DNL-inducing sugar. Furthermore, fructose intake has also been associated with increased intestinal inflammation and permeability. Thus, it comes to no surprise that diets high in fructose lead to hepatic steatosis and can promote disease progression. Other types of carbohydrates, however, like fiber, are thought to have a beneficial role in NAFLD, as low fiber intake has been linked to NAFLD onset and progression, probably by impacting intestinal microbiome (fiber promotes bacterial growth), another known player in NAFLD (Berná & Romero-Gomez, 2020; S. M. B. Duarte et al., 2019).

- Proteins: There are not many studies demonstrating a relation between protein and NAFLD, and the ones that do so have reported contradictory data. Whilst some studies suggest that protein seems to have a protective effect against fatty liver (Xu et al., 2020), others suggest that it might actually be detrimental (Lang et al., 2020). The contradictions in these studies might be due to, among other things, the source of protein, i.e., animal vs plant-derived, or even the types of protein (and thus amino acids) used (Khazaei et al., 2023). Regardless, the mechanism through which high protein diets can lead to improved steatosis might be through increasing energy expenditure (due to increased amino acid catabolism, an energy costing process), whilst a possible justification for how high protein diet promotes hepatic steatosis is through increasing DNL substrate availability (amino acids).

- Micronutrient deficiencies: Micronutrient deficiencies can also play a role in NAFLD. The liver is a key organ that plays an essential role in micronutrient metabolism. Deficiencies in several micronutrients, like vitamins, more specifically vitamins A, C, D and E, and minerals, like zinc, copper, and magnesium, have been shown to be a risk factor for NAFLD onset and progression. This is thought to be due to the roles these micronutrients play as antioxidants, antifibrotic, lipoprotectors and even as modulators of the immune system (Pickett-Blakely et al., 2018).

1.2.5.2. Obesity

Between 50% to 90% of people with obesity have NAFLD. Obesity is defined as excessive accumulation of fat that can present a health risk, and it is caused by excessive energy intake which includes higher ingestion of fats and carbohydrates (*Obesity*, n.d.). As explained in section 1.2.4.3., fats stored in the body come not only from dietary fats, but also from dietary sugars that are converted into fats through DNL. Regardless of their origin, fats are stored preferentially in adipose tissue. However, when the storage capacity of this organ is overwhelmed, like in obesity, fats can start to be deposited in ectopic places, like the liver. Furthermore, obesity is also associated with increased lipolysis at the adipose tissue level, which further increases the amount of free fatty acids in circulation that are available to be up taken by the liver, further increasing hepatic steatosis. In addition, obesity is characterized by low-grade inflammation. In fact, it has been observed that the adipose tissue, intestine and even skeletal muscle of people with obesity often release pro-inflammatory signals that can act in the liver promoting hepatic inflammation, which contributes to NAFLD progression (Y. Luo

& Lin, 2021). Thus, obesity is a risk factor not only to hepatic steatosis onset, but also for disease progression into NASH and even HCC (Fabbrini et al., 2010). Thus, and despite being hard to detangle the effects of diet and obesity in NAFLD, it comes to surprise that obesity is one of the best established NAFLD risk factors (Polyzos et al., 2018). Nevertheless, and even though NAFLD is clearly more prevalent in patients with obesity, about 10-20% of the NAFLD population is lean (Kuchay et al., 2021).

1.2.5.3. Metabolic syndrome

Metabolic syndrome is defined as a combination of high triglycerides, abdominal obesity, hypertension, and hyperglycaemia or diabetes, that predispose an individual to cardiovascular disease. Several of the previously mentioned traits are also known risk factors for NAFLD, thus, it is widely accepted that NAFLD is the liver expression of metabolic disease. Furthermore, several studies confirmed that NAFLD is four times more prevalent in people with metabolic disease, and that several of the previously mentioned characteristics of metabolic syndrome were also associated with worse NAFLD phenotypes, and *vice versa* (Godoy-Matos et al., 2020).

1.2.5.4. Insulin resistance

Insulin is a molecule produced by the beta cells of the pancreas and its secretion peaks in response to high levels of circulating glucose, like what happens after a meal, for example. The insulin will then act on several metabolic organs like the adipose tissue, muscle, and liver. In the adipose tissue, insulin stops lipolysis; in the muscle, insulin stimulates glucose uptake by muscle cells, whilst also promoting glucose storage as glycogen (glycogenesis); In the liver, insulin blocks gluconeogenesis, glycogenolysis and hepatic glucose output, whilst also promoting glycogenesis and DNL (Mu et al., 2019).

Insulin resistance (IR) is a common feature in patients with type 2 diabetes as well as in patients with NAFLD. In fact, around 70% of patients with type 2 diabetes also have NAFLD (Mantovani & Dalbeni, 2021; Younossi, Golabi, et al., 2019). Several studies have shown that insulin resistance can drive and worsen NAFLD, and that NAFLD can drive insulin resistance. Thus, the relationship between NAFLD and insulin resistance is complex, and it seems to be bi-directional. IR happens when organs stop responding to insulin as they normally would, and

it can be split into systemic and hepatic. Whilst systemic IR refers to the impaired response of muscle and adipose tissue to insulin, hepatic IR refers to the specific insulin insensitivity of the liver.

In a situation of systemic IR, adipose tissue lipolysis is not downregulated in response to insulin, which increases both the levels of circulating free fatty acids that will end up being up taken and stored in the liver, as well as the levels of glycerol, a substrate for hepatic gluconeogenesis, whose products can then be used as a substrate for DNL. Insulin resistance in the muscle results in a decrease in the glucose up taken from circulation by the muscle cells and glycogen synthesis is also impaired, which results in higher levels of circulating sugars, that can then be up taken by the liver to be used as precursors of *de novo* lipogenesis. Thus, systemic insulin resistance results in increased hepatic fat accumulation.

In a situation of hepatic IR, insulin fails to block gluconeogenesis and glycogenolysis, and to promote glycogenesis, all of which result in higher substrate availability for DNL. Furthermore, insulin also fails to dampen the hepatic glucose output which leads to hyperglycaemia. Paradoxically, hepatic insulin resistance does not seem to fail to promote *de novo* lipogenesis (Mu et al., 2019). This was initially thought to be due to some sort of pathway selective insulin resistance, but papers have suggested that *de novo* lipogenesis is still being promoted under hepatic resistance conditions due to excess of substrate availability (sugars) (Honma et al., 2018; Ter Horst et al., 2021). Therefore, hepatic insulin resistance also leads to hepatic steatosis.

1.2.5.5. Drug-induced fatty liver disease

Several drugs have been shown to cause hepatic steatosis, and, despite the incidence of drug induced fatty liver disease (DIFLD) in the general population being currently unknown, it is estimated that around 2% of all fatty liver disease cases are linked to chronic medication intake (Kolaric et al., 2021). Different drugs can lead to different NAFLD characteristics. For example, ibuprofen and glucocorticoids (anti-inflammatories), have been shown to induce microvesicular steatosis, whilst others, like paracetamol (analgesic) and tamoxifen (blocks oestrogen signalling), induce macrovesicular steatosis. Furthermore, other drugs, like valproic acid (anti-convulsant) and amiodarone (anti-arrhythmic), have been linked to steatohepatitis. Given that different classes of drugs induce NAFLD, and different NAFLD characteristics, it is not surprising that they might do so through different mechanisms. However, the most

common mechanism is thought to be by promoting lipogenesis and generation of free radicals that lead to oxidative stress in the hepatocytes. Most drugs do not induce NAFLD in all patients taking them, i.e., certain drugs promote fatty liver only in some patients, and, often, simply stopping treatments with these drugs is usually enough to resolve NAFLD (Kolaric et al., 2021).

1.2.5.6. Other underlying diseases

Some underlying diseases have also been shown to lead to NAFLD. These can have a genetic component, like several lipid metabolism disorders, or fall into the infectious or inflammatory categories.

Perhaps not surprisingly, several disorders of lipid metabolism, like abetalipoproteinemia and lipodystrophy have been identified as potential risks to NAFLD development. Abetalipoproteinemia and familial hypobetalipoproteinaemia are both autosomal recessive disorders caused by distinct mutations, but that result in the same outcome, which is impaired VLDL synthesis and secretion, ultimately leading to hepatic fat accumulation. Another example is lipodystrophy, also an autosomal recessive disorder, that can be congenital or acquired, where abnormal fat storage in adipose tissue is impaired, resulting in an increase in fat stored in the liver (Kneeman et al., 2012). Most of these secondary NAFLD causing disorders can be treated with dietary lipid restriction.

Infectious diseases like hepatitis C have also been studied as a secondary cause of NAFLD. Around 55% of these patients present hepatic steatosis that can eventually lead to inflammation and oxidative stress, which accelerates disease progression into fibrosis and puts them at higher risk of developing hepatocellular carcinoma. Evidence suggests that hepatic fat accumulation might favour hepatitis C virus life cycle, and, although the mechanisms through which hepatitis C leads to NAFLD are not fully understood, this might occur through viral impairment of hepatic lipid and glucose metabolism (Adinolfi et al., 2016).

Some chronic inflammatory diseases, like celiac disease, have also been shown to represent a risk for NAFLD development. A study with almost 27000 people reported that celiac patients were three times more likely to develop NAFLD than the general population, particularly during the first year of diagnosis. The mechanism through which celiac disease might put people at higher risk of NAFLD is currently unknown, thus, whether it is the gluten-free diet

or the celiac disease *per se*, or other factor, that drive NAFLD frequency in this population is still an area of active research (Kneeman et al., 2012; Reilly et al., 2015).

1.2.5.7. Genetic predisposition

Some genes have been associated with NAFLD predisposition. Numerous studies in different populations found a relation between NAFLD and a gene called Patatin Like Phospholipase Domain Containing 3, or PNPLA3 for short. In this gene, a single nucleotide polymorphism (known as rs738409 C/G variant), seems to be associated, not only with higher liver fat contents, but also with a more severe fibrosis if the disease progresses to NASH, as well as a higher risk of HCC. Functionally, PNPLA3 is known to be involved in regulating TAG hydrolysis, and thus lipid droplets remodelling, in hepatocytes, as well as stellate cells activation and fibrogenesis. The mutation on the PNPLA3 gene associated with NAFLD, decreases PNPLA3 (TAG) hydrolytic capacity leading to hepatic fat accumulation. Studies in animals carrying the human mutated PNPLA3 variant revealed that silencing it with oligonucleotides improved both NAFLD activity score and fibrosis in these animals. More studies are needed to explore the therapeutic potential of targeting this variant in carrier patients with NAFLD (Sookoian & Pirola, 2017)

1.2.5.8. Intestinal microbiome composition

Several studies in animals and humans found that the composition of the intestinal microbiome might be a risk factor for NAFLD development and progression. Patients with the disease were discovered to have specific intestinal microbiome signatures. However, given that NAFLD patients often present other metabolic imbalances, such as diabetes and/or obesity, it is hard to detangle which microbiome signatures are NAFLD-specific. Thus, better studies with appropriate controls are needed to further our knowledge regarding the role of distinct microbiomes in NAFLD predisposition and progression. The mechanisms through which the microbiome might be contributing to NAFLD are not totally understood yet. However, several studies hypothesize that it might be through altering the gut barrier, by increasing gut permeability. This higher permeability will then result in an increased release of lipopolysaccharides (LPS; present in the membrane of Gram-negative bacteria) and other microbially produced metabolites, like choline and ethanol, from the gut into the liver, that

promote tissue inflammation and impact immunity. Overall, more studies are needed to deepen our understanding of the role that the intestinal microbiome plays in NAFLD, as well as to determine its potential as a therapeutic target (Aron-Wisnewsky et al., 2020).

1.2.5.9. Age

Perhaps not surprisingly, NAFLD incidence has been shown to increase with age, as with advanced age there is higher prevalence of NAFLD risk factors, like the previously mentioned hypertension, obesity, diabetes/insulin resistance and hyperlipidemia. In addition to an increase in the disease incidence, it has also been observed that the disease progression into NASH and cirrhosis is more likely in older patients (Huh et al., 2022).

1.2.5.10. Maternal influence

Several studies have now shown that the presence of obesity and diabetes in pregnancy can increase NAFLD risk in babies, as well as later in life. A study by Brumbaugh and colleagues showed, using magnetic resonance spectroscopy, that neonate babies from obese mothers with gestational diabetes had 68% more fat in their livers than babies from normal weight mothers (Brumbaugh et al., 2013). Additionally, another study concluded that young adults born from obese mothers were at higher risk of developing NALFD when compared to controls born from non-obese mothers (Hagström et al., 2021). Although additional research is needed to explain exactly how maternal obesity and diabetes can influence NAFLD development in the offspring, managing the future mothers weight seems to be a favorable approach.

1.2.5.11. Gender

It has also been shown that NAFLD is more prevalent in men than pre-menopausal women, but this shifts after women reach menopause, suggesting that oestrogen might have a protective role (Huh et al., 2022). In fact, Lee and colleagues have recently shown that this protective effect seems to be mediated by formyl peptide receptor 2 (FRP2), a protein that plays a role in inflammatory response in multiple organs and that is activated by oestrogen. FPR2 is highly expressed in the livers of female mice and silencing it makes females as susceptive to NAFLD as males; likewise, activating FRP2, by supplementing males' diet with oestrogen, made them less susceptive to NAFLD (C. Lee et al., 2022).

1.2.6. Therapeutic strategies

Currently, the most common therapeutic approach to treat/manage NAFLD consists in changes in lifestyle, specifically through changes in dietary behaviours, increased physical exercise and weight loss. Until the present day, there are no FDA-approved drugs for NAFLD treatment, however, there are several drugs being developed for that matter at the moment with some already undergoing clinical trials. Furthermore, drug repurposing is also being explored for the treatment of NAFLD. Given that NAFLD is only harmful in its more advanced NASH stage, and that there are no approved drugs to treat NAFLD patients specifically, these drugs are usually only used in NASH patients that have not responded to the lifestyle change approach. These drugs target several NAFLD characteristics like blood glucose levels, hepatic steatosis, insulin resistance, inflammation, and fibrosis (Mantovani & Dalbeni, 2021). These main approaches to manage and treat NAFLD will be further explored next.

1.2.6.1. Lifestyle change

1.2.6.1.1. Weight loss

The main aim of employing lifestyle changes in NAFLD treatment is to reduce body weight. This comes to no surprise given that excessive body weight, like found in patients with obesity, is one of the most well-known risk factors for NAFLD onset and progression. Indeed, studies have shown that a reduction of only 5 to 10% in weight is enough to significantly improve NAFLD symptoms, such as steatosis and fibrosis (Vilar-Gomez et al., 2015). In fact, evidence showed that a moderate reduction in body weight even in non-obese patients was enough to revert NAFLD to some extent (Gunn, 2021). The improvement of NAFLD symptoms is directly reflected by the levels of lost weight, rather than how that weight loss was achieved. Thus, reduced caloric intake, bariatric surgery and weight-loss drugs that lead to a meaningful weight loss all improve NAFLD. A reduction in body weight happens when there is a negative energy balance, which means that stored energy (like the one in the form of fat) must be used, so that the body can perform its normal functions. Hence, weight loss benefits NAFLD by reducing liver fat, enhancing insulin sensitivity, alleviating adipose tissue inflammation, lowering hepatic oxidative stress, and improving metabolic indicators such as blood lipid levels—all crucial factors involved in NAFLD pathophysiology (Mantovani & Dalbeni, 2021; Romero-Gómez et al., 2017).

1.2.6.1.2. Diet

Several dietary approaches have shown promising results in improving NAFLD. These are usually composed of increased levels of fruits, vegetables, legumes, fibre, whole grains, and mono and polyunsaturated fats, and reduced levels of sugared beverages, trans fatty acids, and red and processed meat (Aboubakr et al., 2021; Houttu et al., 2021). An example of such diet is the Mediterranean diet and switching to this regime can improve NAFLD in several ways. The first one is through weight loss, since patients that swop their usual nutritional regime for the Mediterranean diet often reduce their body weight, which, as explained in the previous section, is known to improve NAFLD symptoms. This reduction in body weight can be a consequence of a reduction in the intake of dense calorie sources (like fats), as well as of reduced energy intake due to increased satiety induced by increased levels of protein intake, for example. Nevertheless, studies have shown that switching to the Mediterranean regime can improve NAFLD symptoms even when no changes in body weight are observed (Mantovani & Dalbeni, 2021). This is because this diet is rich in antioxidants, which are known to reduce hepatic oxidative stress and inflammation; healthy fats, which are known to promote storage of toxic lipids as TAG molecules; and fibre, which supports a healthy gut microbiome. Simultaneously, this diet is also associated with reduced intake of sugars (including fructose), which improves insulin resistance and reduces *de novo* lipogenesis, which are also known players in NAFLD development and advancement (Anania et al., 2018). Thus, for those reasons, the Mediterranean diet is the most recommended diet for NAFLD patients.

1.2.6.1.3. Exercise

Different types of exercise (e.g., aerobic or resistance) have shown positive effects in improving symptoms, such as hepatic steatosis, in NAFLD patients (Hashida et al., 2017). The mechanisms through which exercise can improve NAFLD symptoms are varied, and weight loss is one of them, through previously explained reasons. However, studies have shown that exercise can ameliorate NAFLD symptoms even in the absence of body weight changes (Ok et al., 2018). This is because exercise improves several key players linked to NAFLD onset and progression. For example, evidence shows that exercise improves systemic and hepatic insulin sensitivity; it reduces hepatic steatosis by promoting the breakdown and utilization of stored

fats; and improves inflammation through the release of anti-inflammatory cytokines. As expected, and just like with diet, exercise-induced benefits in NAFLD patients are only sustained whilst the exercise regime is maintained. Additionally, studies have also shown that patients with mutations on PNPLA3 do not respond as well to lifestyle changes as a NAFLD-therapeutic option. Thus, in situations where patients do not comply, quit, or do not respond to the lifestyle change-therapeutic approach, drugs can be used instead (Cigrovski Berkovic et al., 2021; Mantovani & Dalbeni, 2021).

1.2.6.2. Drugs

Although it may be hard to group drugs into a single category, since NAFLD symptoms are often interlinked, and so, the same drug can affect different aspects of NAFLD, they can be broadly grouped into drugs that target glucose, lipids or inflammation levels as well as bile acid pathways (Cruz-Ramón et al., 2017; Fu et al., 2021; Tzanaki et al., 2022; Wiering & Tacke, 2023).

1.2.6.2.1. Glucose lowering drugs

T2DM causes increased blood glucose levels due to inefficient insulin signalling. As previously mentioned in section 1.2.5.4., T2DM is a known risk for NAFLD development and worsening, and so, targeting/managing it is one possible approach for pharmacologic NAFLD-treatment. Oral glucose lowering drugs can target different aspects of T2DM, and some examples are GLP-1 receptor (GLP-1R) and PPAR agonists (Fu et al., 2021).

- GLP-1R agonists: GLP-1 is an incretin hormone produced by the intestinal L-cells that enhances insulin secretion in response to a meal. Furthermore, it is also involved in regulating satiety. Thus, several GLP-1R agonists have been developed to treat patients with T2DM and obesity, and some of those, like semaglutide and liraglutide, are currently also being tested for NAFLD treatment (Nevola et al., 2023).

Semaglutide: Semaglutide has been shown to improve several histological markers of NAFLD (Arai et al., 2022; Loomba et al., 2023; Volpe et al., 2022). For example, semaglutide has been tested in patients with NASH on a phase 2 clinical trial. That clinical trial has revealed that, despite no changes in fibrosis were observed, a significant histological improvement in

hepatocytes ballooning and inflammation levels was reported. Furthermore, patients also experienced a significant weight loss compared to placebo, a known therapeutic approach to treat NAFLD. Regarding side-effects, only mild gastrointestinal disorders were reported. A phase 3 trial is currently on the way (Newsome et al., 2021).

Liraglutide: Liraglutide is another example of GLP-1R agonists. Liraglutide has also been shown to have positive effects in NAFLD patients that also present with T2DM (T. Song et al., 2021). Liraglutide is short-lived and it targets the hepatocytes GLP-1R. A phase 2 trial tested its effects in NASH patients where it led to improved histological markers of NASH and to a reduction in steatosis and hepatocyte ballooning, although no changes were observed regarding inflammation and fibrosis levels. Furthermore, glucose tolerance was also improved in liraglutide-treated patients. The reported side-effects were similar to the semaglutide ones where mild to moderate gastrointestinal disorders were reported (Armstrong et al., 2016; Mantovani & Dalbeni, 2021; Nevola et al., 2023).

- PPAR agonists: PPARs are nuclear receptors that regulate gene expression and are split into alpha, beta and gamma. Depending on the subtype, PPARs can be expressed preferentially in certain tissues and perform different functions. For example, PPAR-alpha is mainly expressed in the liver and is involved in lipid metabolism, including fatty acid breakdown, b-oxidation and transportation. PPAR-beta is expressed in tissues like liver, heart, adipose tissue, and gastrointestinal tract, and is involved in lipid and glucose metabolism, as well as energy expenditure. PPAR-gamma is expressed in adipose tissue, but also liver and skeletal muscle. It plays key roles in lipid metabolism and increases insulin sensitivity through promoting adipocyte differentiation. Thus, it comes to no surprise that several PPAR agonists have been developed to treat dyslipidaemia and T2DM, and that some of these, like pioglitazone, are being repurposed to treat NAFLD (Lange et al., 2022).

Pioglitazone: Pioglitazone is a PPAR-gamma agonist originally employed to treat T2DM due to its capacity of improving insulin-resistance. Recently, it has been put through a phase 4 clinical trial to assess its efficacy in treating NASH. This clinical trial showed that pioglitazone improved overall NAS (which includes histological features of steatosis, inflammation, and ballooning), in addition to glucose tolerance (Cusi et al., 2016). Thus, despite not being FDA-approved for NAFLD treatment, possibly due to the serious side effects associated with long term PPAR-gamma agonism (which include peripheral oedema and weight gain), pioglitazone is currently on the international guidelines to treat NAFLD patients that also present T2DM and that do not respond to other therapies (Mantovani & Dalbeni, 2021).

Lanifibranor: Lanifibranor is a pan-PPAR agonist (i.e., targets all PPAR isoforms) and, on the contrary to the other drugs mentioned so far, has not yet been approved by the FDA to treat any disease. Promising pre-clinical results led to a phase 2b clinical trial that showed that this drug led to improved histologic markers of inflammation, ballooning, and fibrosis, whilst also improving metabolic parameters, such as glucose metabolism, in patients with non-cirrhotic NASH (Francque et al., 2021). Given these promising results, and together with the mild side-effects reported, a phase 3 trial is currently on the way, where the impact of lanifibranor on the risk of NASH progression into cirrhosis will be assessed (Lange et al., 2022; Mantovani & Dalbeni, 2021).

1.2.6.2.2. Lipid-lowering drugs

Dysregulated lipid metabolism is a known risk factor for NAFLD onset and progression, and so, lipid-lowering drugs are another potential way through which NAFLD can possibly be treated/managed. Examples of such drugs are Niemann-Pick C1-Like 1 (NPC1L1), Hydroxy-3-methyl-glutaryl-coenzyme A (HMG-CoA) and Stearoyl-CoA desaturase 1 (SCD-1) inhibitors (Liang & Dai, 2022).

- NPC1L1 inhibitors: NPC1L1 is a protein involved in the transport of cholesterol from the intestinal lumen to the enterocytes, thus affecting cholesterol intestinal absorption, a known player in NAFLD pathology. Thus, inhibiting NPC1L1 has been a common approach to treat patients with hypercholesterinaemia (R. Zhang et al., 2022). One such inhibitor is Ezetimibe.

Ezetimibe: Ezetimibe has been commonly used to treat hyperlipidaemia, and a phase 2 trial was carried out to assess its performance in NASH treatment. This trial revealed that Ezetimibe reduced blood cholesterol levels, whilst also improving histological markers of hepatocyte ballooning and fibrosis (Loomba et al., 2015). However, an increase in HbA1c (marker of (pre)-diabetes) and hepatic long-chain fatty acids (known to worsen insulin resistance) have been reported. Thus, the use of Ezetimibe for NAFLD treatment is only likely to be further explored if combined with other side-effect-mitigating drugs (Mantovani & Dalbeni, 2021; Toyoda et al., 2019).

- HMG-CoA inhibitors: HMG-CoA is an enzyme that mediates cholesterol synthesis in the liver. Thus, inhibiting it can lower cholesterol levels. An example of such drug are statins.

Statins: Statins are FDA-approved drugs for the treatment of high cholesterol and prevention of cardiovascular events. They work to lower LDL and TAGs whilst increasing HDL levels, so repurposing statins for NAFLD treatment is a promising approach. Only a few studies have been conducted to investigate the potential of statins in treating NAFLD (Boutari et al., 2022). However, whilst one study showed improved overall NAS and liver biomarkers (Hyogo et al., 2008), another one showed no significant differences in histological nor hepatic biomarkers (Nakahara et al., 2012) in NASH patients. Thus, and given the small size of the tested patients on both studies, further research is needed to assert the effectiveness of statins in treating NAFLD (Boutari et al., 2022; Mantovani & Dalbeni, 2021).

- SCD Inhibitors: Stearoyl-CoA desaturase 1 (SCD-1) is responsible for converting saturated (SFAs) into monounsaturated fatty acids (MUFAs). Saturated fatty acids are more lipotoxic than monounsaturated fatty acids, however, SCD1 has also been shown to shift lipid metabolism away from b-oxidation and towards lipid storage. Thus, inhibiting SCD-1 might be beneficial in NAFLD (Z. Zhang et al., 2014). Despite no SCD-1 inhibitors having been approved by FDA so far, there are a few currently undergoing clinical trials such as the new drug Aramchol.

Aramchol: A phase 2b trial has assessed the efficacy of this drug in treating NASH patients that also presented T2DM. This study showed that patients taking 400mg of Aramchol experienced a reduction in steatosis, NASH resolution, improved liver enzymes and reduced HbA1c. However, no changes in fibrosis levels, or in the percentage of patients that progressed into cirrhosis, were observed (Ratziu et al., 2021). Thus, future studies might assess Aramchol treatment in combination with anti-fibrotic drugs (Jeyakumar & Vajreswari, 2022).

1.2.6.2.3. Bile-pathway targeting drugs

Bile is composed by two bile acids: cholic and chenodeoxycholic acids. As highlighted earlier (see section 1.1.1.), bile is produced in the liver, stored in the gallbladder, and is then shipped to the intestine to aid the digestion of dietary fats when needed. Thus, dysregulation of the bile acid metabolism can lead to dysregulated dietary fat absorption. Indeed, NAFLD patients often present alterations in their bile acid metabolism (X. Zhang et al., 2018), thus targeting this pathway has been suggested as another potential approach to treat NAFLD (Cruz-Ramón et al., 2017).

- FXR agonist: Farnesoid-X-receptors (FXR) are receptors expressed mainly in the liver and intestine, and are key players in keeping bile acid, lipid and glucose homeostasis. Hepatic FXR activation has been shown to reduce bile synthesis, which impairs dietary fat absorption, stimulates production of anti-inflammatory molecules and holds anti-fibrotic activity. Thus, FXR activation might be another potential approach to treat NAFLD (Henry et al., 2023). An example of a FXR agonist is obeticholic acid.

Obeticholic acid: Obeticholic acid (OCA) is a synthetic molecule about one hundred times more potent than its natural form chenodeoxycholic acid. Phase 2 and 3 trials in NASH patients treated with OCA revealed reduced steatosis, hepatocyte ballooning, inflammation, and fibrosis, as well as improved liver biomarkers. However, side effects were reported and included pruritus and raised LDL and reduced HDL levels (Younossi et al., 2022; Younossi, Ratziu, et al., 2019a, 2019b). Thus, other trials are currently on the way where the long-term effects of OCA-treatment will be explored (Henry et al., 2023; Mantovani & Dalbeni, 2021).

1.2.6.2.4. Anti-inflammatory drugs

Given that inflammation is one of the key drivers of NAFLD, mitigating it using anti-inflammatory drugs might improve NAFLD pathology (Wiering & Tacke, 2023).

- Phosphodiesterase (PDE) inhibitors: PDEs are a group of enzymes that are involved in regulating the levels of cellular cAMP and cGMP, key second messengers in several physiological pathways, including inflammation. Thus, drugs that inhibit PDEs can dampen immune responses and, consequently, inflammation, and might thus improve NAFLD symptoms (El-Deen et al., 2020). Pentoxifylline is an example of a PDE inhibitor.

Pentoxifylline: Pentoxifylline has originally been approved as a vasodilation-inducing drug, however, its anti-inflammatory action against TNF-alpha, a key player in NAFLD, made it an attractive candidate for NAFDL treatment. However, two phase 2 clinical trials in NASH patients have shown slightly different results. Whilst both studies reported an improvement of overall NAS, steatosis and hepatic biomarkers, significance was only reached in one of them. Improvement of fibrosis was also reported on both, though this did not reach significance. Notably, TAG levels were increased in Pentoxifylline-treated subjects in one of the studies, which might hold detrimental effects, especially in NAFLD patients. Thus, further studies are

needed to clarify the effectiveness of this drug in treating NAFLD (Du et al., 2014; Mantovani & Dalbeni, 2021).

Overall, several drugs are currently undergoing clinical trials with some of them showing promising results, despite this being often associated with some side-effects. Nevertheless, to this date, there are still no FDA-approved drugs specifically for NAFLD treatment, so additional research and drug development are needed.

1.2.7. Glucagon signalling modulation in NAFLD treatment

1.2.7.1. Glucagon

The liver plays a very important role in keeping energy homeostasis during periods of high metabolic demand like, for example, during fasting and exercise (Trefts et al., 2017). Given that glucose is the main fuel for cells, keeping energy homeostasis is deeply connected to keeping blood glucose homeostasis (normoglycemia). So, under fasting conditions, to prevent hypoglycemia, the liver releases glucose at the same rate as glucose is up taken by the muscles and other peripheral organs (Han et al., 2016). One of the key players in regulating this is glucagon, a 29 amino acid long peptide hormone. Under physiological euglycemic conditions, glucagon is found at a concentration around 7pmol/l, however, under hypoglycemic conditions, such as during exercise, for example, glucagon concentration can increase up to 3 or 4 times its basal levels (Rix et al., 2019).

Glucagon is encoded by the gene glucagon. Glucagon gene is translated into the preproglucagon peptide, which then suffers the action of proteases in the ER leading to the formation of a proglucagon peptide. Depending on the organ where proglucagon is synthesized, this peptide can then be further processed into different peptides. Under physiological conditions, in the pancreas, prohormone convertase 2 processes proglucagon to give rise to Glucagon, GRPP, IP1 and major proglucagon fragment (MPGF); whereas in the gut and brain, proglucagon is processed by prohormone convertase 1/3 to give rise to GLP-1, GLP-2, IP2, Oxyntomodulin and Glicentin. Thus, glucagon is mainly produced by the pancreatic Langerhans islets alpha cells. After being synthesized, glucagon is stored in peptide vesicles until there is a need to be released (Holst, 2022; Rix et al., 2019).

1.2.7.2. Glucagon secretion

Glucagon release from the alpha cells is controlled by several stimuli. Sympathetic stimulation, low blood glucose levels, prolonged fasting, exercise, low free fatty acids, high plasma amino acids and glucose-dependent insulinotropic peptide (GIP) all promote glucagon secretion. On the other hand, GLP-1, insulin, and high blood glucose levels inhibit it. Furthermore, glucagon indirectly inhibits its own secretion by promoting insulin release from the neighboring beta-cells, which in turn inhibits glucagon secretion (Müller et al., 2017; Rix et al., 2019).

Thus, several glucagon secretion stimuli have been identified and, among these, hypoglycaemia is the most (physiologically) potent one. But how do glucose levels control glucagon release? Circulating glucose reaches the pancreas where it is up taken by the alpha-cells and undergoes glycolysis that culminates with ATP production in the mitochondria. The ATP levels will then influence ATP-sensitive potassium channels, thus affecting potassium flux. The efflux of potassium influences the cell membrane polarization and, consequently, the influx of calcium through voltage-dependent calcium channels. This alters the levels of intracellular calcium, which are the principal trigger for glucagon release from alpha cells. Thus, the levels of ATP, potassium and calcium in alpha-cells reflect the levels of circulating blood glucose thus controlling glucagon release (Müller et al., 2017).

1.2.7.3. Glucagon roles

Glucagon binds to its receptor, GCGR, a G-protein-coupled receptor, that is expressed mainly in the liver, but also in the pancreas, kidneys, heart, brain, adipose tissue, and gastrointestinal tract (Svoboda et al., 1994). Thus, glucagon has roles in several organs and impacts a variety of intracellular processes (Rix et al., 2019).

1.2.7.3.1. Glucagon in the liver

- Glucose metabolism: Glucagon is involved in a wide range of functions in several organs, however, one of its most well-known roles is to stimulate glucose production in the liver. In fact, historically, glucagon has been seen as the counterregulatory hormone to insulin. To do so, glucagon first promotes glycogenolysis and, when glycogen stores are depleted, glucagon-stimulated gluconeogenesis kicks in. Simultaneously, glucagon also inhibits glycogenesis and glycolysis (Ramnanan et al., 2011). All of this leads to an increase in glucose synthesis and release, as previously explained (see section 1.1.2.2.).

- Lipid metabolism: In addition to glucose, under low energy availability, glucagon is also involved in keeping energy homeostasis through the metabolism of other fuels, like lipids. Indeed, glucagon stimulates lipolysis and fatty acid b-oxidation (to ultimately generate ATP and ketone bodies), whilst also inhibiting the energy costing process of *de novo* lipogenesis (both processes have been explored in section 1.1.2.) (Galsgaard et al., 2019).

- Amino acids metabolism: Glucagon is also involved in the metabolism of amino acids, one of the substrates used for gluconeogenesis. As previously explained in section 1.1.2, amino acid catabolism produces toxic waste, ammonia, that needs to be converted into urea to be safely excreted by the body in urine. Glucagon stimulates this conversion process, whilst also promoting amino acid catabolism. Glucagon is also involved in sensing the levels of plasma amino acids, since impaired glucagon action results in hyper aminoacidemia that leads to hyperglucagonemia. Furthermore, amino acids have been shown to promote glucagon secretion, as well as alpha-cell proliferation. Thus, glucagon is considered an important part of an endocrine feedback loop termed the liver-alpha cell axis (Galsgaard, 2020; Hayashi & Seino, 2018).

1.2.7.3.2. Glucagon in other organs

In addition to the previously mentioned roles in the liver, glucagon has also been shown to perform functions in other organs. For example, evidence shows that glucagon might also play a role in the brain. Specifically, glucagon reduces food intake and appetite, whilst also increasing satiety. The mechanisms through which glucagon exerts such functions are not fully understood yet, but could stem from glucagon action in the liver or via central nervous system. In the pancreas, glucagon has been shown to regulate the proliferation and differentiation of insulin-producing beta cells, thus being key in maintaining alpha/beta cells islet ratio. In the adipose tissue, studies where glucagon infusions were performed led to an increase in patients' resting energy expenditure. Exactly how this happens is still an area of active research, but research suggest that it might be via fibroblast growth factor 21 (FGF21). Evidence of a role for glucagon in heart rate and contractility is still a matter of debate. This is because, although administration of pharmacologic concentrations has shown an impact on both heart rate and contractility, physiological concentrations did not. Thus, additional experiments are needed to address this (Rix et al., 2019; Zeigerer et al., 2021).

1.2.7.4. Glucagon pathophysiology

Given its involvement in controlling a plethora of intracellular processes across different organs, it comes to no surprise that glucagon dysregulation might also be involved in the pathophysiology of several diseases. For example, altered glucagon homeostasis is often found in NAFLD patients, as well as in well-known NAFLD risk factors, like T2DM and obesity.

- Glucagon in diabetes: Glucagon homeostasis has been found to be dysregulated in diabetes. In fact, patients with T2DM often present hyperglucagonemia during fasting conditions, as well as impaired reduction in glucagon secretion in response to a meal. Given that glucagon promotes hepatic glucose production, this can contribute to hyperglycaemia in T2DM patients. This is not surprising given that glucagon secretion is inhibited by insulin, and insulin resistance, including at the alpha-cell level, is a common finding in T2DM. Reduced insulin secretion (in response to a meal) can also justify the impaired meal-induced regulation of glucagon levels (Hædersdal et al., 2018). Additionally, evidence also supports that increased glucagon levels in T2DM patients might be due to extra pancreatic glucagon secretion, given that experiments performed in totally pancreatectomized subjects showed that glucagon can be secreted from tissues other than pancreas (Lund et al., 2016). Furthermore, altered glucagon homeostasis in T2DM might also be due to incretin dysfunction. Incretins are hormones released from the gut in response to a meal, like GLP-1, that will further stimulate insulin secretion, whilst inhibiting glucagon secretion. Thus, if incretin release is also dysregulated, or target tissues are somewhat desensitized/resistant, this might also contribute to altered glucagon homeostasis. Hence, all the previously mentioned factors might contribute for the pathologic effect of glucagon dysregulation in diabetes (Hædersdal et al., 2018; Rix et al., 2019).

- Glucagon in obesity: Glucagon dysregulation has also been reported in patients with obesity. More specifically, patients with obesity often present hyperglucagonemia, even when normoglycemic. Additionally, in sharp contrast to lean patients, fasting in obese patients fails to increase glucagon release. In fact, glucagon secretion in these patients is downregulated from basal levels in response to fasting (Morita et al., 2021; Stern et al., 2019).

- Glucagon in NAFLD: Disturbed glucagon homeostasis has also been reported in NAFLD. More specifically, both altered glucagon secretion and glucagon resistance have been associated with fatty liver.

NAFLD patients often present altered glucagon secretion, more specifically hyperglucagonemia, and fail to efficiently downregulate glucagon secretion in response to a meal (Galsgaard, 2020; Pedersen et al., 2020), but what causes this? Glucagon secretion is controlled by several factors such as insulin sensitivity, plasma insulin levels, plasma amino acid levels and incretins (see section 1.2.7.2. for more detail). Even though the exact underlying factors that lead to increased glucagon secretion in the context of NAFLD remain an area of active research, these patients also often exhibit other metabolic abnormalities such as hyperinsulinemia, hyperaminoacidemia, insulin resistance and dysfunctional incretin system. Thus, all the previously mentioned factors could potentially contribute to the observed elevation in glucagon secretion. The relationship between NAFLD and hyperglucagonemia is complex and not fully comprehended (Galsgaard, 2020; Wewer Albrechtsen et al., 2019). Consequently, it is still unclear whether the observed hyperglucagonemia in NAFLD patients is merely a consequence of or if it directly contributes to the development/worsening of hepatic steatosis. As mentioned in section 1.2.7.3.2., glucagon receptor is mainly expressed in the liver, but also to a less extent in adipose tissue, although this is a controverse topic (Pedersen et al., 2020; Vasileva et al., 2022b). Nevertheless, a supporting theory for the notion that hyperglucagonemia might contribute to hepatic steatosis proposes that increased glucagon levels could act on adipose tissue to stimulate lipolysis. This process releases fatty acids into the bloodstream, subsequently elevating the levels of fatty acids reaching the liver and potentially increasing hepatic fat content (HAGEN, 1961; Vasileva et al., 2022a). However, this remains controverse, as several animal and human *in vivo* studies have reported that both physiologic and elevated (e.g., through infusions) glucagon levels do not effectively stimulate lipolysis in adipose tissue (Gravholt et al., 2001; Hayashi, 2021; Perry et al., 2020; Vasileva et al., 2022a). Moreover, research involving chronic administration of glucagon analogues demonstrated an improvement in hepatic steatosis (further explored below in section 1.2.7.5.) (Hope et al., 2022; T. Kim, Nason, et al., 2018). Thus, it is plausible that hyperglucagonemia is a consequence of NAFLD rather than directly contributing to its development.

Glucagon resistance is another type of glucagon signalling dysregulation also commonly found in NAFLD patients. Notably, it is also proposed as a potential factor contributing to the previously mentioned hyperglucagonemia. The causes of glucagon resistance are still under investigation, but excessive hepatic fat accumulation has been advanced as a potential

justification (Wewer Albrechtsen et al., 2019). More specifically, hepatic steatosis has been associated with a decrease in hepatic GCGR expression, which might justify the reduced glucagon sensitivity observed in NAFLD patients (Charbonneau et al., 2007; Eriksen et al., 2019; Wewer Albrechtsen et al., 2019). As highlighted in section 1.2.7.3.1., glucagon plays a direct role in lipid metabolism, a key player in NAFLD, by promoting hepatic lipolysis and fatty acids b-oxidation, whilst inhibiting DNL. Thus, in patients with hepatic glucagon resistance, glucagon might fail to increase lipolysis and fatty acid b-oxidation and decrease *de novo* lipogenesis in the liver, all contributing to hepatic steatosis (Galsgaard, 2020).

1.2.7.5. Potential of modulating glucagon signalling in NAFLD treatment

The use of glucagon has been approved by FDA for the specific treatment of severe hypoglycaemia, however, glucagon is also often used for other purposes off-label, such as, in beta-blocker and calcium channel blocker overdose, gastrointestinal motility disorders, and as a diagnostic aid (e.g., colonoscopy) (Morris & Baker, 2023). However, given the short life, low solubility at a physiologic pH and the instability of working with native glucagon, synthetic glucagon analogues (i.e., synthetic molecules that resemble native glucagon), as well as glucagon receptor agonists and antagonists (molecules that activate or inhibit GCGR, respectively), have been developed. The development of such molecules has contributed for a surge in the investigation of glucagon signalling modulation in the treatment of other diseases, such as diabetes and NAFLD.

Given glucagon's role in raising blood glucose levels, glucagon antagonists were, at some point, considered as a promising tool to fight hyperglycaemia in T2DM patients. In fact, studies using glucagon antagonists have shown positive effects in normalizing glycemia, and that this happens through direct and indirect means. Direct because glucagon antagonists bind to hepatic GCGR leading to reduced glucose secretion (reduced gluconeogenesis and glycogenolysis). Indirect because glucagon binding to GCGR also promotes amino acid catabolism, so, glucagon antagonists lead to reduced amino acid catabolism which leads to increased levels of circulating amino acids (hyperaminoacidemia). This hyperaminoacidemia then stimulates pro-glucagon (precursor of both glucagon and GLP-1 peptides) production by the alpha-cells, leading to increased levels of endogenous glucagon as well as GLP-1. GLP-1 then binds to its receptors on the beta-cells promoting insulin secretion, that directly lowers hepatic glucose

output, whilst also promoting increased glucose uptake by peripheral organs, leading to a reduction in blood glucose, thus improving glycemia. Furthermore, insulin will also inhibit native glucagon secretion, which further contributes to reducing blood glucose levels (Capozzi et al., 2022). However, and perhaps not surprisingly due to glucagon's role in lipid metabolism, T2DM patients treated with glucagon antagonists often started to exhibit altered lipid metabolism, including increased levels of LDL, liver enzymes and, importantly, significant hepatic fat accumulation (Lotfy et al., 2014).

The fact that glucagon receptor antagonism resulted in the dysregulation of (hepatic) lipid metabolism, led some researchers to hypothesise that GCGR agonism could be a potential approach to treat fatty liver, in the context of NAFLD. Besides, GCGR agonism has also been shown to promote autophagy in the liver which, is an important player in NAFLD pathophysiology (Khambu et al., 2018). This is because autophagy mediates, among other things, the removal of compromised/damaged organelles, such as mitochondria (mitophagy), a known contributor for oxidative stress. Thus, GCGR agonism might increase mitophagy in the hepatocytes, promoting mitochondrial turnover and leading to improvement of oxidative stress, a known driver of NAFLD. Additionally, autophagy also plays a role in the usage of fatty acids, termed lipophagy. Lipophagy is necessary to degrade TAGs into free fatty acids, so that these become available for b-oxidation (Galsgaard, 2020). Given all the previously mentioned findings, together with the fact that glucagon resistance is often found in NALFD patients, and that glucagon might hold potential in decreasing food intake, whilst also increasing energy expenditure, lipolysis and fatty acid b-oxidation, researchers started to explore the effects of glucagon analogues and GCGR agonists to treat NAFLD patients.

Of course, given that NAFLD patients often also present hyperglycaemia or T2DM, treating them with a hyperglycaemia inducing drug might sound counterintuitive. In fact, early studies using high levels of glucagon analogues have shown a negative impact on glycemia. Thus, therapies using glucagon agonists to target fatty liver simultaneously with glucose lowering drugs (or dual-agonists) (such as GLP-1, for example) were and are currently still being investigated (Patel et al., 2018; ROBERTSON et al., 2020).

Nevertheless, and despite initial studies indicating that glucagon agonism led to hyperglycaemia, recent studies, with lower doses of glucagon agonists, have reported actual improvement of blood glucose levels. For example, a study using the glucagon analogue IUB288 showed, in an acute setting, that, whilst hyperglycaemia is indeed induced immediately after IUB288 administration, this is followed by improved glucose tolerance in treated lean

animals due to better insulin sensitivity and glucose-stimulated insulin secretion (T. Kim, Holleman, et al., 2018). This seems to be mediated via AKT activation, a component of the insulin signalling pathway, which leads to, among other things, expression of glucose transporter 4 (Huang et al., 2018; T. Kim, Nason, et al., 2018). In fact, another paper showed that glucagon infusion initially increases hepatic glucose production through increasing glycogenolysis, however this is only transient. This is because hepatic glucose output goes back to baseline levels after about 2h, even though glucagon continues to be infused, and it is not due to shortage of glycogen stores. So, even though glucagon agonism can lead to an increase in blood glucose levels, this might be only transient (Magnusson et al., 1995). Thus, GCGR agonism might be a promising tool to treat NAFLD at the end. In fact, another study using the previously mentioned glucagon agonist IUB288, showed that treated DIO animals had markedly less hepatic steatosis than vehicle controls (T. Kim, Nason, et al., 2018).

Nevertheless, additional research with other analogues/agonists is needed to address the potential of chronic modulation of glucagon signalling in the treatment of NAFLD and its impact on glycemia. In fact, our group has recently published a study showing that chronic treatment using a novel long-acting glucagon analogue, G108, improved hepatic steatosis, as well as glycemia, in DIO mice. Nonetheless, optimization is needed to mitigate observed side-effects (Hope et al., 2022).

1.3. *In vitro* and *in vivo* models to study NAFLD

NAFLD is a multifactorial disease that englobes several disease stages, and so there are several models available to studying it, from *in vitro* culture systems to *in vivo* animal models, which will be explored next (Fig. 1.6).

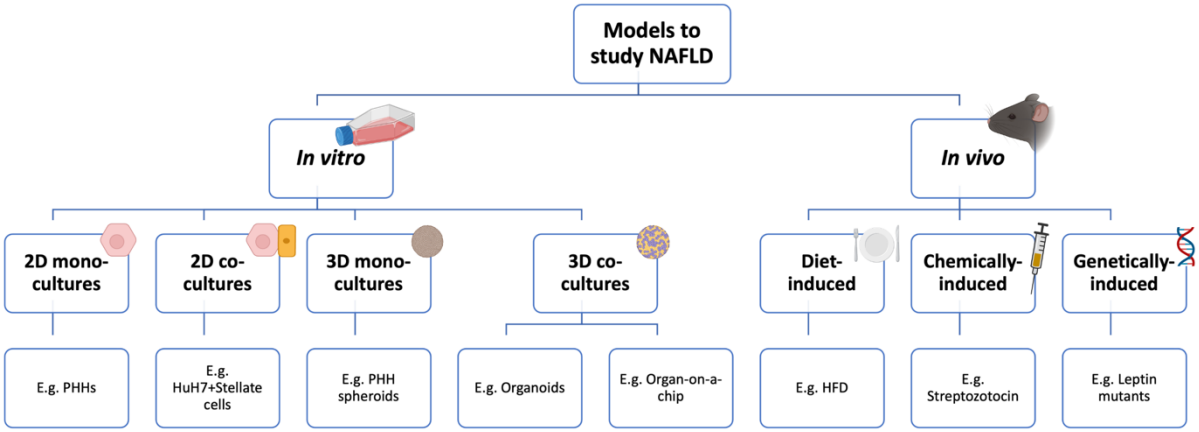


Figure 1.6. Schematic representing some of the currently available *in vivo* and *in vitro* models to study NAFLD. PHH: primary hepatocytes; HFD: high fat diet. *Created on BioRender.*

1.3.1. *In vitro* models

The *in vitro* models to study NAFLD can vary from 2D monocultures to more complex 3D co-cultures (Ramos et al., 2022a).

1.3.1.1. 2D monocultures

2D monocultures are one of the most used *in vitro* models and have provided novel insights into diverse questions. These consist in the culturing of one cell type under two dimensional conditions. Within the 2D monoculture systems, the most widely used model consists in exposing primary human hepatocytes (PHHs) (i.e., isolated from liver tissue) to free fatty acids to induce steatosis. This is because hepatocytes isolated from liver exhibit good and mature hepatic function that resembles true liver functionality. However, these cells only last for a few days in culture, meaning that repeated isolation and a significant amount of liver tissue (which can be hard to get) is needed. In alternative to PHH, hepatocyte like cells (HLCs) differentiated from different stem cells, like, mesenchymal (MSCs), embryonic (ESCs) or induced pluripotent stem cells (iPSCs), seem to be a promising approach, since they can be expanded prior to differentiation and are less invasive to obtain (for iPSCs). However, current differentiation protocols often lead to immature/incomplete differentiation which leads to immature hepatocyte functions. Human hepatoma cells lines (like HepG2) have also been widely used to model NAFLD allowing the observation of phenotypes like inflammation and oxidative stress. However, given that these cells are derived from hepatic cancers, abnormal

genetic alterations might lead to aberrant behaviour which might impact research aims (Ramos et al., 2022a; Soret et al., 2020).

1.3.1.2. 2D co-cultures

The 2D co-culture cell models are more complex than the previously described monocultures, as they consist in the simultaneous culture of more than one cell type, thus resembling more the organ *in vivo*. One example of such model is the co-culture of HuH7 cells (human hepatoma cell line) and hepatic stellate cells (HSCs). Upon exposing co-cultured cells to free fatty acids, both HuH7 cell fat accumulation and stellate cells activation (which is associated with fibrosis severity and NAFLD progression) were observed. However, one of the main drawbacks with this approach consists in finding a culture medium suitable to accommodate both cell types for long term culture. Additionally, the utilization of 2D culture conditions renders them an overly simplistic approach for accurately modelling liver behaviour (Soret et al., 2020).

1.3.1.3. 3D monocultures

3D monoculture cell models are considered to mimic *in vivo* conditions better than 2D models and are, therefore, considered more physiologically relevant. One example are PHH spheroids which are basically defined as clusters of cells that aggregate when grown in suspension. Upon treatment with fatty acids these spheroids exhibit steatosis together with upregulation of several lipogenic genes that are also commonly found overexpressed in NAFLD patients. Even though 3D monoculture models modulate liver function better than 2D ones, these still consist of only one cell type (Soret et al., 2020).

1.3.1.4. 3D co-cultures

3D coculture cell models are one of the most complex *in vitro* models currently available to study NAFLD. One of the most successful models of this kind that convincingly mimics some of NAFLD most complex phenotypes are liver organoids. Briefly, organoids are 3D culture systems that mimic the innate physiology of the organ *in vivo*, and can be derived from several organs including liver. Organoids are usually derived from culturing adult stem cells on a matrix and, although they are not obtained by co-culturing different cell types, they often

develop to a 3D cell structure that can contain more than one cell type. These 3D cultures, when exposed to different treatments that induce NAFLD, allow the successful observation of steatosis, inflammation and even fibrosis (Chi & Kim, 2022; Hendriks et al., 2023). In addition to organoids, another type of 3D co-culture models that looks promising are known as liver buds, where parenchymal (i.e. hepatocytes) and non-parenchymal (i.e. endothelial cells, mesenchymal stem cells) cells are combined to give rise to a 3D mini organ (Takebe et al., 2013a). These liver buds, first developed by Takebe and colleagues, have been shown to recapitulate many liver functions and to recapitulate NAFLD characteristics upon exposure to fatty acids, such as fat accumulation and even liver fibrosis when challenged.

Lastly, another promising model to study NAFLD are the organ-on-a-chip devices. These usually consist in microfluidic devices conceived to incorporate microchannels, chambers as well as porous membranes, that enable the growth and interaction of several cell types that are normally present in an organ, in 2D or 3D conditions. Thus, they aim to replicate *in vivo* structural organization, cell composition, microenvironment, and physiological processes, and, in fact, have shown promising results in modelling NAFLD (Kanabekova et al., 2022; Ramos et al., 2022a; Soret et al., 2020). Despite some of these can be used to study the disease or even to test potential treatments, some argue that, again, the lack of an *in vivo* context is a major disadvantage.

1.3.2. *In vivo* models

In vivo models are also widely used when investigating NAFLD. These usually consist in using rodents where NAFLD is induced through stimulating some of its known risk factors, such as obesity and diabetes, as well pathology drivers, like cellular damage. This can be achieved either through exposure to certain diets, chemicals, or genetic alterations.

1.3.2.1. Diet induced models

There are many dietary models and, depending on their composition, different NAFLD phenotypes or even different stages/severities can be induced. Examples of some of the most widely used NAFLD-inducing diets are the methionine and choline deficient (MCD), and the high fat diet (HFD), for example (Flessa et al., 2022).

- Methionine and choline deficient (MCD) diet: The MCD diet consists in a diet deficient in two essential nutrients, the amino acid methionine, and the nutrient choline. As previously explained in section 1.2.2.1.2., decreased choline levels have been shown to lead to decreased VLDL secretion and increased *de novo* lipogenesis, both of which lead to hepatic fat steatosis. Furthermore, low choline levels also lead to compromised cell membrane integrity, which can make cells more permeable to pro-inflammatory factors leading to inflammation and promoting disease progression. Methionine, on the other hand, is a key player in diverse cellular processes including protein and glutathione synthesis, which are important metabolites that help keep intracellular homeostasis. Thus, methionine deficiency also contributes to hepatocyte dysfunction, inflammation, and fibrosis, all of which contribute to disease progression. Overall, although more severe NAFLD phenotypes can be seen in animals fed the MCD diet, studies have shown that this model induces NAFDL inconsistently, and does not lead to complete metabolic syndrome (Caballero et al., 2010; Stephenson et al., 2018).

- High fat diet (HFD): Several high fat diets exist, where fat percentage can range between 45 to 75% of total calorie intake. Furthermore, the types of fats used – saturated, polysaturated, etc - can also differ. Given that NAFLD is ultimately caused by hepatic fat accumulation, it is easy to understand the rationale behind using chronic high fat diet to induce NAFLD in animals. In fact, among the different diet-induced models, HFD-induced are the ones that resemble the human NAFLD symptoms and pathologies the most, where risk factors such as obesity, insulin resistance and hyperlipidaemia are established, and hepatic steatosis, inflammation and, in some rarer cases (longer HFD exposure), fibrosis can be seen. Additionally, animals kept on a HFD for many months can also exhibit altered gut microbiome, which is a common finding in NAFLD patients, a known player in disease development. There are also a few variations to the original HFD where additional components, such as fructose and/or cholesterol are also added, that usually increase the speed with which NAFLD develops, as well as the severity of the observed NASH features. A potential set back of the diet induced models, and the HFD in particular, is that phenotypes can take longer to develop when compared to other methods, particularly the symptoms of more advance NAFLD (Flessa et al., 2022).

1.3.2.2. Chemically induced models

There are various chemical models of NAFLD as well, but they are usually used to induce the more advanced stage of the disease, NASH. Additionally, these are usually used in combination with the previously mentioned dietary ones, to better recapitulate NAFLD phenotypes. For example, streptozotocin injections in combination with HFD result in fat accumulation, inflammation, and NASH. In alternative, carbon tetrachloride (CCl4) injections also in combination with HFD leads to lipotoxicity, oxidative stress, ballooned hepatocytes and fibrosis.

- Carbon tetrachloride (CCl4) injections: CCl4 injections work by directly inducing liver damage, a known finding in NAFLD. This happens because, when CCl4 is metabolized by the liver, toxic free radicals are generated, which induce oxidative stress, alter cell membrane integrity, impairs hepatocyte function and triggers inflammation. In some cases, CCl4 treatment can also lead to very mild steatosis, but this is thought to be due to impaired hepatocyte lipid metabolism such as impaired mitochondrial fatty acid b-oxidation. Nevertheless, in contrast to what happens during NAFLD development, none of the previous events is caused by lipotoxicity due to excessive hepatic fat accumulation, thus, to make this model more relevant, CCl4 treated animals are often also placed on a HFD (Flessa et al., 2022).

- Streptozotocin injections: Streptozotocin is an antibiotic, and its administration specifically destroys the pancreatic insulin-producing beta cells, which results in impaired insulin homeostasis and eventually leads to diabetes development, a known risk factor in NAFLD. Hence, as previously explained (see section 1.2.5.4.), dysregulated insulin signalling contributes to hepatic fat accumulation and inflammation, thus driving NAFLD onset and progression. Combination of streptozotocin with a HFD regime further accelerates and worsens NAFLD symptoms (Flessa et al., 2022).

1.3.2.3. Genetically induced models

Genetic models are also widely used, but usually only allow for the observation of more severe phenotypes when in combination with either dietary or chemical ones. Examples of such models are mice mutant for the leptin gene, an adipokine with an anorexic effect, and mice carrying the human PNPLA3 polymorphism.

- Leptin signalling mutants: There are two types of animal models targeting leptin signalling, one where leptin receptor is defective (db/db mice), and the other where the leptin protein is defective (ob/ob mice). Leptin signalling increases satiety, thus decreasing food intake, hence, both animal models present increased food intake, obesity, insulin resistance and diabetes, all of which are known to have a detrimental effect in NAFLD onset and progression, as explored earlier in section 1.2.5. Hence, these animals can display moderate to severe liver steatosis and, if combined with an HFD supplemented with cholesterol and fructose, for example, or if combined with a chemical insult such as ethanol, in addition to the previous phenotypes, they also present hepatocyte ballooning and inflammation (Flessa et al., 2022).

- PNPLA3 polymorphism: As previously explained in section 1.2.5.7., PNPLA3 is a protein with lipase activity that is involved in TAGs hydrolysis. A loss-of-function polymorphism has been shown to predispose individuals to NAFLD, and so, transgenic animals carrying such polymorphism can also be used to model increased hepatic steatosis present in NAFLD. Additionally, if these animals are also kept under certain NAFLD-inducing diets, such as high sucrose diets, hepatic NAFLD symptoms are exacerbated (Flessa et al., 2022).

1.3.2.4. Platforms to study NAFLD *in vivo* longitudinally

A common disadvantage to all of the previously mentioned *in vivo* models is that, in order to follow the progression of the disease in the same liver, either indirect (e.g., blood tests) or low resolution (e.g., ultra-sound,) platforms have to be used. In alternative, different animals can be culled at different time points for liver excision for posterior pathologic analysis, adding a lot of inter-individual variability to the results, in addition to leading to a vast number of sacrificed animals. Table 1.1. summarizes the platforms currently available to study NAFLD longitudinally, and respective advantages and disadvantages. So, despite the existence of good models capable of inducing NAFLD phenotypes that resemble the human ones, there are no good platforms to study the onset and progression of the disease or to test drugs, that have an *in vivo* context and cellular resolution without compromising on invasiveness or adding inter-individual variability. Therefore, better platforms are needed.

Table 1.1. Some of the currently available techniques to study NAFLD longitudinally *in vivo*.

Technique	Brief description	Advantages	Disadvantages	References
Ultrasound	Ultrasound tool is used to acquire liver images for posterior analysis and fat quantification.	Non-invasive. Longitudinal power. No inter-individual variability.	Equipment not routinely available in labs. Complex image acquisition and analysis. Low resolution.	(Fernández-Domínguez et al., 2011; Khalid et al., 2021)
MRI	MRI is used to acquire liver images for posterior analysis and fat quantification.	Longitudinal. Non-invasive. Can be used in combination with probes to detect fibrosis.	Expensive equipment and not routinely available in labs.	(Ryu et al., 2015; Waghorn et al., 2021)
Intravital imaging of surgically exposed liver	The liver is surgically exposed and carefully positioned in coverslip for fluorescent microscopy imaging. Images can be obtained only for a short period of time (hours).	Good resolution.	Not truly longitudinal (terminal experiment).	(Davis et al., 2020; Moon et al., 2020)

1.4. Hypothesis and aims

The initial aim of this PhD consisted in carrying out two separate projects that, if successful, would culminate with the development of two novel *in vivo* longitudinal platforms: one to study NAFLD (main project) and the other to characterize tumour vascularization (training project), both taking advantage of the ACE - a natural window to the body. A simplified schematic representation summarizing the two projects, as well as the initial aims of this thesis, can be found in Fig. 1.7.

- Training project: Investigating a platform for the *in vivo* characterization of tumour vascularization.

To get trained in ACE transplantation and imaging techniques, key skills for the main project, a stand-alone training/secondary project was carried out that aimed to develop a platform to track and characterize tumour vascularization *in vivo*.

Tumours rely on vascularization to grow beyond a couple of mm^2, which makes targeting tumour blood supply a promising approach to fight tumour growth. However, different

tumours, and even the same tumour under different conditions, can employ distinct types of vascularization. The identification of the type of vascularization being employed by a tumour is key in choosing which anti-vascularization drug to use. Thus, the goal of developing an *in vivo* longitudinal platform to track and characterize tumour vascularization in the same animal overtime was established. To achieve this, *in vitro* grown fluorescent cancer cells would be transplanted into the anterior chamber of the eye of a host transgenic animal with fluorescent blood vessels. Subsequently, repetitive intravital imaging of transplanted animals would facilitate the tracking tumour growth, as well as the identification of the type of vascularization being employed by the tumour. If successful, this platform could then be used to test potential anti-vascularization drugs targeting specific vascularization types.

- Main project: Investigating a novel *in vivo* longitudinal platform to study NAFLD.

Despite many *in vitro* and *in vivo* models being available to study NAFLD, none allows NAFLD study in the same animal overtime with commonly available lab equipment, without compromising on resolution or invasiveness. Thus, the initial and main aim of this thesis was to develop a novel *in vivo* platform for the longitudinal monitoring of non-alcoholic fatty liver disease, by taking advantage of both pre-existing *in vitro* and *in vivo* NAFLD models. This would be achieved by transplanting an *in vitro* gown 3D liver model with fluorescently labelled lipid droplets into the ACE of a host mouse, followed by NAFLD induction through HFD feeding. Then, intravital longitudinal imaging with fluorescence microscopy of transplanted animals would allow the tracking of NAFLD onset and development, non-invasively, with good resolution and in the same individual overtime. Furthermore, if successful, this novel platform was also aimed to be employed in the optimization of glucagon agonism in NAFLD treatment. This is because it has recently been showed by our group that treating animals that have fatty liver with a GCGR agonist reduces hepatic fat content and improves glycemia, but at the expense of lean mass loss.

<u>Hypothesis:</u>

The ACE can be used to establish novel platforms to characterize tumour vascularization and study NAFLD longitudinally *in vivo.*

<u>General aims:</u>

• Aim 1: Gain expertise in *in vivo* intra-ocular injections and imaging, whilst developing a platform to characterize tumour vascularization *in vivo* (training project).

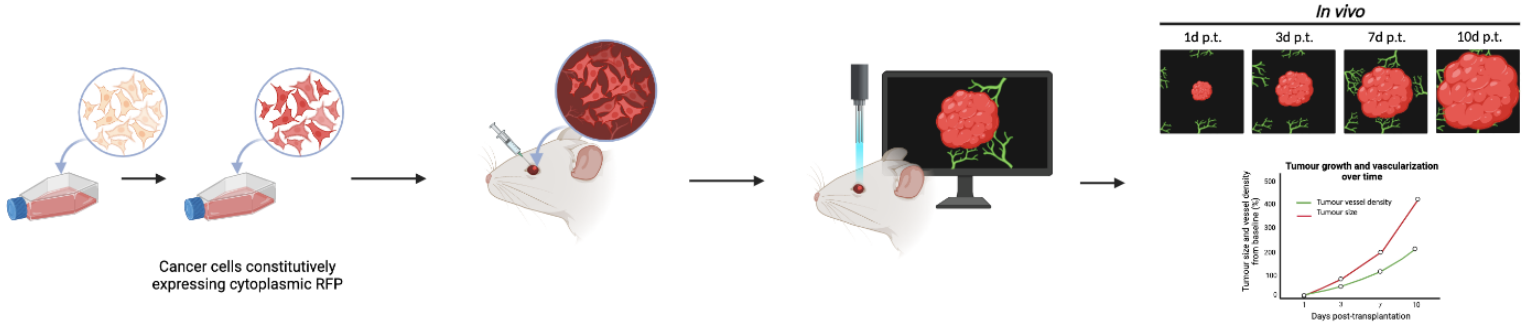
• Aim 2: Establish a novel *in vivo* longitudinal platform to study NAFLD by combining *in vitro* and *in vivo* NAFLD models.

• Aim 3: Optimize GCGR agonism in the treatment of NAFLD, ideally using the novel longitudinal NAFLD platform.

Training project

Aim 1: Gain expertise in *in vivo* intra-ocular injections and imaging whilst developing a platform to characterize tumour vascularization *in vivo*

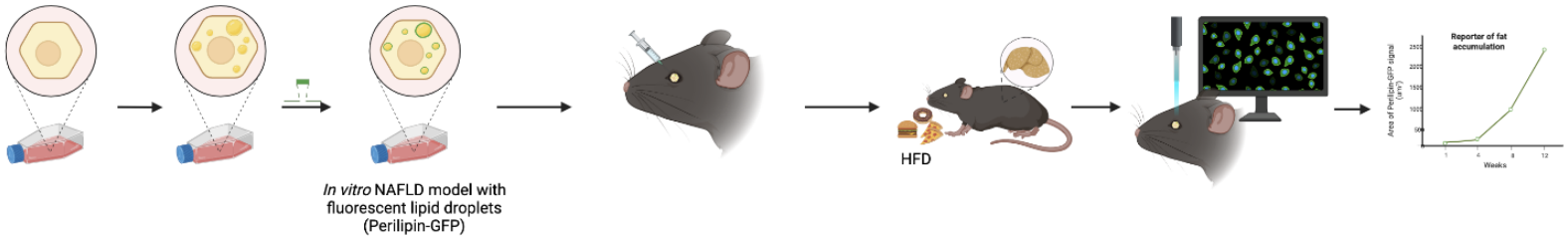
Fluorescently tag cancer cells *in vitro* → Transplant fluorescent cancer cells into the ACE of host transgenic animal that has fluorescent blood vessels → Repeated intra-vital imaging to track tumour growth and to characterize type of vascularization → Quantify tumour growth and vascularization through post-acquisition image analysis



Main project

Aim 2: Establish a novel *in vivo* longitudinal platform to study NAFLD by combining *in vitro* and *in vivo* NAFLD models

Establish NAFLD *in vitro* model → Fluorescently tag lipid droplets → Transplant *in vitro* generated NAFLD model into host animal ACE that vascularizes and engrafts for long term → Induction of NAFLD in host mouse through high fat diet feeding → Repeated *in vivo* intraocular imaging over time, to track changes in fat accumulation → Quantify changes in fat accumulation through post-acquisition image analysis



Aim 3: Use the novel NAFLD platform to optimize glucagon agonism in the treatment of NAFLD

Chronically administrate lower doses of glucagon agonist, whilst trying to mitigate lean mass loss with dietary protein supplementation, in previously established NAFLD platform → Perform intra-vital imaging longitudinally to track hepatic fat accumulation, as well as EchoMRI to track lean mass

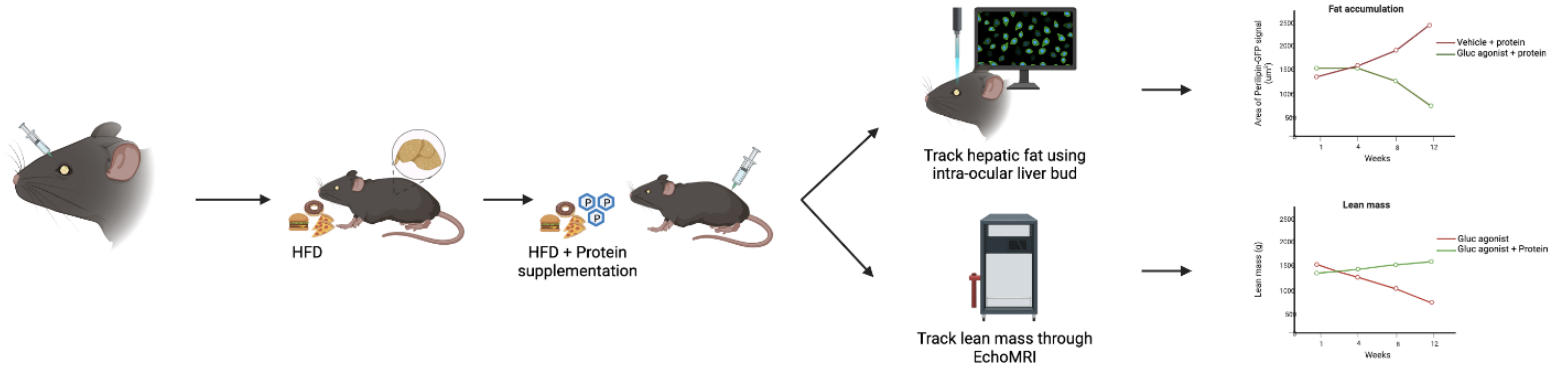


Figure 1.7. Schematic depicting the initial aims of this thesis. ACE: anterior chamber of the eye; p.t.: post-transplantation; RFP: red fluorescent protein; GFP: green fluorescent protein; HFD: high fat diet; Gluc: Glucagon. *Created on BioRender.*

Chapter II: Investigating a platform for the *in vivo* characterization of tumour vascularization

2.1. Introduction

2.1.1. Currently available models to study tumour vascularization

There are several models available to study tumour vascularization, from *in vitro* systems with several degrees of complexity, to more physiologically relevant *in vivo* models (Rahman et al., 2020).

In vitro cultures have been widely used to elucidate different aspects of tumour vascularization biology. These cultures can be simple 2D endothelial cell monolayers to study, for example, the effects of certain growth factors, known to be produced by tumours, on cultured endothelial cells; to co-cultures, where tumour cells are cultured together with endothelial cells and the results of their interactions can be studied; to 3D co-culture models, like spheroids made from tumour and endothelial cells, or vascular organoids, which provide another layer of complexity (Brassard-Jollive et al., 2020; K. Yanagisawa et al., 2020). Despite their usefulness in addressing more basic/molecular questions, *in vitro* models lack the important physiological context of *in vivo* systems.

There are several *in vivo* animal models available to study tumour vascularization longitudinally, across different species, through intra-vital imaging. Zebrafish models take advantage of their transparency, which allows for *in vivo* visualization of tumour blood vessel development (Revskoy et al., 2019). In chicken, implanting tumour cells, or xenografts, in the chorioallantoic membrane, allows for the longitudinal study of tumour-triggered blood vessel development (Eckrich et al., 2020; Javed et al., 2022). Although both previous models hold many advantages, tumour biology and development in fish and birds have many differences from the ones in mammals. Such differences include different drug metabolism and differences in immune system (Chu et al., 2022; Miao et al., 2021). Because of this, mammal models are usually preferred in the research of tumour biology, as they are seen as more relevant. These models can be established, for example, in rabbits, rats and mice.

Mouse models are very popular in cancer research, and they can be used to study naturally occurring or genetically induced tumours, that have many similarities with the human ones, like the MMTV-PyMT model for breast carcinoma (Attalla et al., 2020). Mice models can also be used as recipients to cancer cell lines or human derived tumour xenografts (Xu et al., 2019). In these models, several platforms have been developed to allow for the longitudinal study of tumours, through intravital imaging, in orthotopic locations, such as the mammary gland or

abdomen through artificial 'windows' (Deng et al., 2021; Kedrin et al., 2008), and in heterotopic locations, like subcutaneous imaging in the mouse ear (Bentolila et al., 2018a) and dorsal skinfold chambers (Alexander et al., 2008). However, these procedures often involve complex and technically difficult surgeries and can cause obvious discomfort to the animals post-operatively (Alieva et al., 2014).

2.1.2. The potential of ACE as a platform to study tumour vascularization

Another platform for intra-vital imaging of tumours that is technically simpler, and that causes minimum discomfort to the animals post-operatively, is the anterior chamber of the eye (ACE). The ACE is a clear, fluid-filled space in the front of the eye that is surrounded by the cornea, iris, and lens (Fig. 2.1). The iris of the mouse eye has been used as an optically accessible transplantation site to study various aspects of cell biology. In particular, the ACE has been widely used to enlighten the effects of diabetes on pancreatic islets function, structure, and cell plasticity (Ilegems & Berggren, 2021; Leibiger & Berggren, 2017; Salem et al., 2019a). Furthermore, the ACE has also been used to test drugs that aim to improve insulin secretion, and it paved the way for the study of islet transplantation as a treatment for diabetes (Joo et al., 2018; *Pancreatic Islet Transplantation Into the Anterior Chamber of the Eye - Full Text View - ClinicalTrials.Gov*, n.d.; Speier et al., 2008). The ACE has also been widely used to study cancer biology, including the biology of cancer cells, the interactions between cancer cells and the host immune system, as well as tumour angiogenesis. Here, tumour single cells or 3D structures, like pre-oncogenic islets, are injected into the host ACE and tracked over time through repeated imaging (Balan et al., 2019; Inagaki et al., 2022).

Intravital imaging platforms can be coupled with fluorescence microscopy to allow for the distinction between healthy and tumour tissue, with cellular resolution. Here, tumour cells can be tagged to express fluorescent proteins. In addition, the recipient host mice can also be injected with fluorescent dyes, like dextran, to highlight blood vessels. In alternative, transgenic animals with endogenous fluorescent blood vessel can be used, to allow for the clear observation of tumours vascularization development, as well as for the interactions between tumour cells and tumour vasculature (Alieva et al., 2014). One such transgenic animal is the Tie2-GFP model developed by Motoike and colleagues, that expresses GFP under the control

of the promotor of the endothelial cell marker Tie2. As a result, these mice have green-fluorescent endothelial cells, and thus green-fluorescent blood vessels (Motoike et al., 2000).

A summary of different examples of *in vivo* platforms currently available for longitudinal study of tumour vascularization, using fluorescence microscopy, in rodents, can be found in table 2.1. Nevertheless, no platforms have been developed, to our knowledge, using the ACE that allow the longitudinal tracking of cell-line derived fluorescent tumours with consistent growth rates across animals, that also allow *in vivo* dye-free characterization of tumour vascularization.

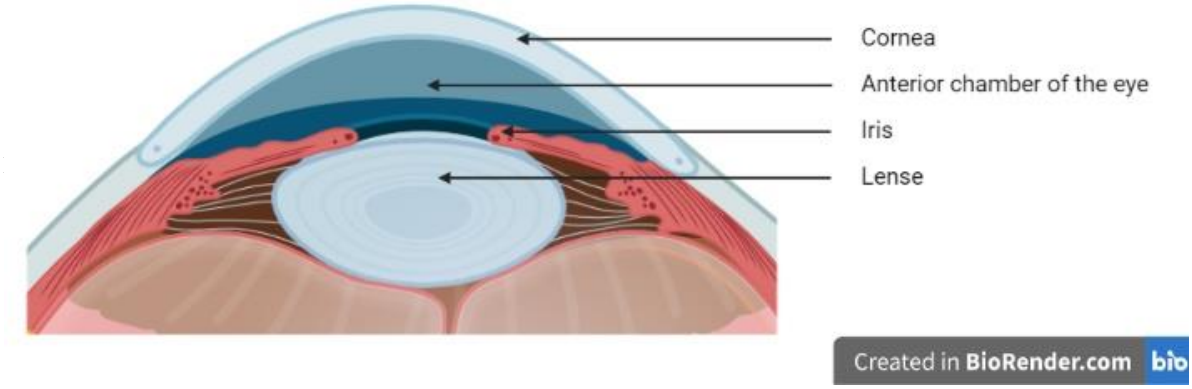


Figure 2.1. Schematic depicting structures in the eye. *Created in BioRender.*

Table 2.1. Examples of *in vivo* platforms to study tumour vascularization longitudinally through intravital fluorescent imaging.

Examples of *in vivo* platforms to study tumour vascularization longitudinally through intra-vital fluorescent imaging						
	Brief description	**Types of tumours studied**	**Reported types of tumour vascularization**	**Advantages**	**Disadvantages**	**References**
Cranial window	Creating a cranial window by either removing the bone and sealing with a coverslip, or by thinning the bone. Fluorescent cells can then be injected.	Orthotopic: brain, bone. Heterotopic: glioma, mammary carcinoma, melanoma an AML.	Angiogenesis; Vascular co-option.	Good resolution; Can be used to study orthotopic tumours.	Complex surgery; Invasive; Post-op care needed; Mostly for heterotopic tumours.	(Auf et al., 2010; Carbonell et al., 2009; D. Duarte et al., 2018; Tsukada et al., 2021)
Abdominal windows • **Mammary** • **Ovarian** • **Pancreatic** • **Liver**	In host mice with specific orthotopic tumours an incision is made in the appropriate area of the abdomen and a window frame is sutured in place resealing the incision.	Orthotopic: Liver, spleen, breast and pancreas.	Angiogenesis.	Good resolution; Can be used to study orthotopic tumours.	Complex surgery; Invasive; Post-op care needed.	(Bochner et al., 2020; Shan et al., 2003; Tanaka et al., 2012)
Lung window	An incision is made through the ribcage exposing the lungs, and a window is fixed in place.	Orthotopic: lung.	Angiogenesis.	Good resolution; Can be used to study orthotopic tumours.	Complex surgery; Highly invasive; Post-op care needed.	(Entenberg et al., 2018)
Surgical orthotopic implantation with whole-body fluorescence imaging	Fluorescent tumours are implanted on orthotopic organs of nude mice and visualized through the skin under whole body imaging.	Orthotopic: breast fat pad, prostate, and pancreas.	Angiogenesis.	Can be used to study orthotopic tumours; Allow tracking of naturally occurring tumour metastasis.	Only suitable for superficial organs; Low resolution.	(M. Yang et al., 2001)

Dorsal skin flaps	Suturing a skinfold chamber on the depilated dorsal skin of the mouse, then surgically removing the skin from the region under the aperture and implanting fluorescent tumour cells or xenografts, finally covering with coverslip.	Orthotopic: melanoma; Heterotopic: gastric adenocarcinoma.	Angiogenesis.	Good resolution; Can be used to study orthotopic tumours.	Complex surgery; Highly invasive; Post-op care needed.	(Cernaianu et al., 2006; Eichhorn et al., 2008; Koehl et al., 2009; Leunig et al., 1992)
Anterior chamber of the eye	A small incision is made through the cornea, and cells (suspension or 3D structures) are injected into the ACE.	Pro-oncogenic islets.	Angiogenesis.	Minimally invasive; No post-op care needed; Good resolution.	Mostly for heterotopic tumours; Limited to early stages of tumour development due to size limitation.	(Balan et al., 2019)
Transdermal imaging (ear)	Cells are injected into the dermis of the mouse ear skin.	Melanoma.	Co-option.	Minimally invasive; No post-op care needed; Can be used to study orthotopic tumours.	Low resolution.	(Bentolila et al., 2018b)

2.1.3. Types of tumour vascularization

Vascularization of solid tumours is key for their development, as it supplies the mass with nutrients and oxygen, whilst also removing waste products. Without a functional vasculature, solid tumours can only rely on diffusion of oxygen and nutrients and, thus, can only grow up to one or two millimetres in diameter. Importantly, vascularization is also a route for tumours to metastasize. There are currently mainly four well established tumour vascularization types: angiogenesis (intussusceptive and sprouting), vasculogenesis (or *de novo* vessel formation), vessel co-option (or vascular co-option) and vasculogenic mimicry (or vascular mimicry) (VM) (Lugano et al., 2020a), a schematic of which can be found in Fig. 2.2. These types can be present simultaneously in the same tumour, and the same tumour can exhibit different types during its growth, or even as an adaptation in response to certain drugs (Belotti et al., 2021; Kuczynski et al., 2016).

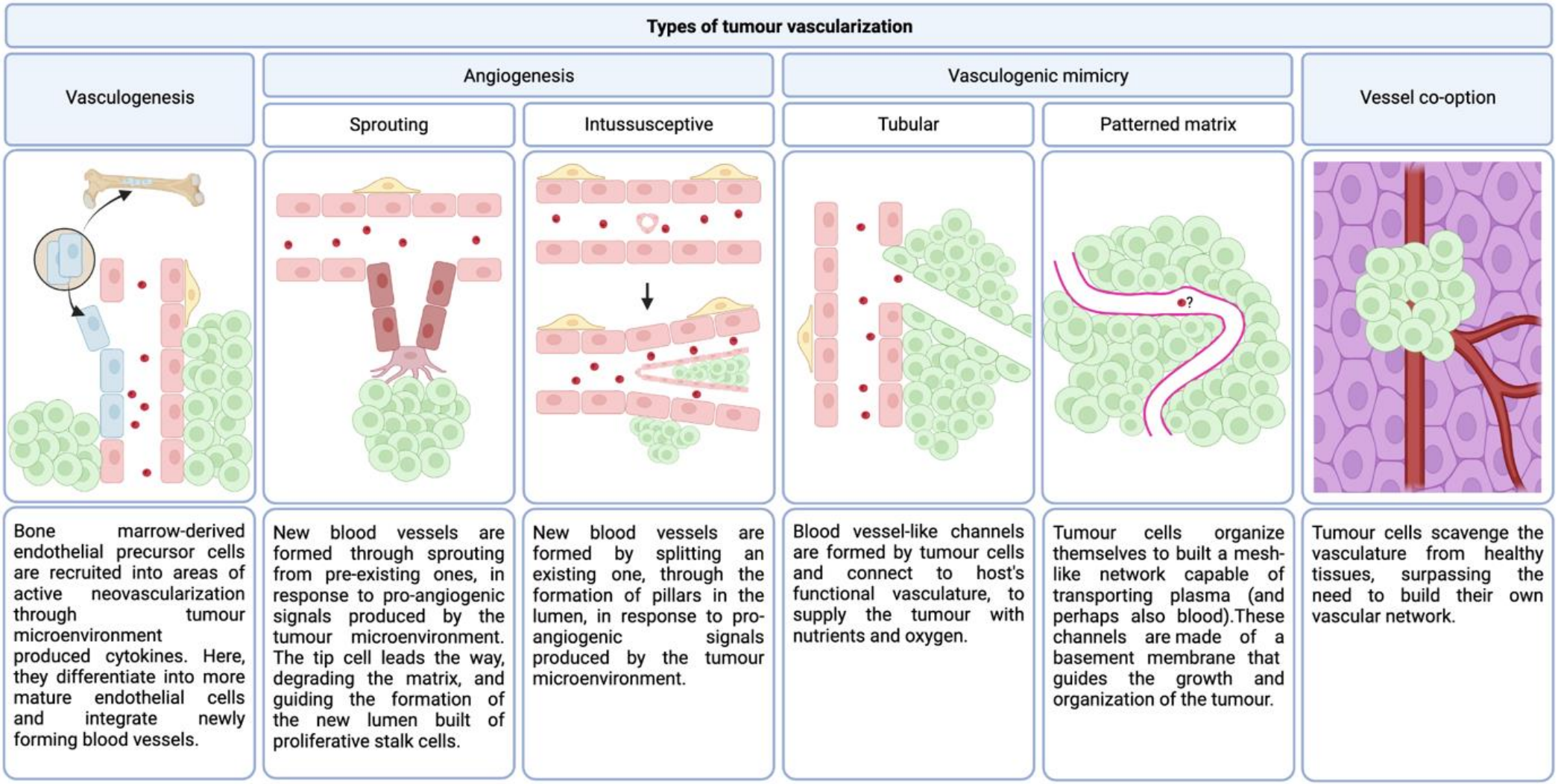

Types of tumour vascularization
Vasculogenesis
Angiogenesis
Sprouting
Intussusceptive
Vasculogenic mimicry
Tubular
Patterned matrix
Vessel co-option
Bone marrow-derived endothelial precursor cells are recruited into areas of active neovascularization through tumour microenvironment produced cytokines. Here, they differentiate into more mature endothelial cells and integrate newly forming blood vessels.
New blood vessels are formed through sprouting from pre-existing ones, in response to pro-angiogenic signals produced by the tumour microenvironment. The tip cell leads the way, degrading the matrix, and guiding the formation of the new lumen built of proliferative stalk cells.
New blood vessels are formed by splitting an existing one, through the formation of pillars in the lumen, in response to pro-angiogenic signals produced by the tumour microenvironment.
Blood vessel-like channels are formed by tumour cells and connect to host's functional vasculature, to supply the tumour with nutrients and oxygen.
Tumour cells organize themselves to built a mesh-like network capable of transporting plasma (and perhaps also blood).These channels are made of a basement membrane that guides the growth and organization of the tumour.
Tumour cells scavenge the vasculature from healthy tissues, surpassing the need to build their own vascular network.
Endothelial precursor cell
Endothelial cell
Tip cell
Tumour cell
Endothelial like-tumour cell
Red blood cell
Pericyte
Stalk cell
Basement membrane
Healthy vascularized tissue
Created in BioRender.com

Figure 2.2. Schematic illustrating and describing the different types of tumour vascularization.

2.1.3.1. Angiogenesis

Angiogenesis consists in new blood vessels forming from precursor ones and can be triggered by hypoxia (Inducible Hypoxia Factor 1alpha, HIF1alpha), genetic alterations in tumour cells that lead to increased production of pro-angiogenic factors, and by tumour-associated inflammation and recruitment of immune cells that produce pro-angiogenic factors (Lugano et al., 2020b; Petrova et al., 2018; Ribatti & Crivellato, 2009). Endothelial cells are usually quiescent (average endothelial cell lifespan is >1 year) (Montezano et al., 2017), but during angiogenesis they proliferate, migrate, and differentiate. Angiogenesis can be intussusceptive or sprouting, with the latter being the most common form.

Intussusceptive angiogenesis consists in the formation of vessels by splitting a pre-existing one into two through the formation of a pillar in the lumen. This type of angiogenesis promotes tumour growth by increasing the complexity and microvascular density within the tumour. The mechanisms that lead to it are less clear compared to sprouting, but the vascular endothelial growth factor (VEGF) is thought to be involved (du Cheyne et al., 2021; Lugano et al., 2020b).

Sprouting angiogenesis consists in a new vessel sprouting from a pre-exiting one and happens in three stages: 1) Tip cell selection: first, one endothelial cell from a pre-existing vessel starts migrating towards the chemotactic gradient of pro-angiogenic factors, while secreting proteins that degrade the matrix to ultimately guide the formation of the new blood vessel. This cell is known as the tip cell; 2) Sprout extension: next, the tip cell leading the way is followed by other endothelial cells called stalk cells, that proliferate and form the lumen and junctional connections of the nascent sprout; 3) Lumen formation: then, the lumen of the newly formed sprout connects to the original parental vessel, and later with other vessels or other sprouts in a process known as anastomosis (Lugano et al., 2020b).

In healthy tissues, angiogenesis is tightly regulated by a balance between pro and anti-angiogenic signals. In tumours, however, this balance is lost and the scale tips towards higher production of pro-angiogenic factors, an event known as the angiogenic switch, that induces sprouting. One of the pro-angiogenic factors that triggers sprouting is the vascular endothelial growth factor (VEGF). In response to VEGF, tip cells start expressing the Notch ligand DLL4, as well as the VEGF receptors 2 and 3 (VEGFR2 and VEGFR3, respectively). In the tip cells, the VEGF pathway inhibits the Notch pathway, promoting sprouting, branching, and increasing

their migratory capacity. Simultaneously, the DLL4 produced by the tip cells activates the Notch signalling in the neighbouring stalk cells, which suppresses VEGFR2 and VEGFR3 expression, whilst increasing VEGFR1 expression (decoy receptor for VEGF), preventing them from acquiring a tip cell phenotype, and increasing their proliferative capacity (Kuczynski et al., 2016).

New blood vessel formation culminates with blood vessel maturation. The Angiopoietin-Tie2 pathway is involved in regulating blood vessel stabilization through recruitment of mural cells. The angiopoietin family composed of Angiopoietins 1, 2 and 3/4 (Ang3 is the mouse orthologue of human Ang4) is also known to play a role in sprouting angiogenesis. Angiopoietins are ligands for the tyrosine kinase receptor Tie2 (also known as TEK) that is expressed in endothelial cells. The angiopoietins 1 and 2 are the most well studied of the four and have been historically seen as agonists and antagonists of Tie2, respectively (Duran et al., 2021a; Yadav et al., 2015).

The binding of Ang1 to Tie2 promotes its phosphorylation, and leads to blood vessels maturation and stabilization, through recruitment of mural cells. The Ang2 function is more complex, as its role in activating/inhibiting Tie2 is now known to be context dependent. Ang1 has more affinity to Tie2 than Ang2, and studies have shown that, in low levels, Ang2 competes with Ang1 to bind Tie2, preventing its phosphorylation, and thus working as an antagonist. In this scenario, Ang 2 prevents vessel maturation, leading to vessel destabilization, which ultimately leads to vessel regression. However, in the presence of VEGF, Ang2 is known to promote angiogenesis, since vessel destabilization is essential for new vessels to sprout from pre-existing ones. Moreover, it has also been showed that, in high levels, Ang2 can also promote Tie2 phosphorylation, thus working as an agonist (Teichert-Kuliszewska et al., 2001).

Being the most common type of vascularization seen in tumours has made angiogenesis a desirable target of new cancer drugs. Several anti-angiogenic drugs targeting different pro-angiogenic factors, like VEGF, have been developed. However, despite a favourable initial response in many types of cancer, these drugs do not always work, as the tumours often have (or develop in response to anti-angiogenic therapies) other types of vascularization (Bar & Goss, 2012; Haibe et al., 2020)

2.1.3.2. Vasculogenesis/*de novo* vessel formation

Vasculogenesis, also referred to as *de novo* vessel formation, consists in the formation of new blood vessels from scratch, and is mainly present during embryonic development, and post-natal in sites with ischemic injury. In this type of vascularization, new blood vessels are formed by the proliferation, differentiation, and association of circulating endothelial precursor cells (EPC), that are recruited from the bone marrow, into sites of active neovascularization (Johnson & Wilgus, 2014). In tumours, vasculogenesis is usually seen as a contributor to vessels being formed by angiogenesis, rather than making vessels from scratch. This type of vascularization is initiated by crosstalk between tumour cells and EPCs in the bone marrow. The process of vasculogenesis in cancer is thought to be regulated by growth factors and signalling pathways that are involved in the regulation of angiogenesis as well. One of those growth factors is VEGF, which is present in the tumour microenvironment and recruits VEGFR2+ EPCs from the bone marrow into the tumour (Nolan et al., 2007).

Evidence of vasculogenesis has been reported in several cancers like melanoma, breast cancer and also RCC (Hashemi et al., 2022; B. Yang et al., 2012; Zarychta & Ruszkowska-Ciastek, 2022). Despite several studies showing that this type of vascularization is important to the progression and spread of tumours, there are currently no FDA-approved drugs for vasculogenesis (Marçola & Rodrigues, 2015).

2.1.3.3. Vessel co-option

In tumours with vessel co-option, pre-existing blood vessels from the healthy organ vasculature are scavenged to support their growth and spread. By co-opting existing blood vessels, tumours can rapidly obtain the blood flow and oxygen they need to grow, thus surpassing the need for the lengthier angiogenesis (Kuczynski et al., 2019a).

This type of vascularization has been widely reported in lung carcinoma, breast cancer and also in metastasis from renal cell carcinoma (Bridgeman et al., 2017a; Donnem et al., 2013; Kuczynski et al., 2019b; Qian, 2013). Co-option has been associated with increased drug resistance and poor prognosis in certain cancers (Bridgeman et al., 2017b; Cuypers et al., 2022), but the specific mechanisms by which tumours co-opt blood vessels, and the best ways to target this process, remain unknown, although tumour cell adhesion and invasion pathways are thought to be involved (Kuczynski et al., 2019b).

2.1.3.4. Vasculogenic mimicry (VM)

VM was the most recently described of the four types of tumour vascularization, and the term was first coined in 1999 by Maniotis and colleagues (Maniotis et al., 1999). VM quickly became subject of many studies that established that, in this type of tumour vascularization, tumour cells line up to form their own fluid-conducting channels, capable of supplying the tumour with the essential nutrients and oxygen it needs to grow (Seftor et al., 2012). So far, VM has been reported in many types of cancer including melanoma, breast cancer, lung cancer and RCC (Andonegui-Elguera et al., 2020; Fernández-Cortés et al., 2019; Williamson et al., 2016; You et al., 2021; Z. Zhang et al., 2019), and it can be split into two subtypes: tubular and patterned-matrix (Folberg & Maniotis, 2004).

VM of the tubular type consists in tumour cell-lined channels that resemble blood vessels structurally, and that carry blood. *In vitro*, aggressive cancer cell lines, that have the capacity for tubular VM, form well defined tubes when seeded on Matrigel, very similar to the tubes formed by endothelial cells under the same conditions (Q. Luo et al., 2020).

VM of the patterned type, on the other hand, leads to the formation of channels that do not resemble blood vessels. These channels are made of a basement membrane rich in fibronectin, collagens, and laminin, that guides the growth and organization of the tumour cells into functional vessels. Also, when seeded on Matrigel, they form thick cord like tubes that can be hollow for short distances, but that are clearly distinct from the ones formed in tubular VM and by endothelial cells. There have been several studies reporting the presence of red blood cells within these channels, but also studies where red blood cells could not be observed (Q. Luo et al., 2020). Clarijs and colleagues suggested that VM channels of this type might work as a lymphatic system, where their primary function would be to carry plasma, but with the incidental accommodation of red blood cells, which would justify the conflicting evidence between studies confirming and denying the presence of such cells within patterned VM channels (Clarijs et al., 2002).

In vivo and *ex vivo* (i.e., biopsies), VM vessels of both types can be distinguished from endothelial blood vessels using a combination of histological features: 1) cell type lining the vessel: VM vessels are lined up by tumour rather than endothelial cells; 2) structure: vessels of the patterned type do not resemble true blood vessels at all, as they are usually less organized. For the vessels from the tubular type, even though they look structurally similar to true blood vessels, their walls are usually thicker and also less organized. Furthermore, while endothelial vessels are surrounded by the stabilizing pericytes, VM channels often do not have these mural

cells, or have them at a lower rate; 3) Laminin and endothelial cell markers expression: endothelial blood vessels express high levels of laminin, whereas VM channels might express it, but at lower levels; also, specific markers of endothelial cells like CD31 or von Willebrand factor are highly expressed in true blood vessels, whereas VM channels might not express them (but sometimes can, if tumour cells transdifferentiate into endothelial cells); 4) Extracellular matrix: While the extracellular matrix surrounding blood vessels may contain polysaccharides that can be detected with a periodic acid Schiff (PAS) stain, the blood vessels themselves would not take up the stain. Since VM channels of the patterned-matrix type are formed by a deposition of ECM rich in molecules like glycogen, these channels can be distinguished from true blood vessels using glycogen-staining dyes, such as PAS. Like true blood vessels, channels of the tubular type might also stain positive for PAS (Q. Luo et al., 2020).

Vasculogenic mimicry is associated with high tumour grade, invasion, metastasis and decreased survival of patients, so understanding it is key for the development of new cancer drugs. Currently, there are no approved drugs that are specifically designed to target vasculogenic mimicry in cancer. However, several existing drugs have shown potential in targeting and reducing vasculogenic mimicry in preclinical and clinical studies, including anti-angiogenic and anti-inflammatory drugs (Q. Luo et al., 2020; Serova et al., 2016).

2.1.3.5. Lymphangiogenesis

In addition to blood vessels, growth of lymphatic vessels can also happen in some tumours by a process known as lymphangiogenesis. Lymphatic vessels are a part of the lymphatic system which, in healthy tissues, plays an important role in the disposal of excess fluid from tissues as well as in the transport of immune cells (Ozdowski & Gupta, 2022). Lymphatic vessels within tumours also serve as an alternative source of oxygen and nutrients, as well as to disseminate cancer cells to distant organs. In cancer, lymphangiogenesis is often regulated by growth factors and cytokines produced by the tumour and its TME, such as vascular endothelial growth factor-C (VEGF-C) (Christiansen & Detmar, 2011). The identification of lymphangiogenesis in tumours relies on three main features: 1) expression of lymphangiogenic factors; 2) occurrence of lymphatic endothelial cells undergoing cell division, assessed through markers of proliferation, like as Ki-67 or PCNA, and 3) increased lymphatic vessel density and invasion (Ran et al., 2010a). This type of vascularization has been reported in several cancers including lung, colorectal and breast, and as well as in RCC (Debiński et al., 2013a; OZARDILI et al.,

2012; Ran et al., 2010b; Saad et al., 2006; J. G. Sun et al., 2009). The specific mechanisms by which lymphangiogenesis is regulated in tumours are still under active investigation, and there are currently no FDA-approved drugs to specifically target it. However, several drugs are currently undergoing clinical trials have shown promising results like VEGF-C, VEGF-D and Angiopoietin 2 inhibitors (C. Wang & Chu, 2021)

2.1.4. Renal cell carcinoma (RCC)

Cancer is a condition where cells in a specific part of the body grow and proliferate uncontrollably. The cancerous cells can invade and destroy surrounding healthy tissue, as well as metastasize to distant organs. Currently, it is estimated that one in two people will develop some form of cancer during their lifetime (*Cancer - NHS*, n.d.). One common cancer is renal cell carcinoma (RCC), which is the main malignant kidney neoplasm and accounts for about 4% of all adult malignancies worldwide (Alzubaidi et al. 2022). Furthermore, RCC is a particularly useful and relevant cancer to work with given that all previously described vascularization types have been observed.

Tumour growth and progression is a complex process that involves several key cellular and molecular mechanisms. It has become apparent, in recent years, that the role of the tumour microenvironment (TME) in tumour initiation and progression is just as significant as the genetic abnormalities initially believed to be the sole cause. The TME refers to the complex network of physical and biological parts that surround the cancer cells. The participants of the TME are tumour cells, growth factors/cytokines, immune cells, stromal cells, extracellular matrix (ECM) and blood vessels (Anderson & Simon, 2020).

Growth factors and cytokines are signalling molecules produced by various components of the TME and that can impact the behaviour of cancer cells and other cells in the microenvironment. The role of immune cells in the TME is complex and they can be broadly categorized into pro and anti-tumorigenic. As the name hints, pro-tumorigenic immune cells can promote tumour growth, through production of growth factors that aid the cancer cells to evade immune surveillance, whilst anti-tumorigenic immune cells play a critical role in recognizing and eliminating cancer cells. The stromal cells support the function of parenchymal cells. In cancer, they are recruited from nearby endogenous tissue stroma and can promote tumour growth by producing growth factors and cytokines. The ECM is the complex of proteins that provide physical support to the tumour cells, and influence tumour progression through the modulation of cell behaviour and signalling pathways. Lastly, blood vessels play a key role in the TME, as they support cancer growth by providing it with nutrients and oxygen, removing waste products and as a route to tumour dissemination (Anderson & Simon, 2020).

As previously described (see section 2.1.3.), there are several types of tumour vascularization. RCC is known to be highly angiogenic, and drugs that target it are one of the main therapies

used to treat this cancer. Sunitinib, a tyrosine kinase inhibitor that targets angiogenesis, is one of the most widely used drugs to treat renal cell carcinoma (RCC). However, while anti-angiogenic drugs can be effective, they do not cure RCC and are not effective in all patients. Some patients, despite an initial positive response, seem to develop resistance to the anti-angiogenic treatment. In some cases, this is because tumours develop other types of vascularization (Kuczynski & Reynolds, 2019; Montemagno & Pagès, 2020; *Resistance to Angiogenesis Inhibitors in Renal Cell Carcinoma – Hematology & Oncology*, n.d.; Serova et al., 2016). Thus, RCC could be a useful tool to study the different types of tumour vascularization and test anti-vascularization drugs.

2.2. Hypothesis and aims

The main objective of this project was to provide training in ACE transplantation and intravital imaging, skills that were going to be necessary to the main project in the next chapter of this thesis, whilst potentially also leading to the development of a novel platform to characterize tumour vascularization *in vivo*.

The anterior chamber of the eye is a well-established model for the study of angiogenesis in tumours. By pairing it with a mouse model with green fluorescent protein (GFP)-tagged endothelial cells (and thus fluorescent blood vessels), it was hypothesized that the ACE could be further used to study other types of vascularization longitudinally. To do so, a cancer cell line tagged with red fluorescent protein (RFP) was used. The chosen cell line was derived from a mouse renal cell carcinoma (RenCa), since all the four previously mentioned vascularization types have been observed in RCC. This carcinoma mimics several aspects of human renal cell carcinoma and is widely used in the field (Cui, 2017; Hirayama et al., 2016; Karashima et al., 2017; Murphy et al., 2017; Salumbides et al., 2009). Thus, by implanting fluorescent tumours in the ACE of host mice with fluorescent blood vessels, this platform would enable, not only the monitoring of tumour growth, but also the identification and characterization of the different types of vascularization happening in these tumours *in vivo*. This information could be valuable for subsequently testing suitable anti-vascularization drugs.

<u>Hypothesis</u>

The anterior chamber of the eye is a viable site to characterize tumour vascularization *in vivo* longitudinally.

Aims

1. Gain expertise in ACE injections and intravital imaging.
2. Define a strategy that leads to the consistent development of tumours in the ACE over a short period of time.
3. Quantify tumour growth over time and characterize the types of tumour vascularization *in vivo*.

2.3. Materials and methods

2.3.1. Animals

Animal procedures were conducted in accordance with the Animals (Scientific Procedures) Act 1986. Tie2-GFP mice were obtained from the Jackson Laboratory, and males with 3 to 6 months old were used in all experiments. Animals that received transplantation of cells were monitored daily for up to 10-days, and no adverse effects were recorded during any experiment.

2.3.2. Cell line

Maintenance: Renca cells were purchased from ATCC and maintained according to supplier's guidelines. Briefly, cells were grown in RPMI-1640 medium containing 10% of FBS, 0.1mM of NEAA, 1mM of Sodium pyruvate, 1x GlutaMAX and Pen/Strep at 37°C and 5% CO_2. They were split twice a week when 80% confluence was reached.
Fluorescent tagging: Renca cells were kindly tagged by Dr Alexandra Milona, where plasmids constitutively expressing RFP (Addgene) were transduced by lentiviral vectors according to standard protocols, prior to antibiotic selection of positive cells.

2.3.3. Generating spheroids *in vitro*

Two methods were used to try to make spheroids out of Renca cells (passage 15 to 35).
Hanging drop: Renca cells were suspended in maintenance medium and aliquoted into 20µl drops (500 cells per drop) on the lid of a petri-dish. The lid was then inverted and placed on the dish that contained PBS, and then incubated for 48h at 37°C and 5% CO_2 (Timmins & Nielsen, 2007). This experiment was conducted also in the presence of 2% GFR-matrigel (Corning).
Low-attachment culture: Spheroids were generated according to published protocols (Badea et al., 2019). Briefly, cells from passage 15 to 45 were trypsinized and re-suspended in maintenance medium containing or not 2% of GFR-matrigel (Corning). 500 cells were seeded per well in an ultra-low attachment plate (NuncSphera, Thermo) that was, or not, then centrifuged at 1000rpm for 5 min at 4°C. The plate was then incubated at 37°C and 5% CO_2, and cohesive 3D spheroids were formed after 48h.
Brightfield images were acquired using a Nikon camera attached to a microscope.

2.3.4. Tube formation vasculogenic mimicry assay

Renca cells were trypsinized and suspended in maintenance medium with or without cobalt chloride (200µM). Then $4x10^4$ cells were seeded per well of a 96-well TC-treated plate uncoated or coated with pre-solidified Matrigel.
Brightfield images were acquired using a Nikon camera attached to a microscope

2.3.5. Transplantation into the ACE

Cell suspension/Spheroids were injected into the anterior chamber of the eye following a previously published protocol (Salem et al., 2019). Briefly, animals were anaesthetized with isoflurane and placed in a stereotactic frame. The cell suspension or one spheroid (in 1xPBS) were aspirated into a blunt cannula inserted in a 100µl screw actuated syringe (Hamilton). Then, a small incision was made in the cornea using a 27G needle, and the cannula inserted in the anterior chamber of the eye. Lastly, 20µl of cell suspension (containing approximately $2x10^5$ cells) or one spheroid were released per eye and the cannula carefully removed.

2.3.6. *In vivo* imaging

Brightfield images were acquired using a Nikon camera attached to a microscope in mice under isoflurane anaesthesia.
Confocal (and multi-photon) fluorescent images were acquired using the Leica SP5/MP FLIM Upright Confocal microscope after ketamine and xylazine anaesthesia. In experiments where Cascade Blue dextran (Thermofisher) was used to highlight blood vessels, animals were injected with the dye via tail vein whilst under anaesthetic.

2.3.7. Post-acquisition image analysis

Post-acquisition image analysis was done using Image J. Movement correction and tumour area quantification were done using the macros kindly provided by Dr Victoria Salem. Tumour growth percentage was quantified as change in RFP area from baseline.

2.3.8. Immunohistochemistry of eye slices

Mice were euthanized and the eyes excised and fixed in 4% PFA (in PBS) overnight at 4°C. They were then transferred to 30% sucrose solution (in PBS) for 2 days, embedded in cryo embedding matrix (OCT, Thermo) and stored at -80°C until needed. The frozen eyes were sliced into 30µm slices using a cryostat and immediately transferred to a poly-D-lysin coated slide. For immunostaining, a standard protocol was then performed using the nuclear dye Dapi at (1ug/ml) and the following antibodies: anti-GFP-AlexaFluor488 conjugate (Invitrogen); CD31 (BD Pharmingen) and AlexaFluor488 (Thermo). Primary antibodies were used at 1:200 and secondary antibodies at 1:1000. *Ex vivo* confocal fluorescent images were acquired using the Zeiss LSM-780 inverted microscope and analysed using Fiji software. For PAS/CD31 double staining, eye slices were prepared as described earlier and stained for CD31 (BD Pharmingen) using Anti-Rat Ig HRP Detection Kit (Cat# 551013, BD Bioscience) prior to Periodic Acid Schiff staining using PAS stain kit (Cat# ab150680, Abcam). Bright field images were acquired using a bright field microscope.

2.4. Results

2.4.1. Renca cells form spheroids *in vitro* that engraft and grow upon transplantation into the ACE of host mice

Experiments were initiated with the injection of a Renca cell suspension containing approximately $2x10^5$ cells into the anterior chamber of the eye (ACE) of host Tie2-GFP mice, following previously published protocols (see methods section 2.3.5). This led to the development of tumours shortly after injection in all mice, that grew overtime (Fig. 2.3) and that could be successfully observed under fluorescence microscopy (Fig. 2.4). Interestingly, within some of the formed tumours, the presence of Tie2 positive single cells infiltrating the tumour could be observed (Fig. 2.5a). This observation was then confirmed *ex vivo* in histologically prepared eye slices (Fig. 2.5b and c).

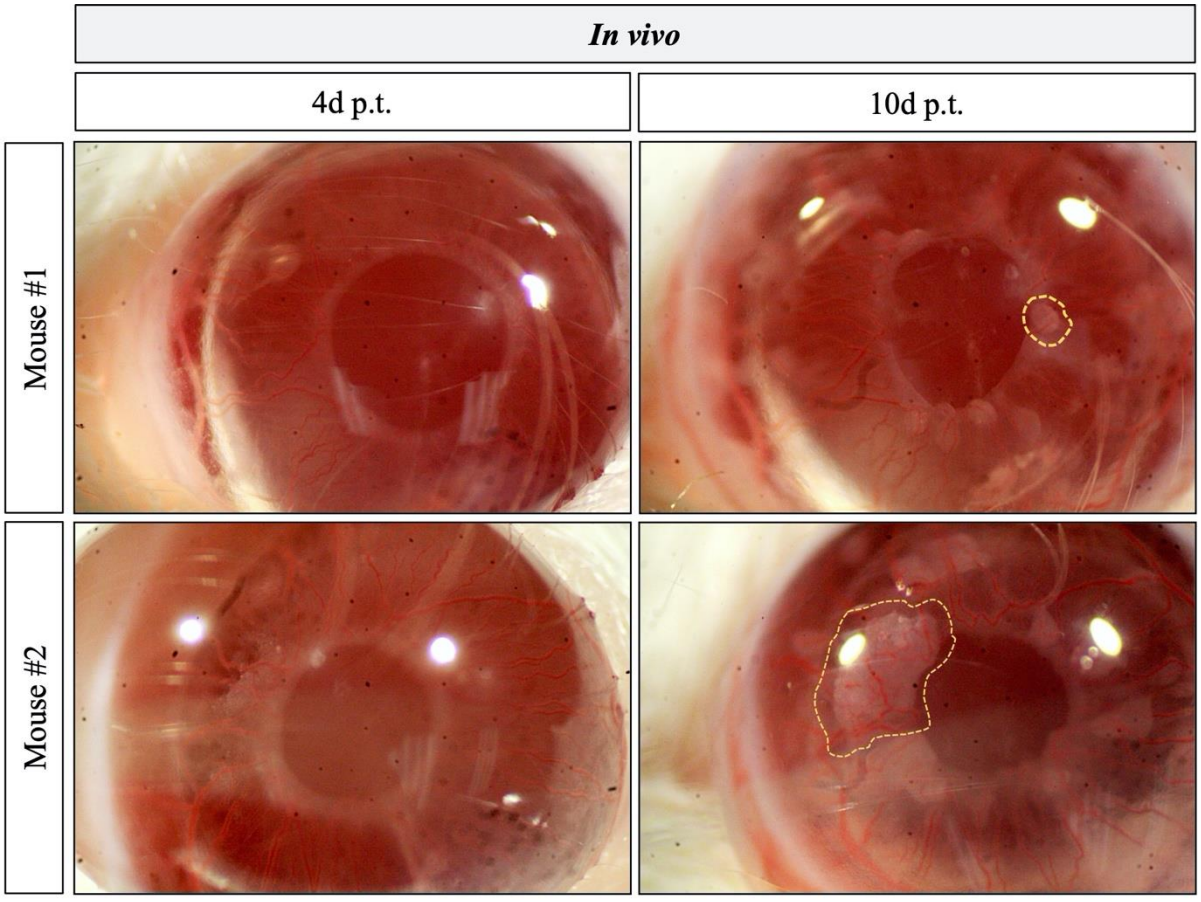


Figure 2.3. Injecting a Renca cell suspension into ACE of host mice leads to development of multiple tumours that grow over time. Bright field images from two mice injected with the same amount of cells, 4 and 10 days after transplantation. Note high variability in the size of tumours formed (dotted line). P.t.- post-transplantation; 4.5x magnification.

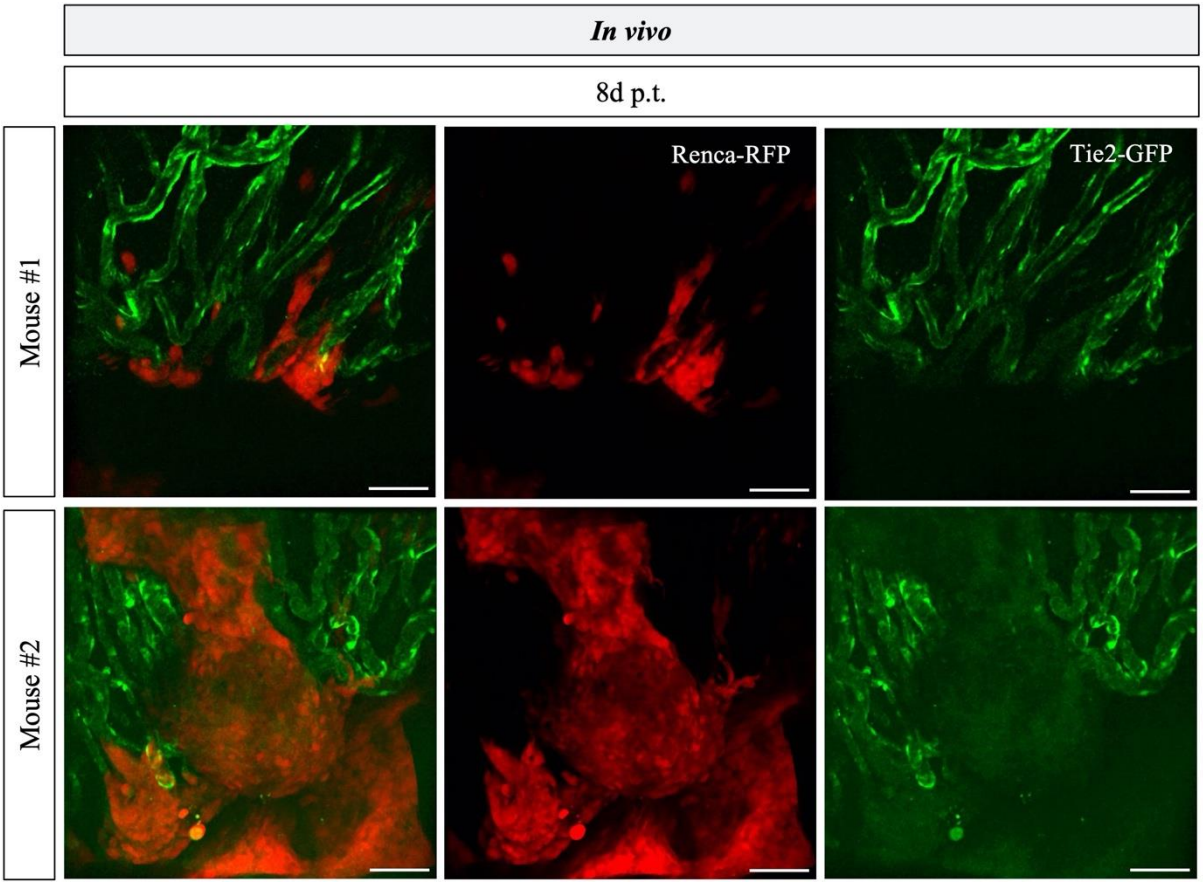


Figure 2.4. Renca tumours and host mouse blood vessels can be visualized under fluorescent microscopy. Confocal *in vivo* images of two animals 8 days post-transplantation with tumour cells in red and blood vessels in green. P.t.- post-transplantation; Scale bars are 100μm.

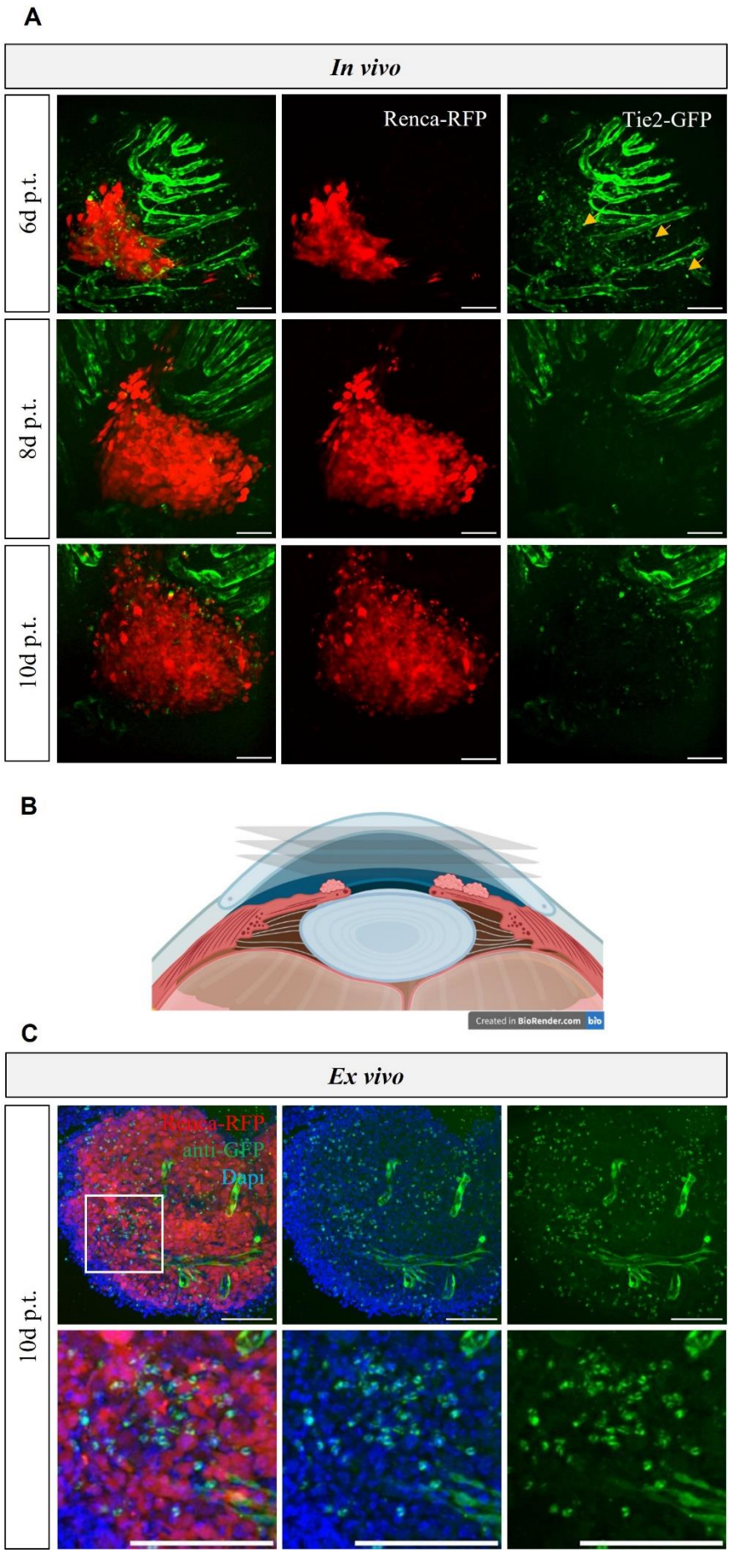

A
In vivo
Renca-RFP
Tie2-GFP
6d p.t.
8d p.t.
10d p.t.
B
Created in BioRender.com
C
Ex vivo
Renca-RFP
anti-GFP
Dapi
10d p.t.

Figure 2.5. Single Tie2-GFP cells can be observed around and within some tumours. A) Confocal *in vivo* images of the same tumour 6, 8 and 10 days post-transplantation, with tumour in red and Tie2-GFP positive cells in green. Arrows point towards potential Tie2-GFP-positive single cells B) Schematic depicting how eye slices were acquired. C) Confocal images of eye slices with nucleous stained by dapi in blue, tumour cells in red and Tie2-positive cells in green. P.t.- post-transplantation; Scale bars are 100μm.

Although the same number of cells were being injected per eye, both the number and size of the resulting tumours were found to be highly variable across injected eyes (Fig. 2.3 and 2.4). This caused two problems: on one side, it was hard to track the growth of the exact same tumour overtime, because there were several per eye and they would eventually merge; on the other side, it was hard to define a consistent experiment duration, since some mice had bigger tumours and had to, therefore, be culled earlier than others. Thus, to have better control over the number and size of tumours formed, spheroids were generated out of Renca cells *in vitro* prior to injection into the ACE.

Spheroids are defined as a cohesive 3D cell mass that resembles the tumour *in vivo* context better than 2D monolayers, particularly regarding distribution of nutrients, oxygen, CO_2, and metabolic waste. Therefore, they are preferred over 2D monocultures in studies of tumour biology as well as for *in vitro* drug screening models, since spheroids replicate the solid *in vivo* tumour better in terms of the resistance to drug penetration (Rossi & Blasi, 2022). Spheroids are formed by spontaneous aggregation of cells followed by binding of cell surface proteins to the extracellular matrix (ECM), thus resulting in a compact cell mass. There are several methods available to generate tumour spheroids out of single cells, the main ones being based on the hanging drop culture, non-adherent culture, and suspension culture (Gunti et al., 2021). The first attempt at generating spheroids out of Renca cells was carried out using the hanging drop culture method, due to its simplicity. This method consists in suspending a certain number of single cells in culture medium, plating the cell suspension into small drops on the lid of a Petri dish, and then inverting the lid, thus promoting cell aggregation by surface tension and gravitational force. However, and even though Renca cells aggregated, they failed to form a cohesive cell mass and thus spheroids (Fig. 2.6, left panel). The non-attachment culture method was then tested where cells are seeded in pre-treated plates to prevent cell attachment. This resulted in a cell aggregate that was more cohesive than the one generated with the hanging drop method. However, those aggregates were still not cohesive enough to be manipulated, since they often disintegrated when aspirated into the Hamilton syringe used for intra-ocular injections (Fig. 2.6, middle panel). Centrifugation of the cell culture plates immediately after

seeding was also tested, in an attempt to accelerate and improve cell aggregation, with the expectation that this would subsequently improve the cohesiveness of the cell mass formed. However, the resulting mass was still not stable enough (Fig. 2.6, right panel). Ivascu and colleagues showed, for the first time, that some tumour cell lines form loose aggregates when seeded under non-adherent culture conditions. However, in the presence of small amounts of basement membrane extract, such as Matrigel, those same tumour cell lines gave origin to compact spheroids (Ivascu & Kubbies, 2006). In fact, studies have been published showing that adding ECM to the culture medium of cell lines that would form spheroids even in its absence can enhance several spheroid characteristics, bringing them closer to their respective *in vivo* tumours (Badea et al., 2019). Hence, next, 2% matrigel was added to the cell suspension before it was aliquoted into the non-attachment plates. This time, following centrifugation of the plate after seeding, compact spheroids were consistently formed (Fig. 2.6, lower right panel).

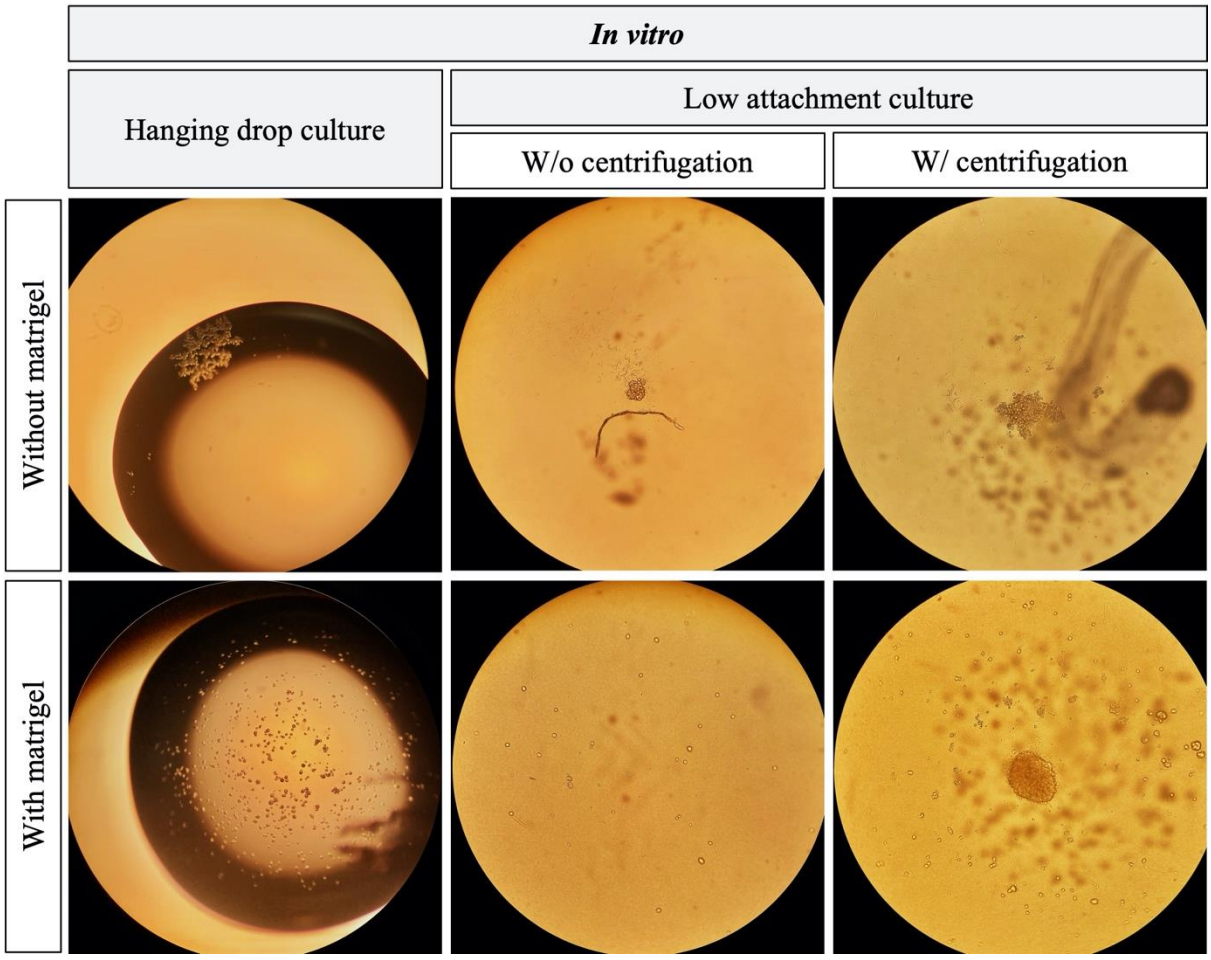
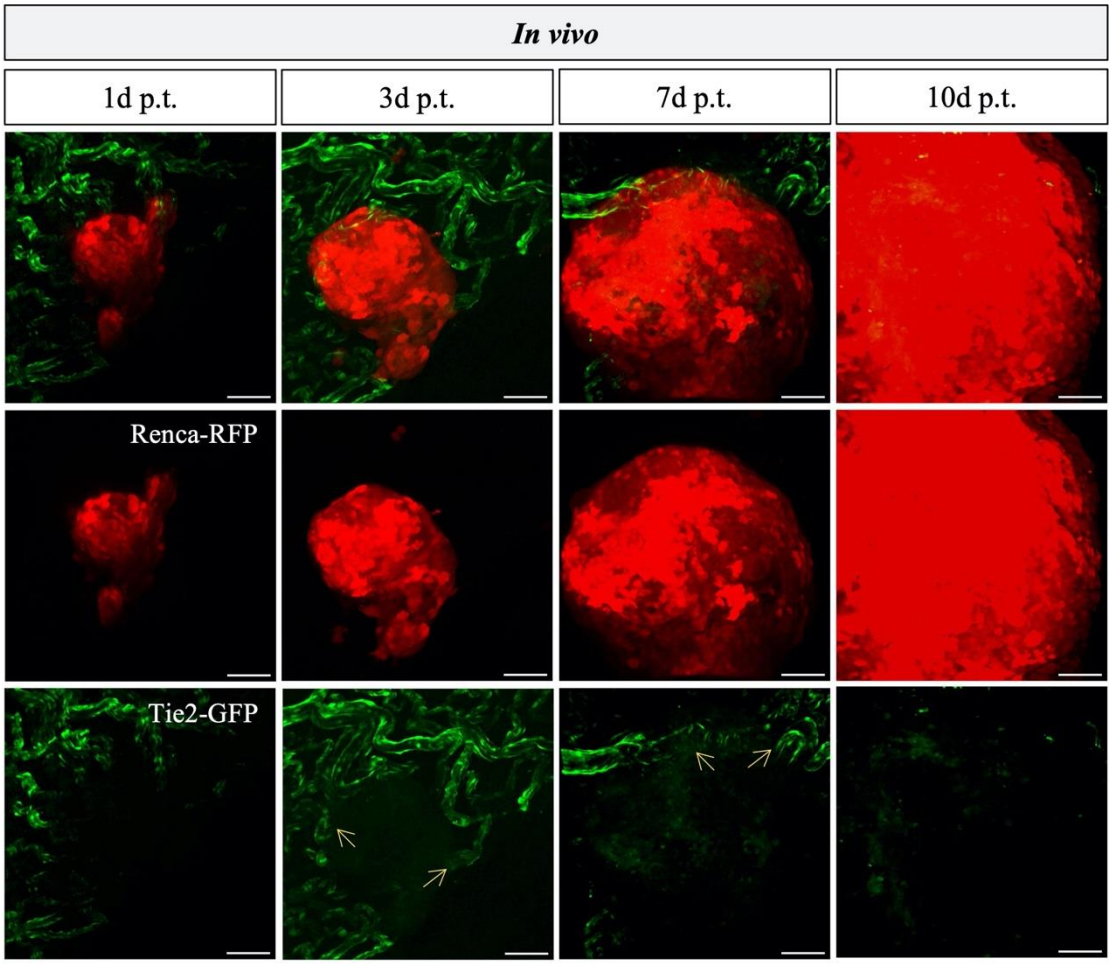


Figure 2.6. Renca cells form cohesive spheroids through low-attachment culture upon centrifugation and in the presence of Matrigel. Different strategies were used to attempt spheroid formation. Magnification is 4x on left panel and 10x on middle and right panels.

Experiments were then carried out to define the number of initial cells that needed to be seeded per well that led to the formation of spheroids with a size compatible with our experimental plan. These experiments showed that spheroids made from initially seeding 500 cells per well were small enough to fit into the Hamilton syringe canula used for the eye injection procedure. Thus, next, one spheroid was injected per eye of host mouse that, as expected, readily engrafted onto the hosts iris, and grew over time (Fig. 2.7a). Furthermore, these spheroids led to the development of tumours of adequate size that could grow for at least 2 weeks, upon ACE transplantation, without causing any visible discomfort to the host mice. This growth could be easily quantified in post-acquisition image analysis, and it revealed the high reproducibility of tumour growth rate between different tumours in different animals (Fig. 2.7b).

A



B

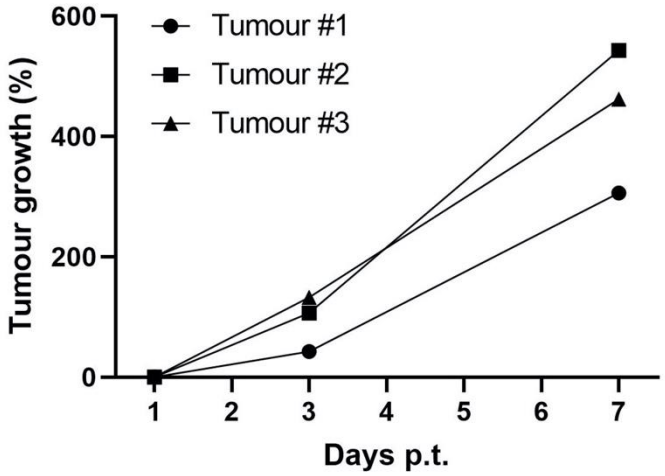


Figure 2.7. *In vitro* generated Renca spheroids engraft and grow overtime upon transplantation into ACE. A) *In vivo* confocal images of the same tumour spheroid (red) and surrounding host vessels (green) taken on days 1, 3, 7 and 10 after transplantation. Arrows point towards blood vessels that stopped being observed once within the tumour mass. Scale bars are 100μm. B) Graph showing tumour growth (as change in area percentage from baseline) over time of three independent tumour spheroids, upon transplantation into host mice ACE. p.t. – post-transplantation.

2.4.2. Intra-spheroid blood vessel fluorescence is lost due to Tie2-GFP down-regulation

Although tumour cells and blood vessels could clearly be observed through fluorescence microscopy, blood vessel fluorescence was consistently lost within, and only within, the tumour mass (Fig. 2.7a, lower panel). However, and even though blood vessel fluorescence could not be observed within the tumours, it was likely that tumours were getting vascularized because new channel-like looking structures were being formed overtime, as seen on the RFP channel (Fig. 2.8). Thus, it was possible that the lack of GFP signal from intra-tumour blood vessels was due to a laser penetration issue since signal intensity does decrease with depth. To test this hypothesis, imaging experiments were conducted using a multi-photon confocal, which is known to penetrate deeper into tissues than the previously used single-photon approach. Single and multiphoton imaging of the same tumour was performed, however, GFP-positive intra-tumour blood vessels could still not be seen (Fig. 2.9a). It was then hypothesized that blood fluorescence loss was due to Tie2 and, consequently, GFP downregulation. To assess this hypothesis host mice were injected with a fluorescent dye that highlights blood vessels. Indeed, the intra-tumour blood vessels were highlighted, whilst there was still no visible GFP signal (Fig. 2.9b). These experiments suggest that lack of GFP signal in intra-tumour blood vessels is not due to a laser penetration issue, and supports the hypothesis of Tie2-GFP downregulation.

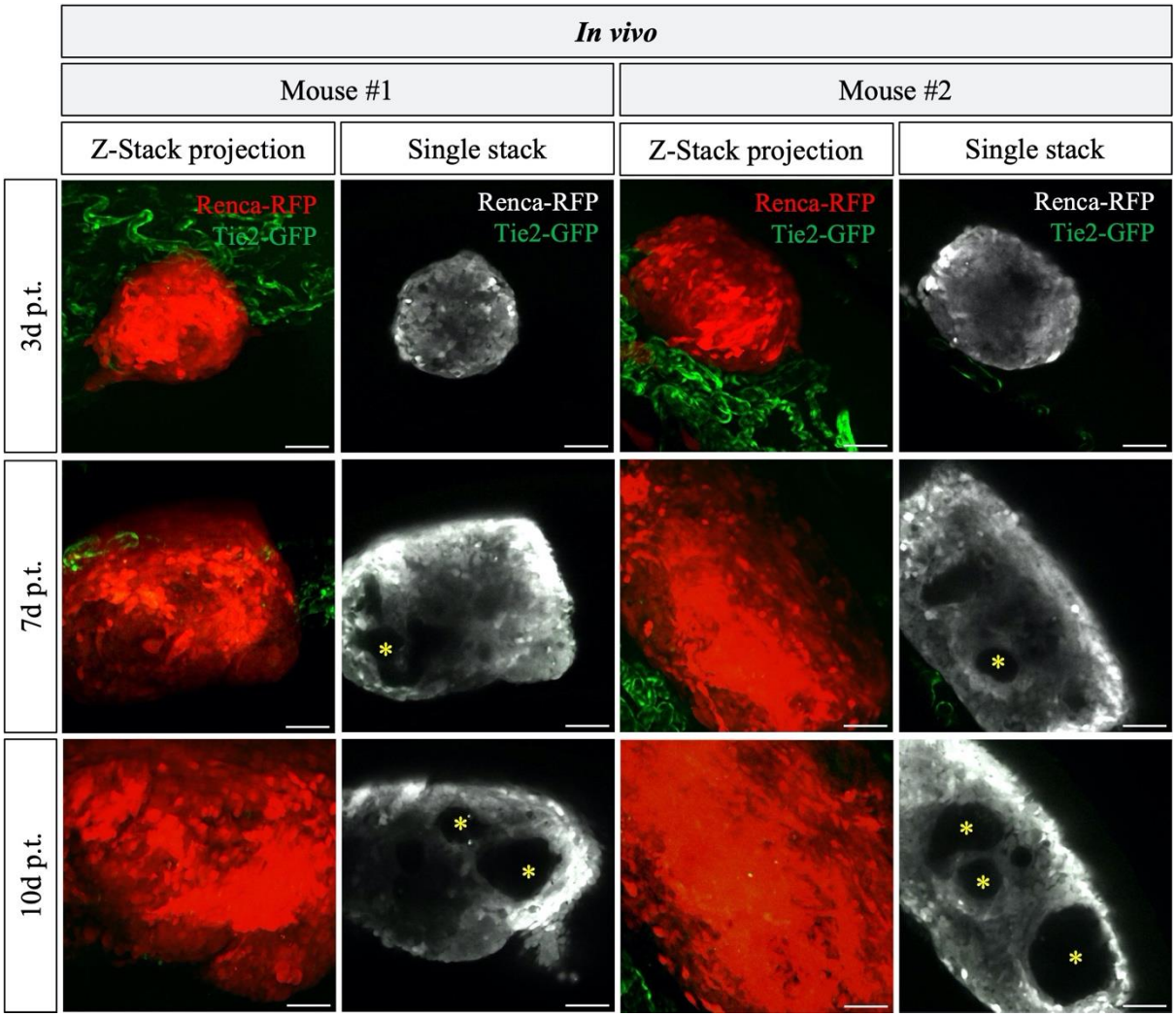


Figure 2.8. Channel-like looking structures developing in Renca spheroids overtime upon transplantation into ACE. *In vivo* confocal images of two tumour spheroids, taken on days 3, 7 and 10 post-transplantation. Coloured panels show a Z-stack projection of tumour spheroids (red) and hosts blood vessels (green); Grey panels show a single stack of tumour spheroids (grey) and host blood vessels (green). * Denotes new channels developing overtime. p.t. – post-transplantation. Scale bars are 100μm.

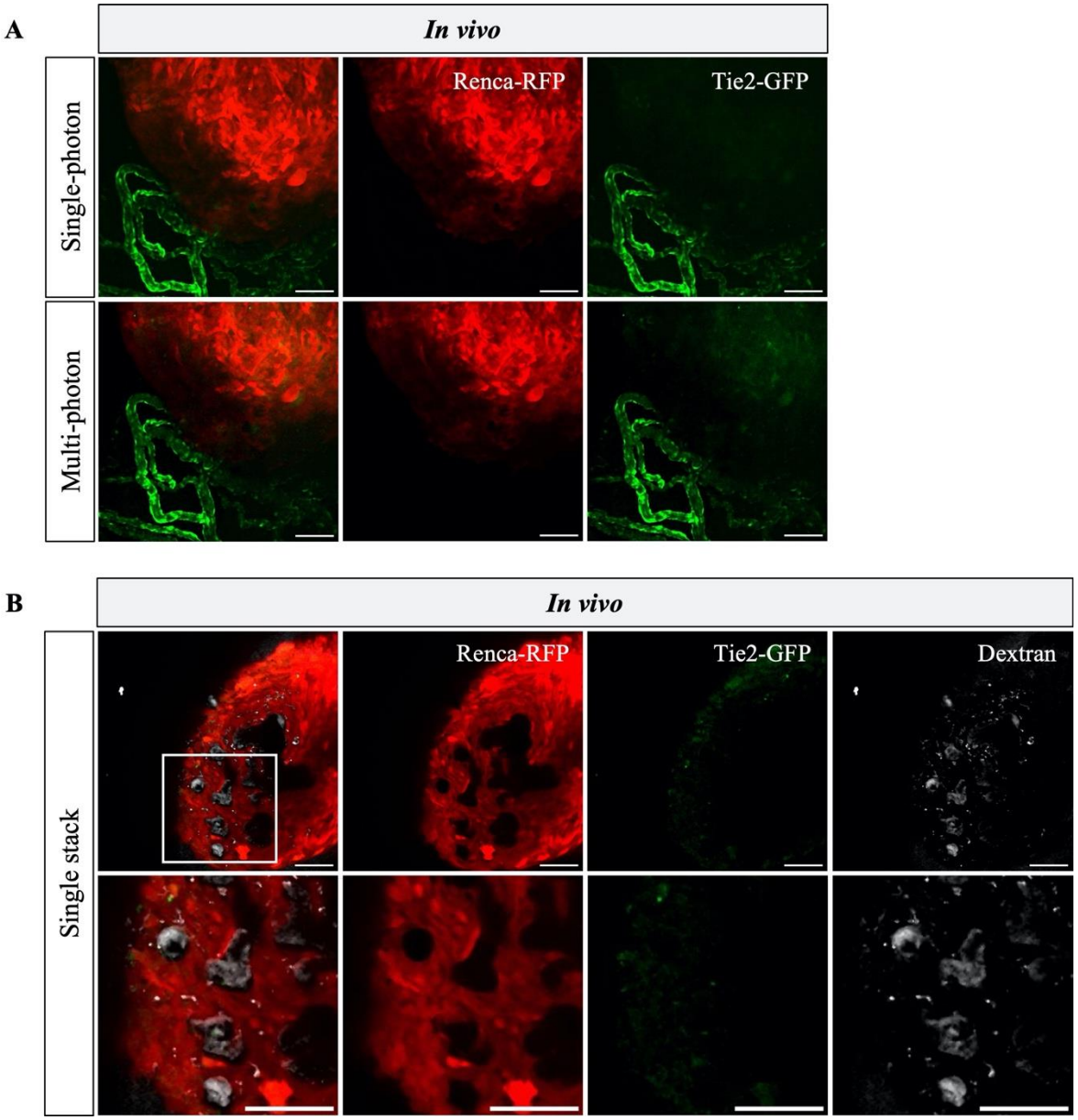


Figure 2.9. Loss of blood vessel fluorescence within tumours is likely not due to laser penetration issues. A) *In vivo* confocal and multi-photon images of the same tumour (red) and surrounding blood vessels (green) taken on day 8 post transplantation. B) *In vivo* confocal single stack image of cascade-blue dextran (grey) highlighting blood vessel within the tumour spheroid (red). Note that no Tie2-GFP expression (green) can be seen. Scale bars are 100μm.

To further address the nature of the intra-spheroid channels, additional experiments were carried out to characterize them *ex vivo*. To do so, host animal eyes were excised and sliced as previously described (see section 2.3.8.)(Fig. 2.5b), followed by immunostaining of the resulting eye slices. Immunostaining of excised eyes with anti-GFP further validated the presence of intra-tumour channels and supported the down regulation of GFP as the reason for the lack of fluorescence in channels within the tumour seen *in vivo*, since no GFP-positive channels could be seen within tumours (Fig. 2.10 upper panel), in contrast to the GFP-positive

blood vessels in nearby healthy tissue (Fig. 2.10 lower panel). Occasionally, one or two GFP-positive cells could be observed in intra-spheroid channels (Fig. 2.10 and Fig. 2.11), however further experiments are needed to ascertain their nature.

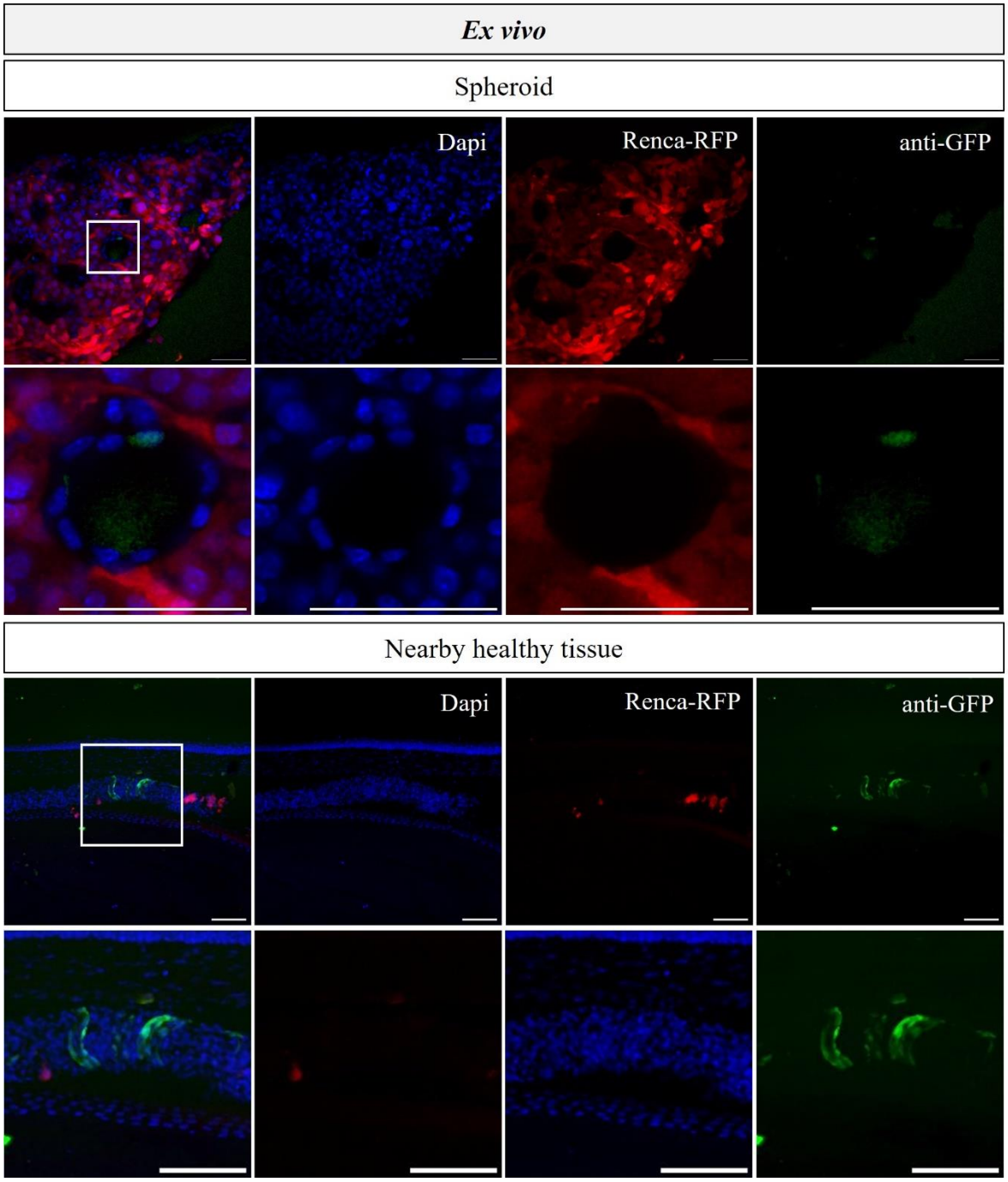


Figure 2.10. Loss of blood vessel fluorescence within tumours is likely caused by Tie2-GFP down-regulation. Confocal images of eye slices stained for anti-GFP, showing the spheroid (red) and blood vessels (green). Scale bars are 50μm in upper panel, and 100μm in lower panel.

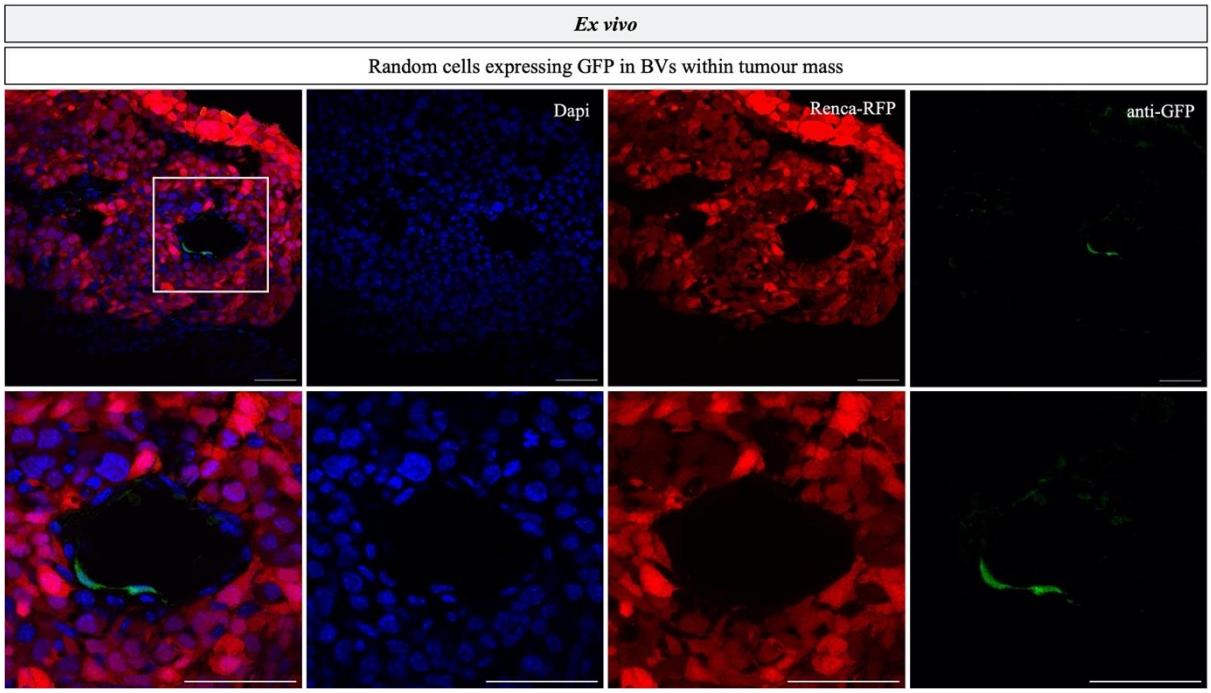


Figure 2.11. Occasionally, a few GFP+ cells could be seen in intra-tumour blood vessels. Confocal images of eye slices showing the tumour spheroid (red), blood vessels stained with anti-GFP (green) and dapi nuclear staining dye (blue). Scale bars are 100μm.

2.4.3. Cancer cell-lined channels are present in Renca spheroids

Additional experiments were then performed to confirm the endothelial origin of the intra-tumour channels, by staining eye slices with CD31, another endothelial cell marker. As expected, these channels were positive for CD31 (Fig. 2.12). Surprisingly however, even though most of these channels were indeed of endothelial origin, a few channels that seemed to be lined by cancer cells were found in around 60% of all excised tumours (Fig. 2.12). Around one to two such channels were usually present within each spheroid.

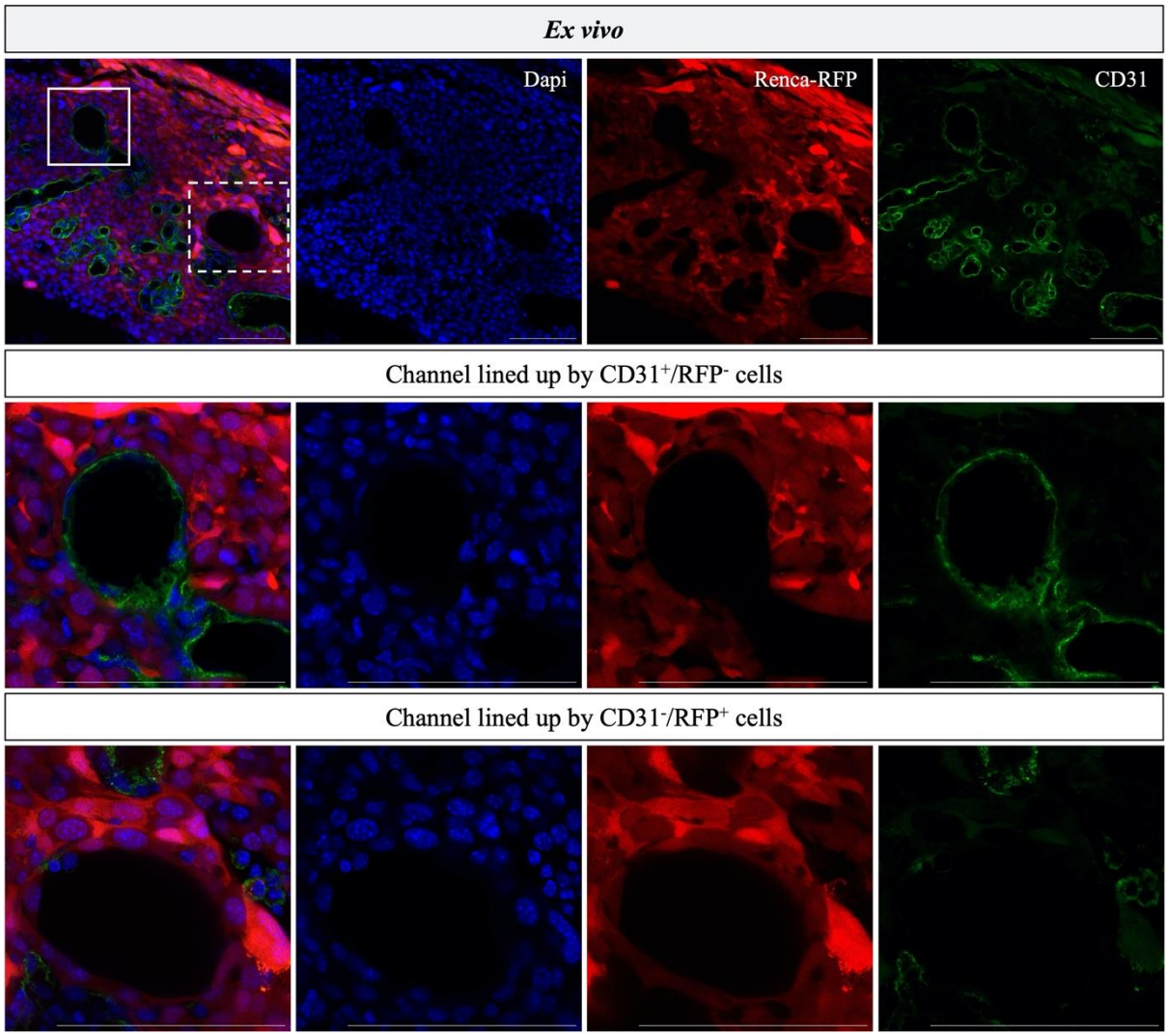


Figure 2.12. Presence of channels lined by endothelial cells and channels lined by tumour cells within spheroids. Confocal images of eye slices stained for CD31 (green) showing the spheroid (red). Scale bars are 100μm.

One of the most recent types of tumour vascularization to be described is vascular mimicry (VM), where tumour cells line up to form their own fluid-conducting and cancer cells-carrying channels, simultaneously providing nutrients to the tumour, whilst also enhancing its invasion and metastasis capacity. Hence, it was hypothesized that the channels lined up by cancer cells found in the excised tumours were of VM origin. There are currently no established markers of VM, but there are a set of characteristics that a channel must have to be considered VM: 1) it is lined by cancer cells, 2) it is positive for PAS staining, 3) ideally contains red blood cells/or is showed to be connected to functional vasculature and 4) tumour cells have the capacity to form tube-like structures *in vitro*. Thus, double staining for PAS and for the endothelial cell marker CD31was performed in excised eye slices. These revealed that potential tumour-cell lined VM channels were positive for PAS whilst negative for CD31, however no red blood

cells were ever detected within these channels, in sharp contrast to their neighbouring endothelial blood vessels (Fig. 2.13). Renca cells were then assessed for their capacity to form tube-like structures by seeding them on Matrigel, a well-known approach frequently used to test the VM capacity of tumour cell lines *in vitro*. However, when Renca single cells were seeded on Matrigel, they invaded the matrix and formed spheroids (Fig. 2.14). Abnormal tumour vascularization, including VM, is known to be stimulated by hypoxia, so Renca cells tube formation capacity was additionally assessed in a hypoxic environment by supplementing the culture medium with cobalt chloride, a well know chemical hypoxia model (Muñoz-Sánchez & Chánez-Cárdenas, 2019). However, the single cells still formed spheroids instead of tube-like channels (Fig. 2.14).

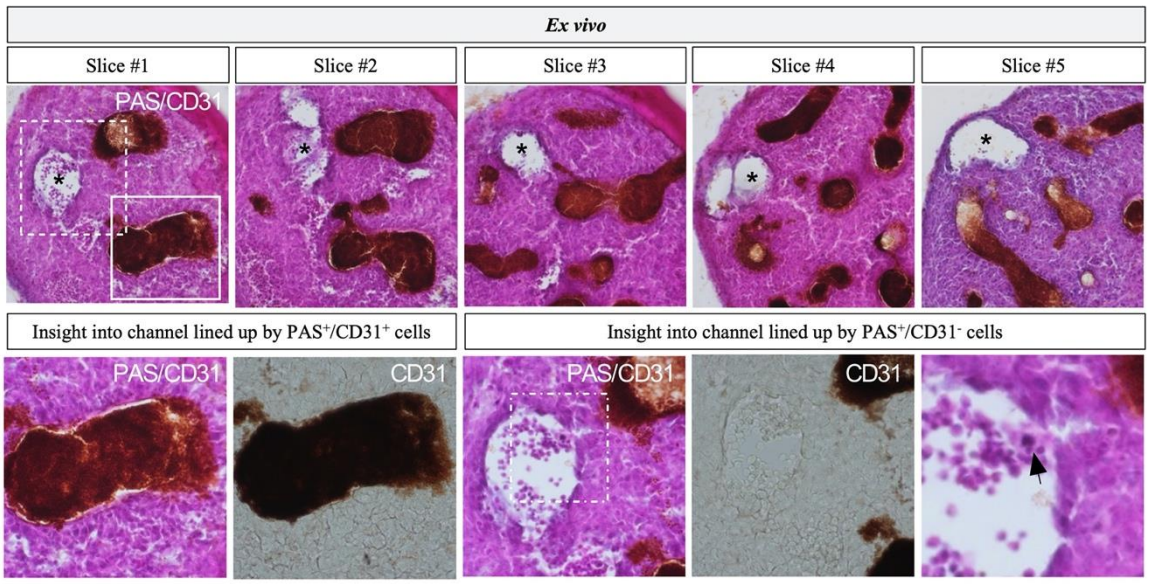


Figure 2.13. Channels lined by tumour cells are positive for PAS and negative for CD31, and do not seem to be perfused with blood. Bright field images of 5 consecutive eye slices stained for CD31 (brown) and PAS (pink). Full square shows zoomed region containing PAS+/CD31+ channel, and dotted square shows zoomed region containing PAS+/CD31- channel. Magnification is 10x on upper panel and 20x on lower panel.

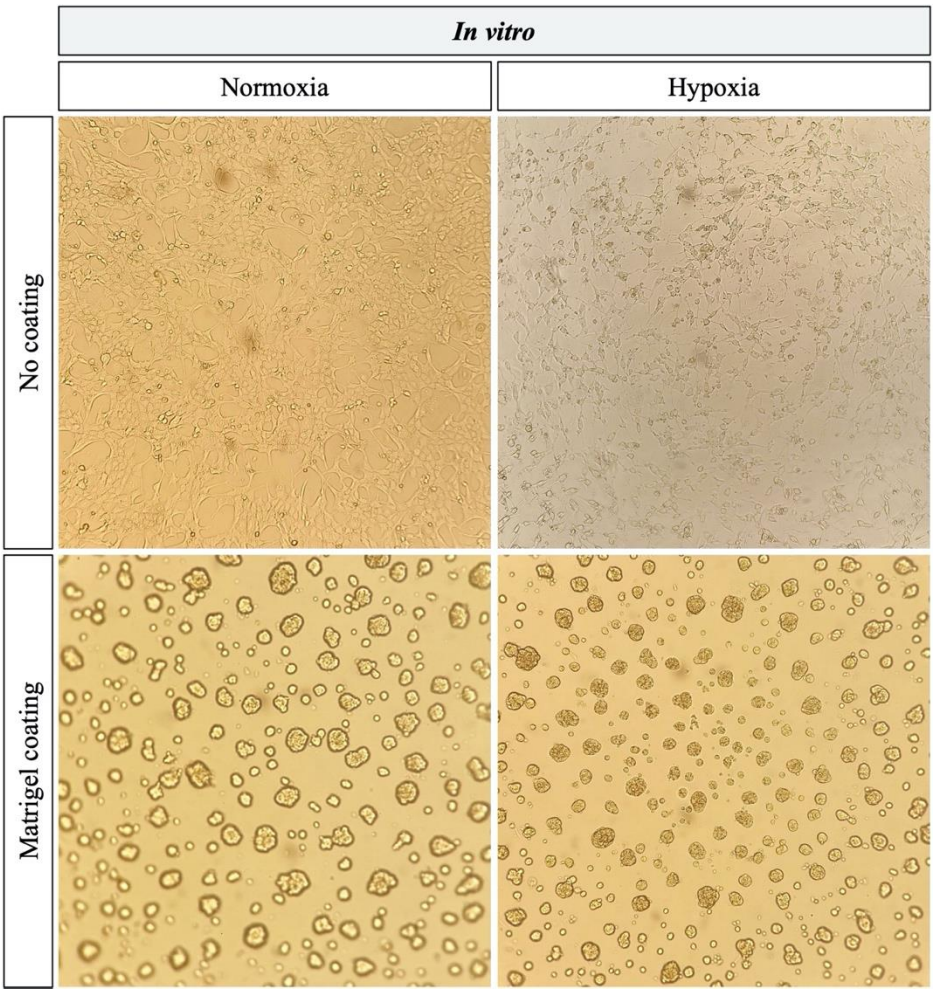


Figure 2.14. Renca cells do not form tube-like structures when seeded on Matrigel, instead they form spheroids. Bright field images of Renca cells two days after being cultured on TC-treated wells vs Matrigel, in normoxic vs hypoxic conditions induced with chloride cobalt. 4x magnification.

2.5. Discussion and future studies

This chapter aimed to develop a novel *in vivo* platform to track tumour growth and that would allow to characterize the different types of tumour vascularization in the same animal over time. While attempting to do so, it was demonstrated, for the first time, to our knowledge 1) that Renca cells can form spheroids, 2) Renca spheroids vascularize through angiogenesis and grow over time upon transplantation into the anterior chamber of the eye of host mice, 3) endothelial cells from intra-spheroids blood vessels experience Tie2 downregulation *in vivo*, and 4) the presence of intra-spheroid channels of tumour origin, whose nature and purpose can be subject of further studies.

The aim of using this platform to characterize tumour vascularization *in vivo* could not be achieved due to the Tie2-GFP downregulation. However, it was shown, by exclusion, that angiogenesis seems to be the main type of vascularization employed by Renca spheroids when transplanted into the anterior chamber of the eye. As explained earlier in this chapter, there are 4 main types of tumour vascularization: angiogenesis, *de novo vessel* formation, vessel co-option and vasculogenic mimicry.

Vessel co-option consists in tumours scavenging existing blood vessels from healthy tissue to get hold of a supply of oxygen and nutrients. Vessel co-option has been reported in lung metastases of Renca tumours (Bridgeman et al., 2017c), in response to anti-angiogenic drugs. However, the anterior chamber of the eye is naturally avascular, thus, and since the formation of new channels could be observed as the tumour grew and occupied the ACE, vessel co-option was probably not involved.

De novo vessel formation consists in new vessels being formed by bone marrow-derived circulating endothelial precursor cells. Even though blood vessels-endothelial cells could not be observed within the tumours *in vivo* due to Tie2-GFP down-regulation, Tie2-GFP positive single cells could occasionally be observed within some of the tumours formed by injecting a suspension of Renca cells into the ACE. This observation was confirmed in *ex vivo* IHC experiments. Thus, the fact that single Tie2-GFP positive cells could never be observed near or within the spheroids *in vivo* or *ex vivo,* nor CD31 positive cells in *ex vivo* experiments, suggests that the newly formed blood vessels are not being formed by *de novo* vascularization. Notably, whilst Tie2 is expressed in endothelial precursor cells, CD31 may or may not be expressed, depending on their degree of differentiation (Hristov et al., 2003; Obi et al., 2012). In addition, it is important to notice that Tie2 expression is not restricted to blood vessels

endothelial cells and endothelial progenitor cells. Tie2 is also expressed by lymphatic endothelial cells, several cancer cells, and hematopoietic cells including monocytes and macrophages (de Palma et al., 2007; Duran et al., 2021b; Korhonen et al., 2022). Thus, the single cells observed in tumours originated from Renca single cells injections might not have been of endothelial origin. Regardless, the point is that no GFP nor CD31 positive cells could be observed at any point (*in vivo* or *ex vivo*) within the intra-ocular spheroids.

Vasculogenic mimicry happens when tumour cells self-organize to form their own fluid-conducting channels. The presence of tumour cell-lined channels was reported in 60% of all excised tumours, and, on average, one to two such channels were observed per spheroid (data not shown). The experiments carried out in this chapter did not address the exact nature of these channels, however, the fact that not all tumours had them, and that they represented only a small percentage of the total intra-tumour channels suggests that, even if these are VM channels, this is not the main type of vascularization present in these spheroids.

Thus, angiogenesis seems to be the main type of vascularization employed by Renca spheroids upon transplantation into the anterior chamber of the mouse eye.

Blood vessel fluorescence was reported to be lost *in vivo* exclusively within Renca spheroids. An initial hypothesis was formulated suggesting that this was due to a laser penetration issue, a well-known limitation of fluorescence microscopy (St Croix et al., 2005). However, it has been demonstrated, through the use of multiphoton microscopy, which allows roughly five times the imaging depth of the confocal approach (Coste et al., 2020), that this was not the case. This conclusion has been further supported by experiments conducted involving dextran tail-vein injections.

The transgenic animal model Tie2-GFP, which possesses fluorescent blood vessels, was employed as host animals. In this model, a green fluorescent protein gene was inserted under the control of the promotor region of the Tie2 gene, meaning that GFP expression is dependent on Tie2 expression. Thus, and together with the *ex vivo* experiments performed using an anti-GFP antibody that stained vessels in nearby healthy tissue, whilst not staining intra-tumour blood vessels, it was concluded that the loss of blood vessel fluorescence within spheroids is likely due to Tie2 downregulation. Additional experiments directly assessing Tie2 levels (e.g., IHC with anti-Tie2 antibody) should be performed to further validate that GFP down-regulation is indeed a consequence of Tie2 down-regulation. Furthermore, whether that down-regulation is exerted through the direct interaction between Renca cells and host animal

endothelial cells or is an EC response to the TME was not addressed with the experiments performed.

There are several hypotheses that might justify why Tie2 downregulation occurred in intra-spheroid blood vessels. The Ang-Tie2 pathway promotes vessel stabilization and maturation. During tumour angiogenesis, existing vessels need to be destabilized (lose stabilizing mural cells, for example) so that new vessels can sprout. Tie2 is involved in vessel maturation and its function needs to be reduced to allow new vessels to form in response to the rapidly growing and highly angiogenic tumours (Holash et al., 1999), like the Renca spheroids. Because of this, Tie2 activation, which promotes blood vessel stabilization, has been seen as a possible approach to fight cancers. Such approach has been shown to reduce tumour-BVs leakiness and, thus, metastasis; whilst also improving blood perfusion, and consequently, tumour drug delivery, in several cancer models (Park et al., 2016).

In human RCC, changes in Ang-Tie2 pathway have been widely described. These changes are usually reported at the angiopoietins rather than Tie2 expression levels (Bullock et al., 2010; X. Wang et al., 2014; Yamakawa et al., 2004). However, it has been shown that Ang2 decreases Tie2 expression in breast tumours compared to untreated tumours (Mazzieri et al., 2011). In fact, Currie and colleagues reported specific Tie2 down-regulation at the RNA and protein level in advanced stages of the disease in biopsies from patients with RCC (Currie et al., 2002), albeit probably not to the same extent as the level of down-regulation seen in Renca spheroids. In contrast to the Tie2 downregulation mainly observed in advanced human RCC samples, Renca spheroids exhibited Tie2 down-regulation from the start. Naturally occurring tumours do not start as an already established solid mass, but that was what was being accomplished when transplanting 3D spheroids into the ACE. Thus, it was hypothesized that Renca spheroids were behaving more like advanced RCC, even immediately after being injected. This idea was supported by the finding that in Renca tumours formed by transplanting single cells into the ACE, GFP-positive blood vessels could be observed in excised eye slices. In other words, whilst Renca tumours originated from single cells might resemble earlier stages of RCC, Renca spheroids might resemble more advanced stages of the disease. Nevertheless, it is important to note that whether the blood vessels within the single cell derived-Renca tumours were also of angiogenic origin, or if they were co-opted, for example, could not be ascertained. Therefore, care should be taken when drawing comparisons between the two approaches.

Another possible cause for the Tie2 downregulation in intra-tumour channels is the fact that blood pressure is often altered in large and abnormal cancer vessels. Idowu and colleagues showed that reduction of the mean arterial pressure, in a mouse model of hypotension, leads to

the reduction of Tie2 expression through GATA3, without altering expression levels of Tie2 ligands (Idowu et al., 2021). Many tumours exhibit reduced microvascular pressure (Jain et al., 2014; Siemann, 2011), which can lead to accumulation of vascular contents and elevated interstitial fluid pressure. The vast amounts of vascular contents (including red blood cells) in intra-tumour vessels, seen in the histologic preparations of tumour slices double stained for CD31 and PAS, is an indicator of low blood pressure. Thus, it is possible that the Tie2 downregulation seen in Renca spheroids is due to low microvascular pressure.

The occasional presence of GFP-positive cells in a few intra-tumour blood vessels of unknown nature was also reported. GFP expression in host mice is under the control of the Tie2 gene. Tie2 is a well-known marker of endothelial cells, however, other cell types, like macrophages as well as a subset of tumour associated monocytes, have been reported to express Tie2 in several cancers, including RCC (L. Chen et al., 2016; Ji et al., 2013; Turrini et al., 2017). Thus, additional experiments are needed to determine the exact nature of these occasional cells in intra-tumour blood vessels.

In retrospective, given that the aim of this platform was to enable the observation and characterization of tumour vascularization *in vivo*, the use of a host mouse where blood vessel fluorescent was not dependent on the expression of an endothelial cell protein involved in angiogenesis should have been considered instead. In other words, it would have been more appropriate to use animals where the GFP production was not under the control of the Tie2 promotor. In fact, as an alternative, mice like the ones generated by Balan and colleagues, where all the cells that have ever expressed Tie2 would express fluorescence thereafter, regardless of changes in Tie2 expression, could have been used instead (Balan et al., 2019).

Ex vivo experiments revealed the presence of tumour lined channels in 60% of all excised spheroids. It was initially hypothesized that these channels could be formed through VM. Currently, there are four characteristics to consider tumour-lined channels to be of VM origin: 1) they are lined by cancer cells, 2) are positive for PAS staining, 3) ideally contain red blood cells/or are connected to functional vasculature and 4) the tumour cells have the capacity to form tube-like structures *in vitro*.
The experiments carried out with PAS/CD31 double staining revealed that the tumour lined CD31 negative channels were PAS positive, which could support that these were formed by VM. Matrigel was used to make the Renca spheroids *in vitro*, which is a complex mixture of

extracellular matrix components that has been used as a supportive matrix for cell culture. Matrigel contains various growth factors, extracellular matrix proteins, and glycosaminoglycans, which are polysaccharides that can be detected by PAS staining. Thus, and given that the whole spheroids seemed to stain positive for PAS, a conclusion regarding the PAS content of those channels might not be accurate, since the staining was not specific to the channels. Red blood cells were never observed within these channels. However, it has been suggested that some VM channels might transport just plasma, which still provides the tumour tissue with nutrients and oxygen (Clarijs et al., 2002). In the future, it would be worth assessing the tumours-cell lined channels for the presence of fibrinogen, a protein that circulates in blood plasma, to assess whether they carried it or not. With the experiments performed, whether these channels were connected to functional blood vessels could not be addressed. Thus, further experiments should be performed to check if tumour lined channels ever anastomose with blood vessels. Renca cells capacity to form channels *in vitro* was also evaluated. Like endothelial cells, tumour cells with VM capacity form tube like structures when seeded on Matrigel. However, when Renca cells were seeded on Matrigel, they invaded the matrix and formed spheroids. This was not surprising, since Matrigel is a commercial ECM, and invasive cancer cells are able to migrate away from the original tumour mass, traversing the confining basement membrane and moving through the three-dimensional (3D) ECM by means of single or collective cell migration (He et al., 2016; Winkler et al., 2020). Retrospectively, this experiment was performed using Renca single cells that had been previously cultured as a monolayer, and it has been shown that 2D cultures can exhibit different characteristics when cultured under 3D conditions (Birgersdotter et al., 2005; Fontoura et al., 2020). Thus, in the future, it would be interesting to repeat this experiment by seeding spheroids, or single cells derived from spheroids, instead, on Matrigel.

Given the lack of red blood cells within these channels, as well as the highly metastatic nature of RCC, which is known to spread through the lymphatic system, another possible explanation for the nature of these channels is through the novel concept of lymphangiogenic mimicry (Karinen et al., 2021a; Q. S. Wang et al., 2018). As explored in section 2.1.3.5., lymphangiogenesis consists in the development of lymphatic vessels within tumours, in a similar way to blood vessels during angiogenesis, and has been widely reported in RCC (Debiński et al., 2013b). Lymphangiogenesis has also been shown to happen in several tissues surrounding the anterior chamber of the eye, like the naturally avascular cornea (in response to injury, xenografts transplantation, and to some growth factors) and in some ocular cancers (Nakao et al., 2012). LYVE-1-positive cells, a marker of endothelial lymphatic cells, have been

identified in the iris as well (Kaser-Eichberger et al., 2015). The emerging concept of lymphangiogenic mimicry, first coined by Wang and colleagues, consists in cancer cells forming lymphatic vessel-like channels capable of carrying cancer cells to lymphatic nodules, hence increasing metastatic capacity (Q. S. Wang et al., 2018). These channels are positive for lymphatic endothelial cells markers. Thus, it is possible that the CD31-negative tumour cell-lined channels could be formed by lymphangiogenic mimicry. In the future, it would be interesting to assess the expression of LYVE-1 in the CD31-negative channels. In addition to expressing lymphatic endothelial cells markers, another characteristic of tumour cell lines that have lymphangiogenic mimicry capacity is, just like in VM, to form tubes when seeded on Matrigel (Karinen et al., 2021b). However, as discussed earlier, the Renca cells formed spheroids instead under those conditions.

Another plausible explanation for the nature of the channels lined by the cancer cells is that they could resemble structures like the tubules found in the kidneys, as described by Guo and colleagues. Guo and colleagues have shown that human urine-derived stem cells (USCs), originated from the renal glomerular parietal stem cell population, form spheroids *in vitro* when seeded in ultra-low attachment plates, and that these differentiate into renal tubular epithelial cells in three-dimensional (3-D) culture, in the presence of extracellular matrix, after 7 days. Under 3D conditions, these spheroids exhibit tubule-like structures (Guo et al., 2020). The Renca cell line used in this project was isolated from a renal cell carcinoma that arose spontaneously in a mouse. Renal cell cancer is a disease in which malignant cells form in the tubules of the kidney. Given the anatomical source of the Renca cells, and that spheroids were generated in a very similar way, also using ultra-low attachment plates and in the presence of ECM, it is possible that these channels might be the tubule-like structures observed by Guo and colleagues. In future experiments, it would be interesting to have a look at histologic preparations of the *in vitro* spheroids, to look for the presence of these tubule-like structures. However, if this was the case, such structures would have probably been observed immediately upon *in vivo* spheroid transplantation using the RFP channel (since they form *in vitro*) even before spheroids become vascularized. Nevertheless, the structures described by Guo and colleagues only formed after 7 days, and spheroids were never kept in culture for more than 2/3 days pre-transplantation, so this might justify why such channels could not be observed immediately after *in vivo* transplantation.

Like all animal models, this platform has limitations worth noting. Tumours usually arise in well vascularized areas. This platform takes advantage of the anterior chamber of the eye as a

natural window to the body, however, the ACE is naturally avascular. Thus, the types of vascularization induced by implanting tumours in this area might not mimic the types of vascularization of the RCC in its original location. Nonetheless, this platform could still be useful to test drugs targeting angiogenesis, which is the most widely prevalent vascularization type observed in tumours, including RCC. Additionally, due to the small size of the ACE, this platform can only be used to study the early stages of tumour spheroid development.

In conclusion, given all the previously mentioned findings, and even though the initial aim of establishing an *in vivo* longitudinal platform to characterize tumour vascularization could not be achieved, it is possible that the platform developed in this chapter can still be used to test candidate drugs belonging to the two main tumour vasculature targeting drug groups: anti-vascularization and vascularization-normalizing drugs. More specifically, both candidate anti-angiogenic or Tie2-normalizing drugs can potentially be tested in this platform having tumour growth rate and rescue of blood vessel fluorescence as a readout, respectively. A schematic of how this platform was generated and a suggestion regarding how it could be employed can be found in Figure 2.15.

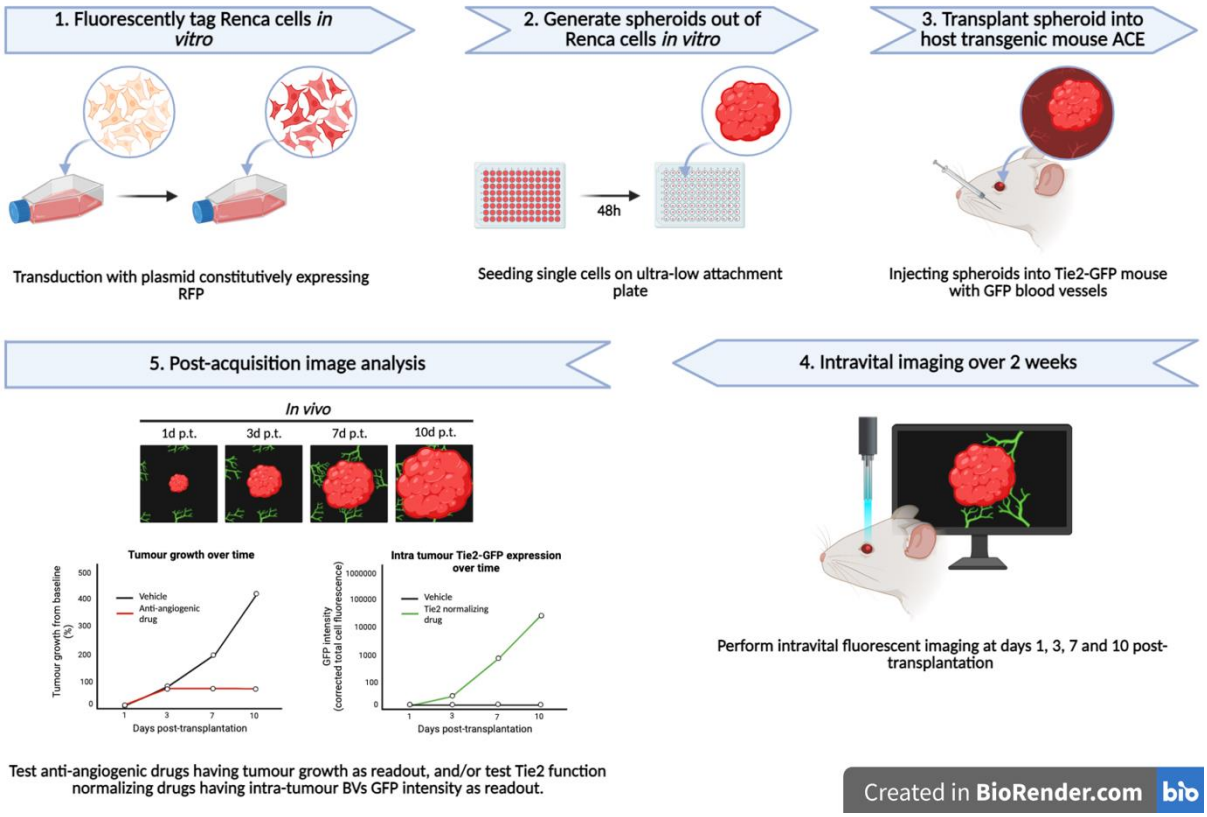


Figure 2.15. Schematic representing how this platform was developed and how it can potentially be used. Renca cells were first fluorescently tagged *in vitro* to express cytoplasmic red fluorescent protein (RFP). Then, spheroids were generated using ultra-low attachment plates, followed by injection into the anterior chamber of the eye of a host mouse. Tumour growth is then tracked through repeated intra-vital imaging and quantified through post-acquisition image analysis. Finally, potential anti-angiogenic drugs can be investigated having as a read-out tumour growth. In addition, drugs targeting specifically the normalization of Tie2 function, known to play a role in angiogenesis, could also potentially be tested having as readout rescue of the Tie2-GFP expression in intra-tumour blood vessels. *Created in BioRender.*

Chapter III: Investigating a novel *in vivo* longitudinal platform to study NAFLD

3.1. Introduction

3.1.1. Sources of hepatocytes to establish *in vitro* models

There are several options available to model liver diseases *in vitro*. Given that hepatocytes are the effectors of most liver functions, these cells are the common player across all *in vitro* liver models available. These hepatic cells used to set up *in vitro* models can be primary (hepatocytes isolated from liver), immortalized (usually cell lines established from hepatic cancers) or hepatocyte like cells (HLCs) (stem cells differentiated into hepatocytes). Working with each of those brings several advantages and disadvantages. Primary hepatocytes are the most efficient ones at recapitulating hepatocyte function because they are native liver cells, however, with the currently available protocols, they can only be cultured *in vitro* for a limited amount of time. This makes them unsuitable to be targeted, for example, by molecular techniques like, Crispr, and, because they cannot be extensively expanded, they also require repeated isolation. Immortalized hepatocytes, on the other hand, can be expanded and cultured for a long time *in vitro*, however, since they are isolated from tumours, they usually carry genetic alterations that can influence hepatocytes behaviour and function. HLCs are differentiated from stem cells, which means that they can be extensively expanded before differentiation and, thus, have an almost unlimited source. However, most differentiation protocols currently available lead to the generation of hepatic cells with immature hepatic functions/behaviour (Ramos et al., 2022b).

3.1.2. *In vitro* differentiation of stem cells into HLCs

During gastrulation, endoderm, mesoderm, and ectoderm are formed. Endoderm will give origin to hepatocytes, whilst the hepatic non-parenchymal cells, such as liver sinusoidal endothelial cells, originate from mesoderm. The endoderm then further specifies into hindgut, midgut, and foregut. Cells from the foregut further differentiate into hepatic endoderm, which then differentiates into foetal hepatocytes that, post-natal, further develop into fully mature hepatocytes. During embryogenesis, the development of the liver is a gradual process that involves a series of interactions between the endoderm and mesoderm tissues. Many pathways that govern liver development have been identified over the last few years, and this knowledge has been applied to generate several models to study liver disease *in vitro* (Lynch et al., 2009; Zorn, 2008).

In general, differentiation of cells *in vitro* can be promoted using cocktails of growth factors, small molecules, epigenetic modifiers, or combinations of any of these. Growth factors are proteins biologically made that are isolated and purified for *in vitro* use. Small molecules are low molecular weight compounds, that, therefore, can easily diffuse into cells, and can be obtained from natural compounds, synthetic chemistry or even a combination of both. Epigenetic modifiers are molecules that can modulate gene expression through targeting epigenetic marks on the DNA or histones, like chromatin modifiers, for example, thus influencing which genes transcription is promoted or repressed. In addition to the previously mentioned methodologies, other approaches can be used to further improve cell differentiation. These include co-culture with other cell types, e.g., non-parenchymal cells, where cell-cell interactions promote the activation of key signalling pathways involved in cell-fate specification; mechanical and physical cues, like, for example, matrix stiffness, that better mimics the native tissue environment; and culture dimension, where culturing cells in 3D has been shown to improve cell differentiation success in comparison to 2D approaches, through better mimicking tissue spatial organization, cell-cell interactions and even oxygen and nutrient gradient. Furthermore, research has also shown that transplanting cells previously differentiated *in vitro* into an *in vivo* setting promotes further cell differentiation and maturation (Ramos et al., 2022b)

HLCs can be obtained from differentiating stem cells into the hepatic lineage. These stem cells can have different origins, like adult stem cells (isolated from adult tissues), embryonic stem cells (ESCs) (isolated from the inner cell mass of blastocysts) and induced pluripotent stem cells (iPSCs) (adult cells genetically reprogramed to acquire a stem phenotype), and they can have different degrees of stemness. Thus, depending on the degree of stemness of the initial cells (i.e., how committed they already are for the hepatocyte lineage), different protocols can be used to generate HLCs.

There are several protocols available to differentiate pluripotent stem cells, like ESCs and iPSCs, into HLCs. However, the most efficient ones – those yielding cells capable of closely mimicking native primary hepatocytes in their hepatocyte functions – typically adhere to the same three-step approach: 1) induction of definitive endoderm, 2) hepatic endoderm specification and 3) hepatic maturation.

1) The formation of definitive endoderm involves a complex sequence of events that are regulated by multiple signalling pathways. BMP, Nodal and Wnt all promote endoderm specification *in vivo*, so using compounds *in vitro* that mimic their action will lead to endoderm specification. One of those compounds is Activin A, which binds to the same receptors as Nodal, thus mimicking its function and promoting definitive endoderm specification (Zorn, 2008).

2) For the next stage of embryonic liver development, the endoderm is patterned into midgut, hindgut, and foregut, and this is specified by the activation of specific transcription factors like Haematopoietically Expressed Homeobox (HHEX). The activation of HHEX transcription factor guides the patterning of endoderm into foregut, the precursor of liver. Growth factors such as fibroblast growth factor (FGF) and epidermal growth factor (EGF) activate HHEX expression, so these molecules can then be added to the definitive endoderm cells to promote specification into foregut. Adding BMP4 then promotes hepatic endoderm specification from foregut (J. M. Rossi et al., 2001; Zorn, 2008).

3) Lastly, hepatic maturation is achieved by adding molecules like HGF, Oncostatin M and Dexamethasone, that synergistically promote the expression of liver-specific genes, such as hepatocyte nuclear factors (HNFs), albumin, drug metabolizing genes (like cytochrome P450 enzymes), whilst simultaneously promoting cell survival and polarity and inhibiting cell proliferation. Altogether, these events will contribute to functional hepatic characteristics (Zorn, 2008).

When it comes to differentiating HLCs from adult stem cells, the choice of differentiation protocols depends on the tissue where the cells were isolated from, and how committed they already are towards the hepatic lineage. For example, LGR5-positive stem cells isolated from liver have been shown to have the capacity to generate both bile duct cholangiocytes and mature hepatocytes. These cells are more committed to the biliary lineage but can be differentiated into HLCs *in vitro*, upon exposure to certain growth factors as shown by Huch and colleagues (Huch et al., 2013).

3.1.3. Liver spheroids and organoids as *in vitro* NAFLD models

As previously explained in chapter I, depending on the aim or questions to be studied, different *in vitro* NAFLD models with different degrees of complexity can be used. Primary hepatocytes,

hepatic tumour-derived cell lines and HLC can all be used to create 2D and 3D NAFLD models. Two of the most widely used models that recapitulate liver function and NAFLD characteristic are organoids and spheroids (Soret et al., 2020).

Spheroids are 3D structures created by the natural clustering of one (like primary hepatocyte spheroids) or more (usually co-culture with non-parenchymal cells) cell lines in a fluid environment with or without the presence of an extracellular matrix. As mentioned in the previous chapter, there are several methods available to generate spheroids, but the most commonly used ones are the hanging drop method, and culture on ultra-low attachment (ULA) plates (S. M. Kang et al., 2021). A summary of different culture strategies available to generate hepatic spheroids in NAFLD research can be found on table 3.1.

In the past, the word 'organoid' has been utilized to describe the resulting products of a range of different 3D culture methods, that imitate the structure and function of an organ with varying degrees of accuracy. As a result, what is considered as an organoid by some researchers might be considered a spheroid by others. In this thesis, organoids, or more specifically hepatic organoids, were defined has complex 3D structures that can be created by culturing pluripotent stem cells (PSCs), liver tissue stem cells, liver progenitor cells, or liver parenchymal cells, in a scaffold, that lead to the development of self-organizing structures that recapitulate the functionality of the tissue of origin (Prior et al., 2019). The scaffolds used to make hepatic organoids are designed to mimic the spatial organization of the liver, allowing for the accurate modelling of the organ's structure and function. There are several strategies available to generate liver organoids. The source of the initial cells seeded on the scaffold influences the complexity of the resulting organoids in terms of cell types present and capacity for liver functions.

The mammalian liver po'sesses a remarkable regenerative ability, and two modes of damage response have been described: 1) A massive proliferative response of mature hepatocytes upon, for example, partial hepatectomy and 2) the ''oval cell'' response that emanates from the biliary tree when most hepatocytes are affected by chronic liver disease, and thus, cannot proliferate, or are too slow to respond. Huch and colleagues took advantage of the lessons learned from the hepatic oval cell response and generated liver organoids by embedding bi-potent liver progenitor cells, found in the bile ducts, on Matrigel, followed by differentiation into hepatic liver organoids though exposure to certain growth factors (Huch et al., 2013). More recently, Hu and colleagues took advantage of the hepatocyte proliferative response and generated liver

organoids, that could be cultured for long-term, by embedding single hepatocytes in matrigel and culturing them in a proliferation-inducing medium (Hu et al., 2018). A summary of different strategies available to generate hepatic organoids can be found in table 3.2.

Table 3.1. Summary of different strategies to make liver spheroids *in vitro*.

Starting cell type(s)	Brief description	Advantages	Disadvantages	References
Monoculture				
Primary hepatocytes	Spheroids were formed by seeding primary hepatocytes on ULA plates.	Mature hepatocytes; Keep mature hepatocytes characteristics/function for days; Easy and quick to set up.	Absence of biliary and non-parenchymal cells; Not suitable for expansion; Not suitable for long term culture.	(Kozyra et al., 2018)
HepG2	Spheroids were generated by seeding HepG2 cells on ULA plates.	More sensitive to drugs than 2D cultures.	HepG2 cells are derived from hepatic cancer and can thus carry genetic alterations that alter hepatic functions; Absence of other non-parenchymal and biliary cells.	(Štampar et al., 2019)
	Spheroids are formed by encapsulating HepG2 cell suspension in a semipermeable alginate capsule. The alginate capsule forces the cells together, thus promoting cell aggregation and spheroid formation, whilst allowing access to nutrients and oxygen in the culture medium.	Improved hepatic function compared to 2D culture.	HepG2 cells are derived from hepatic cancer and can thus carry genetic alterations that alter hepatic function; Absence of other non-parenchymal and biliary cells.	(Khalil et al., 2001)
ESCs	ESCs were initially differentiated into the hepatic lineage under 2D culture, and then spheroids were made by culturing committed cells on ULA plates where they underwent further hepatic maturation.	Better hepatic function than when cultured 2D.	Absence of other non-parenchymal and biliary cells.	(Subramanian et al., 2014)
iPSCs	Spheroids were generated by seeding iPSCs on agarose plates. Spheroids were then differentiated into mature hepatocytes through exposure to certain growth factors.	Differentiated spheroids remained stable for one year in culture.	Absence of non-parenchymal and biliary cells.	(Rashidi et al., 2018)
Co-culture				

iPSC-HLC + HAMECs	iPSCs and human adipose microvascular endothelial cells (HAMECs) were co-cultured on agarose to promote spheroid formation. Spheroids were then exposed to a cocktail of growth factors to promote hepatic maturation.	Spheroid hepatic function was somewhat improved by co-culture with HAMECs.	Absence other non-parenchymal cells and biliary cells; Endothelial cells were not isolated from liver; Endothelial cells distribution was not homogeneous within spheroid.	(Pettinato et al., 2019)
HepG2 + LX-2	Spheroids are formed by seeding immortalized hepatocytes (HepG2) and immortalized HSCs (LX-2) on ULA plates.	Develop fibrosis in response to fatty acids treatment; Respond to anti-steatosis drug treatment.	HepG2 cells are derived from hepatic cancer and can thus carry genetic alterations that alter hepatic function; Absence of other non-parenchymal and biliary cells.	(Pingitore et al., 2019)
Primary hepatocytes + primary NPCs	Primary hepatocytes and all NPCs were isolated at once. Spheroids were then generated by co-culturing hepatocytes and non-parenchymal cells mixture on ULA plates.	Co-culture with NPCs improved spheroids hepatic function.	Amount of each type of non-parenchymal cells is variable across batches.	(Baze et al., 2018)
Hepatocytes + LSECs + HSCs + KCs	Hepatocytes, liver sinusoidal endothelial cells, hepatic stellate cells and Kupfer cells were individually isolated from liver. Spheroids were formed after co-culturing all cell types on ULA plates.	Good hepatic functions; All cells used were isolated from liver; Can be used to model NASH due to presence of HSCs.	Loss of liver sinusoidal endothelial cells and Kupfer cells from spheroid after a few days in culture. Absence of biliary cells.	(van Os et al., 2022)

Table 3.2. Summary of different strategies to make liver organoids *in vitro*

Starting cell type (s)	Brief description	Advantages	Disadvantages	References
Parenchymal cells				
Hepatocytes	Hepatocytes are isolated from mouse liver, embedded in Matrigel and cultured in defined medium, originating 3D liver organoids with extensive bile canaliculi networks.	Good hepatic maturation; Engraft onto liver upon transplantation; Can be expanded and stably kept in culture for several months.	Low plating efficiency; Slow growth; Organoids seem to form by recapitulating regenerative response rather than liver development; Absence of non-parenchymal cells	(Hu et al., 2018)
Stem cells				
ASCs	Stem cells, or bile duct fragments containing stem cells, are embedded in Matrigel resulting in the development of liver organoids that can be further differentiated into the hepatocyte lineage.	Easily and quickly established; Can be expanded and stably kept in culture over months;	Organoids seem to form by recapitulating regenerative response rather than liver development; Immature hepatocyte function; Absence of non-parenchymal cells;	(Huch et al., 2013)
iPSCs	iPSCs are first differentiated into foregut spheroids that are then embedded in Matrigel in the presence of a defined medium that leads to the formation of organoids containing hepatocytes, cholangiocytes, Kupfer and stellate-like cells	Multiple liver cell lineages develop;	No endothelial cells; Immature hepatic-like cells; High inter-batch variability;	(Ouchi et al., 2019)
	iPSCs are cultured on Matrigel and exposed to a sequential cocktail of growth factors to induce mesoderm and endoderm lineages, followed by hepatoblasts. These then differentiate into hepatocytes and cholangiocytes forming an hepatobiliary organoid that also contains some endothelial-like cells.	Multiple liver cell lineages develop; Functional hepatobiliary structures that produce bile acid; Organoids engraft upon transplantation into ectopic spleen for at least 8 weeks.	No Kupfer or stellate cells present in the organoids; Reduced hepatic function; Organoids' hepatic-like cells are not well-kept overtime upon transplantation, with some migrating into liver.	(Wu et al., 2019)

	iPSCs are first differentiated into definitive endoderm followed by specification into hepatic lineage. An enrichment step for Epcam+ cells is then carried out followed by embedding of sorted cells in Matrigel, giving rise to liver organoids that can be further differentiated into functional hepatocytes.	Can engraft onto liver upon transplantation.	Immature hepatic functions; Absence of non-parenchymal cells.	(Akbari et al., 2019)
mESCs	mESCs were first differentiated into definitive endoderm followed by hepatic specification. The cells were then dissociated and embed in Matrigel where they were further committed to the hepatic lineage.	Can engraft onto liver upon transplantation.	Differentiation into hepatocyte-like cells was done on cell aggregates derived from organoids; Absence of non-parenchymal cells.	(S. Wang et al., 2019)
Multi-lineage				
Hepatic endoderm cells (from iPSC) + HUVECs + MSCs	Three cell types are co-cultured on Matrigel where they self-organize to form a liver bud.	Multiple liver cell types; Vascular network *in vitro*; Vascularize upon *in vivo* transplantation even in ectopic places.	Needs to be transplanted *in vivo* to further maturation; Lack HSCs, Kupfer cells and cholangiocytes; Bud architecture does not recapitulate liver tissues architecture.	(Takebe et al., 2013b)

3.1.4. Strategies available to generate vascularized *in vitro* grown 3D models

A functional vasculature is present in almost all tissues in the body and plays key roles in keeping healthy tissue function. Blood vessels play a fundamental role in supplying cells with oxygen and nutrients, whilst also removing waste products. Additionally, BVs are also essential for tissues to be exposed to hormones, signalling molecules, and immune system cells, whilst also playing important roles in thermoregulation, tissue repair, wound healing, and keeping tissue osmotic balance (Tucker et al., 2022). 3D models, including spheroids and organoids, hold several advantages against 2D ones. However, a common problem of working with such models is that many of them do not vascularize upon *in vivo* transplantation. Because of that, pre-vascularization, i.e., creating a functional microvasculature in *in vitro* generated tissues, prior to *in vivo* transplantation, has emerged as a promising strategy in tissue engineering. By generating a microvasculature before *in vivo* transplantation, the *in vitro* grown tissues are better equipped to establish rapid and efficient blood supply upon transplantation, promoting tissue integration and survival. Thus, given all the previously mentioned roles that vascularization plays in the maintenance of healthy tissues/organs, several strategies have been developed with the aim of pre-vascularizing *in vitro* models.

During tissue formation, vascularization is first promoted through vasculogenesis (or *de novo* vessel formation), where progenitor endothelial cells infiltrate the tissues and fuse to give rise to primitive tubes. Later, angiogenesis kicks in, where new vessels are formed from pre-existing ones. When new blood vessels anastomose with pre-exiting ones a new vasculature is formed and, overtime, these are perfused with blood and further matured when perivascular cells attach to their walls (Tucker et al., 2022). Current approaches available to generate vascularized 3D *in vitro* models can be based on mimicking either vasculogenesis or angiogenesis. Below are the main strategies that can be, and have been, employed to generate vascularized 3D models *in vitro* (Strobel et al., 2023).

3.1.4.1. Co-culture with ECs

Endothelial cells (ECs) are the building blocks of blood vessels thus, co-culture of parenchymal cells with ECs is one of the most common ways to generate vascularized 3D tissues. Here, a process that resembles vasculogenesis takes place, where the ECs organize themselves to give origin to primitive-like tubes. However, this approach often leads to the formation of unstable

vessels due to lack of stabilizing mural cells. Regardless, different studies have shown that adding ECs to their cultures (including to 3D organoid and spheroid cultures) is enough to promote *in vitro* vascularization and, in some cases, engraftment and vascularization success upon *in vivo* transplantation (Dissanayaka et al., 2014; S. Kang et al., 2012; D. H. Lee et al., 2004; Osaki et al., 2018; Pham et al., 2018; Shi et al., 2020; Verseijden et al., 2010). A specific example is the approach by Peng and colleagues, where 3D hepatic organoids (derived from hepatocytes) were co-cultured with ECs on ultra-low attachment plates, which led to the development of vascularized 3D hepatic organoids (Peng et al., 2018).

3.1.4.2. Co-culture with ECs and vessel stabilizing cells

Given that co-culture of parenchymal cells with ECs can lead to unstable blood vessels, additional cells can be added to the culture to promote vessel stabilization and maturation. Among these, one of the most chosen ones are MSCs, given that they play roles in promoting angiogenesis, produce paracrine signals that promote EC survival, and are well known to exhibit pericyte-like characteristics (blood vessel stabilizing cells) (Cristante et al., 2021; Melchiorri et al., 2014). Thus, generation of spheroids *in vitro* through the co-culture of parenchymal cells with ECs and MSCs has been previously done (Ying Tsang et al., 2021). Additionally, co-transplantation of MSCs, ECs and organoids has also shown to increase vascularization success upon *in vivo* transplantation (Sharmin et al., 2016). Another example that demonstrates the success of co-culturing these two cell types with parenchymal cells *in vitro* are liver buds.

Takebe and colleagues first came up with a way of generating liver buds capable of vascularizing for long-term upon *in vivo* transplantation. They did so by co-culturing iPSC-derived hepatic endoderm cells with human umbilical vein endothelial cells (HUVECs) and MSCs, on a Matrigel layer. This resulted in all cell types working together to self-organize into a 3D structure that presented characteristics of a foetal liver and that they called liver bud. Additionally, they also showed that these liver buds could be further matured (regarding hepatic functions) upon *in vivo* transplantation into ectopic locations (Takebe et al., 2013b, 2014). Since then, other people have followed and modified their approach to generate new liver bud models. For example, Ramachandran and colleagues generated liver buds, following Takebe's approach, from adult human primary hepatocytes, liver sinusoidal endothelial and mesenchymal stem cells. They did so using Upcyte cell lines, which consist in primary cells

that have been genetically reprogramed to transiently proliferate. These cells can thus undergo a finite number of divisions (20-40 population doublings), but after removing the proliferation-inducing factors they (mostly) behave like the original primary cells (Ramachandran et al., 2015). Li and colleagues then followed the same approach to generate even more complex liver buds that, in addition to the three initial cell types, also included HSCs. In their approach, all three cell types (HLCs, ECs and HSCs) were differentiated from MSCs (J. Li et al., 2019a).

3.1.4.3. Co-culture with stromal vascular fraction

Tissues are made of parenchymal cells, which carry most of an organ's function, but also of stromal cells, which are defined as a heterogenous group of connective tissue cells that provide support for parenchymal cells. Whitin the stromal cells, there is a stromal vascular fraction (SVF). SVF often refers to specifically adipose tissue derived SVF, since its where its most commonly isolated from. This fraction is specifically composed of all cell types present within the vascular niche, that go beyond endothelial and perivascular cells, including endothelial progenitor, mesenchymal stem, hematopoietic and immune system cells (Valentin et al., 2016). Due to containing stem cells, SFV can be cultured on its own to generate 3D vascularized organoids (Muller et al., 2019), or in co-culture with parenchymal cells. Co-culturing parenchymal cells with cells from the stromal vascular fraction has led to the formation of 3D vascularized structures that have a more complex and relevant microvascular cellular composition than 3D models generated from parenchymal cells alone. A specific example is the work by Nunes and colleagues that generated a 3D vascularized structure capable of hepatic functions that engrafted and vascularized upon *in vivo* transplantation. This was achieved by co-culturing SVF cells and HepG2 cells embedded in collagen (Nunes et al., 2013).

3.1.4.4. Co-culture with isolated micro vessel fragments

Whilst co-culture of parenchymal cells with stromal vascular fraction has proved useful in the successful vascularization of 3D *in vitro* grown tissues, these do not completely recapitulate the complex cellular organization and matrix composition of microvessels seen *in vivo*. Thus, another approach using microvessel fragments (MVF) isolated from tissues has been developed. This approach consists in isolating intact 3D MVFs by digesting away the other tissue cellular components, such as the parenchymal cells. The resulting MVFs, that still retain

their 3D structure, can then be co-cultured with parenchymal cells, leading to the development of a vascularized 3D structure (Strobel et al., 2021). For example, Nalbach and colleagues showed that co-culture of pancreatic islet-cells with MVFs leads to the formation of pre-vascularized islet organoids that have superior vascularization, viability and functionality upon *in vivo* transplantation when compared to islets alone (Nalbach et al., 2021).

Even though generating vascularized 3D liver models *in vitro* adds an additional layer of complexity to traditional 3D models, these still lack the important *in vivo* context. The *in vivo* setting is especially important for the accurate modelling of multifactorial diseases such as NAFLD. Thus, and as previously explored in section 1.3.2., NAFLD *in vivo* models are also available, where the disease is induced through diet, chemicals, or genetic alterations. Nonetheless, given the difficulty of tracking what is happening in the animal's liver over time due to the liver natural position deep in the body, as well as the lack of minimally invasive techniques commonly available in labs to allow liver visualization with good resolution, these models are also not ideal on their own. Thus, better platforms are needed to model NAFLD longitudinally *in vivo*. One such platform that has been widely used to provide good resolution and non-invasive longitudinal power to study a wide range of biological processes, is the anterior chamber of the eye (ACE).

3.1.5. The potential of the ACE as a platform to study NAFLD longitudinally *in vivo*

The anterior chamber of the eye (ACE) has been used as a transplantation site for the longitudinal tracking of several biological processes for more than 150 years. The fact that the iris is highly vascularized contributes for the successful engraftment of different tissues in this location. In fact, the ACE has been used for the transplantation, as mentioned in the previous chapter, of tumours, as well as of healthy tissues from several origins including heart, muscle, prostate, brain, kidney, and liver (Gupta & Chowdhury, 1992; Ilegems & Berggren, 2021; Robert et al., 1998). Consequentially, the ACE has been used to study several biological processes, such as, tissue vascularization, regeneration, and rejection, as well as, immune responses, the initial stages of fertilized egg development, and numerous metabolic processes (Ahlgren & Bengtsson, 1962; Chang et al., 2020; Kistler et al., 2014; Tun et al., 2022). Furthermore, the ACE is also compatible with drug testing, as several studies have shown that cells transplanted into the ACE respond to systemically administered drugs. Nevertheless,

when it comes to using the ACE as a transplantation site, nothing has brought as many novel insights as the transplantation of pancreatic islet (Ilegems & Berggren, 2021; Salem et al., 2019b).

Indeed, research using islets transplanted into the ACE has revealed key insights into islet vascularization, innervation, engraftment and survival, as well as, into islet development and the roles it plays in glycemia control (S. N. Yang & Berggren, 2019). Pancreatic islets, or islets of Langerhans, are small cellular clusters that contain the previously mentioned alpha and beta cells responsible for glucagon and insulin production, respectively, both key players in keeping normal blood glucose levels. Thus, given the previously mentioned roles of (dysregulated) glycemia and insulin signalling in NAFLD onset and progression (see section 1.2.5), islet dysregulation can be tightly connected to NAFLD.

Given the previously mentioned experiments and findings using the ACE as a transplantation site, the question arose as to whether the ACE could also serve as a suitable platform for studying the effects of non-alcoholic fatty liver disease (NAFLD) in the liver. In fact, in the 1930s, Hans Popper transplanted a small piece of liver tissue into the ACE of the same individual. Despite the tissue initially vascularizing and connecting to the iris vasculature, the transplanted tissue rapidly degenerated and eventually disappeared. This is not surprising given that getting adult tissue to engraft in ectopic places is notoriously difficult (Böck & Popper, 1937; Gupta & Chowdhury, 1992). Later, in the 1980s, Rao and colleagues transplanted a suspension of primary hepatocytes into the ACE, however, and even though they were reported to engraft onto the iris for several weeks, no signs of vascularization were mentioned or evident from figures of histological preparations of excised eyes. This means that engrafted hepatocytes probably relied on diffusion of oxygen and nutrients, from the aqueous liquid that fills the ACE, to remain viable, rather than blood perfusion (Rao et al., 1986). This is not surprising, given that triggering and sustaining vascularization depends on the production of pro-angiogenic signals, which the hepatocytes alone, under physiologic conditions, might not be able to do. Nevertheless, establishing a connection to the host's vasculature is crucial for transplanted cells to be exposed to the host's physiological environment, enabling them to experience a true *in vivo* context.

Despite the potential impact on normal cellular roles when transplanting tissues or cells into ectopic locations, the aforementioned studies employing pancreatic islets have convincingly demonstrated their utility as precise indicators of what is going on with *in situ* islets. This includes effectively monitoring changes in beta-cell function and islet volume/mass in response

to various stimuli, like diabetes and drugs (Ilegems & Berggren, 2021). Thus, this chapter aimed to explore whether liver cells transplanted into the ACE would be capable of accumulating fats and whether they could be used as reporters of the host animal liver, in the context of NAFL.

3.2. Hypothesis and aims

There are several *in vitro* hepatic models available to study NAFLD, however, they lack the important *in vivo* context. Likewise, there are plenty of *in vivo* models to study this disease, but these lack the important resolution, or have it, but at the cost of needing expensive lab equipment or animal well-being (for being so invasive). Thus, it was hypothesized that *in vitro* generated liver models transplanted into the ACE could successfully vascularize and accumulate fat in response to host animals being fed a high fat diet, thus being capable of modelling NAFLD. This platform would give the *in vitro* model an *in vivo* context, and the *in vivo* model better resolution at minimum discomfort.

Hypothesis

In vitro generated liver model can engraft and vascularize upon transplantation into the anterior chamber of the eye, and can be used to track NAFLD initiation and initial progression overtime when host is challenged with high fat diet.

Aims

1. Generate liver model *in vitro* capable of vascularizing for long-term upon *in vivo* ACE transplantation
2. Assess if engrafted liver model accumulates fat in response to feeding host HFD
3. Fluorescently tag lipid droplets of liver model cells
4. Use intra-ocular liver model to track NAFLD initiation and progression *in vivo* through intravital imaging

3.3. Materials and methods

3.3.1. Animals

Animal procedures were conducted in accordance with the Animals (Scientific Procedures) Act 1986. Animals used in this project were C57Bl/6J and SCID purchased from Charles River. Animals that received transplantation of cells were monitored daily for up to 60-days, and no adverse effects were recorded during any experiment.

3.3.2. Cell lines

3.3.2.1. Liver organoids

Isolation: The liver organoids were generated before the beginning of this PhD by Dr Alexandra Milona. They were generated and maintained following (Huch et al., 2013) protocol. Briefly, bile ducts were dissected from the mouse liver and bile duct fragments were seeded on growth factors reduced Matrigel (Corning).

Maintenance: (Bile duct/stock) organoids were expanded once a week, re-fed every two days with expansion medium and kept at 37°C, 5% CO_2. Expansion medium was composed of Advanced DMEM/F12 (Invitrogen) supplemented with 1% Pen/Strep (Gibco), 1% Hepes (Thermofisher), 1x GlutaMax (Thermofisher) 1% B27 (Gibco), 1.25 mM N-Acetylcysteine (Sigma), 10 nM gastrin (Sigma), 50 ng/ml EGF (Peprotech), 10% rSpondin1 conditioned media, 100 ng/ml FGF10 (Peprotech), 25 ng/ml HGF (Peprotech) and 10 mM Nicotinamide (Sigma).

Differentiation: liver organoids were split as usual, seeded and kept for two to four days under the usual expansion medium. Then, the medium was changed to contain 50 ng/ml EGF (Invitrogen), 100 ng/ml FGF10 (Peprotech), 50 nM A8301 (Tocris Bioscience), 10nM Gastrin 12 (Sigma) and 10 μM DAPT (Sigma-Aldrich), and 30 μM dexamethasone (Sigma) for the last three days of the differentiation. Differentiation medium was changed every other day for a period of nine to fourteen days.

Fluorescent tagging: undifferentiated liver organoids were kindly tagged by Dr Alexandra Milona, where plasmids expressing GFP under the control of FoxO1 gene (Addgene) were transduced by lentiviral vectors according to standard protocols prior to antibiotic selection of positive cells.

3.3.2.2. Hepatic endothelial cells

Isolation: Endothelial cells were isolated from liver, based on a previously published protocol. Briefly, two mice from 2 to 6 weeks old were culled, livers were excised and minced into small pieces and digested in collagenase type I (200 U/ml, Gibco) for 1h with constant rotation. The digested suspension was then passed through a 70μm cell strainer to remove large undigested blocks and washed with PBS2.5%BSA. The pellet was then incubated in 0.125%Trypsin0.01%EDTA to obtain a single cell suspension for 10 minutes. Trypsin was discarded and the pellet washed with PBS2.5%BSA. Endothelial cells were then isolated with miniMACs kit (Milteny Biotech). Briefly, cells were incubated with FC blocking solution at 4°C for 30 minutes, washed twice in PBS2.5%BSA and further incubated with rat anti-mouse CD31 (BD Pharmingen), rat anti-mouse CD105 (BD Pharmingen) and biotinylated isolectin B4 (BD Pharmingen) for 30 minutes at 4°C. After two more washes with buffer, the pellet was incubated with anti-rat and streptavidin-conjugated microbeads for 15 min at 4°C, and loaded into the columns according to manufactures instructions. Finally, the cells were washed and seeded onto plates pre-coated with 0.1% gelatine (Sigma) in commercial endothelial cells medium (Cat#M1168, Generon) at a density of $3x10^5$ cells/cm^2.
Maintenance: Cells were re-fed every two days and kept in a 37°C and 5% CO_2 atmosphere. They were split once a week with TryplX (Gibco) and kept for a maximum of 2 passages.

3.3.2.3. Mouse mesenchymal stem cells

Maintenance: OriCellTM STRAIN C57BL/6 MOUSE Mesenchymal Stem Cells (Cat# MUBMX-01001) isolated from bone marrow were purchased from Cyagen and kept according to manufactures instructions. Briefly, cells were kept in OriCellTM Mouse Mesenchymal Stem Cell Growth Medium in a 37°C and 5% CO_2 atmosphere, re-fed every other day and split with TryplX when 80% confluent.

3.3.2.4. Human embryonic stem cells

Maintenance: hESCs were kept on a matrigel layer (1:20) in maintenance medium. Cells were kept at 37°C and 5% CO_2, re-fed every other day and passaged with accutase when 70%

confluent. Maintenance medium: KSR medium supplemented with 10 ng/ml of bFGF (Peprotech).

Differentiation: For differentiation experiments, hESCs (WiCell Research Institute) were passaged as usual and seeded at 5 x 10^5 cells per (Matrigel-coated) well of a 6-well plate (Corning) in maintenance medium. 24h later, the cells were differentiated into definitive endoderm by exposure to definitive endoderm medium for 3 days, followed by 5 more days in Hepatic endoderm medium to generate hepatic endoderm cells. At this stage, cells were trypsinized and used to make liver buds. Definitive endoderm medium: RPMI/B27 supplemented with Activin A (100ng/ml)(Qkine) and Torin (15nM)(Bio-techne); Hepatic endoderm medium: DMEM containing 20% KSR medium supplemented with BMP4 (20ng/ml)(Peprotech) and bFGF (10ng/ml); Hepatocyte maturation medium: HCM medium (Lonza) supplemented with HGF (20ng/ml)(Peprotech) and OSM (20ng/ml)(Biotech).

3.3.3. Assessing fat storing and *de novo* lipogenesis capacity *in vitro*

To assess fat storage capacity cells were treated with water-soluble oleic acid (300uM, Sigma) overnight, or for 3 days with re-feeding every day. To assess DNL, cells were treated with differentiation medium, or differentiation medium supplemented with 1720nM insulin or supplemented with 5.5mM glucose, 10mM fructose and 1720nM insulin, as previously shown (Kozyra et al., 2018). For lipid droplet staining, cells were incubated with LipidTOX (ThermoFisher) for 40 minutes, stained with DAPI, washed, and mounted in Vectashield (VectorLabs).

3.3.4. RT-qPCR

RNA extraction: organoids were collected from Matrigel and washed in cold 1xPBS. The organoids pellet was then snap frozen in liquid nitrogen, and 500ul trizol (Fisher Scientific) and 1 steel bead (Qiagen) were added per Eppendorf. The samples were then mechanically homogenized for 3 minutes at 30Hz using a tissue homogenizer. 500ul chloroform were then added to each Eppendorf followed by centrifugation at 12000g for 15 minutes. The supernatant was then transferred to a new Eppendorf, 500ul of 70% isopropanol were then added to it and the tubes were gently inverted, before being centrifuged at 16000g for 15 minutes. The

supernatant was then discarded, and great care was taken not to disturb the RNA pellet. The pellet was then washed with 70% ethanol and let to air dry. Finally, the RNA pellet was re-suspended in RNAse-free water, the concentration measured using a spectrophotometer (NanoDrop) and stored at -80ºC until needed. cDNA synthesis: cDNA was made from 1ug of total RNA samples using the iScript™ cDNA Synthesis Kit (Bio-Rad) as per manufactures instructions. qPCR: qPCR was performed using iTaq™ Universal SYBR® Green (Bio-Rad) as per manufactures instructions, and the primers used were cyclophilin (housekeeping)(M_Ppif_1), G6Pase (m_g6pc_1) and ApoC2 (M_Apoc2_1)(kickstart primers, Bio-Rad, UK).

For data on Figure 3.15, RNA was extracted using Tri Reagent (Sigma), and cDNA using the Protoscript II reverse transcriptase (NEB). Then, qPCR was done with Sybr Green Jumpstart Taq ready Mix (Merk) using a StepOnePlus real time PCR system (Applied Biosystems) and the primers from Table 3.3.

The relative quantification of target gene expression was calculated using the $2^{-\Delta Ct}$ method with normalization to the respective housekeeping genes.

Table 3.3. List of primers used in data from Fig. 3.15.

Gene	Forward Primer (5'- 3')	Reverse Primer 3'-5'
AFP	TGGGACCCGAACTTTCCA	GGCCACATCCAGGACTAGTTTC
ALB	CCTTTGGCACAATGAAGTGGGTAACC	CAGCAGTCAGCCATTTCACCATAGG
FoxA2	GGGAGCGGTGAAGATGGA	TCATGTTGCTCACGGAGGAGTA
Sox17	GGCGCAGCAGAATCCAGA	CCACGACTTGCCCAGCAT
Sox2	GCCGAGTGGAAACTTTTGTCG	GCAGCGTGTACTTATCCTTCTT
Oct4	TCGAGAACCGAGTGAGAGGC	CACACTCGGACCACATCCTTC
RPL22	TCGCTCACCTCCCTTTCTAA	TCACGGTGATCTTGCTCTTG

3.3.5. Generation of engraftable liver model

3.3.5.1. Using liver organoids

3.3.5.1.1. Seeding 3D differentiated organoids and ECs in ULA plates

Bile duct organoids were first differentiated, and endothelial cells isolated as previously mentioned (see sections 3.3.2.1. and 3.3.2.2., respectively). Then, differentiated organoids were collected from Matrigel with cold PBS, and washed twice in cold PBS through centrifugation. Endothelial cells were tripsinized and re-suspended in 1:1 medium, which

consisted in an equal mixture of EC medium and Organoid differentiation medium. One organoid and 2000 ECs were cultured per well of 96-well ULA plate (Corning). Medium was changed every day.

3.3.5.1.2. Seeding 3D differentiated organoids, ECs and MSCs in ULA plates

Organoids and ECs were prepared as previously described in section 3.3.5.1.1. MSCs were kept as explained in section 3.3.2.3. and were tripsinized into a single cell suspension. Then, one organoid, 2000 ECs and 570 MSCs were re-suspended in warm 1:1 medium (ECs medium : Organoid differentiation medium with Dex) and immediately seeded per well of 96-well ULA plate. Medium was changed every day.

3.3.5.1.3. Seeding differentiated organoid-derived single cells, ECs and MSCs in ULA plates

ECs and MSCs were prepared as previously explained (see section 3.3.5.1.1. and 3.3.5.1.2., respectively). Differentiated organoids were collected from Matrigel with cold PBS and washed twice through centrifugation. They were mechanically dissociated into smaller cell clusters, and then incubated with 0.125%Trypsin0.01%EDTA for 20 min to obtain a single cell suspension. Then, 450 single cells from differentiated organoids, 315 ECs and 90 MSCs were re-suspended in warm 1:1 medium (ECs medium : Organoid differentiation medium with Dex) and immediately seeded per well of 96-well ULA plate. Medium was changed every day.

3.3.5.1.4. Seeding differentiated organoid-derived single cells, ECs and MSCs on Matrigel

Pre-chilled flat bottom 96-well plates (Thermofisher) were coated with cold diluted Matrigel (2:1 mixture of Matrigel : ECs medium) and incubated for 30-60 minutes at 37°C. Single cells from differentiated organoids, ECs and MSCs were prepared as previously explained (see sections 3.3.5.1.3., 3.3.5.1.1. and 3.3.5.1.2., respectively). Cells were seeded according to the ratio optimized by Takebe and colleagues (10:7:2, HLCs:ECs:MSCs). Then, Matrigel coated plates were removed from 37°C and $4x10^4$ single cells from differentiated organoids, $2.8x10^4$ ECs and $8x10^3$ MSCs were re-suspended in warm 1:1 medium (ECs medium : Organoid

differentiation medium with Dex) and immediately seeded per well. Medium was changed every day.

3.3.5.2.Using HLCs

3.3.5.2.1. Seeding hHE cells, ECs and MSCs on Matrigel

Matrigel coated plates, ECs and MSCs were prepared as previously described (see sections 3.3.5.1.4., 3.3.5.1.1. and 3.3.5.1.2.). hESCs were differentiated into HE cells as previously described (see section 3.3.2.4.). Cells were seeded according to the ratio optimized by Takebe and colleagues (10:7:2, hHE cells:ECs:MSCs). Then, hHE cells were tripsinized and, when 96-well plates were used, $4x10^4$ single cells from differentiated organoids, $2.8x10^4$ ECs and $8x10^3$ MSCs were re-suspended in warm 1:1 medium (ECs medium : Hepatocyte maturation medium) and immediately seeded per well. When 384-well plates were used, $2.1x10^4$ hHE cells, $1.5x10^4$ ECs and $4.2x10^3$ MSCs were re-suspended in warm 1:1 medium (ECs medium : Hepatocyte maturation medium) and immediately seeded per well. Medium was changed every day.

3.3.6. Transplantation of *in vitro* models into the ACE

In vitro models were injected into the anterior chamber of the eye following a previously published protocol (Salem et al., 2019a). Briefly, animals were anaesthetized with isoflurane and placed in a stereotactic frame. Then, organoids and LBs were aspirated (in 1xPBS) into a blunt cannula inserted in a 100µl screw actuated syringe (Hamilton). Then, a small incision was made in the cornea using a 27G needle, and the cannula inserted in the anterior chamber of the eye. Lastly, 1-3 organoids/LBs were released per eye and the cannula carefully removed.

3.3.7. *In vivo* imaging

In vivo intra ocular imaging was performed as previously shown (Speier et al., 2008). Bright field images were acquired using a Nikon camera attached to a microscope, whilst animals were under isoflurane anaesthetic.

3.3.8. Immunocytochemistry

Cells were fixed with 4% PFA for 30 min. For immunostaining a standard protocol was then performed using the following antibodies: anti-GFP-AlexaFluor 488 conjugate (Invitrogen); rat CD31 (BD Pharmingen), rat CD105 (BD Pharmingen), rabbit HNF4a (abcam), rabbit CD44 (abcam), mouse anti-albumin (Merck, A6684, 1:100), rabbit anti-AFP (Abcam, ab169552, 1:500), rabbit anti-E-cadherin (CST, #3195, 1:200), AlexaFluor 488 (Thermo) and AlexaFluor 633 (Thermo). Dapi (Invitrogen) was used to counterstain the nucleous and slides were mounted with Vectashield (VectorLabs). Primary antibodies were used at 1:200, unless specifically mentioned otherwise, and secondary antibodies at 1:1000. Confocal fluorescent images were acquired using the Zeiss LSM-780 inverted microscope and analysed using Fiji software.

3.3.9. Immunohistochemistry of eye slices

Mice were euthanized and the eyes excised and fixed in 4% PFA (in PBS) overnight at 4C. They were then transferred to 30% sucrose solution for 2 days, embedded in cryoembedding matrix (OCT, Thermo) and stored at -80°C until needed. The eyes were sliced (5, 10 or 30um) using a cryostat and immediately transferred to poly-D-lysin/Superfrost Plus slide (VWR).
For immunostaining, a standard protocol was then performed using the following antibodies: anti-GFP AlexaFluor 488 conjugate (Invitrogen); CD31 (BD Pharmingen) and AlexaFluor 488 (Thermo). Primary antibodies were used at 1:200 and secondary antibodies at 1:1000.
Ex vivo confocal fluorescent images were acquired using the Zeiss LSM-780 inverted microscope and analyzed using Fiji software.

3.3.10. Albumin ELISA

Albumin levels were measured using the human Albumin ELISA kit (Merk) in medium samples of HLCs on day 13 of the differentiation protocol. Medium had been changed 24h prior to collection. Medium incubated for 24h without cells was used as control. After medium samples were taken, HLCs were collected and counted.

3.3.11. Statistical analysis

Statistical test used were Unpaired t-test and One-way ANOVA, on GraphPad Prism.

3.4. Results

3.4.1. Attempting to generate liver model capable of vascularizing *in vivo* using liver organoids

3.4.1.1. Differentiated liver organoids only

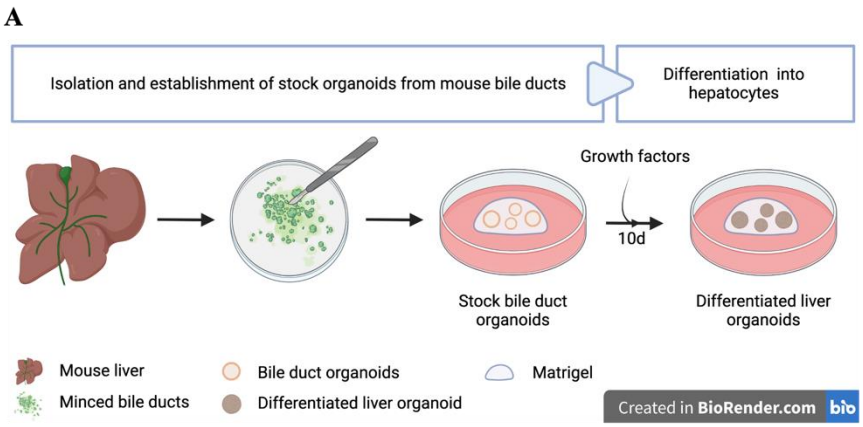
3.4.1.1.1. Isolation and validation of hepatic organoids

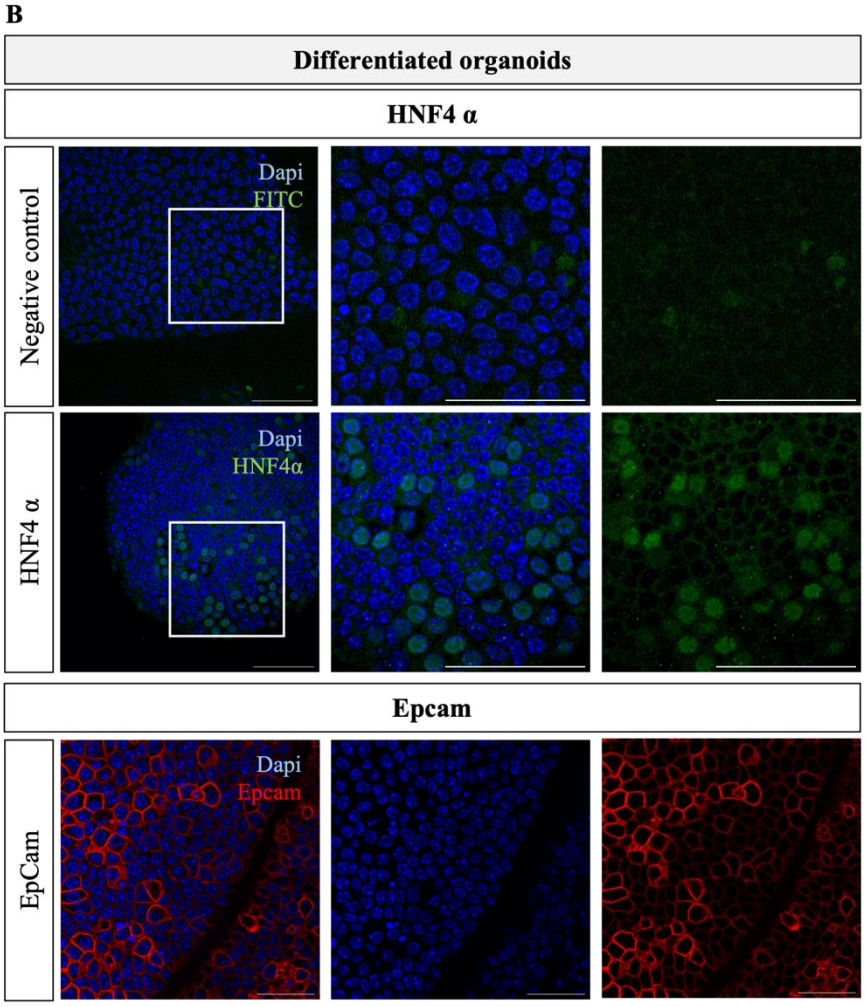
This chapter aimed to develop a platform that was easy and quick to set up in any lab. To do so, attempts were carried out to generate an engraftable NAFLD model *in vitro*, using liver organoids isolated from adult mouse tissue first. Liver organoids were specifically chosen (as opposed to other primary models) due to the advantages mentioned earlier in this chapter, including good hepatic function and possibility of long-term culture (essential for the following aim of fluorescent tagging of lipid droplets). These organoids were isolated from mouse bile ducts and were kept as a stock of undifferentiated bile duct organoids, as originally shown by Huch and colleagues. Bile duct organoids can be kept in culture for months and have been shown to have the capacity to commit into the hepatocyte-lineage upon exposure to a defined cocktail of growth factors. Thus, for experiments, bile duct organoids were differentiated into the hepatocyte lineage, also as previously shown, and are hereafter referred to as differentiated liver organoids (Huch et al., 2013) (see section 3.3.2.1.) (Fig. 3.1a).

The differentiation of bile duct organoids into the hepatocyte lineage was validated by assessing the expression of hepatocyte markers, such as, hepatic nuclear factor 4a (HNF4a), through immunostaining (Fig. 3.1b), and glucose-6-phosphatase (G6Pase) and apolipoprotein C2 (ApoC2), through qPCR (Fig.3.1c). Not surprisingly, due to the reported heterogeneity of the cells that compose the same organoid, HNF4a expression was present in many, but not all organoid cells. The expression of the liver stem cell and immature hepatocyte marker, EpCam, was also assessed through immunofluorescence. EpCam expression in the developing liver *in vivo* gradually decreases as the hepatocytes mature (Huch & Dollé, 2016). However, and as shown by Huch and colleagues, some EpCam expression was still retained in differentiated organoids (Fig. 3.1b). qPCR experiments revealed that differentiated organoids expressed G6Pase and ApoC2, whilst stock bile duct organoids did not. However, but as expected, differentiated liver organoids ApoC2 and G6Pase expression levels were still greatly reduced when compared to liver tissue. Overall, these findings align with Huch and colleagues' research, as they demonstrate the potential of bile duct organoids to differentiate into the

hepatocyte lineage. However, like many existing differentiation strategies and protocols, liver organoid hepatocyte-like cells still exhibit immaturity rather than achieving full maturation.
Experiments were then carried out to assess whether the differentiated liver organoids were capable of performing hepatic functions. Organoids capacity to accumulate fat was evaluated first, given that this is a key requirement to model NALFD *in vitro*. As previously explained in chapter I, the fat that accumulates in the liver of NAFLD patients has three main sources: uptake of diet-derived fats, uptake of fats from the circulating pool of non-esterified fatty acids (NEFA) and *de novo* lipogenesis. To investigate differentiated organoids capacity for fat uptake, organoids were exposed to oleic acid (OA) and their response was assessed through staining with a lipid-specific dye – LipidTOX. These experiments showed that differentiated liver organoids were capable of accumulating fat when challenged, and that the extent of fat accumulation seemed to increase with longer exposer to OA (Fig. 3.2a). Then, experiments were carried out to evaluate differentiated liver organoids capacity for *de novo* lipogenesis. *De novo* lipogenesis consists in the synthesis of fat from non-lipid precursors like, for example, sugars, with fructose being the most potent DNL-inducing one. Thus, differentiated organoids were next exposed to glucose and fructose in the presence of insulin, as previously done (Kozyra et al., 2018). Despite a trend showing that the differentiated organoids exposed to sugars accumulated more fat than vehicle controls, this difference did not reach statistical significance, even after 7 days of treatment (Fig. 3.2b). Thus, additional experiments, using higher concentration of sugars, should be performed. Overall, these experiments suggested that differentiated organoids can effectively accumulate fat when challenged with fatty acids and may also be capable of DNL although additional experiments are needed to address this.

Thus, bile duct organoids that can be differentiated into liver organoids with hepatic functions were successfully established, as originally showed by Huch and colleagues.


A
Isolation and establishment of stock organoids from mouse bile ducts
Differentiation into hepatocytes
Growth factors
10d
Stock bile duct organoids
Differentiated liver organoids
Mouse liver
Minced bile ducts
Bile duct organoids
Differentiated liver organoid
Matrigel
Created in BioRender.com


B
Differentiated organoids
HNF4 α
Negative control
Dapi
FITC
HNF4 α
Dapi
HNF4α
Epcam
EpCam
Dapi
Epcam

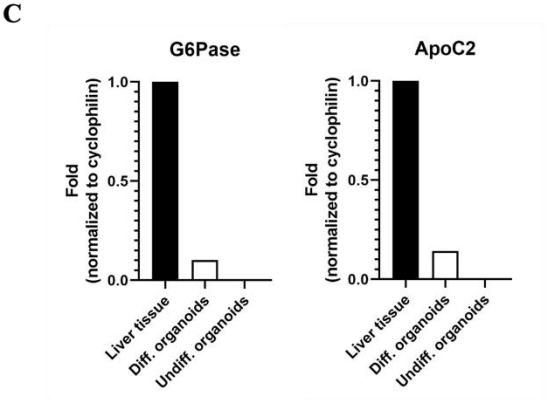

C
G6Pase
ApoC2
Fold
(normalized to cyclophilin)
1.0
0.5
0.0
Liver tissue
Diff. organoids
Undiff. organoids

Figure 3.1. Validation of the differentiation of isolated liver organoids. A) Schematic illustrating isolation and differentiation of liver organoids. Briefly, mice livers were digested, and bile ducts collected. Bile ducts were then minced and cultured in matrigel. For differentiation into hepatocyte-lineage, organoids were cultured in differentiation medium containing growth factors for approximately 10 days. B) Confocal images of differentiated liver organoids expressing hepatic-lineage markers HNF4a (green) and EpCam (red), and nuclear dye dapi (blue). Scale bars are 30µm and 50µm for insets. C) qPCR data showing that differentiated organoids express hepatocytes markers G6Pase and ApoC2 in sharp contrast to undifferentiated ones, but still to a less extent than hepatocytes from liver tissue.

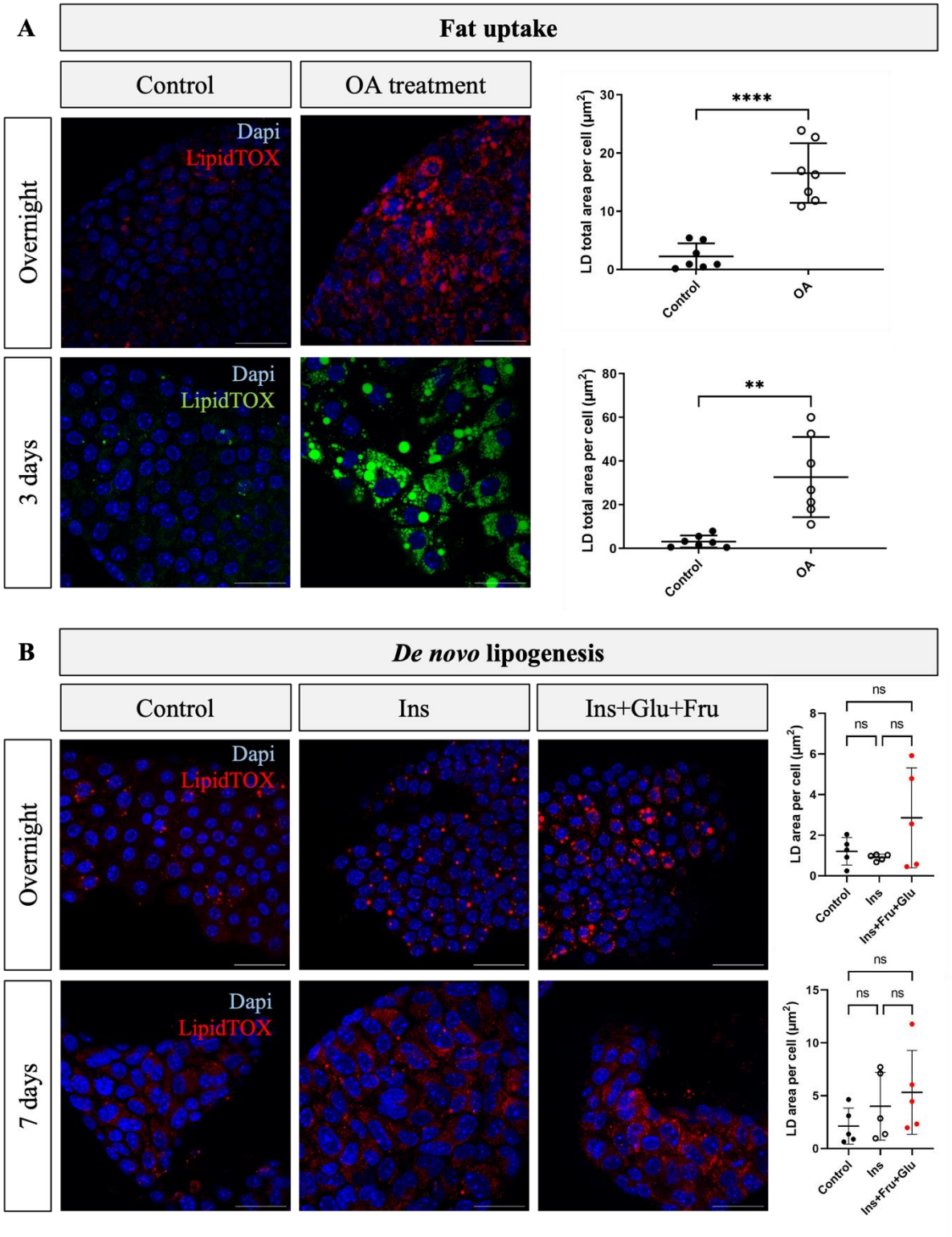


Figure 3.2. Liver organoids differentiate into functional hepatic organoids capable of fat uptake, and maybe *de novo* lipogenesis. A) Confocal images of differentiated liver organoids treated with oleic acid (OA) overnight or for 3 days, and stained with lipidTOX (green or red) and nuclear dye dapi (blue). Graphs showing quantification of lipid droplet area per cell, in controls and oleic acid treated organoids. Unpaired t-test; ** p-value < 0.01, **** p-value < 0.0001; B) Confocal images of differentiated liver organoids treated with insulin or insulin (Ins), glucose (Glu) and fructose (Fru), overnight and for 7 days, and stained with lipidTOX (red) and nuclear dye dapi (blue). Graphs with quantification of lipid droplet area per cell, in controls and oleic acid treated organoids. Scale bars: 30μm. Each symbol represents one organoid. One-way ANOVA; ns: p-value > 0.05.

3.4.1.1.2. Transplantation of differentiated liver organoids into ACE

Huch and colleagues showed that liver differentiated organoids can engraft onto mice liver upon orthotopic transplantation (Huch et al., 2013). Thus, next it was investigated if the differentiated liver organoids were also capable of engrafting onto the iris after being injected into the anterior chamber of the eye (ACE) of a host animal. Differentiated organoids were transplanted into the ACE as previously explained (see section 3.3.6.). However, even though they seemed to adhere to the iris, they never vascularized and eventually started shrinking until completely disappearing after a few days (Fig. 3.3 and data not shown).

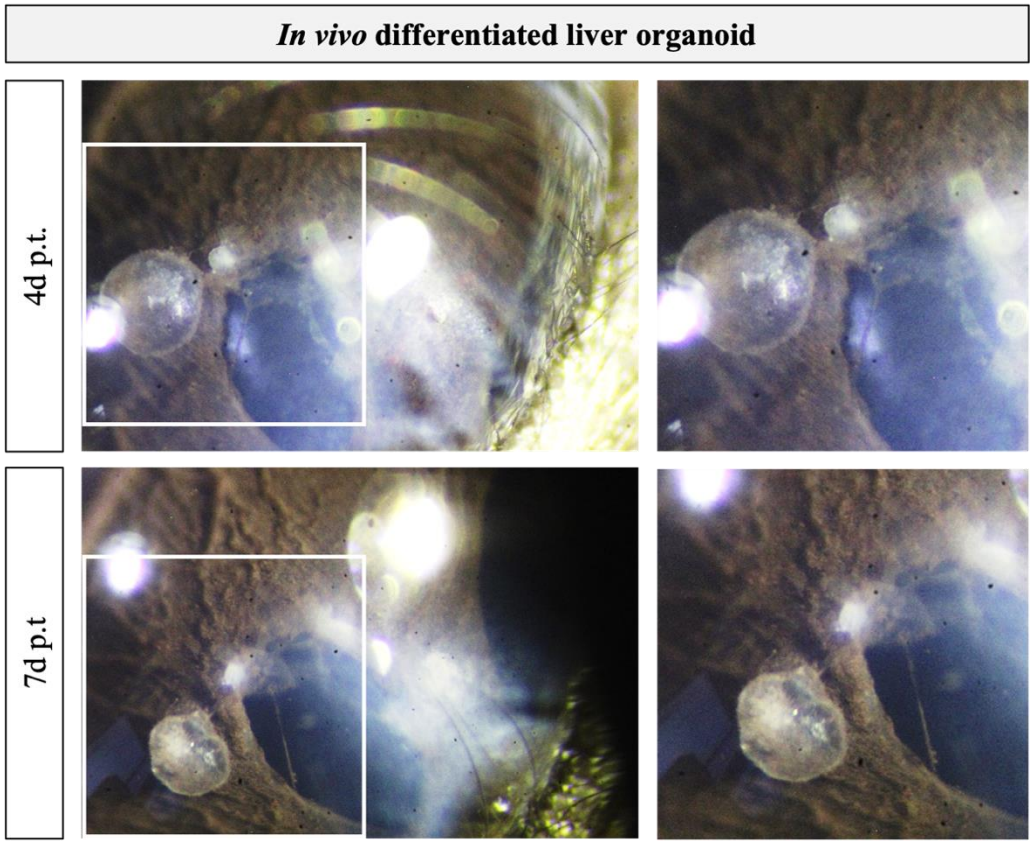


Figure 3.3. Differentiated liver organoids do not vascularize after transplantation into the anterior chamber or the eye. Bright field images of the same mouse taken 4 and 7 days post-transplantation (p.t). 4x magnification and insets are digitally zoomed in areas

3.4.1.2. Differentiated liver organoids enriched with endothelial cells

Differentiated liver organoids did not vascularize upon transplantation into the ACE. Angiogenesis, the most common type of post-natal vascularization in healthy tissues, is triggered by pro-angiogenic factors. Even though hepatocytes are known to express pro-angiogenic factors at low levels constitutively, and higher levels in response to stress situations, like liver regeneration (Fernández et al., 2009), the fact that liver organoids did not vascularize *in vivo* was not surprising, since generation of engraftable and vascularized adult organoids is notoriously difficult (H. Li et al., 2021). It has been shown that depending on the transplantation site, organoids vascularization can stem from the organoid itself, or from the hosts vasculature (Daniel & Cleaver, 2019). Since the differentiated liver organoids do not have endothelial cells, and given that endothelial cells are also known to produced proangiogenic factors key in triggering angiogenesis, it was hypothesised that enriching differentiated organoids with ECs could improve engraftment/vascularization rate. Successful co-culture of 3D liver organoids (established from hepatocytes) and endothelial cells (isolated from human umbilical vein) has previously been done. However, despite the successful development of an EC-rich organoid, no experiments were conducted to assess its vascularization capacity upon *in vivo* transplantation (Speier et al., 2008). As mentioned in chapter I, liver ECs play a key role in efficient fat uptake by the liver. This is because of their characteristic fenestrations, that allow for the easy movement of fats from blood to the hepatocytes. Hence, considering that the project's objective involved transplanting the *in vitro* generated model into a host mouse to induce NAFLD through high-fat diet feeding, it became evident that the utilization of endothelial cells specifically isolated from the liver held significance for the prospective success of this platform.

3.4.1.2.1. Isolation and validation of hepatic endothelial cells

To isolate ECs from mouse liver, a previously published protocol by Marelli-Berg and colleagues was followed and optimized (Marelli-Berg et al., 2000). Briefly, the mouse liver is collected, digested, and dissociated into single cells that are then labelled with antibodies against markers of ECs. The cells are then incubated with magnetic microbeads conjugated with the appropriate secondary antibody, and finally sorted using magnetic cell sorting (see methods section 3.3.2.2.) (Fig. 3.4a). The identity of the isolated endothelial cells was assessed

through immunofluorescent staining against the endothelial cell markers CD31 and CD105. These experiments revealed that most cultured cells were indeed ECs (Fig. 3.4b). Isolated ECs function was also investigated through the tube formation assay. Briefly, whilst endothelial cells exhibit a cobble form under usual maintenance conditions, i.e., when seeded on gelatine-coated plates, they have the capacity to form tube-like structures when seeded on Matrigel. Both characteristics were observed in the ECs isolated from mouse liver (Fig. 3.4c). Thus, ECs were successfully isolated from mouse liver tissue.

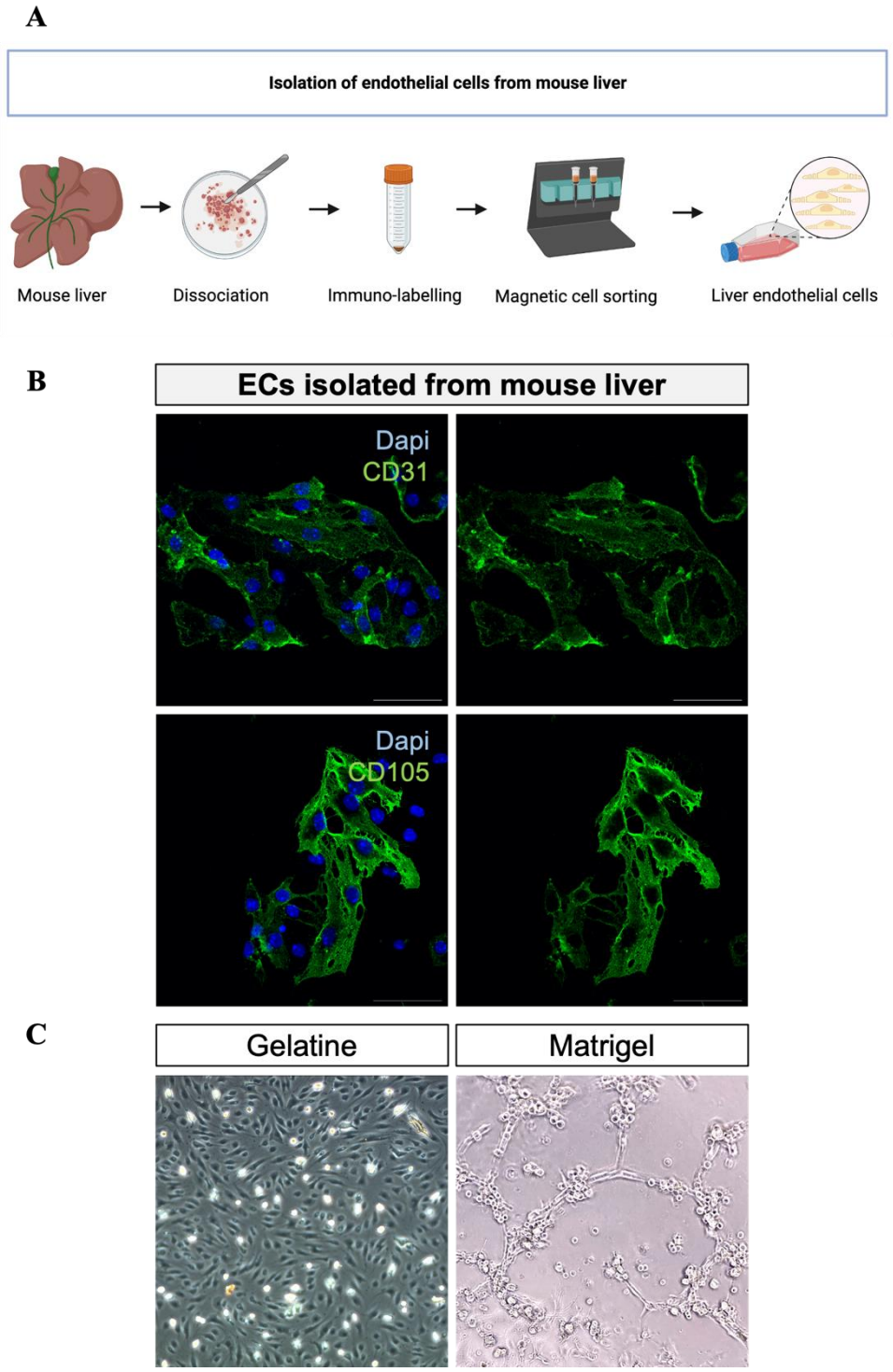


Figure 3.4. Validation of endothelial cells isolated from mouse liver. A) Schematic illustrating how endothelial cells were isolated. Briefly, mouse livers were minced and dissociated into single cells. Cells were then incubated with antibodies against endothelial cell markers, followed by incubation with anti-rat microbeads. Finally, labelled cells were separated using a magnetic cell sorter, and plated; *Created in BioRender*. B) Confocal images of isolated endothelial cells stained for CD31, CD105 (green) and dapi (blue). Scale bars are 50um; C) Brightfield images of isolated endothelial cells seeded on gelatine vs matrigel coated plates. 10x magnification. ECs: endothelial cells.

3.4.1.2.2. Co-culture of differentiated liver organoids and endothelial cells on ULA plates

Next, differentiated organoids were co-cultured with hepatic endothelial cells, as previously shown (Peng et al., 2018) (see methods section 3.3.5.1.1.). Briefly, one organoid and 2000 ECs were seeded per well of a 96-well ultra-low attachment (ULA) plate (Fig. 3.5a). These plates undergo a special treatment to prevent cell attachment to its surface, thus promoting ECs adhesion to the organoid instead. Because organoids size can vary widely within the same well, organoids were filtered through cell strainers, so that only organoids larger than 100µm would be used for co-culturing experiments. A few days after co-culturing, the ECs could be observed coating the differentiated organoids surface (Fig. 3.5b).

To have a better look at the interaction between differentiated organoids and ECs, immunofluorescent staining experiments were performed on EC-coated organoids. These confirmed that ECs were indeed attached to the organoid surface, but that their distribution was uneven (Fig. 3.5c).

Nevertheless, differentiated organoids were successfully enriched with primary hepatic endothelial cells.

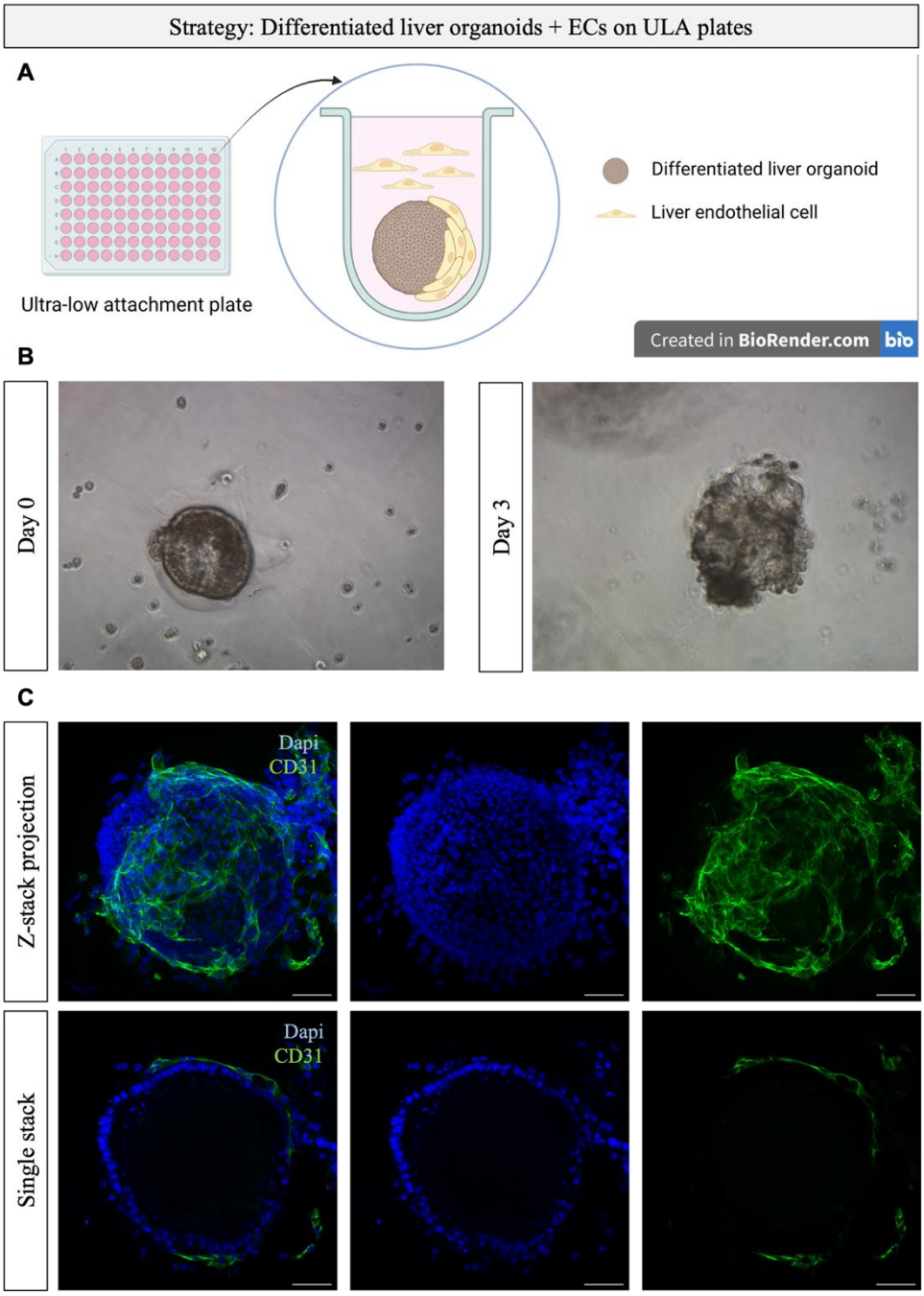


Figure 3.5. EC-rich liver organoid made from co-culturing differentiated liver organoids and endothelial cells (ECs) on ultra-low attachment (ULA) plate. A) Schematic of how EC-rich liver organoids were made. B) Bright-field image of EC-rich liver organoid 0 and 3 days after co-culture with endothelial cells. B) Confocal images of EC-rich liver organoid stained for endothelial cell marker CD31 (green) and nuclear dye Dapi (blue). Upper panel shows z-tack projection and lower panel single stack. Scale bars are 50µm.

3.4.1.2.3. Transplantation of differentiated liver organoids enriched with ECs into the ACE

The EC-rich differentiated organoids were then transplanted into the ACE of host mice as previously explained (see section 3.3.6.). Despite a few blood-perfused vessels initially

forming around some of the transplanted organoid's surface, these did not look robust and eventually retracted after only a few days (Fig. 3.6). This was followed by the shrinking of the organoid that eventually disappeared (Fig. 3.6 and data not shown).
Thus, EC-rich organoids cannot be used to model NAFLD *in vivo* using the ACE.

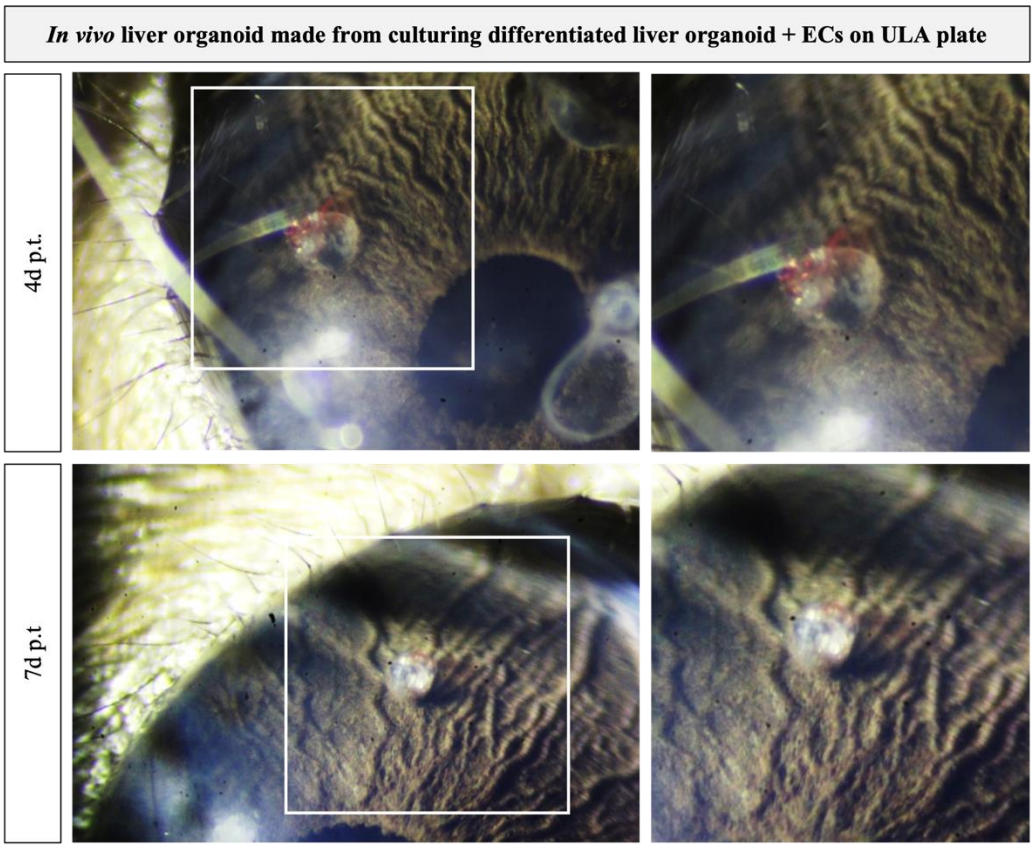


Figure 3.6. Liver organoid made from differentiated liver organoids and endothelial cells (ECs) briefly vascularize after transplantation into the anterior chamber or the eye. Bright field images of the same mouse taken 4- and 7-days post-transplantation (p.t.).

3.4.1.3. Differentiated liver organoids enriched with endothelial and mesenchymal stem cells

3.4.1.3.1. Co-culture of differentiated organoids with endothelial and mesenchymal stem cells on ULA plates

Mature blood vessels are made not only from endothelial cells, but also from stabilizing mural cells. Mesenchymal stem cells (MSCs) have been shown to differentiate into blood vessel-stabilizing perivascular cells when co-cultured with endothelial cells (Koike et al., 2004; Takebe et al., 2012, 2013b). Thus, given that the blood vessels formed around the EC-rich

differentiated organoids quickly regressed, next mesenchymal stem cells (MSCs) were also added into the co-culture system. Even though the isolation of MSCs from bone marrow was planned to be carried out by us in the lab, the optimization of such protocols is often time-consuming. Thus, to quickly assess whether this approach would lead to the formation of an engraftable structure capable of vascularizing upon *in vivo* transplantation, initial experiments were carried out with commercially available MSCs. For the MSCs to have the capacity to differentiate into blood vessel stabilizing cells, their stemness must be preserved, so their stemness was first validated through CD44 immunostaining experiments (Fig. 3.7). Then, differentiated liver organoids, ECs and MSCs were co-cultured on ULA plates (Fig. 3.8a) as explained in section 3.3.5.1.2.. Generation of vascularized liver organoids from co—culturing HLC, ECs and MSCs in ULA plates has been previously done, although no transplantation experiments were conducted to validate whether these could actually vascularize *in vivo* (Ying Tsang et al., 2021). After only a few days, the ECs and MSCs coated the organoid's surface (Fig. 3.8b). To assess the distribution of MSCs and ECs on the differentiated organoids, immunofluorescent staining experiments using antibodies against ECs and MSCs markers (CD31 and CD44, respectively) were then performed. To enable the visualization of the differentiated organoid, this time organoids that expressed cytoplasmic GFP constitutively (FoxO1-GFP) that were available in the lab were used (see methods section 3.3.2.1). These experiments confirmed that the co-culture of those 3 cell types resulted in an organoid coated with ECs and MSCs (Fig. 3.8c). Thus, EC-MSC-rich differentiated liver organoids were successfully generated.

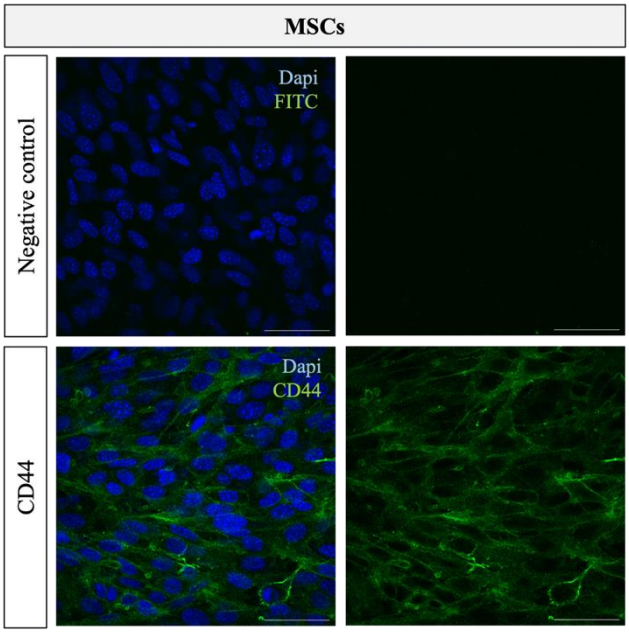


Figure 3.7. Mesenchymal stem cells stain positive for CD44. Confocal images of cultured mesenchymal stem cells stained for CD44 or IIAB-only (FITC) (green) and nuclear dye dapi (blue). Scale bars are 50μm.

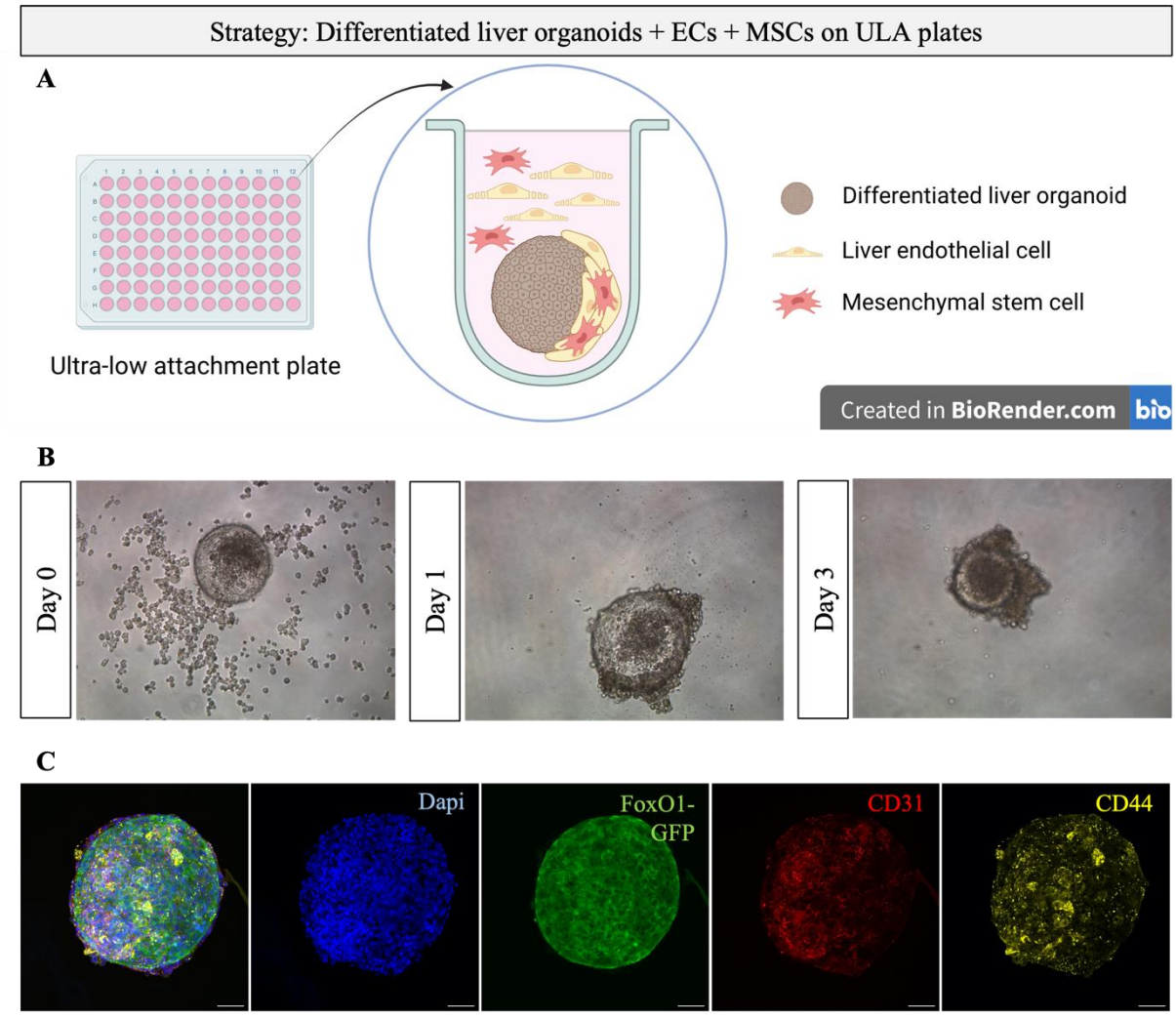


Figure 3.8. Liver organoid made from differentiated organoids, endothelial cells (ECs) and mesenchymal stem cells (MSCs) on ultra-low attachment (ULA) plate. A) Schematic of how liver organoids were made. B) Bright-field images of liver organoid 0, 1 and 3 days after co-culture with liver endothelial and mesenchymal stem cells. C) Confocal images of liver EC-MSC-rich organoids stained for CD31 (red), CD44 (yellow) and nuclear dye dapi (blue), and showing FoxO1-GFP liver organoids in green. Scale bars are 50μm.

3.4.1.3.2. Transplantation of differentiated liver organoids enriched with endothelial and mesenchymal stem cells into the ACE

EC-MSC-rich organoids were then transplanted into the ACE. This time, visibly more robust blood vessels formed around the organoid. However, the blood vessels seemed to disappear

between 7 and 14 days post-transplantation (Fig. 3.9). To confirm this, eyes from mice 7 and 14 days post-transplantation were excised and sliced. As expected, while vessels surrounding the organoid could clearly be seen on day 7 (Fig. 3.10a), by day 14 these were completely gone, and so was most of the liver organoid (FoxO1-GFP), as evidenced by the reduced GFP signal observed (Fig. 3.10b).

Thus, EC-MSC-rich organoids cannot be used to model NAFLD in the specified *in vivo* setting.

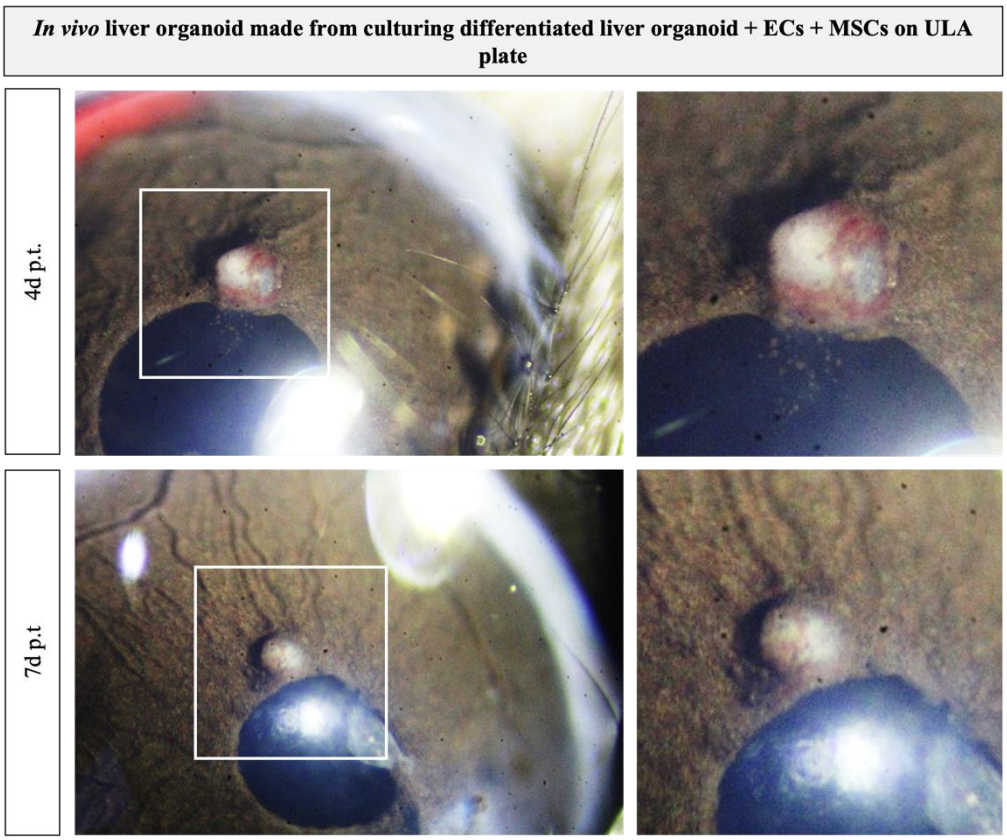


Figure 3.9. Liver organoids made from differentiated liver organoids, endothelial cells (ECs) and mesenchymal stem cells (MSCs) briefly vascularize after transplantation into the anterior chamber or the eye. Bright field images of the same mouse taken 4 and 7 days post-transplantation (p.t.). 4.5x magnification and insets are digitally zoomed in areas.

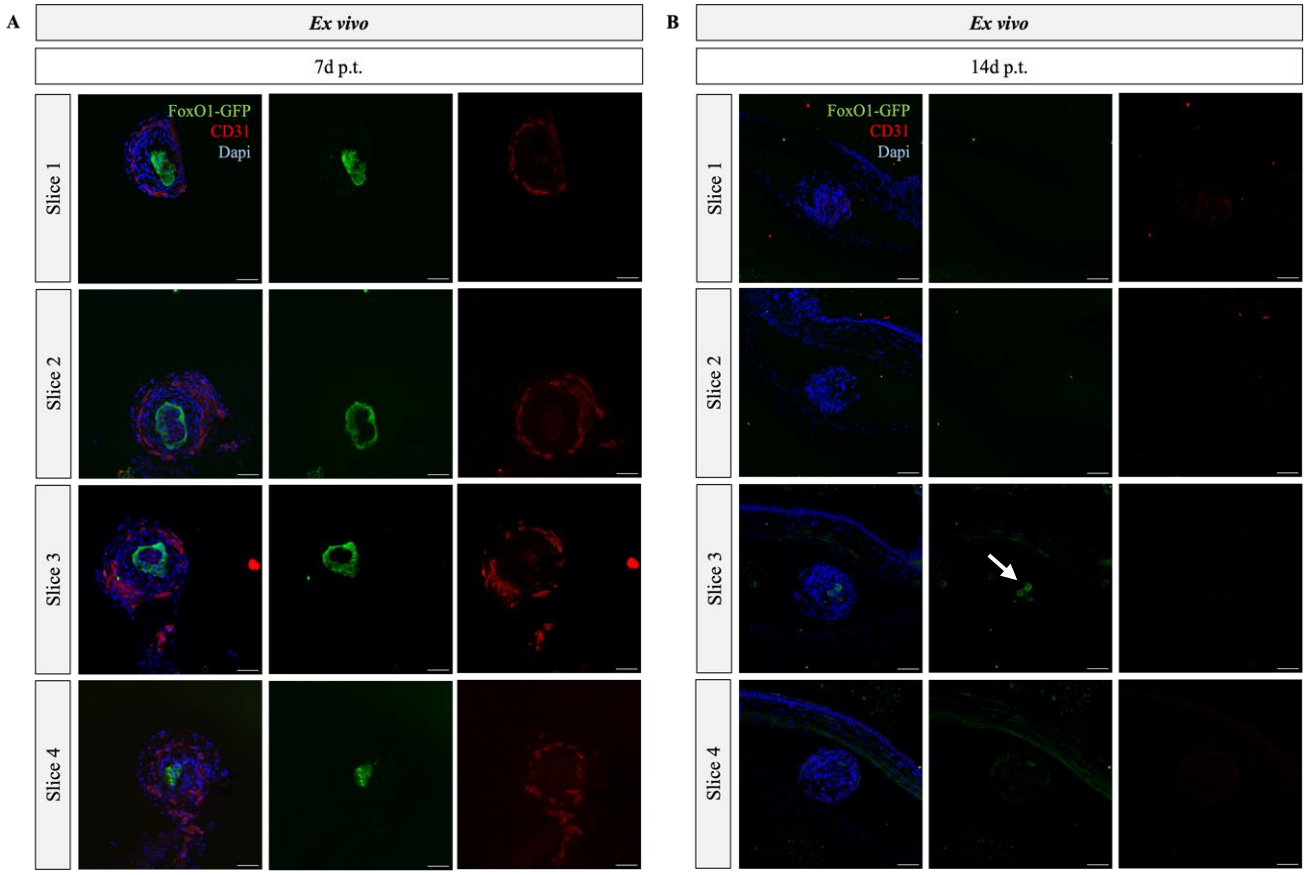


Figure 3.10. Blood vessels regress over time from liver organoids transplanted into anterior chamber of the eye. Slices of excised liver organoids made from co-culturing differentiated liver organoids (green), endothelial cells (ECs) (Red) and mesenchymal stem cells (MSCs) stained with nuclear dye dapi (blue) on ultra-low attachment (ULA) plate, A) 7 and B) 14 days post-transplantation. Arrow points to a few GFP-positive cells. Scale bars are 50 μm.

3.4.1.4. Aggregates made from differentiated liver organoid-derived single cells, endothelial and mesenchymal stem cells on ULA plates

3.4.1.4.1. Co-culture of single cells from differentiated organoids with endothelial and mesenchymal stem cells on ULA plates

The previous co-culture systems led to the formation of differentiated liver organoids whose surface was coated with ECs and MSCs. These structures appeared to get vascularized through the development of blood vessels on their surface, however BVs quickly regressed. Thus, experiments were carried out that aimed to generate more homogenously vascularized liver organoids. To do so, differentiated liver organoids were dissociated into single cells, that were then co-cultured with ECs and MSCs (Fig. 3.11a) on ULA plates. As mentioned earlier in this chapter's introduction, co-culture of HLCs and non-parenchymal cells (ECs and hepatic stellate cells) in ULA plates has been previously done, and specific co-culture of organoid-derived single cells and other cell types, including endothelial cells, has also been previously published

(Choi et al., 2021; S. Wang et al., 2019). This strategy led to the formation of cell aggregates that were stable enough to be manipulated (Fig. 3.11b). However, immunofluorescent staining experiments revealed that ECs distribution in the resulting cell aggregate was neither homogeneous nor consistent between experiments (Fig. 3.11c).

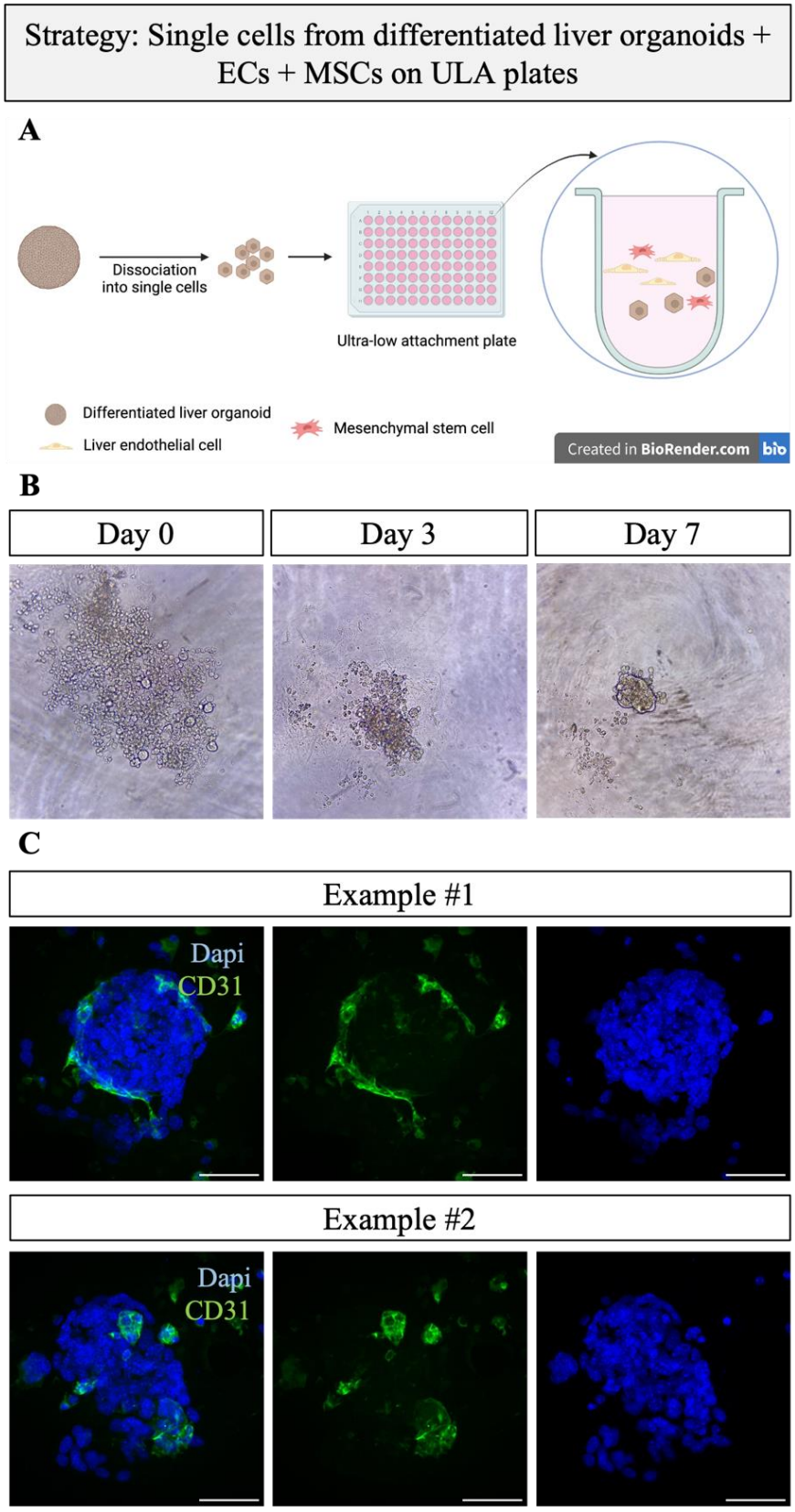


Figure 3.11. Liver spheroids made from co-culturing differentiated liver organoids-derived single cells, endothelial cells (ECs) and mesenchymal stem cells (MSCs) on ultra-low attachment (ULA) plate. A) Schematic of how liver spheroids were made; B) Bright-field image of liver spheroid 0, 3 and 7 days after co-culture with liver endothelial and mesenchymal stem cells. C) Confocal images of liver spheroids stained for CD31 (red), and nuclear dye dapi (blue). Scale bars are 50μm.

3.4.1.4.2. Transplantation of aggregates made from differentiated liver organoid-derived single cells, endothelial and mesenchymal stem cells into the ACE

Even though the previous strategy did not lead to the expected structure with homogenous ECs distribution, they were still assessed for their vascularization capacity upon transplantation into the ACE. However, those aggregates never vascularized, and eventually disappeared from the ACE (Fig. 3.12 and data not shown).

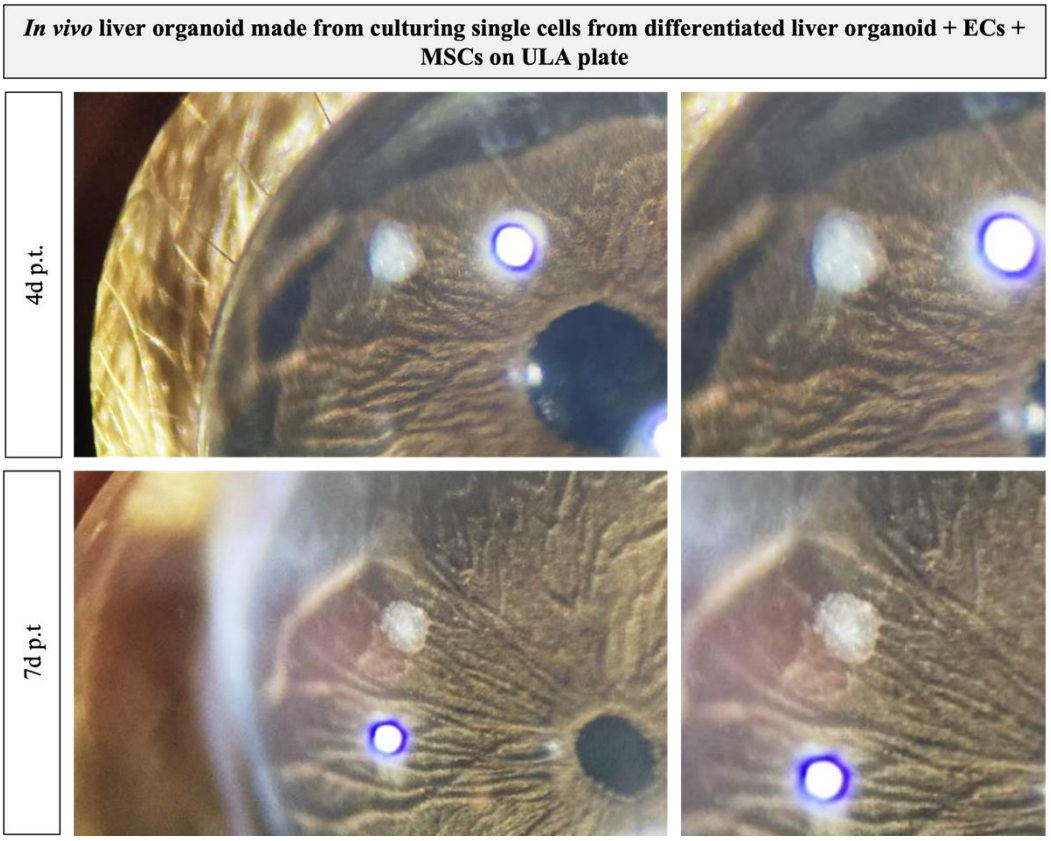


Figure 3.12. Liver spheroids (LS) made from culturing differentiated liver organoids-derived single cells, endothelial cells (ECs) and mesenchymal stem cells (MSCs) on ULA plate do not vascularize after transplantation into the anterior chamber or the eye. Bright field images of the same mouse taken 4 and 7 days post-transplantation (p.t.). 4x magnification and insets are digitally zoomed in areas.

3.4.1.5. Liver buds from differentiated liver organoid-derived single cells, endothelial and mesenchymal stem cells

Takebe and colleagues replicated *in vitro* the complex interactions between different cell types that happen during liver organogenesis *in vivo*. They did so by co-culturing induced pluripotent stem cell (iPSC)-derived hepatic endoderm cells (HE) with ECs and MSCs on Matrigel. Upon

seeding, they observed that the three cell types organized themselves into a 3D structure that they called liver bud (LB). These LBs could be further matured upon exposure to growth factors that promoted HE cells differentiation into mature hepatocyte like cells (HLCs). Furthermore, LBs presented homogenous distribution of all cell types and, more importantly, were capable of vascularizing for long term upon transplantation into several ectopic locations, including brain, sub renal capsule and mesentery (Takebe et al., 2014). Thus, it was hypothesised that liver buds could be obtained by co-culturing single cells derived from differentiated liver organoids, ECs and MSCs on matrigel (Fig. 3.13a), and that these could vascularize upon transplantation into the ACE. However, after several attempts, liver buds never formed (Fig. 3.13b).

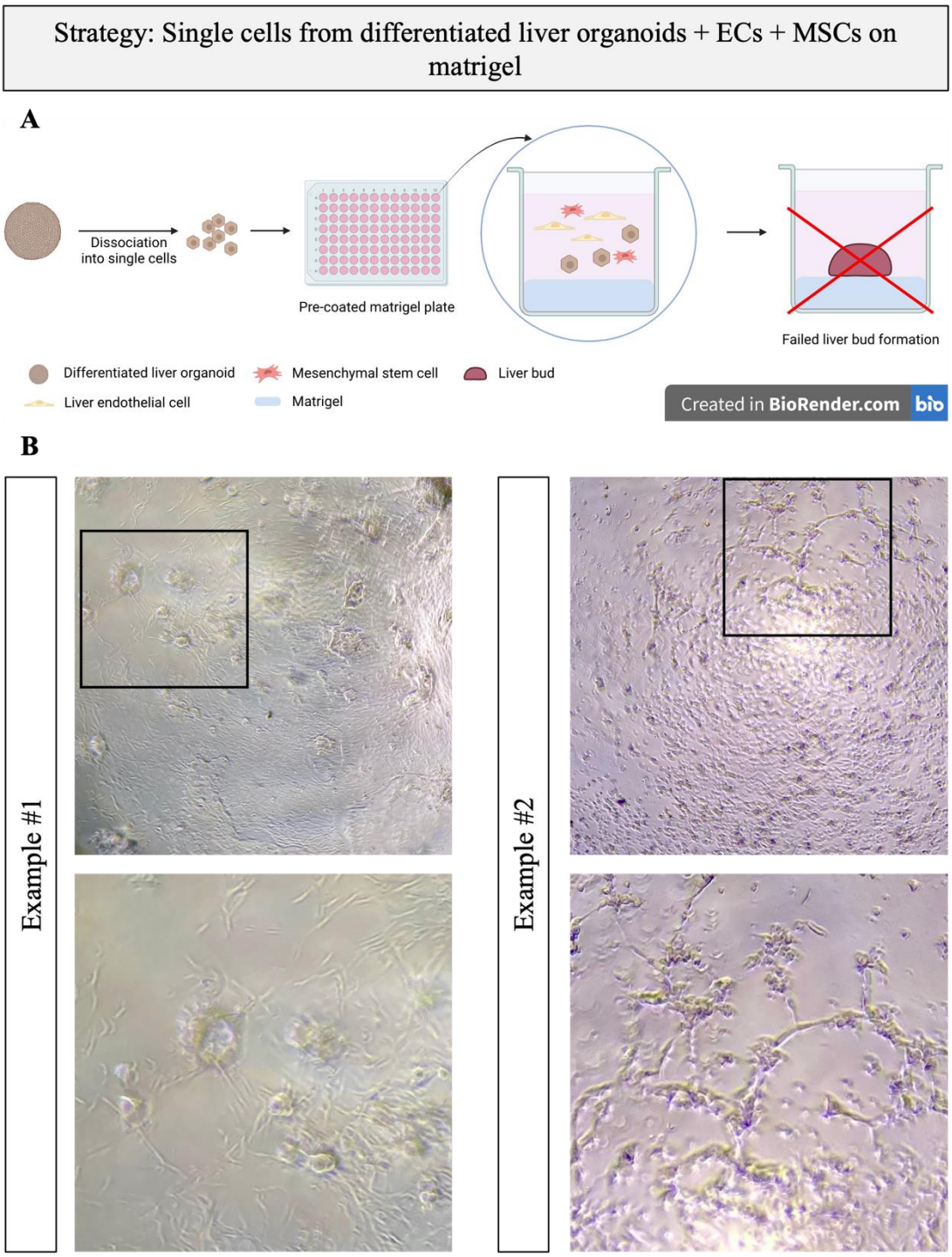


Figure 3.13. Liver buds failed to form when co-culturing single cells from differentiated organoids, endothelial cells (ECs) and mesenchymal stem cells (MSCs) on matrigel. A) Schematic illustrating how liver bud formation was attempted. B) Bright-field images of two failed attempts, 2 days after co-culture. 4x magnification and insets are digitally zoomed in areas.

3.4.2. Attempting to generate liver model capable of vascularizing *in vivo* using hepatocyte like cells

The initial aim of this project was to establish an *in vitro* NAFLD model out of primary cells isolated from adult mouse tissues, so that it could be quickly established in any lab. However, considering the previous unsuccessful attempts to generate a structure capable of long-term vascularization upon transplantation into the ACE, a decision was made to alter this strategy. Since Takebe and colleagues had shown that liver buds made from hepatocyte like cells (HLCs), ECs and MSCs could engraft upon transplantation into several ectopic organs (Takebe et al., 2013b), it was next decided to adopt their approach using HLCs differentiated from embryonic stem cells (ESCs).

Takebe's approach to generate liver buds consisted in first differentiating human induced pluripotent stem cells (hiPSCs) into hepatic endoderm (HE) cells, followed by their co-culture with ECs (from human umbilical vein, HUVECs) and MSCs (from human bone marrow) on Matrigel for the bud generation stage, and finally inducing hepatic maturation of HE cells-containing buds into HLCs (Fig. 3.14).

There are several protocols available to differentiate mouse ESC into HE cells and HLCs, however, these usually require optimization for each specific mESC cell line. Thus, for the sake of time, a collaboration was established with a lab at Imperial College London that was doing this routinely . Dr Wei Cui's lab routinely differentiates human embryonic stem cells (hESCs) into HE cells and HLCs. Thus, it was next investigated whether liver buds made using human HE cells and mouse ECs and MSCs would form, and if so, if they vascularized for long-term upon transplantation into the ACE.

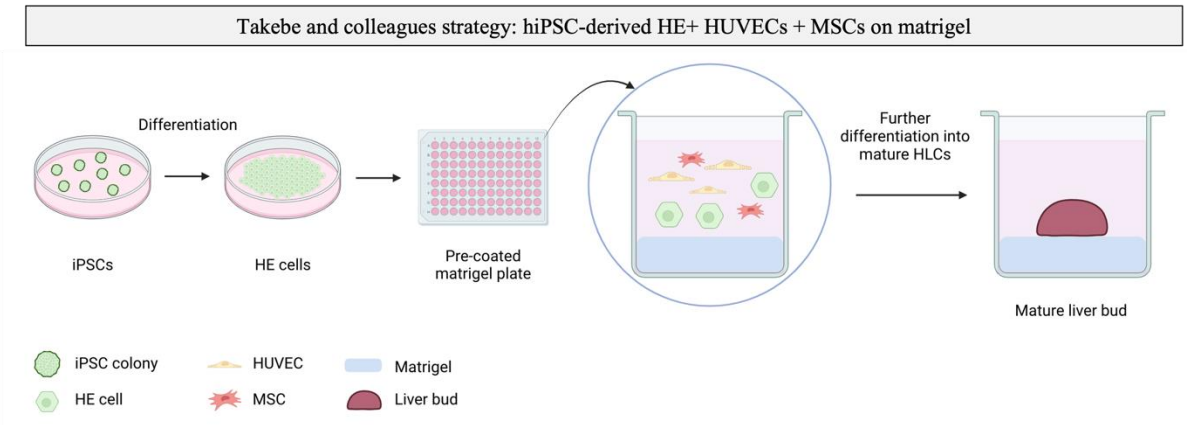


Figure 3.14. Schematic representing Takebe and colleagues' approach to generate liver buds.

3.4.2.1. Liver buds from human HLC

3.4.2.1.1. Differentiation of hESCs into HLC

Dr Wei Cui's lab routinely differentiates hESCs into HLCs. Their approach to generate HLCs from hESCs is based on the 3-step differentiation strategy previously explained in section 3.1.2. Briefly, hESCs are first differentiated into definitive endoderm cells, that are then committed into the hepatic endoderm lineage, and finally matured into HLCs. Representative images of the validation experiments of the successful differentiation of hESCs into definitive endoderm cells, hepatic endoderm and HLCs can be found in Fig. 3.15 and were kindly provided by Faiza Farhan. Overall, these experiments showed that, whilst the differentiation protocol is successful, this is only to some extent, since not all cells expressed albumin, and most cells still exhibited immature hepatocyte markers, as indicated by alpha-foetal protein (ACE) expression.

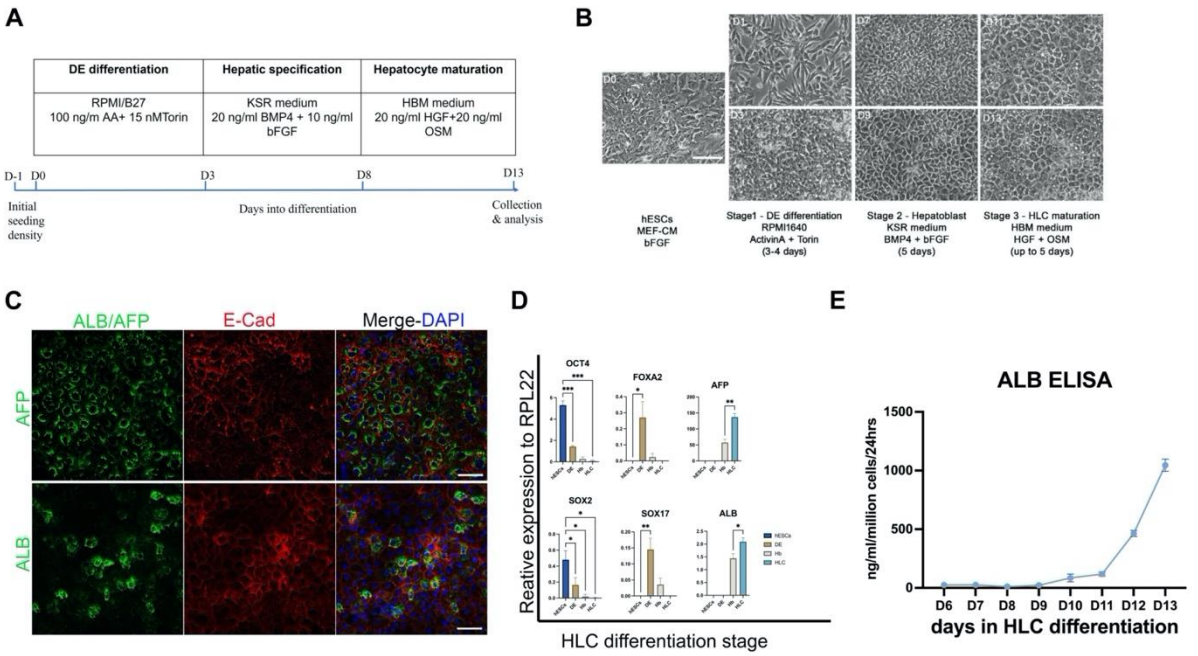


Figure 3.15. hESCs are successfully differentiated into HLCs. A) Schematic depicting differentiation strategy used. B) Bright field images of hESCs at different stages (days 0, 1, 3, 7, 9, 11 and 13) of the differentiation protocol; Scale bar = 100µm. C) HLCs stained for alpha-foetal protein (AFP) or albumin (Alb) (green), e-cadherin (E- Cad)(red) and dapi (blue); Scale bar = 50µm. D) Expression levels of the stem cell markers Oct4 and Sox2, definitive endoderm markers Foxa2 and Sox17, and hepatocyte markers AFP and Alb, in cells at different stages of the differentiation protocol. One-way ANOVA; *: p-value < 0.05; **: p-value < 0.01; ***: p-value < 0.001; E) Albumin production by cells at different stages (days 6, 7, 8, 9, 10, 11, 12, and 13) of the differentiation protocol. DE: definitive endoderm; Hb: Hepatoblast. MEF-CM: Mouse embryonic fibroblasts conditioned medium.

3.4.2.1.2. Liver bud formation from hHE cells

Cells for the bud formation experiments were handed over to our lab at the HE stage. Then, hHE cells were co-cultured with mouse hepatic ECs and MSCs on Matrigel coated plates, as previously described, in a 1:1 mixture of ECs and hepatic maturation inducing medium (Fig 3.16a) (see section 3.3.5.2.1.). These experiments were first carried out in matrigel-coated 96-well plates, and buds successfully started forming after only a few hours (Fig. 3.16b, upper panel). However, the resulting LBs were too big to be injected into the ACE, so the experiment was then repeated using a lower total number of cells, whilst keeping the same cell type ratio, as also previously done by Takebe and colleagues (Takebe et al., 2017). Given that seeded cells need to be in close contact with each other for the bud to form, this time they were seeded on smaller (Matrigel-coated) wells of 384-well plates. As a result, LBs, that were small enough to be transplanted into the ACE, formed (Fig. 3.16b, lower panel). Additionally, these buds consistently presented an even ECs distribution (Fig. 3.16c).

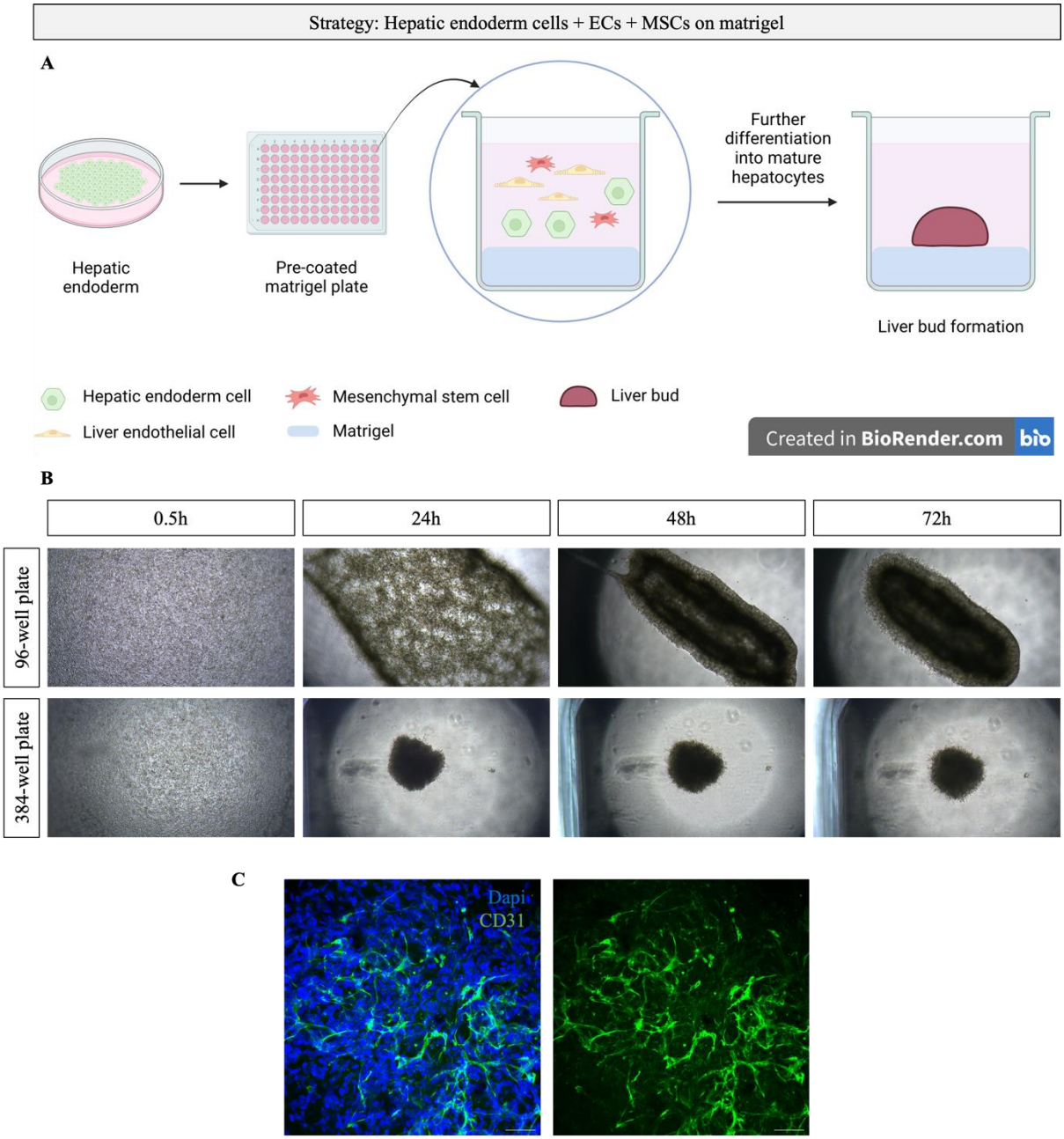


Figure 3.16. Liver buds made from co-culturing parenchymal human and non-parenchymal mouse cells. A) Schematic representing how liver buds were made. B) Pictures of liver buds forming 0.5, 24, 48 and 72h after seeding, in 96 and 384-well plates. 4x magnification. C) LB's stained with CD31 (green) and Dapi (blue) at 72h after seeding. Scale bars = 50µm.

3.4.2.1.3. Transplantation of liver buds from hHE cells into the ACE

LBs capacity of vascularizing *in vivo* upon ACE transplantation was then assessed.

Up to this point, all the cells used when attempting to establish the engraftable *in vitro* model were syngeneic, i.e., from the same genetic strain as the recipient host animal (C57BL/6). However, because the HLCs used to make these buds were from human origin, to avoid rejection issues, for these experiments severe combined immunodeficiency disease (SCID)

animals were used as hosts. As the name suggests, these animals lack a working immune system, which prevents xenogeneic transplanted tissues, i.e., from a different species, from being rejected.

Finally, the transplantation of these LBs into SCID animals ACE consistently resulted into visibly vascularized LBs, and at least 50% of them remained vascularized for the whole duration of the experiment, so over 2 months (Fig. 3.17). The initial vessels were big and often leaky, but gradually normalized, probably as a result of blood vessel maturation.

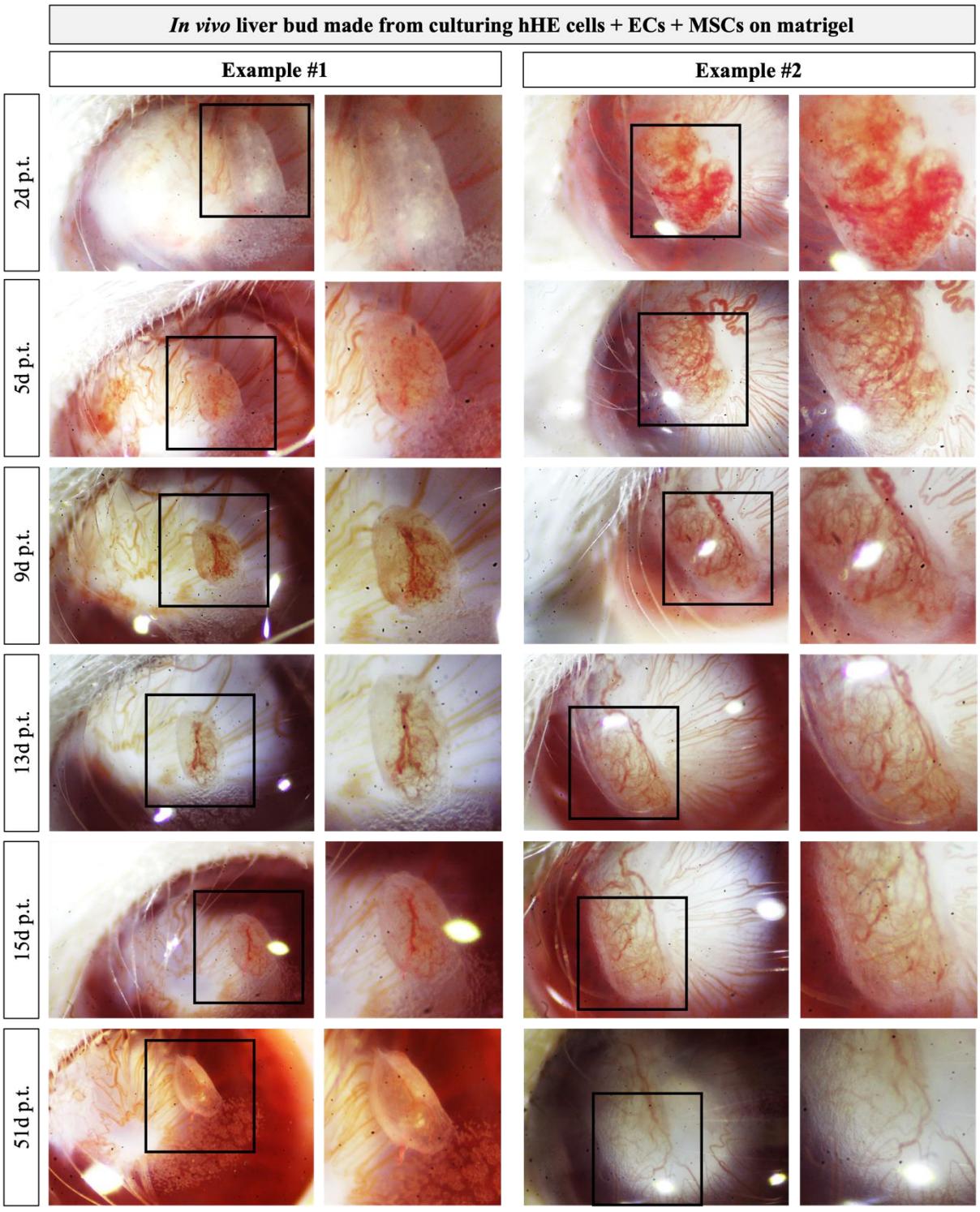


Figure 3.17. Liver buds transplanted into host ACE vascularize for long term. Two examples of LBs transplanted into the ACE, imaged at days 2, 5, 9, 13, 15 and 51 post-transplantation. 4.5x magnification. Insets are digitally zoomed images of boxed areas.

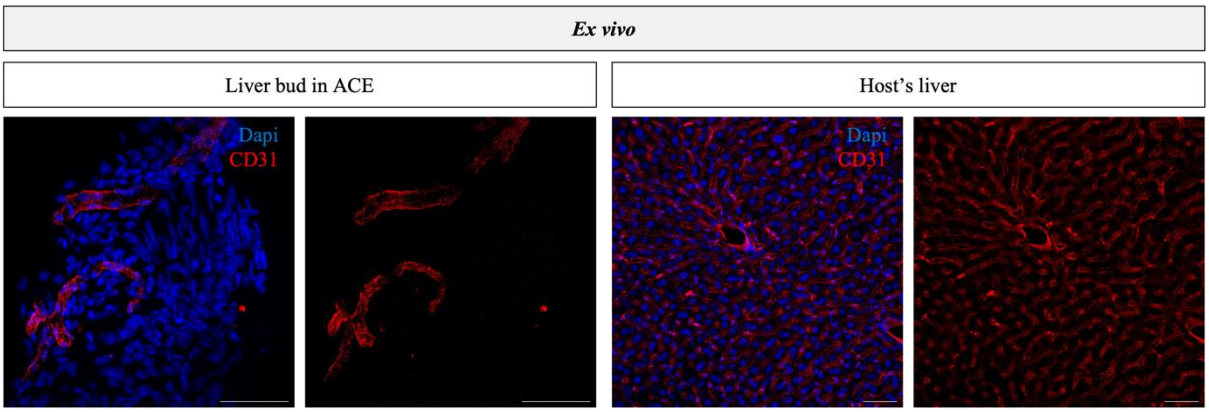


Figure 3.18. Liver buds remain vascularized two months post-transplantation, but BVs density is lower than in liver tissue. Liver buds and liver tissue were sliced and stained with Dapi (blue) and CD31 (red). Scale bars = 50μm.

3.4.2.1.4. Assessing whether intra-ocular liver buds from hHE cells accumulate fat

Given that some LBs were capable of long-term vascularization, it was next assessed whether they could accumulate fat in response to the host mouse being fed an HFD, and, if so, how that fat accumulation would compare to *in situ* hepatic fat accumulation. Thus, host animals were put on a HFD 2 weeks post-transplantation, where they remained for 6 more weeks. Animals were then culled at day 60 p.t., the eyes excised, sliced and stained with the lipid dye LipidTOX. Whilst obvious lipid droplets could be observed in the host animal liver, this was not the case in liver buds (Fig. 3.19).

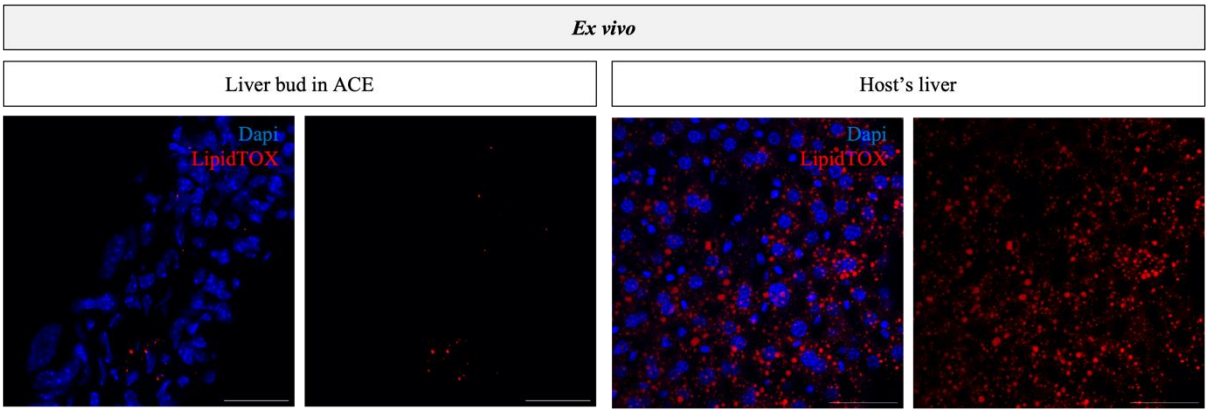


Figure 3.19. Liver buds fail to accumulate fat in response to host being fed an HFD. Liver buds and liver tissue were excised, sliced, and lipid droplets were stained with LipidTOX (red) and nucleous with Dapi (blue). Scale bars = 50μm.

3.5. Discussion and future perspectives

This chapter aimed to develop a minimally invasive novel platform to track the initial stages of NAFLD in the same animal overtime. Whilst trying to do so it was shown, that 1) co-culture of differentiated liver organoids with hepatic ECs originates an EC-coated organoid, that, upon *in vivo* transplantation, can sometimes vascularize, but the vessels are unstable and quickly regress; 2) adding MSCs to that co-culture strategy results in an EC-MSC-coated organoid that is still only capable of vascularizing for short term upon *in vivo* transplantation, although with visibly more stable vessels; 3) co-culture of differentiated organoid-derived single cells with ECs and MSCs on ULA plates originates aggregates with uneven cell distribution that are not capable of vascularizing upon *in vivo* transplantation; 4) co-culture of differentiated organoid-derived single cells with ECs and MSCs on Matrigel fails to produce liver buds; 5) co-culturing cells from different species (human HE cells and mouse ECs and MSCs) still leads to the formation of liver buds following Takebe's approach; 6) at least some of those liver buds are capable of vascularizing for long-term (≥ 2 months) upon *in vivo* transplantation into the ACE, although further experiments are needed to assess whether or not they are capable of accumulating fat.

Transplanting an *in vitro* generated liver model into the ACE means that these will be in an ectopic place, which could potentially impact their success in replicating liver functions that are key for modelling NAFLD, such as fat uptake, synthesis, and storage. The natural occurring liver position within the body is key for several liver roles. An example of this is the filtering of potential gut-derived pathogens from the blood, that reaches the liver via portal vein, before that blood joins systemic circulation. Additionally, bile is produced in the liver by the hepatocytes, stored in the gallbladder and then carried into the intestine via bile ducts when needed, to aid fat digestion. Thus, liver's location near the intestine (and portal vein connection) is also essential for the normal digestion of diet-derived fats. The liver position near the pancreas is also key for its ability to quickly regulate glycemia, since glucose level-stimulated pancreatic insulin and glucagon secretion promote liver glucose uptake and release, respectively. Nevertheless, experiments where pancreatic islets were transplanted into the ACE, showed that intra-ocular islets efficiently regulated glycemia in animals with compromised *in situ* pancreatic islets (S. N. Yang & Berggren, 2019).
Despite the challenges associated with working with an ectopic liver model, in this chapter it was hypothesized that transplanting the *in vitro* generated liver model into the ACE would not

greatly impact its capacity to uptake, synthesise and store fats. As mentioned previously in chapter I, a study by Donnelly and colleagues revealed that the fats that accumulates in the livers of NAFLD patients have three origins: 1) DNL, 2) NEFA pool and 3) diet. 1) DNL refers to the generation of fats from non-fat precursors, such as sugars, with fructose being the most potent-DNL inducing one. To assist in regulating blood glucose levels, the liver possesses the ability to extract a significant amount of glucose derived from the diet and the intestine from portal blood before it enters systemic circulation. Additionally, evidence suggests that this first pass clearance effectiveness is even bigger for fructose (Tappy & Le, 2010). Given that DNL consists in the conversion of sugars into fats, and that the liver might be exposed to higher sugar levels than the rest of tissues (including the ACE) due to its physical proximity and direct connection to the intestine (portal vein), this could indeed impact the DNL rate in ACE liver models compared to the liver *in situ*. However, DNL was estimated to contribute only by 25% of the fats that accumulate in the livers of NAFLD patients (Donnelly et al., 2005a). 2) NEFA pool is the highest contributor to hepatic fat in NAFLD patients (60%). The NEFA pool refers to the group of circulating non-esterified fatty acids that is found in systemic circulation, so, in theory, vascularized liver models in the ACE could be exposed to the NEFA pool. 3) Only 15% of hepatic fats in NAFLD patients are derived directly from diet. Moreover, of these 15%, only a portion (SCFA) flows directly from the intestine to the liver via portal vein since the rest (MCFA and LCFA) must enter systemic circulation first as part of chylomicrons. The fats in the chylomicrons can then enter the liver by either spilling into the NEFA pool, or as part of chylomicron remnants bound to the liver to be recycled. Thus, in theory, some dietary fats could also reach the vascularized liver models in the ACE via NEFA pool and uptake of chylomicron remnants. Therefore, in theory, it was possible for an ectopic vascularized liver model to accumulate fat in response to the host being challenged with an HFD. In fact, research has shown that hepatocytes transplanted into ectopic places, like the spleen, accumulate fat, similarly to the hepatocytes *in situ*, in response to Dex treatment (Lupp et al., 1998). However, the spleen is also connected to the portal circulation. Nevertheless, there are some medical conditions where lipids can accumulate in patients' eyes thus further validating that fats can travel through the blood that irrigates the eye (Broekhuyse, 1971, 1972; Fraunfelder et al., 1976; Hall et al., 2020; Secondi et al., 2019).

Importantly, research has suggested that intestinal microbiota can play a key role in NAFLD development and progression, given that gut microbiota derived substances (like pro-inflammatory LPS) reach the liver via portal vein and worsen NAFLD. Since the ACE is not connected to the portal system, liver models would not be exposed to such substances.

Additionally, the ACE is probably not compatible with modelling advanced NAFLD stages (NASH), since it is a relatively immune privileged location, and the immune system is a known important contributor to disease progression into NASH. However, the initial aim of this chapter was to develop a platform to track the initial stages of NAFLD that would also allow us to test drugs directly targeting hepatic fat accumulation, such has glucagon analogues/GCGR agonists, which is the root cause of NAFLD in first place. Thus, NAFLD severity and progression could be milder in intra-ocular liver models when compared to the liver *in situ*.
In addition to studying the initial stages of NAFLD longitudinally, it was hypothesised that this novel platform, had it worked, could also potentially be used to test NAFLD targeting drugs, such as glucagon analogues/GCGR agonists. The potential of GCGR agonists in lowering hepatic fat resides in the fact that they directly increase hepatic lipolysis and fatty acids b-oxidation, whilst also reducing DNL rate, all resulting in depletion of hepatic fat storages. Most oral drugs reach the liver via portal vein, which could indeed be a problem, since the liver models were going to be in an ectopic location with no access to such route (Vaja & Rana, 2020). However, several drugs, including GCGR agonist, can be administered subcutaneously, thus quickly entering systemic circulation, and therefore circumventing the potential problem posed by orally administered drugs.

Experiments were conducted to assess the differentiation success of stock bile duct organoids into the hepatocyte lineage. These experiments revealed that HNF4a was consistently expressed in differentiated organoids (although it was not homogeneously expressed in all cells within the same organoid); that most cells still retained EpCam expression (although levels varied in the cells within the same organoids) and that G6Pase and ApoC2 expression levels were much higher in differentiated vs undifferentiated organoids (where no expression was detected), but still greatly reduced when compared to liver tissue. These experiments, despite being in accordance with the results from the paper that originally generated this model (Huch et al., 2013), revealed that the differentiation protocol was somewhat, but not completely, successful in generating mature HLCs. *In vitro* differentiation of stem cells into mature HLCs that resemble and behave as primary hepatocytes has been widely recognised as a challenging task (C. Chen et al., 2018). As previously explained in this chapter's introduction, in addition to exposure to certain growth factors, several other approaches can promote differentiation and maturation of undifferentiated/immature cells into the hepatocyte lineage, such as co-culture with non-parenchymal cells, as well as *in vivo* transplantation (i.e., due to vascularization that exposes cells to host blood). Therefore, as the project was initially designed with the goal of

co-culturing differentiated liver organoids alongside liver hepatic endothelial cells (non-parenchymal cells), and subsequently transplanting the resulting structures into a host animal ACE, it was hypothesized that further maturation of the differentiated liver organoids could be achieved further down the line.
Regardless, functional experiments revealed that these differentiated organoids were already capable of accumulating fat when challenged with oleic acid, and potentially, DNL-inducing substrates, *in vitro*, which are key to accurately model NAFLD.
It is important to note that, due to the fact that hepatocytes-only were not routinely available in the lab, liver tissue was used as a positive control for the qPCR experiments assessing the levels of hepatic markers in undifferentiated vs differentiated organoids. This is not ideal as the liver comprises cell types beyond hepatocytes. As such, the reduced expression levels of the hepatic markers might be underestimated in the organoids (when compared to primary hepatocytes), due to the diverse cell composition of the liver.

Hepatocytes are known to produce several pro-angiogenic factors, such as VEGF, and angiopoietin 1 and 2, in response to stress situations like wound healing or hepatectomy (Peng et al., 2021). These pro-angiogenic factors can then promote the proliferation and migration of LSECs (Shimizu et al., 2001). In fact, research has shown that overexpressing VEGF in hepatocytes is enough to promote their engraftment and trigger neovascularization upon *in vivo ex situ* transplantation (Ajioka et al., 1999). Huch and colleagues showed that the differentiated organoids used in the experiments carried out in this chapter were shown to engraft to some extent upon transplantation into the liver, although no evidence of vascularization was shown (Huch et al., 2013). Nonetheless, and given that the levels of pro-angiogenic factors expressed by the organoids were not assessed, an attempt was made to transplant them into the ACE. However, no evidence of vascularization could be seen, and they soon disappeared from the ACE, probably due to immune system intervention.

One of the strategies used to generate tissues *in vitro* capable of engrafting and vascularizing upon *in vivo* transplantation is co-culture with ECs. LSECs play an important role in the capacity of the liver to efficiently uptake fats (McMahan et al., 2016). This was the reason why LSECs were chosen for this project as opposed to other endothelial cell types/lines. To isolate ECs from mouse liver a previously published protocol was followed and optimized (Marelli-Berg et al., 2000). Whilst more recent papers were available that offered a higher yield and purity of hepatic LSECs, these usually involved complex techniques, such has *in situ* digestion

of liver tissue through portal vein cannulation. Given that no one in our department was familiarized with such methodology, Marelli-Berg and colleagues approach was chosen for its ease of use and in sake of time. Briefly, this protocol consisted in extracting and digesting liver tissue, followed by incubation of the resulting single cell suspension with EC specific antibodies prior to magnetic cell sorting. The liver is not only composed by sinusoidal endothelial cells (LSECs), but also portal and central ECs. Antibodies against CD31, CD105 and Isolectin-B4 were used to specifically label hepatic ECs. However, even though these are specific markers of ECs, they are not specific to LSECs. Despite this, LSECs are the most abundant population of ECs in the liver, so the vast majority of isolated ECs should be LSECs (DeLeve & Maretti-Mira, 2017; Duan et al., 2018; Ruan et al., 2021; X. Sun & Harris, 2020). In addition, two of the characteristics that make LSECs so effective at quickly and efficiently transferring fat from blood to hepatocytes are their high endocytic capacity and the presence of fenestrations on their surface (McMahan et al., 2016). However, some studies have suggested that these fenestrations are quickly lost, and their endocytic capacity rapidly declines, upon short-term *in vitro* culture (DeLeve & Maretti-Mira, 2017). No experiments were conducted to assess whether this was the case in the cultured primary ECs. Therefore, this could potentially impair the capacity for the *in vitro* liver model to uptake fat from circulation upon *in vivo* transplantation.

Since differentiated organoids did not vascularize upon *in vivo* transplantation and, as explored in section 3.1.4.1., co-culture with ECs is one of the strategies used to generate pre-vascularized tissues, given the simplicity and practicality of this approach, co-culture of 3D differentiated organoids and hepatic ECs was attempted. This strategy led to the formation of ECs-coated organoids that could occasionally trigger vascularization upon ACE transplantation. However, the new vessels were clearly unstable and quickly regressed over time. This finding was not completely surprising. Whilst some research has demonstrated that co-culture with ECs alone can generate structures capable of vascularizing upon *in vivo* transplantation, other studies show that such approach often results in the formation unstable primitive-like tubes rather than mature vessels. This instability is attributed to the lack of vessel-stabilizing cells in the co-culture system. Hepatic ECs are known to have a somewhat long lifespan that can vary from months to years, however, when vessels are not properly matured, through interaction with vessel-stabilizing cells, ECs can undergo apoptosis leading to vessel regression.
To overcome this, MSCs were also added to that co-culture system. As explored in section 3.1.4.2., MSCs are widely known to have vessel stabilizing characteristics, whilst also

producing paracrine signals that promote angiogenesis and ECs survival. However, this approach was only somewhat successful. Indeed, this strategy led to the formation of ECs-MSCs-coated organoids that quickly vascularized upon ACE transplantation. The new vessels looked notoriously more mature and stable, when compared to organoids co-cultured with ECs only. However, these too regressed only a few days post-transplantation. This was not expected, since, as referenced in section 3.1.4.2., formation of pre-vascularized tissues, through co-culture with ECs and MSCs, have been shown to be capable of long-term vascularization by several researchers upon transplantation into various ectopic locations. Thus, next it was hypothesised that the problem laid with the organoids employed, or more precisely, in the methodology used for generating those pre-vascularized organoids, rather than with the cell types themselves. Indeed, the way the ECs-MSCs-coated organoids were generated led to the distribution of those cells only on the organoids outside surface. Thus, subsequently, an effort was made to create uniform pre-vascularized organoids following Takebe's approach, first by co-culturing differentiated organoid-derived single cells with ECs and MSCs under low-attachment conditions, and then on a Matrigel layer. However, culturing the three cell types under low attachment conditions led to the formation of aggregates with non-homogenous ECs distribution, that failed to vascularize upon *in vivo* transplantation. Likewise, seeding those cells on a Matrigel layer was also unsuccessful since it failed to produce a bud.

Using single cells derived from organoids in co-culture experiments has been previously done (Choi et al., 2021). However, the digestion of these 3D structures can impact the resulting single cells fitness, which might justify why the three cell types failed to properly interact to form homogenous aggregates and LBs.

On the other hand, in Takebe's approach, to recapitulate the cellular interactions that happen during embryogenesis, liver buds were formed using hepatic endoderm cells, not differentiated HLCs (the single cells derived from differentiated organoids used in this chapter can be considered HLCs). Thus, this could potentially justify why the buds failed to form. Alternatively, single cells derived from undifferentiated (stock/bile duct) organoids could have been used instead. However, stock organoids resemble more hepatoblasts (cells with bi-potent differentiation capacity into hepatocytes and cholangiocytes lineage) rather than hepatic endoderm cells, meaning that they would still be more differentiated/committed into the hepatocyte lineage than the cells used by Takebe and colleagues (Chi & Kim, 2022; Kulkeaw et al., 2020). Additionally, the organoids differentiation protocol takes 14 days of exposure to a cocktail of growth factors. Many cell lines do not last that long in *in vitro* culture, (like the hepatic ECs isolated for the co-culture experiments), and others can start undergoing

spontaneous differentiation (MSCs). Moreover, one of the difficulties of co-culture systems is finding a culture medium that is compatible and suitable for all cell lines. For all the aforementioned reasons, it was hypothesised that co-culturing undifferentiated liver organoid-derived single cells with ECs and MSCs for 14 days was likely not compatible with Takebe's LB formation approach.

Given how successful Takebe's LBs were at vascularizing upon transplantation into several ectopic places (cranial window, sub-renal capsule, and mesentery), the generation of LBs that more closely resembled Takebe's was attempted. To do so, ECs, MSCs and HE cells were co-cultured on a Matrigel layer. To quickly and effectively differentiate ESCs into HE, a collaboration was established with Dr Wei Cui's lab that routinely differentiates hESCs into hHE cells. This meant that human parenchymal and mouse non-parenchymal cells would be co-cultured together. Even though, to our knowledge, no one has attempted to make LBs following Takebe's approach using cells from different species before, co-culture of human hepatocytes/HLCs and mouse non-parenchymal cells (and vice-versa) has been previously done (Hsu et al., 2021; Sengupta et al., 2020). Indeed, the co-culture of human parenchymal and mouse non-parenchymal cells led to the successful formation of LBs. However, these were too big to be transplanted into the ACE. Therefore, smaller LBs were subsequently generated by reducing the number of total cells, whilst keeping the same cell type ratios, as previously shown in a more recent publication from Takebe and colleagues (Takebe et al., 2017).

As previously noted (see section 3.1.5.), transplantation of *in vitro* grown tissues into the ACE of host animals might lead to immune system-mediated rejection, which might confound the results regarding LBs *in vivo* vascularization capacity. To avoid that, all the cell types used for experiments up to this point were derived from animals from the same genetic background as the future host (C57Bl/6). Thus, in experiments using LBs made from mouse and human cells, LBs had to be transplanted into severe combined immunodeficiency disease (SCID) animals. SCID animals have an impaired immune system since they lack mature T and B lymphocytes, which are important mediators of immune responses (J. Chen et al., 2022; Takebe et al., 2012). Thus, transplanting LBs of mixed species origin into SCID animals eliminates the risk of immune system-mediated LB rejection.

Transplantation of these LBs into the ACE led to quickly vascularized structures that remained vascularized throughout the whole experiments (> 2 months). However, it was hard to define the success rate at which LBs vascularized for long term upon ACE transplantation. This is because, despite being clear that all LBs quickly vascularized shortly after transplantation into

the ACE, approximately half of the LBs seemed to lose their 3D structure and flatten overtime. Since none of the LBs cell types were fluorescently tagged, it could not be determined with certainty whether LBs were flattening and merging with the host tissue, or whether they were completely disappearing (i.e., dying). Thus, additional experiments are needed to assess this.

Nevertheless, the number and size of LB's blood vessels that clearly remained in the ACE until the end of the experiment, seemed to decrease as time passed by, and *ex vivo* experiments confirmed that blood vessel density was notoriously lower in LBs compared to liver tissue. Some blood vessel regression was expected, since it is part of the maturation process of newly developed vasculatures to remove redundant vessels (Lokmic & Mitchell, 2008). Furthermore, a modest decrease in blood vessel density was also evident in Takebe's results (Takebe et al., 2013b). However, in contrast with the evidence reported in this chapter, they reported that LBs blood vessel density was similar to the host's liver tissue.

Nevertheless, the LBs were still vascularized and so, in theory, its cells could be exposed to the hosts blood and, consequently, to circulating fats. Hence, the ability of transplanted LBs to accumulate fat in response to the host animal being fed a high-fat diet for approximately 6 weeks was assessed. However, LBs failed to accumulate fat, in sharp contrast to the host's liver. This could be potentially explained by several scenarios:

1) Even though the protocol used in Dr Wei Cui's lab consistently leads to the successful differentiation of hESCs into hHLCs, the approach carried out in this chapter to originate LBs required the adaptation of the last differentiation step. This is because, to recapitulate embryonic liver development whilst keeping all three cell types viable under the same co-culture conditions, liver buds are made by initially co-seeding cells at the HE stage with ECs and MSCs, in a 1:1 mixture of EC maintenance and hepatic maturation medium. This means that the third stage of the HLC differentiation protocol – hepatic maturation – is induced using a 1:1 mixture of ECs and hepatic maturation mediums. However, and even though this was the exact approach that Takebe and colleagues employed in the original protocol, this could have prevented the full and successful differentiation of LBs-HE cells into mature HLCs, and thus their capacity to perform hepatocyte-specific functions. This could justify why LBs were incapable of accumulating fat after challenging host animals with HFD. Therefore, additional experiments assessing the identity of *in vitro* LBs parenchymal cells should be performed, like, for example, immunofluorescent staining against albumin/AFP and fat transporters, as well as fat staining upon *in vitro* exposure to fatty acids.

2) Another possible justification is the fact that LBs-HLCs might have dedifferentiated upon *in vivo* transplantation. In this situation, LB-HE cells could have been successfully

differentiated into HLCs *in vitro*, but then dedifferentiated into less mature cells upon ACE transplantation, thus also affecting their capacity for fat uptake and storage. Dedifferentiation of hepatocytes/HLCs upon *in vivo* transplantation is a well-known concern in the field (Lupp et al., 2003). In fact, even *in situ* hepatocytes can undergo dedifferentiation in response to certain hepatic regeneration stimuli (H.-S. Kim et al., 2019). However, other research has shown that hepatocytes transplanted into ectopic places, including the spleen, do not dedifferentiate and remain functional for long term (J. Li et al., 2019b; Mito et al., 1979). Thus, additional experiments should be performed to assess the identity of intra-ocular LBs parenchymal cells, like, for example, albumin/AFP staining of excised LBs.

3) Another possible explanation is that the ECs that compose the LBs blood vessels might not allow the LBs exposure to circulating fats. This can be caused by two things. On one hand, the hepatic ECs used to make the LBs might have lost their fenestrations prior to *in vivo* transplantation due to extended *in vitro* culture, as explained earlier (DeLeve & Maretti-Mira, 2017). This could significantly impair the LBs exposure to circulating fats, and thus its capacity to accumulate fat in response to the host animal being fed an HFD. On another hand, the BVs within the LBs might be of hosts origin (i.e., stemmed from the iris) rather than of hepatic ECs origin. The ACE is filled with the aqueous humour and is, under physiological conditions, immune privileged. This is because of the blood-aqueous barrier that selectively controls the molecules that pass from the blood to the aqueous humour. This selectivity is, at least in part, due to the iris blood vessels ECs having tight junctions and lacking fenestrations, which makes them impermeable to large molecules (Labelle, 2017). Research in pancreatic islets transplanted into the ACE has shown that, depending on how long the islets remain in *in vitro* culture prior to transplantation, the newly formed islet blood vessels can originate from the islet itself or from the host animal tissue (in this case, the iris) (Xiong et al., 2020). However, this is because islets ECs disappear with extensive *in vitro* culture, but CD31 staining of LBs at the transplantation day revealed that ECs were still widely present. Nevertheless, if LBs ECs died during/shortly after transplantation and the LBs blood vessels stemmed from the iris, they may not allow for LBs to be exposed to circulating fats. Therefore, additional experiments are needed to address this question, like, for example, making liver buds using hepatic ECs isolated from the Tie2-GFP animals used in the previous chapter II. In this situation, presence of GFP signal in intra-LBs BVs would indicate that they were of hepatic ECs origin, whereas absence of GFP signal would indicate BVs of host animal origin.

4) Finally, if none of the previous hypotheses proves to be true, another possibility is that LBs might not have been able to accumulate fat in response to the host being fed an HFD,

because the ACE might simply not be compatible with such aim. Even though, in theory, *in vitro* grown liver models transplanted into the ACE could accumulate fat due to all the previously mentioned reasons, this might simply not be the case.

It is important to note that the generated LBs were missing other hepatic cells that play important roles in NAFLD onset and progression, like Kupffer cells and HSCs. As explained in section 1.2.2.1, these cells are involved in mediating NAFLD-associated inflammation and fibrosis, which are important drivers of NAFL progression into NASH. Thus, LBs missing these cells would probably not be able to model the whole spectrum of non-alcoholic fatty liver disease. However, the ACE is probably not compatible with modelling NASH anyway, since it is a relatively immune privileged location that is also not exposed to the gut's microbiome, both known important contributors to NASH development. Nevertheless, this chapter's aim was to develop a platform to track the initial stages of NAFLD that could also be used to test drugs directly targeting hepatic fat accumulation, which is the root cause of NAFLD in first place. Thus, although the presence of additional hepatic non-parenchymal cells would make this platform more relevant, this was not detrimental to successfully accomplish the initial aim of modelling the initial stages of NAFLD.

Chapter IV – Optimization of chronic GCGR-agonism in the treatment of NAFLD

4.1. Introduction

4.1.1. A new glucagon analogue, G108, improves glycemia and possibly hepatic steatosis in obese mice

Our group has recently published a study on the effects of G108 chronic treatment in a diet-induced obese (DIO) mouse model (Hope et al., 2022). G108 is a new long-acting glucagon analogue and was generated by incorporating a fatty acid tail in the C-terminus of a peptide whose sequence was based on both endogenous glucagon and oxyntomodulin (a GLP-1R/GCGR co-agonist). In that study, it was concluded that, at a sub-anorectic dose, chronic GCGR agonism using G108 lead to improved glycemia and hepatic steatosis. Despite these two promising outcomes, other G108 treatment-induced outcomes were reported that affected plasma amino acid levels, energy expenditure, and lean and fat masses. More specifically, it was showed that G108 treatment leads to hypoaminoacidemia (low plasma amino acid levels), that subsequently, leads to an increase in energy expenditure that decreases fat mass, whilst also leading to loss of lean mass (Hope et al., 2022). Given that this chapter aimed to explore G108's potential to treat fatty liver and improve blood glucose levels, all the other previously mentioned outcomes of G108-chronic treatment will be considered as secondary/side effects. The side effects of glucagon chronic treatment will be further explored below.

4.1.2. Side effects of G108 chronic administration: hypoaminoacidemia, increased energy expenditure, and fat and lean mass loss.

4.1.2.1. G108 chronic treatment induces hypoaminoacidemia

Amino acids are the building blocks of proteins and so balanced amino acid levels must be kept to maintain normal cell function. There are 20 different amino acids, and they can be split into essential (EAA) and non-essential (NEAA) categories, depending on whether or not they can be synthesized in the body (Lopez & Mohiuddin, 2023). As previously explained (see section 1.2.7.), glucagon acts on the hepatic GCGR to, among other things, promote amino acid catabolism directly through activation of catabolic pathways, as well as by promoting amino acid uptake from the plasma into the liver (Miller & Birnbaum, 2016). Thus, it not surprising that, in a chronic setting, glucagon receptor agonism might lead to low plasma amino acid levels.

The connection between glucagon signaling and hypoaminoacidemia has been previously reported in a plethora of studies, using both native and synthetic glucagon. For example, Bromer and Chance reported a drop in plasma amino acids in rabbits injected with glucagon obtained through crystallization. This drop in amino acids was sustained for longer when the glucagon halftime was increased through zinc complexation (Bromer & Chance, 1969). Also, hyperaminoacidemia and hypoaminoacidemia have been reported in diseases where glucagon levels are decreased (pancreatectomy) and increased (glucagonoma), respectively (Barazzoni et al., 1999; Boden et al., 1980). Additionally, altered plasma amino acid levels have also been reported in studies using glucagon analogues. Several GCGR multi-agonists (i.e., drugs that target more than one receptor) have been shown to induce hypoaminoacidemia in patients. In fact, hypoaminoacidemia is now widely used as a read out for GCGR agonism (W. Li et al., 2020).

The study with the glucagon analogue G108 further confirmed these observations and the role of the hepatic GCGR in glucagon mediated hypoaminoacidemia. Indeed, it was shown that plasma total amino acid levels drop in response to chronic G108 treatment, and experiments carried out in knock-out animals validated that this is dependent on the hepatic GCGR. Furthermore, some individual essential and non-essential amino acids, like lysine and alanine, for example, were reported to be preferentially affected over others, like phenylalanine and glutamate. Accordingly, G108 also led to the upregulation of genes involved in amino acid catabolism (Hope et al., 2022).

4.1.2.2. G108-induced hypoaminoacidemia leads to increased energy expenditure and consequentially fat mass loss

Energy is essential for all types of biological processes, and energy balance is reached when the amount of energy spent (energy expenditure) is the same as the amount of energy ingested (food intake). When the intake of energy is higher than the energy spent, excess energy is stored, mainly in adipose tissue. Equally, when more energy is spent than ingested, energy stored in adipose tissue is used, leading to a reduction in fat mass. Energy expenditure is defined as the amount of energy the body uses and can be split into three main sections: basal metabolic rate, which is the energy spent during rest; thermic effect of food, which is the energy used during digestion, absorption, and food processing; and, lastly, physical activity, which is the energy expended during movement (Hills et al., 2014).

For over six decades, it has been widely recognized that glucagon has the capacity to elevate energy expenditure, as supported by numerous studies using both native glucagon and glucagon/GCGR analogues/agonists/co-agonists. For example, acute glucagon administration in rats enhances whole body oxygen consumption, a readout of energy expenditure (Davidson. et al., 1960; Hills et al., 2014). This observation has been widely validated in human studies as well (Kleinert et al., 2019).

Given that amino acids are the building blocks of proteins it is not surprising that altered levels might impact distinct processes in the body. The idea that altered plasma amino acid levels might impact energy expenditure has been hinted in several studies. For example, low protein diets, which might lower plasma amino acid levels, can lead to increased energy expenditure. These diets are known to affect not only EE, but also food intake. Nevertheless, studies showed that low protein diets result in an increase in EE even in the absence of increased energy intake (Pezeshki & Chelikani, 2021). Despite most of these studies not validating that plasma amino acid levels were effectively reduced by the low protein diets, it is widely known that diet protein restriction results in reduction of, at least, some plasma essential amino acids, since the human body cannot produce them (Sjøberg et al., 2020). Furthermore, several other studies have shown that diet restriction of specific amino acids results in increased EE as well. Many of these studies also report a concomitant increase in food intake, which brings up the question of whether, in these situations, increased energy expenditure is a consequence of increased energy intake (thermic effect of food), rather than a response to hypoaminoacidemia *per se* (Hasek et al., 2010; Lees et al., 2017; Pezeshki & Chelikani, 2021). However, pair feeding studies have shown that, even when animals are fed the same number of calories on both control and amino acid restricted diets, there is still a significant increase in energy expenditure on the latter. This suggests that the increased energy expenditure in response to low protein diets is indeed due to low availability of proteins/amino acids (Malloy et al., 2006).

Though there is plenty of evidence suggesting that both glucagon and hypoaminoacidemia can, independently, lead to increased energy expenditure, whether glucagon-induced hypoaminoacidemia is what drives energy expenditure in glucagon-treated individuals is still an area of active research. In fact, in our recently published study, this relationship was further validated. Firstly, it was shown that chronic G108 treatment, which leads to hypoaminoacidemia, also leads to increased energy expenditure, as seen in experiments performed using metabolic cages. Furthermore, increased energy expenditure seemed to be

responsible for the reduction of fat mass observed in G108-treated animals. This is because rescuing plasma hypoaminoacidemia with a high protein diet prevented G108-mediated increase in energy expenditure, and fully rescued fat mass loss. Moreover, feeding mice with a diet specifically designed to contain the same (reduced) levels of amino acids as the ones measured in plasma of the mice chronically treated with G108, also led to an increase in energy expenditure and fat mass loss. Altogether, these results support the idea that glucagon-mediated increased energy expenditure and fat mass loss are caused as a response to hypoaminoacidemia (Hope et al., 2022).

4.1.2.3. G108-induced hypoaminoacidemia leads to lean mass loss

The human body consists in 70-90% of lean mass, which is calculated as total body weight minus fat mass. Lean mass thus includes the weight of organs, like muscles, but also of body fluids. A healthy human has around 40-50% muscle mass, and this is tightly regulated by a balance between muscle protein synthesis and degradation. Thus, when the level of proteolysis surpasses the level of protein synthesis, muscle mass is lost (Wolfe, 2006).

There are several pathways controlling protein degradation, with the main ones being the autophagy-lysosome and the ubiquitin-proteosome pathways. The autophagy lysosome pathway is responsible for elimination of insoluble proteins and defective cytoplasmic organelles. In this process, a sequence of actions results in the creation of an autophagosome that contains the structures intended for breakdown. Later, the autophagosome fuses with a lysosome, producing an autolysosome where the actual degradation takes place. Examples of genes involved in this pathway are Map1lc3b and Bnip3 (Xia et al., 2021). The ubiquitin pathway, on the other hand, is responsible for the degradation of short-lived and misfolded soluble proteins. Here, ubiquitin ligases tag proteins intended for degradation with ubiquitin, which will then be recognized by the proteosome, where protein degradation takes place. A gene involved in this pathway is Fbxo32 (aka Atrogin-1), which is part of the F-box only family, that encodes a muscle specific ubiquitin ligase (Sandri, 2013).
Muscle protein synthesis is regulated by several stimuli like exercise, protein intake (diet), amino acid availability, hormones (like insulin), age and even sleep. There are several pathways known to regulate protein synthesis in response to the previously mentioned stimuli, with the most well-known one being the mTOR. Upon activation, mTOR leads to the activation

of S6K, which promotes translation initiation, as well as repression of 4EBP1, a known suppressor of translation initiation. This, in combination with the role that mTOR also plays in directly inhibiting proteolysis, leads to muscle protein synthesis (Baptista et al., 2010; Dossou & Basu, 2019).

Studies conducted with both native glucagon and glucagon analogues provided evidence that this peptide hormone is associated with lean mass loss. In human studies, patients were infused short term with physiological levels of glucagon, which led to a decrease in muscle markers of protein synthesis. Although a conclusive loss in lean mass was not reported, the scale of muscle turnover was skewed towards muscle loss (Pacy et al., 2005). Other studies that show endogenous glucagon leading to lean mass loss are the ones mentioned in one of the previous sections regarding glucagonoma. Indeed, in addition to hypoaminoacidemia, loss of lean mass is also a known symptom in these patients (Barazzoni et al., 1999).
Studies with glucagon analogues have reported an effect on lean mass as well. For example, two studies using the glucagon analogue IUB288 in lean mice reported that animals experienced a loss of lean mass (Habegger et al., 2013; Okun et al., 2021). Additionally, another study on obese mice revealed that a GLP-1R/GCGR co-agonist also led to lean mass loss after a 13-day treatment (Day et al., 2012).

The muscles are the main storage site of amino acids. In fact, it has been acknowledged since the 1960s that, in the event of reduced nutrient intake, muscle protein acts as the main storage to replenish blood amino acids absorbed by other tissues (Wolfe, 2006). There are several studies linking low plasma amino acids with lean mass loss as well. One of the most common causes of lean mass loss is ageing. Several studies have shown a link between sarcopenia, i.e., patients experiencing loss of muscle mass due to age, and low plasma amino acid levels (Y et al., 2022; Yamada et al., 2018). Sarcopenia can also happen in association with other diseases. For example, another study evaluated the plasma amino acid levels in patients suffering from heart failure, before and after spending one year at a rehabilitation center. The authors reported a notable and significant correlation between low baseline serum concentration of branched chain amino acids, and the occurrence of skeletal muscle mass loss one year later (Tsuji et al., 2019).

There have been reports linking both glucagon and hypoaminoacidemia, independently, with lean mass loss. However, whether glucagon leads to lean mass loss via hypoaminoacidemia is

still an area of active research. The recent study published by our group supports this hypothesis. First, it was showed that animals chronically treated with G108, that thus present with hypoaminoacidemia, experience lean mass loss, as evidenced by MRI readings, grip strength tests and expression levels of proteolysis markers in muscle samples. Furthermore, rescue of plasma amino acid levels in G108-treated animals through diet supplementation with either protein or total amino acids (EAA and NEAA) alleviated loss of lean mass. Additionally, feeding mice with a diet with matched levels of amino acids to the ones found in the plasma of G108 treated animals, resulted in lower plasma amino acids, and also led to lean mass reduction (Hope et al., 2022). Thus, these results suggest that glucagon-induced lean mass loss is mediated by hypoaminoacidemia. The exact mechanisms and pathways through which glucagon mediated-hypoaminoacidemia induces lean mass loss are currently not fully understood, but but some suggest is through mTORC1 .

4.1.3. Partial mitigation of G108-induced side-effects does not prevent improved glycemia or hepatic steatosis

The study published by our group previously showed that G108-chronic treatment improves glycemia and potentially hepatic steatosis, whilst also leading to some secondary effects such as hypoaminoacidemia-mediated lean mass loss (Hope et al., 2022). To address whether G108 could be used to improve glycemia and hepatic fat without the lean mass loss side effect, several strategies were considered to rescue plasma amino acid levels. The most common way to increase plasma amino acids is through diet supplementation. Providing G108-treated animals with a diet with twice as much protein partially rescued plasma amino acid levels and lean mass loss (Hope et al., 2022). Remarkably, G108 chronic agonism still improved glucose tolerance and fatty liver, even after the side effects were partially mitigated (Hope et al., 2022). However, even though high protein supplementation helped mitigating the lean mass loss side effect, a complete rescue was not achieved.

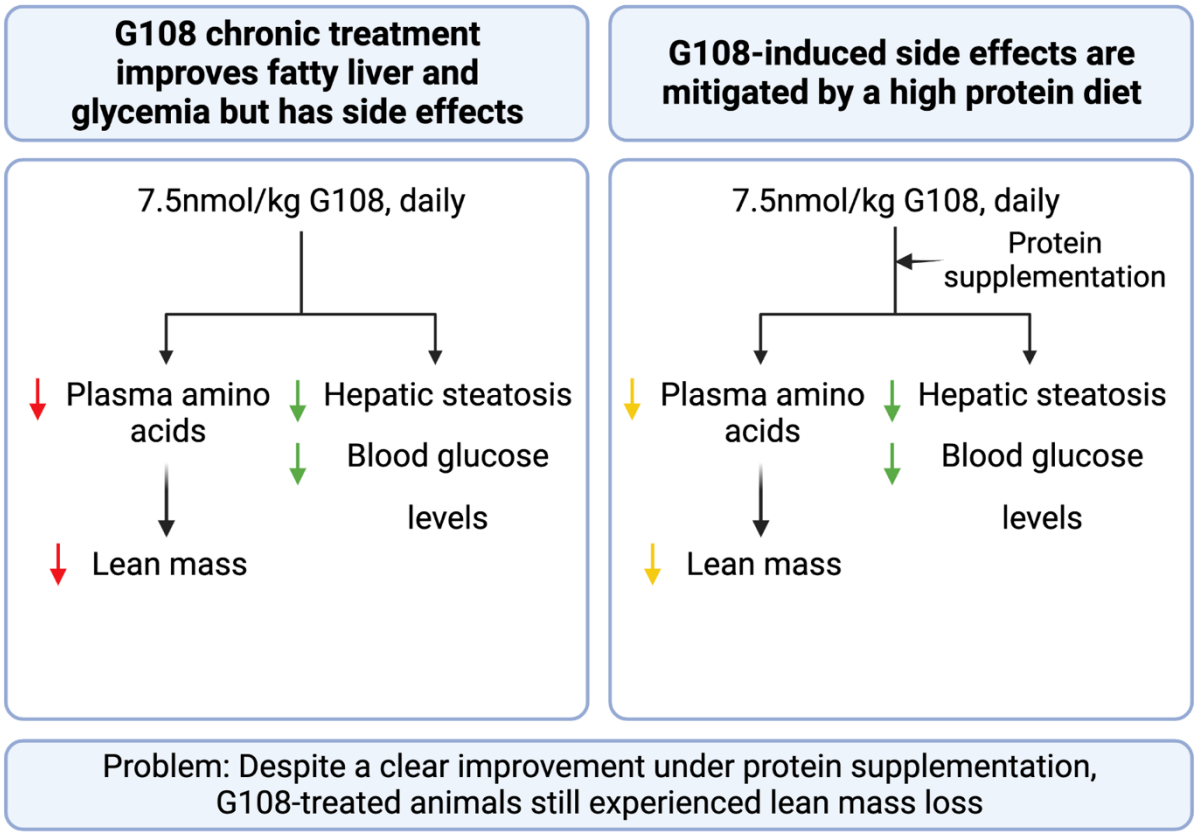


Figure 4.1. Schematic depicting relevant findings of (Hope et al., 2022). Daily treatment of DIO-mice with 7.5nmol/kg of G108 improves hepatic steatosis and glycemia, whilst also leading to hypoaminoacidemia-induced lean mass loss. Providing the treated animals with a diet high in protein only partially rescued hypoaminoacidemia and, consequently, lean mass loss, whilst still allowing the beneficial effects on fatty liver and blood glucose levels.

4.2. Hypothesis and aims

Our group has recently published a study on the effects of chronic GCGR agonism in DIO-mice using a novel glucagon analogue, G108 (Hope et al., 2022). That study uncovered that daily administration of 7.5 nmol/kg G108 improves glycemia, and potentially reduces hepatic steatosis (not all samples were tested and objective quantification was not performed), however it also promoted hypoaminoacidemia-induced lean mass loss. Loss of lean mass was successfully reduced by providing the animals with a diet higher in protein. High protein supplementation was effective at preventing loss of lean mass to some extent, whilst still allowing the benefic effects of GCGR agonism on hepatic steatosis and glycemia, suggesting that these might be governed by distinct pathways. Because lean mass loss is a serious side effect, and it was only partially rescued it in the initial study (Hope et al., 2022), this chapter aimed to test whether a complete rescue of lean mass loss was possible without affecting the glycemia and hepatic fat positive effects of G108 chronic treatment.

Hypothesis

It is possible to completely prevent lean mass loss in G108-chronically treated animals whilst still improving glycemia and hepatic steatosis.

Aims

1. Assess contribution of high protein diet only to the outcomes reported on G108-treated high protein diet fed animals.
    - Include high protein diet vehicle control group in all experiments.
2. Test strategies to completely prevent lean mass loss in G108-chronically treated mice:
    - Test lower G108 doses of 5 and 2.5 nmol/kg.
    - Test lower G108 doses of 5 and 2.5 nmol/kg in the context of high protein supplementation.
3. Assess whether G108-chronic treatment still improves glycemia and hepatic steatosis after complete mitigation of lean mass loss.
    - Perform objective quantification of hepatic fat content in all samples.

4.3. Materials and methods

4.3.1. Animals

Animal procedures were conducted in accordance with the Animals (Scientific Procedures) Act 1986. Mice used in this chapter were male C57Bl/6 (Charles River UK) housed in a temperature-controlled room (21ºC) with a 12h light/dark cycle. All mice had access to water and respective diets Ad libitum throughout the whole study unless mentioned otherwise.

4.3.2. Chronic G108 treatment

Fifty 4-week-old male mice were provided with accesses to 60kcal% high fat diet (D12492, Research diets) ad libitum for 4 weeks to induce obesity. The number of animals for this study was chosen based on previously published study (Hope, 2022; Hope et al., 2022). Then, they were single housed and provided with a diet containing 45kcal% fat and either standard (SP) (20kcal%) (D08091803, Research Diets) or high (HP) (40kcal%) (D08091801, Research Diets) protein for 2 weeks prior to the beginning of the study (table 4.1). During the study, mice were injected subcutaneously daily between 9 and 11 am for 22 days, with equal volumes (50ul) of vehicle (water for injections), 2.5nmol/kg or 5nmol/kg G108 solutions. G108 solutions were prepared by diluting G108 powder in water for injections everyday immediately before injections.

Table 4.1. Animal diets composition.

	Fat (kcal%)	Protein (kcal%)	Carbohydrate (kcal%)
High fat	60	20	20
Standard protein (SP)	45	20	35
High protein (HP)	45	40	15

4.3.3. Body weight and food intake

Body weight was measured daily and food intake every other day with the same weighing scale.

4.3.4. Lean and fat mass MRI measurement

Lean and fat mass were measured using an EchoMRI analyser (EchoMRI-100H) in the morning, one day before the beginning of injections and then again at days 13 and 21. The animals were inserted into a transparent cylindrical Perspex tube which was then cautiously placed inside the MRI analyser. After the scan, values were recorded, and the animals were returned to their respective cages.

4.3.5. Grip strength

Grip strength measurements were taken one day before the beginning of injections, and then again at day 21. To measure the forelimb grip strength of mice, a dedicated grip strength meter was used. Each mouse was gently placed on a grip strength bar and allowed to grip it. The grip was then released by gently pulling the mouse's tail, and the maximum force applied to the bar was measured and recorded. This process was repeated three times, with a one-minute interval between each measurement. Finally, the average of all recorded measurements was calculated

4.3.6. Plasma amino acid quantification

Total plasma amino acids were measure in terminal plasma samples acquired on day 22 of the study, using a commercial kit (MAK002, Sigma).

4.3.7. Intra-peritoneal glucose tolerance test (Ip-GTT)

Due to the cohort size and limited number of researchers available, ip-GTTs were performed over two days (24 mice on day 13 and 26 mice on day 15). On the morning of the test, mice were injected with either vehicle, 2.5 or 5 nmol/kg of G108 and body weight was recorded as per usual. They were then fasted of food and water for 5h and moved to the procedure room 1h prior to the beginning of the test for acclimatization. A baseline blood glucose measurement was taken via tail venesection using a glucose monitor (GlucoRX), followed by intra-peritoneal injection of 2g/kg of a glucose solution (in water). Blood glucose measurements were also taken at 20, 40, 60 and 90 minutes post glucose challenge. At the end of the test, mice were returned to the respective cages and access to food and water was restored.

4.3.8. Histology: double ORO and haematoxylin staining

Liver samples were consistently collected from the same lobe and same region within the lobe across different animals. Liver samples were snap frozen and later mounted on a holder with OCT and sliced into 5µm slices using a cryostat. Slices were collected onto SuperFrost slides (Cat# 17284884, Fisher Scientific) and stored at -80ºC until needed.

For ORO and haematoxylin staining, slides were removed from -80ºC and let to equilibrate at room temperature for 10 minutes. Slides were then dipped in a 4% PFA solution, rinsed in 60% triethyl phosphate and immersed in 1% ORO solution (Cat# A12989.14, VWR) (in 60%triethly phosphate) for 25 minutes. Excess ORO solution was then removed by rinsing slides in 60% triethyl phosphate followed by distilled water. Lastly, haematoxylin counterstain was performed by dipping slides on haematoxylin solution (Sigma), followed by washing in distilled water. Slides were mounted in aqueous mount (Sigma) and sealed with coverslips.

ORO-stained slides were imaged within 2 days of staining protocol using an automated slide scanner, and quantification of hepatic fat percentage was performed using an automated macro developed by Dirk Doorman from LMS Microscopy facility that quantified the percentage of positive ORO staining area per total area imaged. ORO staining scoring was performed by a blind researcher that classified an average of 3 slices per liver sample from 1 to 10 (with 1 being no hepatic fat observed).

4.3.9. RT-qPCR

RNA extraction: liver and quadricep samples were collected to an Eppendorf and snap frozen in liquid nitrogen. 1 steel bead (Cat#69989, Qiagen) was added to each Eppendorf, followed by 1ml TRizol (Cat# 15596026, Fisher Scientific), and samples were then mechanically homogenized for 3 minutes at 30Hz using a tissue homogenizer (Brand and Model). 500ul chloroform were then added to each Eppendorf followed by centrifugation at 12000g for 15 minutes. The supernatant was then transferred to a new Eppendorf, 500ul of 70% isopropanol were then added to it and the tubes were gently inverted, before being centrifuged at 16000g for 15 minutes. The supernatant was then discarded, and great care was taken not to disturb the RNA pellet. The pellet was then washed with 70% ethanol three times and let to air dry. Finally, the RNA pellet was re-suspended in RNAse-free water, the concentration measure using a spectrophotometer (NanoDrop) and stored at -80ºC until needed.

cDNA synthesis: cDNA was made from 1ug of total RNA samples using the iScript™ cDNA Synthesis Kit (Cat#1708891, Bio-Rad) as per manufactures instructions.
qPCR: qPCR was performed using iTaq™ Universal SYBR® Green (Cat# 1725122, Bio-Rad) as per manufactures instructions, and the list of primers used (KiCqStart primers) can be found in the table below.

Table 4.2. List of primers used in qPCR experiments.

Gene	**Catalog number**
Cyclophilin	M_Ppif_1
B-actin	M_B020004C17Rik_1
4ebp	m_4ebp1_1
Fbxo32	m_fbxo32_1
Map1lc3b	m_map1lc3b_1
Bnip3	m_bnip3_1
Ass1	m_ass1_1
Asl	m_asl_1,
Cps1	m_cps1_1
Arg	m_arg_1
Fasn	m_Fasn_1
Cpt1a	M_Cpt1a_1

4.4. Results

4.4.1. Lean mass loss is completely prevented by 2.5nmol/kg G108 dose in the context of high protein supplementation

The study presented in this chapter aimed to fully mitigate lean mass loss induced by G108 chronic treatment and then assess whether the improvement of NAFLD features is still maintained. Simultaneously, this study also aimed to address the effects of HPD alone on the outcomes reported in the original publication, given that this group was missing in that study (Hope et al., 2022). Two strategies were defined in an attempt to completely prevent lean mass loss. 1) First, it was assessed whether simply lowering G108 dose (from 7.5) to 5 or 2.5 nmol/kg was enough to prevent lean mass loss; 2) Secondly, it was tested whether lowering G108 dose to 5 or 2.5 nmol/kg under high protein conditions was enough to prevent lean mass loss. While doing so, the impact of increased protein intake alone on lean mass, glycemia, and/or hepatic fat accumulation over time was also explored. Thus, for this study an additional control group was included, that was missing in the initial publication, of vehicle treated mice fed a high protein diet. Thus, the experiments in this chapter were performed in the following 6 groups: Veh, SP and Veh, HP: Animals treated with vehicle and kept under standard or high protein diets, respectively; 2.5, SP and 2.5, HP: animals treated with 2.5 nmol/kg G108 and kept under standard or high protein diets, respectively; 5, SP and 5, HP: animals treated with 5 nmol/kg G108 and kept under standard or high protein diets, respectively. A schematic of this study's experimental design can be found in Fig. 4.2.

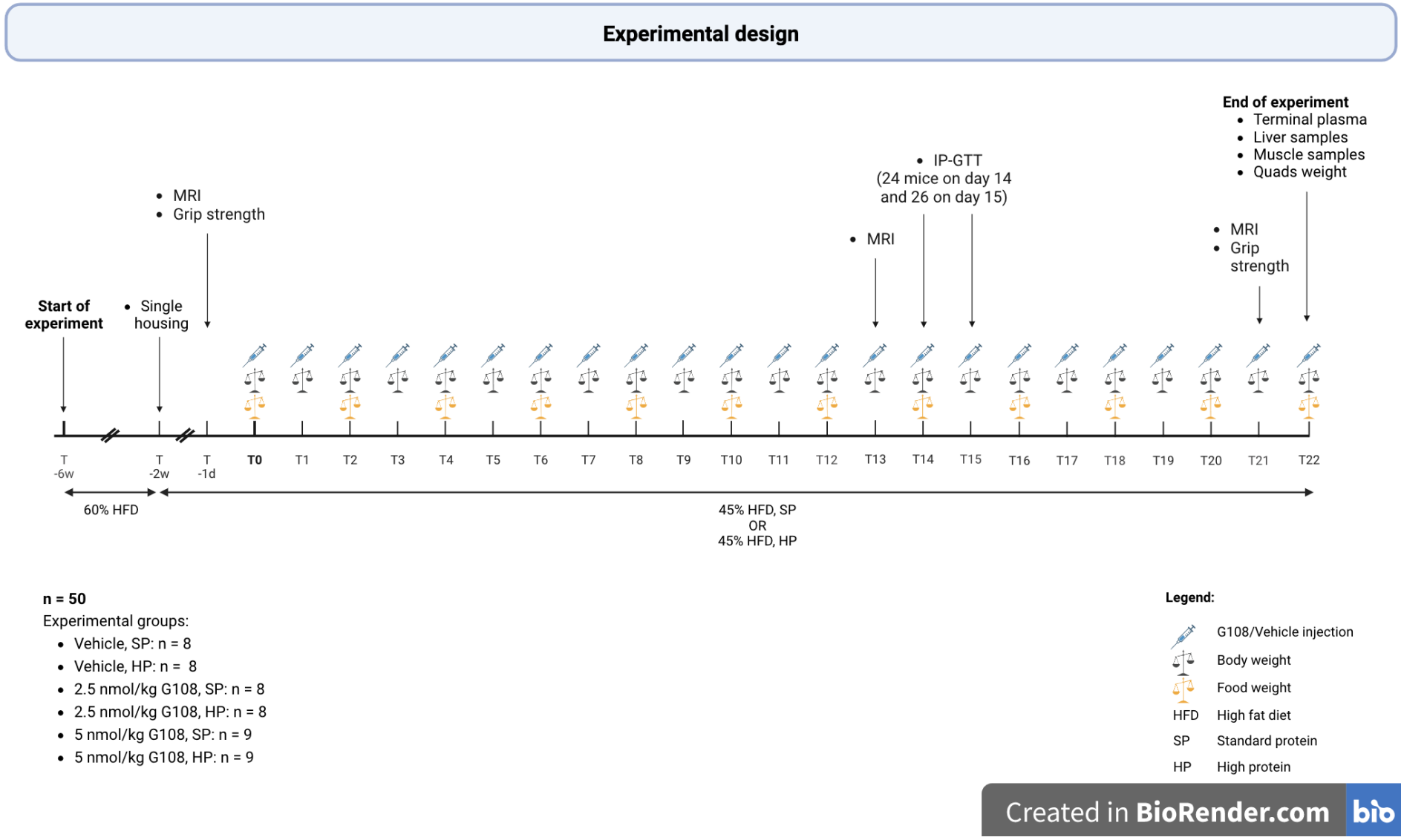


Figure 4.2. Schematic of study's experimental design. *Created in BioRender.*

The effect of the two pre-determined approaches to mitigate lean mass loss in G108-treated animals was first studied on body weight and food intake. First, regarding body weight, there was no significant difference caused by dietary protein content, as evidenced by the similar trends in body weight of vehicle-treated mice kept under SP and HP conditions. Body weight was also not affected with the lower 2.5 nmol/kg dose of G108, irrespectively of dietary protein amount (Fig. 4.3). However, animals treated with the higher 5 nmol/kg dose, and kept under standard protein conditions, exhibited body weight loss since early on the study, with this difference reaching significance from day 6 (Fig. 4.3a). By the end of the study, 5, SP animals had lost nearly 4g of body weight (11% of baseline body weight), in sharp contrast to both Veh, SP and HP controls that gained 1.6g (5.5%) and 0.9g (3.3%), respectively (Fig. 4.3b and c). Feeding animals injected with 5 nmol/kg G108 a high protein diet seemed promising in preventing body weight loss in the first 12 days of the study. However, shortly after that they also started to lose weight, with such drop reaching significance from day 16 (Fig. 4.3a). By the end of the study, animals from the 5, HP group had lost a total of 0.5g (1.5%) body weight (Fig. 4.3). Although the difference in body weight between 5, HP and Veh, HP animals did not reach statistical significance, the trend towards body weight loss is clear. Thus, despite high protein supplementation clearly blunting body weight loss induced by chronic 5 nmol/kg G108 treatment, this was still not enough to completely prevent it over time (Fig. 4.3a). Overall, these results show that body weight preservation was only completely achieved in mice treated with the lower 2.5 nmol/kg G108 dose, irrespective of dietary protein content.

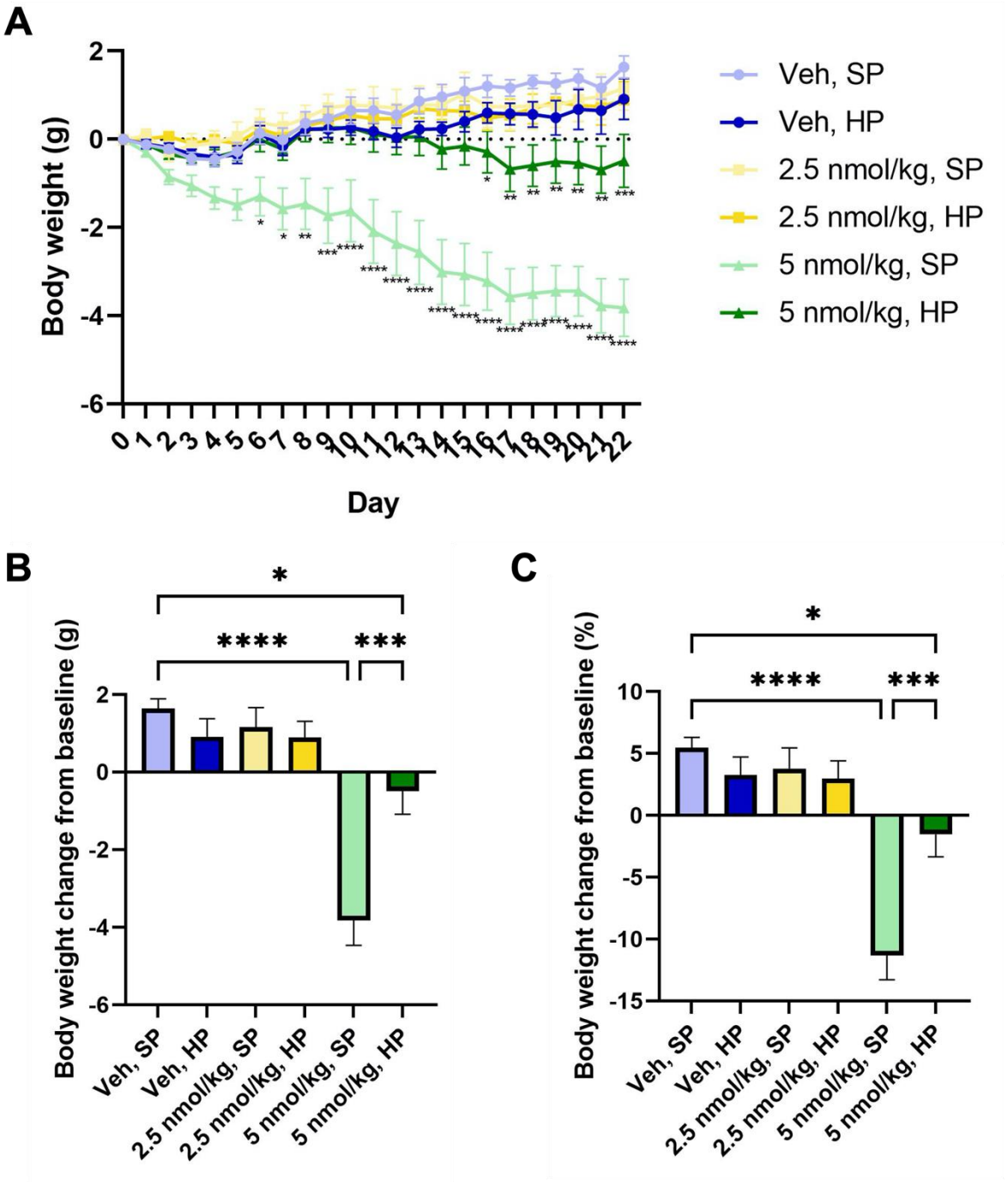


Figure 4.3. Chronic G108 treatment with 5 nmol/kg, but not 2.5 nmol/kg, leads to body weight loss. A) Graph depicting daily change in body weigh from baseline; Graphs depicting total body weight change from baseline in B) grams and C) percentage. Data expressed as ± SEM Two-way ANOVA with post-hoc Dunnett's and Tukey's tests. *: p-value < 0.05; **: p-value < 0.01; ***: p-value < 0.001; ****: p-value < 0.0001. Indicates significance compared to Veh, SP.

Regarding the effects on food intake, all animals kept on a high protein diet started eating significantly less than the ones from the vehicle SP group between the 14th and 16th day of the study (Fig.4.4a). Indeed, total food intake data showed that all groups fed a high protein diet ate slightly, but significantly, less than their counterparts kept on a standard protein (Veh, SP:

59.1g vs Veh, HP: 53.9g; 2, SP: 60.2g vs 2, HP: 54.5g; 5, SP: 59.8g vs 5, HP: 54.1g). There were, however, no differences caused by G108 treatment in food intake, regardless of dosage (Fig. 4.4). Thus, these results show that, indeed, higher dietary protein content alone, but not G108 treatment, is responsible for a slight reduction in food intake in G108, HP groups.

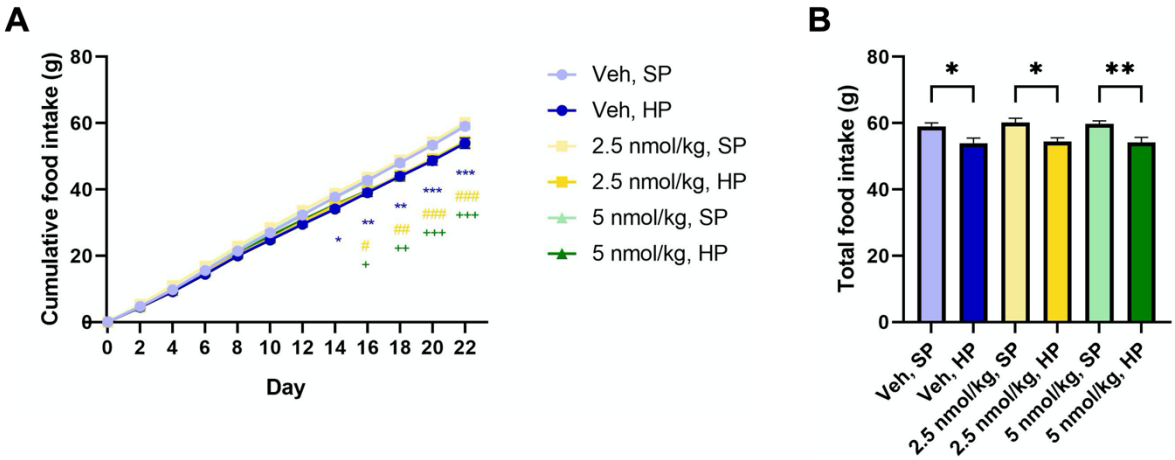


Figure 4.4. High protein diet, but not G108, reduces food intake. A) Daily and B) total food intake from baseline. Data expressed as ± SEM. Two-way ANOVA with post-hoc Dunnett's and Tukey's tests. *, # and +: p-value < 0.05; **, ## and ++: p-value < 0.01; ***, ### and +++: p-value < 0.001. On a), * indicates significance of Veh, HP; # indicates significance of 2.5, HP; and + indicates significance of 5, HP; compared to Veh, SP.

Next, an assessment was conducted to determine whether the observed changes in body weight were attributed to alterations in fat and/or lean mass content. Despite an initial non-significant difference at day 13 of the study, by day 21, fat mass content was similar between vehicle SP and HP controls, with both having gained 1.6g (19.6% of baseline fat mass) and 1g (17.1%) of fat mass, respectively, throughout the study (Fig. 4.5). Consistent with the body weight data, the lower 2.5 nmol/kg dose did not lead to any change in fat mass either, regardless of protein content (Fig. 4.5). However, after only 13 days of daily G108 injections, mice treated with the higher 5 nmol/kg dose, and kept under standard protein conditions, had already lost 1.3g (14.6%) of fat mass, in contrast to vehicle SP controls that had already gained 0.9g (10.7%). This trend continued until the end of the study. High protein supplementation significantly attenuated fat mass loss in animals treated with 5 nmol/kg G108. By day 21 of the study, the 5, HP group increased its fat mass in 0.3g (4.6%), whilst the SP and HP controls had an increase of 1.6g (19.6%) and 1.1g (17.1%), respectively. Despite the control groups gaining around four times more fat mass than the animals from the 5, HP group, this disparity did not reach statistical significance (Fig. 4.5). Overall, these results show that fat mass is completely preserved in animals treated with the 2.5 nmol/kg dose, regardless of dietary protein content,

but for the animals treated with 5 nmol/kg dose fat mass preservation is only partially achieved under high protein supplementation.

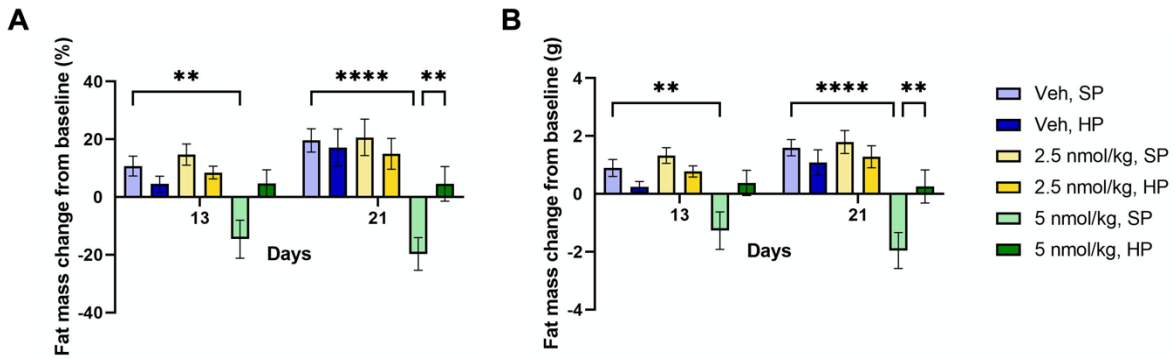


Figure 4.5. Chronic G108 treatment with 5 nmol/kg, but not 2.5 nmol/kg, leads to fat mass loss. Change in lean mass from baseline in A) grams and B) percentage, at days 13 and 21 of the study. Data expressed as ± SEM. Two-way ANOVA with post-hoc Tukey's test. **: p-value < 0.01; ****: p-value < 0.0001.

The impact of G108 chronic treatment on lean mass and muscle function was investigated next. Regarding the lean mass, MRI data showed that there was no significant difference between vehicle SP and HP groups, with both having lost 0.1g (0.5% of baseline lean mass) and 0.5g (2.1%) lean mass, respectively, by day 21. For the 2.5nmol/kg dose, after 13 days into the study, animals kept on a standard protein diet had lost 0.8g (3.6%) of lean mass, which was a significantly higher drop compared to the respective Veh, SP control. This trend was maintained until the end of the study (day 21) (p-value=0.05) (Fig. 4.5). However, higher protein intake completely rescued the lean mass loss seen in standard protein conditions, since animals from the 2.5, HP group lost only 0.5g (2.3%) of lean mass, which was very similar to the lean mass lost in vehicle HP controls. For the higher 5nmol/kg dose, animals kept under standard protein conditions had already lost a significant amount of lean mass by day 13 (2.2g/10.1%), and such loss was maintained until the end of the study (day 21). High protein supplementation was enough to cut G108-induced lean mass loss in half, to only 1.1g (4.9%), by day 21. However, animals in this group still lost significantly more lean mass when compared to the vehicle SP control group. Animals from the 5, HP group lost more than double the amount of lean mass compared to vehicle HP control (4.9% vs 2.1%). Whilst this difference did not reach statistical significance, it was close (p-value=0.07) (Fig. 4.6a and b). Overall, these results show that lean mass was only completely preserved in animals receiving the lower 2.5 nmol/kg G108 dose, and specifically only under conditions of high protein supplementation.

The impact of G108-chronic treatment on muscle size and function was assessed next by comparing terminal quadriceps weight, and grip strength before (baseline) and after (day 21) the respective treatments, respectively. Extensive lean mass loss might translate into smaller muscles, so quadriceps weights were compared across the different groups. However, by the end of the study, no differences in quadriceps weight were observed between any of the groups (Fig. 4.6c). Regarding muscle function, no significant differences were seen in animals treated with either vehicle or 2.5nmol/kg G108 dosage, irrespectively of dietary protein levels. However, in line with the lean mass loss data, animals treated with the higher 5nmol/kg dose kept under a standard protein diet had significantly reduced strength by the end of the study (120.1g at baseline vs 95.7g at day 21). In contrast to the lean mass data, high protein supplementation was enough to completely prevent loss of muscle function in animals chronically treated with 5 nmol/kg G108 (Fig. 4.6d). Overall, these results indicate that muscle function was only impaired in animals treated with the higher 5 nmol/kg G108 dose, and only under standard protein conditions.

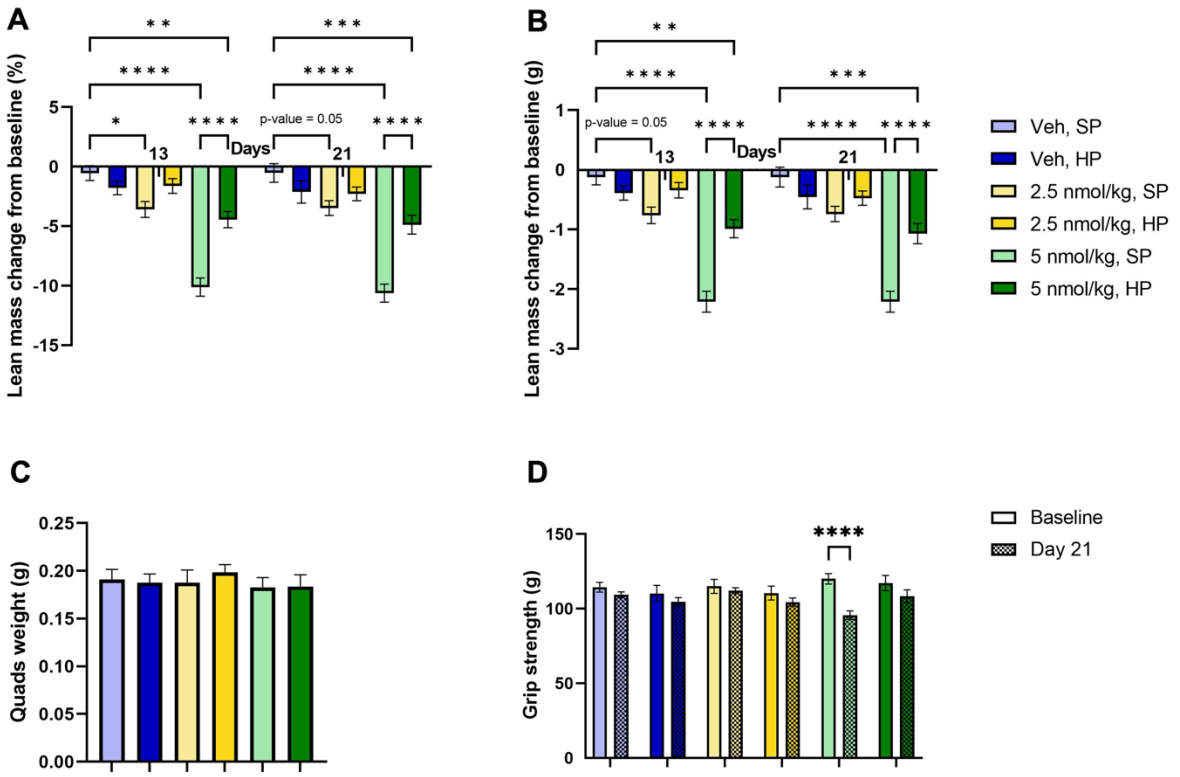


Figure 4.6. Lean mass loss is completely prevented by high protein supplementation in mice chronically treated with 2.5 nmol/kg, but not 5 nmol/kg G108. Change in lean mass from baseline in A) grams and B) percentage, at days 13 and 21 of the study. C) Quadricep muscles weight at day 22 of the study; D) Grip strength at baseline and at day 21 of the study. Data expressed as ± SEM. Two-way ANOVA with post-hoc Sidak's and Tukey's test. *: p-value < 0.05; **: p-value < 0.01; ***: p-value < 0.001; ****: p-value < 0.0001.

As explained in section 4.1.2.3., loss of muscle mass happens when the rate of muscle degradation surpasses the rate of muscle synthesis. Thus, to have a more in dept look at muscle turnover, the expression levels of markers of protein degradation and synthesis on quadriceps samples were analyzed. Specifically, the markers of the autophagy pathway Mapl1c3b and Bnip3, and of the ubiquitin pathway Fbxo32 were investigated. The expression levels of 4ebp1, a known repressor of protein synthesis, were also studied. Surprisingly, no obvious differences could be observed between any of the groups regarding the expression levels of the protein degradation markers Bnip3, Mapl1c3b and Fbxo32 (Fig. 4.7b, c and d). Unexpectedly, although this did not reach statistical significance, high protein diet seemed to promote 4ebp1 upregulation, as indicated by the slightly increased expression levels seen in Veh, HP compared to Veh, SP and 2.5, HP compared to 2.5, SP (Fig. 4.7a). Furthermore, a statistically significant increase was observed between 5, HP and 5, SP groups. G108 treatment did not seem to affect 4ebp1 expression levels, as evidenced by the similar expression levels between Veh, SP; 2.5, SP and 5, SP groups as well as the similar expression levels between their counterparts Veh, HP; 2.5, HP and 5, HP groups (Fig. 4.7a). Overall, these results show that, in contrast to what was previously reported in the original study (Hope, 2022; Hope et al., 2022), with these lower doses, G108-chronic treatment did not lead to a visible change in protein synthesis nor degradation markers.

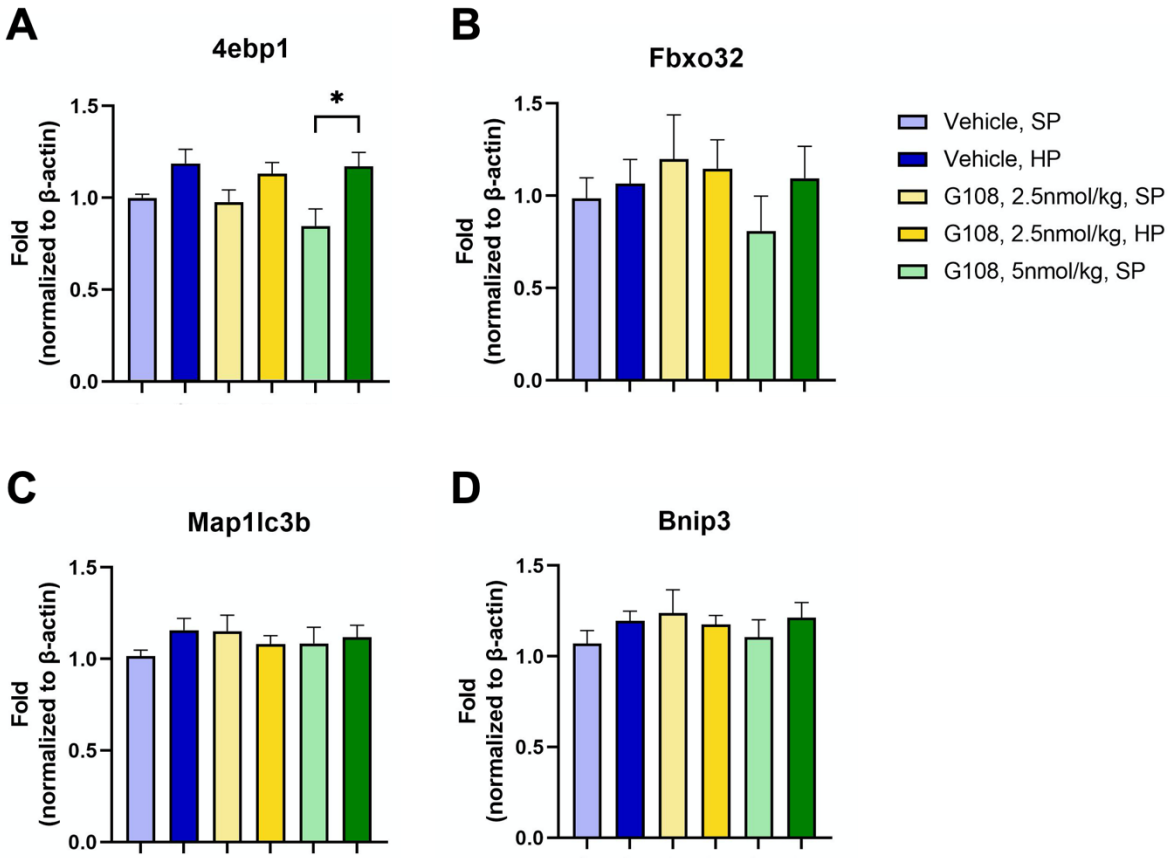


Figure 4.7. Expression levels of muscle turnover markers do not reflect lean mass loss. qPCR of markers of muscle turnover A) Eukaryotic translation initiation factor 4E-binding protein 1 (4ebp1); B) F-box only protein 32 (Fbxo32); C) Microtubule associated protein 1 light chain 3 beta (Mapl1c3b); D) BCL2 interacting protein 3 (Bnip3). Data normalized to b-actin. Data expressed as ± SEM. Two-way ANOVA with post-hoc Tukey's test. *: p-value < 0.05.

Our group has previously shown that G108-induced lean mass loss happens due to a whole-body response to hypo aminoacidemia. Thus, the hepatic expression levels of genes involved in amino acid catabolism, as well as plasma amino acid levels, were investigated across the different groups at the end of the study (day 22). Specifically, the expression levels of *Cps1*, *Ass1*, *Arg* and *Asl* genes involved in the urea cycle, a key pathway in amino acid catabolism, were analyzed. RT-qPCR on liver samples showed that, although not significantly, the expression levels of most tested genes, namely *Cps1*, *Ass1* and *Asl*, were upregulated by higher dietary protein, as indicated by the increased fold of Veh, HP compared to Veh, SP groups (Fig. 4.8 a, b and d). Furthermore, and as expected, expression of all tested amino acid catabolic genes was increased by both 2.5 and 5nmol/kg G108 doses under standard protein conditions (Fig. 4.8). Despite *Cps1* and *Ass1* expression being upregulated by both G108 doses when compared to the respective Veh, SP control, this did not reach statistical significance for the 2.5, SP group (Fig 4.8 a and b). As expected, HP supplementation did not prevent G108-mediated increased expression of the tested genes. In fact, and in line with the previously

mentioned observation that a high protein diet on its own seems to promote upregulation of most aa catabolism genes, high protein seemed to further upregulate the expression levels of all tested genes in the context of G108 treatment (Fig. 4.8). This trend of high protein further up regulating the expression levels of genes involved in amino acid catabolism in the context of G108 did not reach statistical significance for the 2.5 nmol/dose, but it did so for the higher 5 nmol/kg dose on *Arg* and *Asl*, as evidenced by the comparison between 5, SP and 5, HP groups (Fig. 4.8 c and d). Overall, this data shows that both high protein diet and G108 treatment increase the expression of genes involved in the catabolism of amino acids, and that together these two factors have an additive effect.

Next, amino acids levels were measured in terminal plasma samples. Vehicle control animals kept under a high protein diet exhibited slightly higher levels of plasma amino acids, than when raised under standard protein conditions (5.3 vs 4.2 nmol/ul, respectively), although not significantly. As expected, animals kept under a standard protein diet, and treated with either dose of G108, had significantly decreased plasma amino acid levels, when compared to vehicle SP controls, of 2.3 nmol/ul each. High protein supplementation completely rescued amino acid levels in animals treated with both doses to 3.8 nmol/ul each (Fig. 4.8e). Overall, these results confirm that G108 promotes plasma hypoaminoacidemia, that HP diet fully rescued hypoaminoacidemia in animals treated with G108, but that there is no difference between the two doses tested.

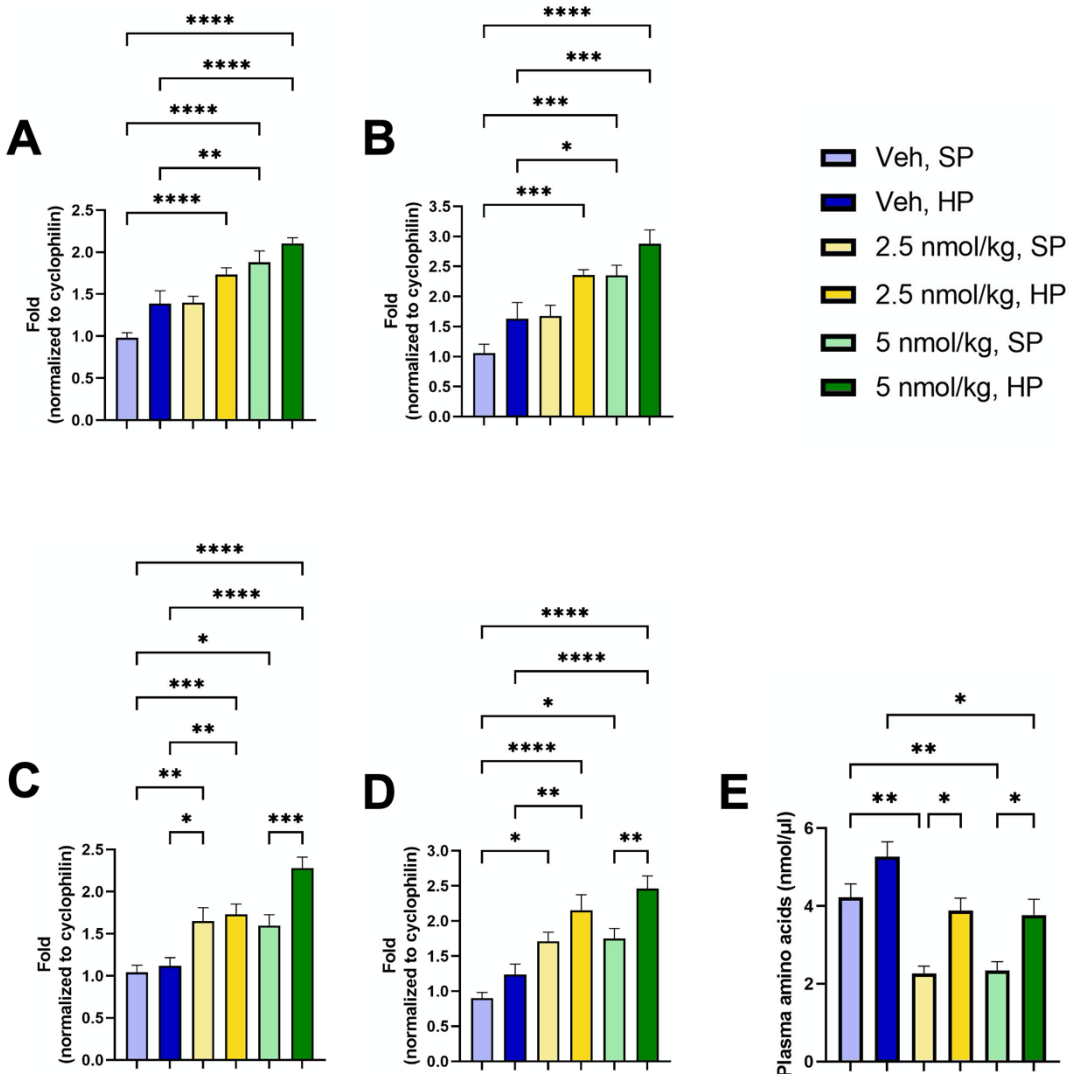


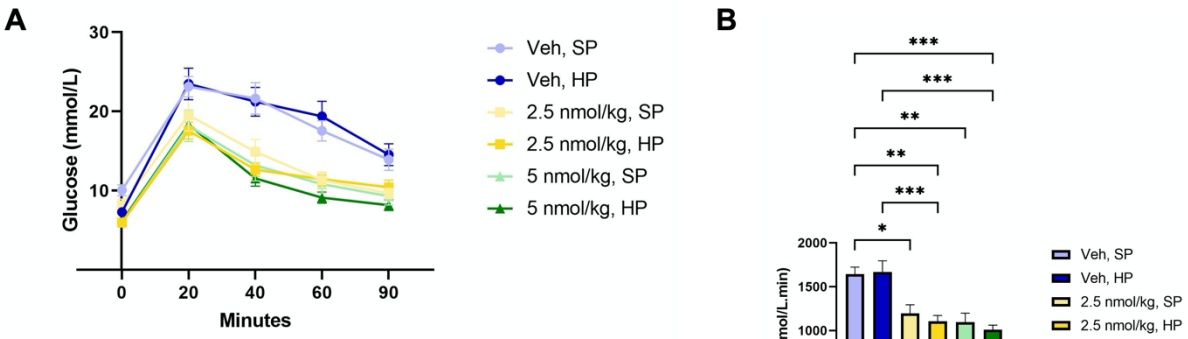
Figure 4.8. G108-chronic treatment with both 2.5 and 5 nmol/kg dose induces hypoaminoacidemia, that is completely rescued by high protein supplementation. A) Expression levels of genes involved in hepatic amino acid catabolism (urea cycle) Carbamoyl phosphate synthase 1 (Cps1), B) Arginosuccinate synthase 1 (Ass1), C) Arginase (Arg) and D) Arginosuccinate lyase (Asl). Data normalized to cyclophilin. E) Plasma total amino acid levels at the end of the study (day 22). Data expressed as ± SEM. Two-way ANOVA with post-hoc Tukey's test. *: p-value < 0.05; **: p-value < 0.01; ***: p-value < 0.001; ****: p-value < 0.0001.

4.4.2. Improved glycemia and hepatic steatosis are still maintained after complete mitigation of lean mass loss

Experiments were then conducted to assess whether the improved NAFLD features of glycemia and hepatic steatosis previously reported after chronic G108 treatment, in DIO mice, (Hope et al., 2022) were still preserved after complete mitigation of lean mass loss. The groups treated with the higher G108 dose were also tested as a positive control.

Dietary protein content did not influence whole glucose excursion after glucose loading, as evidenced by the similar profiles and areas under the curve (AUC) of vehicle SP and HP control

groups. However, baseline glucose levels were slightly, but significantly, lower on vehicle control animals kept on a high protein diet (10.1 vs 7.3 mmol/l in SP vs HP groups, respectively). G108-treatment significantly improved glucose tolerance in a similar fashion with both doses and regardless of protein level supplementation (Fig. 4.9). So, overall, these results show that the complete mitigation of lean mass loss, achieved in animals treated with 2.5 nmol/kg dose and kept under high protein conditions, does not prevent G108-mediated improvement of glycemia in DIO mice.



Compared to Veh, SP					
	0 min	20 min	40 min	60 min	90 min
Veh, HP	*	ns	ns	ns	ns
2.5 nmol/kg, SP	ns	ns	ns	**	ns
2.5 nmol/kg, HP	**	*	**	**	ns
5 nmol/kg, SP	**	ns	*	**	ns
5 nmol/kg, HP	**	*	**	***	*

Figure 4.9. G108-chronic treatment still improves glycemia after complete mitigation of lean mass loss. ip-GTT A) profile and B) area under the curve. In a) * indicates significance compared to vehicle, SP group. Data expressed as ± SEM. Two-way ANOVA with post-hoc Dunnett's and Tukey's test. *: p-value < 0.05; **: p-value < 0.01; ***: p-value < 0.001.

The impact of G108 chronic treatment on hepatic steatosis was then investigated. To do so, liver samples from each animal were stained with the fat dye Oil Red O (ORO), and representative images from each group can be found in Fig. 4.10a.

The differences in ORO staining were first evaluated by blind relative-scoring. Here, stained liver sections were scored from 1 to 10 according to the amount of positive ORO staining (with 1 representing less hepatic fat). The results suggested that, despite no significant difference (p-value=0.4), vehicle animals fed a high protein diet seemed to have slightly less hepatic fat, as evidenced by the lower 5.1 score, than vehicle animals kept under standard protein conditions, that had a scoring of 7.2. Both 2.5 and 5 nmol/kg G108-treated groups kept under standard protein conditions had significantly improved hepatic steatosis than the respective Veh, SP control group, as indicated by the lower scoring of 3.3 and 2.1, respectively. HP supplementation did not prevent the reduction in hepatic fat accumulation seen with both G108

doses that were still significantly lower than vehicle SP control. However, when compared to Veh, HP group, and despite the clear trend, the decrease in hepatic steatosis was only significant with the higher 5nmol/kg G108 dose (Fig. 4.10b).

Subsequently, the percentage of ORO positive staining in each sample was also objectively quantified through automated post-acquisition image analysis. The results obtained supported the blind-scoring ones. Again, despite not significant, controls fed a high protein diet had nearly 4% less hepatic fat than controls kept under a standard protein diet (11% vs 14.7%, respectively). The percentage of hepatic fat was also significantly reduced with both G108 doses under standard protein conditions, with the 5, SP group having half the hepatic fat of the 2.5, SP group (2.5% and 5%, respectively). Higher protein intake did not prevent the reduction in hepatic fat percentage. However, and just like in the blind-scoring results, despite the 2.5, HP group having more than two times less hepatic fat than the Veh, HP controls (5% vs 11%, respectively) this did not reach significance, whereas the 5, HP group did (Fig. 4.10c). Overall, these results show that G108-mediated improvement of hepatic steatosis is still preserved, even after complete mitigation of lean mass loss, as evidenced by the reduced scoring and percentage of ORO staining in the 2.5, HP group.

As explored in section 1.2., hepatic fat accumulation is tightly regulated by the mechanisms governing hepatic fat acquisition and disposal. Four main pathways are involved in keeping this balanced: fat uptake (directly from diet and from the NEFA pool), *de novo* lipogenesis, fatty acid b-oxidation and fat exportation in very low-density lipoproteins. Glucagon is widely known to suppress *de novo* lipogenesis and promote b-oxidation, thus experiments were then conducted to gain insight into how G108 was reducing hepatic fat under the defined experimental settings. To do so, the expression levels of Carnitine palmitoyl transferase I (*Cpt1a*), involved in fatty acid b-oxidation, and Fatty acid synthase (*Fasn*), involved in *de novo* lipogenesis, were measured. First, higher levels of dietary protein seemed to downregulate *Fasn*, as evidenced by the reduced fold of Veh, HP compared to Veh, SP groups, although this did not reach a significant level. G108 treatment with both 2.5 and 5 nmol/kg doses also led to a downregulation of *Fasn* expression when compared to Veh, SP controls, with this drop reaching significance with the higher 5 nmol/kg dose. Despite *Fasn* being downregulated by both high protein and G108 individually, when in combination, these factors do not seem to have a synergistic effect. In fact, it is quite the contrary, since 2.5, HP and 5, HP groups have slightly higher expression levels than 2.5, SP and 5, SP groups, respectively, although not significantly. Indeed, the 2.5, HP, but not the 5, HP, group showed increased *Fasn* expression when compared to the respective Veh, HP control group. As evidenced by comparing Veh, SP

and Veh, HP groups, dietary protein levels did not seem to have a great effect on *Cpt1a* expression. G108 treatment, on the other hand, led to its up regulation with both 2.5 and 5 nmol/kg doses, with this reaching significance only for the higher 5 nmol/kg dose (p-value=0.07 for Veh, SP vs 2.5, SP). High protein supplementation did not seem to impact *Cpt1a* expression levels in G108-treated animals, with both 2.5, HP and 5, HP groups being increased in comparison to Veh, HP, although this only reached significance for the latter (Fig. 4.10e). Overall, these results suggest that G108 still reduces hepatic steatosis even under conditions of complete mitigation of lean mass loss. However, exactly how this happens is presently unclear, since G108 seems to reduce hepatic fat accumulation, at least in part, by up-regulating fatty acid b-oxidation and down-regulating *de novo* lipogenesis, but high protein diet somewhat mitigates these effects.

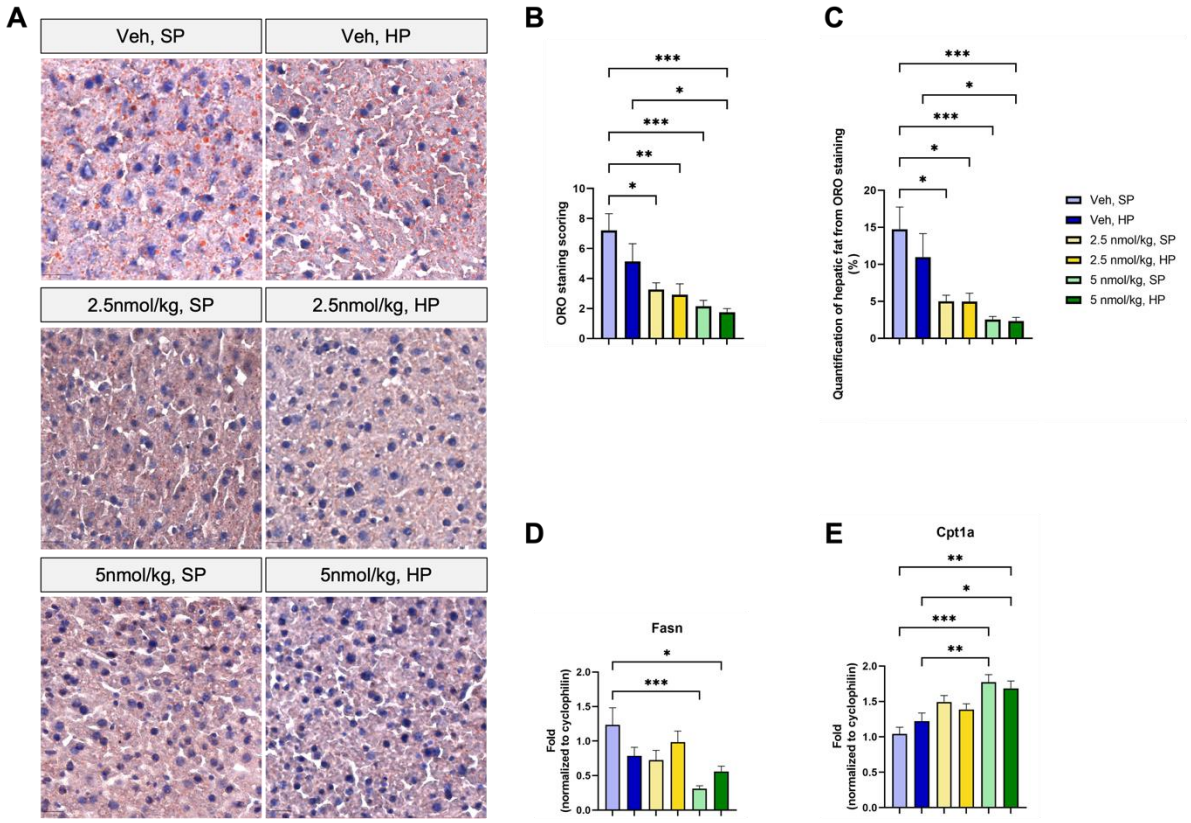


Figure 4.10. G108-chronic treatment still improves hepatic steatosis after complete mitigation of lean mass loss. A) Representative images of liver samples stained with oil red o (ORO) (bright red) and haematoxylin (blue). B) ORO staining scoring by blinded individual. C) Quantification of ORO staining as percentage. Expression levels of genes involved in hepatic fat metabolism D) Fatty acid synthase (Fasn) and E) Carnitine palmitoyl transferase I (Cpt1a). Data expressed as ± SEM. Two-way ANOVA with post-hoc Donnett's and Tukey's test. *: p-value < 0.05; **: p-value < 0.01; ***: p-value < 0.001. Scale bars = 20μm.

4.5. Discussion and future perspectives

This chapter aimed to define a strategy to significantly improve hepatic steatosis and blood glucose levels in diet-induced obese mice using the novel glucagon analogue G108, whilst completely preventing the previously reported side effect of lean mass loss. Altogether, this study 1) validated that G108 chronic treatment indeed leads to a quantifiable reduction in hepatic steatosis; 2) reported some high protein diet only-influenced outcomes; 3) defined a strategy to mitigate lean mass loss that still improves hepatic fat and glycemia; and 4) by confirming that the reduction in hepatic fat and blood glucose levels still happens under conditions of complete rescue of hypoaminoacidemia, this study further confirmed that G108 exerted such effects through separate pathways (Fig. 4.11).

In contrast to the original G108 study, the results presented in this chapter showed that food intake was significantly and consistently reduced in groups fed a high protein diet, regardless of whether they were receiving drug or vehicle treatment.

This was not surprising as high protein diets are known to have a satiating effect, and several studies have shown that animals kept on a high protein diet often display decreased food intake when compared to animals kept on a standard protein regime (French et al., 2017; Morell & Fiszman, 2017; Paddon-Jones et al., 2008; Vu et al., 2017).

In addition to distinct protein levels, the SP and HP diets used in this study also had higher and lower carbohydrates levels, respectively. The notion that higher dietary carbohydrate levels can increase appetite and accelerate hunger return has been prevalent for some time, and several recent studies and clinical trials have supported these ideas (Chandler-Laney et al., 2014; Ebbeling et al., 2018; Geiselman & Novin, 1982). Thus, the experiments performed in this chapter are not enough to pinpoint whether animals raised on the high protein diet had decreased food intake due to increased protein levels or decreased carbohydrate levels, or both.

The reduced food intake observed in animals from HP fed groups could be problematic because of two-fold: first, one of the aims of this study was to test G108 potential on reducing hepatic steatosis on a diet induced obesity mouse model. This model was chosen because chronic high fat dietary intake is known to lead to hepatic fat accumulation (Van Herck et al., 2017). Since both SP and HP diets have the same percentage of fat, and animals kept on a HP diet ate less, this means that animals feeding on the high protein diet ingested less fat than the ones feeding on the standard protein diet. This might lead to HP groups accumulating less hepatic fat than SP groups. Regardless, since the appropriate controls were used, G108-treated groups can

always be compared to the vehicle HP group to assert G108-specif effects, including on hepatic steatosis, thus discriminating from any food-intake related effect. Secondly, the aim of providing mice with a high protein diet was to increase their protein intake. Given that animals kept on the high protein diet ate significantly less than the ones kept on standard protein conditions, one could be unsure whether higher protein intake was actually achieved. However, high protein diet had twice as much protein than the standard one (40 vs 20 kcal%, respectively), so for animals kept on high protein diet to eat less protein than the animals on standard protein diet, they would have had to eat two times less food, which was not the case.

Changes and differences in lean mass were evaluated using several tests, specifically, echo-MRI, grip strength, quads weight and expression levels of markers of muscle protein turnover. Altogether, the results showed that complete prevention of G108-induced lean mass loss was achieved only when using a lower 2.5 nmol/kg dose, and specifically under high protein dietary supplementation.

All groups seemed to have lost lean mass during the study, with both vehicle controls included. This might have been because the animals were being injected and weighed daily, which can be stressful, and it has been shown that chronic stress can induce loss of muscle mass in mice (Allen et al., 2010; Fushimi et al., 2023). Additionally, and despite not reaching statistical significance either, vehicle control animals kept on a high protein diet lost four times more lean mass than the ones kept under standard protein conditions. This was unexpected given that high protein diets are known to preserve and increase muscle mass (Carbone & Pasiakos, 2019). Regardless, given that animals were all handled by the same researcher throughout the whole study, and that the appropriate controls were used, this potential stress/dietary protein content-induced trend towards loss of lean mass does not pose a problem.

The MRI data indicated that animals treated with 5 nmol/kg dose experienced lean mass loss, in both standard and high protein dietary conditions, when compared to vehicle control animals kept on a standard protein diet. When compared to vehicle controls fed a high protein diet, only the 5, SP animals had significantly lost more lean mass. Animals from the 5, HP group also lost more lean mass, in fact twice as much, than vehicle controls kept under the same dietary protein conditions, yet this difference did not reach statistical significance (p-value = 0.07). Despite this, it is likely that this trend would have reached statistical significance if the study had continued for a few more days, hence the conclusion that lean mass loss was not completely prevented in the 5, HP group either. Mice treated with 2.5 nmol/kg dose kept under standard protein conditions also lost more lean mass than Veh, SP controls, with this difference reaching

significance at day 13 of the study. Despite not reaching significance at day 21, 2.5, SP animals still lost 7 times more lean mass than the respective controls. Furthermore, when comparing Veh, SP and 2.5, SP groups, the p-value was of 0.05, when data was plotted as change in percentage, and 0.07 when data was plotted as change in grams. As such, this difference would have probably reached significance again if the study had continued for a few more days, thus the conclusion was drawn that lean mass loss was not completely prevented in the 2.5, SP group either. It seems that animals treated with the 2.5 nmol/kg dose kept under high protein conditions lost slightly, but insignificantly, more lean mass than animals form the Veh, SP group. There was, however, no difference in lean mass change from baseline between the 2.5, HP and Veh, HP groups. Thus, the slight reduction in lean mass seen in the 2.5, HP animals seems to be a dietary protein content-, rather than G108-, mediated effect, which led to the conclusion that G108-mediated lean mass loss was completely prevented in animals from the 2.5, HP group.

Grip strength experiments performed at baseline and at day 21 of the study showed that only mice treated with the 5 nmol/kg dose kept under standard protein conditions had significantly impaired muscle strength. Even though, according to the MRI data, animals treated with 2.5nmol/kg kept under the standard protein diet, as well as the ones treated with 5 nmol/kg kept on the high protein diet, also lost lean mass, these results suggest that such losses were not enough to compromise muscle function.

In contrast to the results from the initial G108 study (Hope, 2022, p. 90), loss of lean mass was not reflected in quads weight, as no differences were detected between any of the groups. First, the doses used in the experiments detailed in this chapter were 33% (5 nmol/kg) and 67% (2.5 nmol/kg) lower than in the original study (7.5nmol/kg) (Hope, 2022; Hope et al., 2022), which resulted in a more modest loss of lean mass, comparatively. Secondly, weighing of muscle samples as a method to detect potential muscle mass loss is experimentally challenging, since, for example, some quadricep tissue can be lost during separation from the femur. Additionally, the quadriceps frequently exhibited fat, and despite efforts to remove it, this factor might have also influenced the accuracy of the results. In sum, muscle weighing might not be an accurate read out of muscle mass content, at least when compared to MRI, and this might justify the lack of results reproducibility.

To have a more detailed look into what was happening between the different groups regarding muscle protein turnover, the expression levels of markers of muscle proteolysis (*bnip3*, *map1lc3b* and *fbxo32*) and synthesis (*4epb1*) were measured on quads samples. These genes were specifically chosen because the original G108 study had previously demonstrated their

responsiveness to G108-chronic treatment. Unexpectedly, and in contrast with previous observations (Hope, 2022, p. 124), there were no significant G108-induced differences in the expression levels of the tested genes. This was unexpected given that the MRI data showed that 2.5, SP; 5, SP and 5, HP groups all lost more lean mass than vehicle controls, and muscle mass is controlled by the ratio of muscle degradation and synthesis. In the original study, despite reaching statistical significance, proteolysis markers *bnip3* and *map1lc3b* were only 1-fold upregulated in G108- vs vehicle-treated animals, under the same standard protein conditions (Hope, 2022, p. 124). Given that in the experiments conducted in this chapter G108 dosage was reduced in approximately 33% (5 nmol/kg) and 67% (2.5 nmol/kg), it is not surprising that the effect on proteolysis markers expression is also flattened. Additionally, the original study ran for slightly longer than this one (27 days vs 22 days of G108/vehicle treatment) which might have further contributed for a less obvious effect on markers of muscle turnover. Furthermore, as explained in section 4.1.2.3., loss of muscle mass happens when the rate of muscle degradation surpasses the rate of muscle synthesis. However, muscle is a highly plastic tissue, so gene expression can fluctuate overtime, which could justify the lack of differences on muscle proteolysis/synthesis markers at the time point quadriceps were collected.

Despite no differences could be seen in the expression levels of the tested genes between vehicle and G108 treated animals kept under the same dietary protein conditions, high protein levels seemed to upregulate *4ebp1* expression. Indeed, all animals kept under a high protein diet, i.e., Veh, HP; 2.5, HP and 5, HP groups, presented higher expression levels of *4ebp1* than their counterparts Veh, SP; 2.5, SP and 5, SP groups. Given that high protein diets usually promote muscle synthesis, and that *4ebp1* is a repressor of protein synthesis, the opposite result was expected. mRNA levels do not always reflect what is happening protein wise, so, looking into protein levels and/or activation status (e.g., phosphorylation status), could provide us with further information. For example, protein translation, and thus muscle synthesis, is controlled by 4ebp1 phosphorylation status rather than quantity, where translation is promoted by 4ebp1 repression through phosphorylation (Ma & Blenis, 2009). Thus, performing western blot to compare 4ebp1 phosphorylation levels across the different groups would have provided additional information regarding whether protein synthesis was being affected.
No studies were available to substantiate the findings reported in this study regarding the upregulation of 4ebp1 expression by a high-protein diet. Nevertheless, if protein synthesis is indeed being suppressed by HP diet, these results agree with the MRI data that showed that Veh, HP animals had lost, not significantly, but four times more lean mass than animals from

the Veh, SP group. In fact, all animals kept on a HP diet (regardless of G108/vehicle treatment) seem to have lost more lean mass and express higher *4ebp1* levels when compared to Veh, SP animals.

The original study using the G108 compound showed that the lean mass loss observed in G108-chronically treated animals happens as a response to hypoaminoacidemia (Hope et al., 2022). That study revealed that mice treated with a 7.5 nmol/kg G108 dose had significantly reduced plasma amino acid levels, that were only partially rescued under high protein dietary conditions. These results fitted with echo-MRI data showing that lean mass loss was also only partially mitigated on animals injected with 7.5 nmol/kg G108 kept on a high protein diet (Hope et al., 2022).

The data on hepatic amino acid catabolic genes produced in this study recapitulated the results from the initial publication, where G108 treatment led to their upregulation regardless of dietary protein content (Hope et al., 2022). This is because glucagon receptor agonism, and thus G108, promotes the upregulation of amino acid catabolic genes, and the high protein supplementation rescues plasma amino acids by increasing amino acid availability, not by inhibiting amino acid catabolism.

Chronic treatment with both 2.5 and 5 nmol/kg G108 doses led to a significant reduction in plasma amino acid levels under standard protein conditions, when compared to vehicle controls kept on the same diet. Both doses reduced plasma amino acids to the same level. MRI data showed that animals treated with the higher 5 nmol/kg dose kept under SP conditions lost three times more lean mass than animals treated with 2.5 nmol/kg kept on the same diet. So, given the claim in the original study that hypoaminoacidemia is the driver of lean mass loss, and that animals on the 5 nmol/kg dose lost significantly more lean mass than animals on 2.5nmol/kg dose, a difference in plasma amino acid levels between these two groups was expected. However, this was not the case. Furthermore, protein supplementation fully rescued amino acid levels on animals treated with both 2.5 and 5 nmol/kg doses to levels seen in control vehicle animals kept under standard protein conditions. However, MRI data showed that, under HP conditions, animals treated with the higher dose still experienced significant lean mass loss, whereas animals treated with the lower dose displayed a complete prevention of lean mass loss. Hence, given that hypoaminoacidemia is proposed as the driver of lean mass loss, lower plasma amino acid levels were expected on the 5, HP group, at least when compared to the Veh, SP animals, and potentially also when compared to the 2.5, HP group. In the original study it was showed, through mass spectrometry, that some amino acids were preferentially reduced by

G108-chronic treatment, whilst others were unchanged (Hope et al., 2022). In addition, a study performed on obese Zucker rats showed that a high protein diet preferentially upregulated some amino acids, like lysine and glutamine, whilst not affecting, or sometimes even downregulating others, like alanine and glycine, respectively (French et al., 2017). Therefore, differences between the afore mentioned groups could potentially be observed in specific, rather than total, plasma amino acids' levels. Additional experiments assessing plasma levels of such amino acids, like alanine or lysine, would address this question. Another possible explanation for the previously mentioned results is as follows: G108-induced hypoaminoacidemia is a result of increased amino acid catabolism induced by chronic glucagon agonism. Animals treated with higher levels of G108 had slightly higher expression levels of the hepatic amino acid catabolic genes *cps1* and *ass1* than animals treated with a lower G108 dose. Hypoaminoacidemia is what directly stimulates lean mass loss, but amino acid availability also conditions protein turnover and consequently muscle mass balance. It is possible that, when mice are treated with the lower 2.5 nmol/kg dose, HP supplementation is sufficient to rescue hypoaminoacidemia, whilst the leftover amino acids are also enough to be used for protein synthesis in the muscle. On the other hand, in animals treated with the higher 5nmol/kg dose, the HP might be enough to rescue plasma hypoaminoacidemia, but there are no amino acids left to be used for protein synthesis, since amino acid catabolism is more strongly promoted by a higher G108 dose. However, if this was the case, the expression of muscle synthesis marker *4ebp1* should be reduced in 2.5, HP animals, when compared to 5, HP. Nevertheless, additional experiments where animals treated with the 5 nmol/kg dose are provided with a diet slightly higher in protein could help address this hypothesis. Another potential explanation might be the influence of the time of day or the interval between G108 administration and sample collection. It is possible that the data obtained at this timepoint may not accurately reflect the true differences between doses due to it being a non-representative moment in the overall response timeline.

Next, glucose tolerance was assessed across the different groups through an ip-GTT. During a glucose tolerance test, a glucose bolus is given to the animal, in this case via intra-peritoneal injection, and blood glucose levels are measured at several time points, including at baseline (i.e., before glucose bolus is given). The quicker the glucose is cleared from the blood, the smaller the area under the curve, and the higher the glucose tolerance (Virtue & Vidal-Puig, 2021).

The ip-GTT data revealed that all G108 treated groups displayed significantly improved blood glucose tolerance, regardless of dietary protein level, when compared to the respective vehicle controls.

Given that a healthy/lean control group was not included in this study, whether control groups had a normal or impaired glucose tolerance could not be assessed. This means that the experiments conducted in this study cannot determine whether G108 improved disrupted or normal glucose tolerance. Nevertheless, and although comparing results performed in different experiments is not the best practice, other studies have reported similar glucose excursion rates to the ones observed in this study, in healthy C57Bl/6J mice of similar age, thus suggesting that vehicle control animals had a normal glucose tolerance (Fisher-Wellman et al., 2016). Regardless, G108 treatment significantly lowered glycemia and improved glucose tolerance, even after lean mass loss was completely mitigated.

Remarkably, animals receiving vehicle and kept under the high protein regime had significantly lower basal blood glucose levels than controls kept on the standard protein diet. Despite this, there were no differences regarding overall blood glucose excursion between those two groups, as evidenced by the similar AUCs. Yet, for the standard and high protein diets to be isoenergetic, whilst having the same percentage of fat and different percentages of protein, the percentage of carbohydrates had to differ between the two diets (35% on SP and 15% on HP). Thus, whether exposure to the high protein diet resulted in improved basal blood glucose levels due to increased dietary protein, and/or due to decreased carbohydrates, was not addressed. Importantly, there are studies suggesting that both can improve glycemia individually, as further explored below.

There have been conflicting results on whether high protein diets are a beneficial strategy for improving glycemia long term. Additionally, many studies claiming that high protein diets improve glycemia compare diets that also vary in carbohydrate levels (Drummen et al., 2018; Gannon et al., 2003). Nonetheless, there is evidence that high protein diets affect glucose homeostasis through various metabolic pathways, one of which is insulin secretion. Insulin promotes glucose uptake from the blood and into organs, and its secretion can be directly modulated by the amino acid products of protein digestion (Y. Yanagisawa, 2023). In fact, in a study done back in the late 70s, researchers observed that infusing amino acids for one hour starting immediately before a GTT, in diabetic patients, significantly improved glucose tolerance in response to the glucose oral bolus, due to a sustained increase in insulin levels (Seino et al., 1977). Whilst Veh, HP animals had lower basal glucose levels, glucose tolerance was similar between the two controls. Nevertheless, diabetes first starts as increased fasting

blood glucose levels, so, perhaps, control animals raised on a high protein diet had lower fasting blood glucose levels than Veh, SP animals due to increased plasma insulin levels. Although plasma insulin levels were not measured in this study, plasma total amino acids were indeed elevated in Veh, HP compared to Veh, SP mice. Thus, amino acid-induced increased insulin levels could be the reason why control animals kept on the high protein regime presented lower basal blood glucose levels than animals fed a standard protein diet.

The content of carbohydrates in meals, which are broken into glucose molecules by the body, is known to affect glycemia as well. In fact, several studies have shown that diets higher in carbs can lead to increased blood glucose levels when compared to low carb diets, and switching to a low carbohydrate diet has showed promising results in patients with diabetes (Foley, 2021; *Low-Carb Diets Position Statement (May 2021) | Diabetes UK*, n.d.; Pavlidou et al., 2023; Stentz et al., 2016). Since the standard protein diet had higher levels of carbohydrates, this could be another possible explanation of why Veh, SP animals had significantly higher fasting basal glucose levels than the controls kept on the high protein diet. In addition to the higher percentage of carbohydrates in the SP diet, food intake data showed that animals under standard protein conditions ate slightly, but significantly, more than animals under high protein conditions. This might have further exacerbated the difference in carbohydrates consumption, and thus fasting basal glucose levels, between control groups.

Additionally, another contributor to the observed lower basal blood glucose levels in Veh, HP animals could be hepatic fat content. Veh, HP animals had slightly reduced hepatic steatosis than animals from the Veh, SP group. The liver is a very important organ in regulating glycemia. As explored earlier in section 1.1.2.2., the liver is responsible for keeping normal glycemia through up-take and release (gluconeogenesis and glycogenolysis) of glucose from and into the blood. Such tasks can be influenced by deranged hepatic fat content (L. Li et al., 2019). Thus, lower hepatic steatosis in Veh, HP animals could also justify the lower basal blood glucose levels.

ORO staining experiments revealed that vehicle controls kept on a high protein diet seemed to accumulate considerably less hepatic fat than when kept under a standard protein regime, though this was not significant. This was evidenced by the blind scoring, as well as by the automated quantification performed through post-acquisition image analysis. Despite not reaching statistical significance, a difference of over 25% less hepatic fat might be meaningful.

Hepatic steatosis is a result of increased hepatic fat accumulation, influenced by levels of ingested fats, circulating pool of NEFA, and *de novo* lipogenesis, as well as by deficient fat handling, which is influenced by fatty acid b-oxidation and VLDL secretion.

The food intake data revealed that all groups fed a high protein diet ate slightly, but significantly, less than the corresponding treatments on standard protein. Given that SP and HP diets had the same levels of fat (45 kcal%), this means that HP groups consumed slightly less fat than the SP groups, and this could have contributed to the lower percentage of hepatic steatosis observed in Veh, HP livers.

It is important to note that, in addition to different protein levels, the SP and HP diets used in this study also had higher and lower levels of carbohydrates, respectively. This is because balanced diets are composed by fats, carbohydrates and proteins, meaning that for a diet to remain isocaloric when the levels of protein vary, the levels of at least one of the other macronutrients has to change as well. In fact, other studies have investigated the effects of different dietary protein levels on liver steatosis using diets that also had distinct levels of carbohydrates. For example, the previously mentioned study on obese Zucker rats, as well as a study in mice, reported that animals kept on a high protein diet accumulated less hepatic fat than the ones on standard protein. Similar to the diets used for our study, the carbohydrate levels were also lower in their high protein compared to normal protein diet (French et al., 2017; Schwarz et al., 2012). Thus, with the experiments performed in this chapter it is unclear if the reduced levels of hepatic fat observed in the control animals kept under the high protein diet regime are indeed due to the higher protein levels, or due to lower carbohydrate content. Importantly, there is evidence that both increased dietary protein levels and reduced carbohydrate levels can improve hepatic steatosis independently.

High protein diets are often used as an approach to reduce hepatic steatosis (De Chiara et al., 2019). The mechanisms through which high protein diets might affect hepatic fat accumulation are not completely understood. However, one way might be through increasing energy expenditure, that can create an energy deficit, thus promoting lipid b-oxidation whilst supressing fat synthesis in the liver (Schwarz et al., 2012). The energy expenditure levels were not assessed in this chapter, however increased energy expenditure would probably be reflected as lower body weight, since, in addition to liver, other tissues fat reserves are affected (for example, adipose tissue). In fact, the body weight data revealed a potential trend where the control animals raised on the high protein diet put on slightly less weight than Veh, SP animals over the course of the study. The fat mass data also supported this, as Veh, HP animals gained slightly less fat mass than SP controls over time. Of course, these modest differences might

also be a simple consequence of the slightly reduced food intake rather than increased energy expenditure.

Another possibility is that high protein diets or, more specifically, increased amino acids levels from high protein diets, directly stimulate glucagon release, which can then decrease *de novo* lipogenesis, whilst also increasing hepatic fatty acid b-oxidation (J. Zhang et al., 2022). Glucagon levels were not measured in this study, however, the expression levels of the *de novo* lipogenesis marker *Fasn* were slightly downregulated in Veh, HP compared to Veh, SP animals, though this did not reach statistical significance. Furthermore, the marker of fatty acid b-oxidation *Cpt1a* was also marginally up-regulated in control animals fed a high protein diet. These results are in line with McGarry and colleagues' observations that, when DNL is upregulated, *Cpt1a*, and thus fatty acids b-oxidation, is repressed (McGarry et al., 1977).

Regarding low carbohydrate diets, these are thought to improve fatty liver through decreasing *de novo* lipogenesis (Pichon et al., 2006). As previously explored in section 1.1.2.1, during *de novo* lipogenesis, fats are made from non-lipid precursors, with the main substrate for this process coming from carbohydrate's catabolism. Briefly, upon ingestion, carbohydrates are broken down into sugars that are internalized by cells and converted into pyruvate through glycolysis. The resulting pyruvate can then be used for energy by entering the TCA cycle, or, in situations of energy excess, can serve as a *de novo* lipogenesis substrate. Thus, diets richer in carbohydrates promote DNL by increasing substrate availability. As discussed earlier, standard and high protein diets had a different percentage of carbohydrates of 35kcal% and 15kcal%, respectively. Thus, mice on the SP diet had 20% more substrate available for *de novo* lipogenesis than mice on the HP diet. Furthermore, animals fed the standard diet ate significantly more than the ones on high protein conditions, which brings those 20% higher levels of DNL substrate availability even higher. In agreement with this, the ip-GTT results showed that Veh, HP animals had significantly lower basal blood glucose levels than Veh, SP animals, which supports the idea that sugar availability is indeed increased in control mice kept on the standard protein regime. As previously mentioned, the expression of the DNL marker *Fasn* was slightly upregulated in Veh, SP compared to Veh, HP animals, though this did not reach statistical significance. Moreover, *Cpt1a* levels, a marker of fatty acids b-oxidation, were slightly upregulated in the HP diet. As previously mentioned, higher levels of DNL are enough to inhibit *Cpt1a* expression (McGarry et al., 1977).

In this study, it was not assessed if the levels of plasma free fatty acids or VLDL exportation rate contributed to the reduced hepatic steatosis observed in Veh, HP animals. However, studies in mice have shown that animals fed the same amount of fat accumulate less hepatic fat under

high protein conditions at least in part due to increased VLDL secretion (Schwarz et al., 2012). Nevertheless, the slightly reduced fat consumption, together with the reduced rate of DNL and slight increase in fatty acid b-oxidation, could justify why control animals kept on a high protein regime presented 25% less hepatic fat than the ones fed the standard protein diet. Whether these differences were caused by increased high protein and/or decreased carbohydrate dietary levels is currently unknown.

ORO staining experiments also revealed that G108 chronic treatment effectively reduced hepatic steatosis in a dosage dependent way, independently of dietary protein content and, thus, under conditions of complete lean mass loss mitigation. This was evidenced by the results of both the blind scoring, as well as by the automated quantification performed through post-acquisition image analysis. Animals treated with the higher 5 nmol/kg dose had significantly reduced hepatic steatosis when compared to both vehicle SP and HP controls. Animals treated with the lower 2.5 nmol/kg dose experienced similar reductions in hepatic fat accumulation under SP and HP diets, that were significantly lower than Veh, SP controls. However, the high protein diet seemed to have a benefic effect on hepatic fat on its own and, thus, despite the 2.5 nmol/kg treated animals having less than half of the hepatic fat of Veh, HP controls, this difference did not reach statistical significance. Regardless, and in addition to improving glycemia, the aim of this study was also to improve hepatic steatosis in diet-induced obese mice through G108 treatment, whilst completely preventing lean mass loss, which was accomplished by a lower G108 dose together with dietary protein supplementation (i.e., Veh, SP vs 2.5, HP comparison).

Experiments were conducted with the aim of providing additional insights into the mechanisms by which G108 improves hepatic steatosis. G108 is a glucagon analogue and GCGR agonist, and glucagon is known to reduce *de novo* lipogenesis, whilst also increasing fatty acids b-oxidation.

Indeed, under SP conditions, G108-treated animals exhibited decreased *Fasn* expression levels, a marker of *de novo* lipogenesis, in a dose dependent fashion. HP diet on its own also seemed to downregulate *Fasn* expression. Unexpectedly, however, HP in the context of G108 treatment seemed to upregulate *Fasn* expression when compared to G108-treated groups kept on a standard protein regime.

Whilst it is clear that products of both carbohydrates and amino acid catabolism can be used as substrates for DNL, whether diets rich in protein can actually promote DNL is not so clearly defined (Cross et al., 2023). For example, a recent study claimed that, in rats, a high protein diet blunted DNL markers when compared to a low protein diet (Margolis et al., 2016). Yet,

another study in humans claimed that a high protein diet promoted DNL (Charidemou et al., 2019b). In both studies, however, the high protein diets also had lower levels of carbohydrates compared to the low protein diet, meaning that the differences observed might be due to different carbohydrate, rather than protein, levels. Nevertheless, the study on humans, showed, *in vitro*, that treating hepatocytes with individual specific amino acids was enough to increase markers of DNL, thus supporting the hypothesis that a higher dietary protein content (rather than lower carbohydrate quantities) might directly promote DNL. Therefore, although there is evidence that high protein diets can promote DNL, this is still not entirely clear. Many studies refer to the products of carbohydrate catabolism (as opposed to amino acids catabolism, for example) as being the main substrate for DNL (F. W. B. Sanders et al., 2018; F. W. B. Sanders & Griffin, 2016; Z. Song et al., 2018). However, no studies can be found comparing how strongly carbohydrates/sugars vs proteins/amino acids promote DNL when under similar levels. Nevertheless, if the assumption is made that sugars are stronger promotors of DNL than amino acids, but that increased amino acids levels can also promote DNL, a possible explanation for the results observed is as follows: 2.5, HP vs 2.5, SP and 5, HP vs 5, SP had increased DNL because their sugar (substrate) availability was the same (evidenced by similar basal blood glucose levels), however, the levels of plasma amino acids were higher in the HP groups, which led to an increase in DNL in high protein fed G108-treated animals. These assumptions also fit with the previously discussed results regarding the levels of accumulated hepatic fat in the control groups, where the Veh, HP group had lower DNL than Veh, SP group, because their sugar availability was lower (evidenced by lower basal glucose levels), and despite their plasma amino acid levels being higher.

Cpt1a was also individually upregulated by HP and G108, in a dose dependent way, however, just like with *Fasn*, HP in the context of G108 treatment led to a slight downregulation in comparison to G108, SP groups. As previously mentioned, higher levels of DNL are known to inhibit *Cpt1a*, therefore this is in accordance with the *Fasn* data.

It is important to notice that, even though there was evidence that DNL might be slightly increased and b-oxidation slightly reduced, in G108-HP compared to G108-SP groups, this did not translate into a noticeable difference in hepatic steatosis levels. This is not surprising, since there is evidence that increased/decreased DNL/b-oxidation do not always correlate with increased hepatic fat accumulation, as other pathways might come into play to regulate hepatic fat accumulation (like increased VLDL secretion, for example) (Cross et al., 2023).

Importantly, even though the G108 doses are expressed as nmol/kg, they were not adjusted to the body weight of each animal, for convenience. Instead, each group baseline body weight average was used. This means that slightly heavier and lighter mice could have received less and more than the intended doses, respectively. This could justify some of the variability observed in data within G108-treated groups.

Finally, even though the study lined out in this chapter showed promising results of G108 improving hepatic fat and glycemia, it was also showed that G108 dosage must be tightly regulated to prevent lean mass loss even under high protein dietary condition. NAFLD patients often present glucagon resistance (Galsgaard, 2020). However, the animals used in this study were not assessed for glucagon sensitivity. Thus, in the future, additional experiments should be performed to optimize G108 usage in treating NAFLD in the context of glucagon resistance.

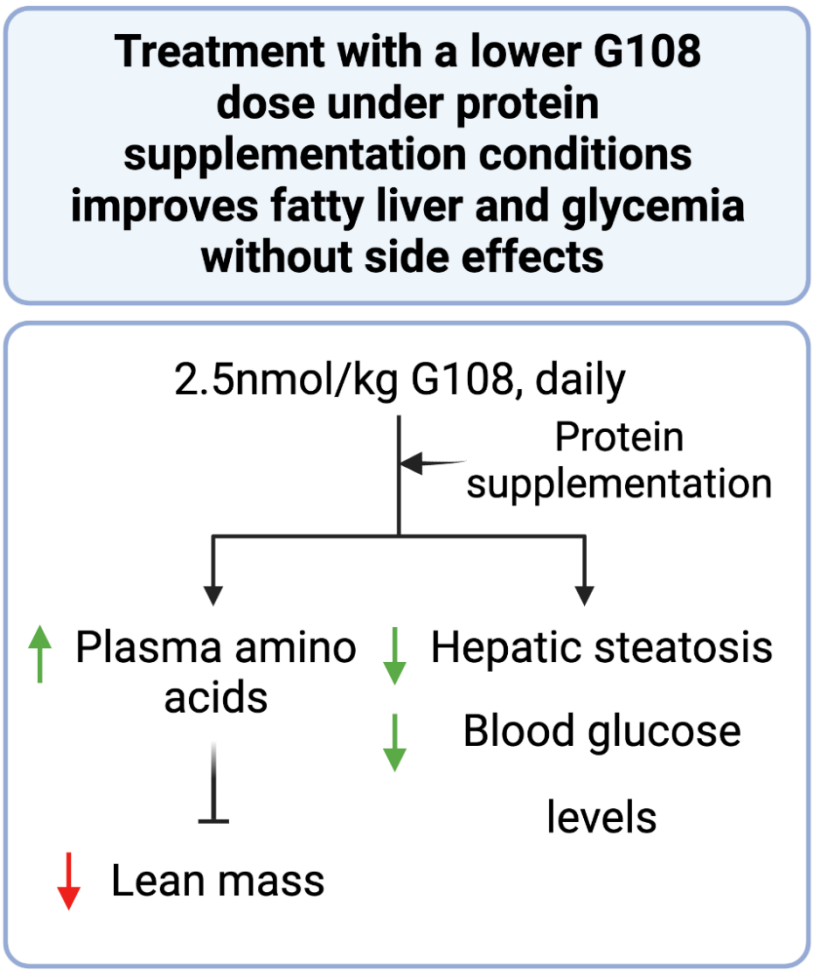


Figure 4.11. Schematic summarizing study's findings. Lowering G108 dose to 2.5 nmol/kg in the context of dietary protein supplementation improved hepatic steatosis and glycemia without any lean mass loss.

Chapter V - Concluding remarks

Three general aims were defined at the beginning of this PhD: 1) Gain expertise in *in vivo* intra-ocular injections and imaging, whilst developing a platform to characterize tumour vascularization *in vivo* (training project); 2) Establish a novel *in vivo* longitudinal platform to study NAFLD by combining *in vitro* and *in vivo* NAFLD models; 3) Optimize GCGR agonism in the treatment of NAFLD using the novel longitudinal platform if it works.

1) The main goal of this aim was to gain expertise in intra-ocular injections and intravital imaging, skills that would be essential for the main project. Additionally, it was also proposed that, whilst developing those skills, a novel platform could be developed to characterize tumour vascularization *in vivo*. However, this could not be achieved due to technical issues. Nevertheless, whilst trying to do so, interesting findings came to light. First, it was shown that Renca cells could form spheroids *in vitro* following a previously published approach. Such spheroids were capable of vascularizing through angiogenesis and grow over time upon transplantation into the anterior chamber of the eye of host mice. However, upon transplantation into the *in vivo* setting, the endothelial cells that composed the intra-spheroid blood vessels experienced a down-regulation in Tie2 expression, which resulted in GFP downregulation. This renders this platform unsuitable for the longitudinal *in vivo* characterization of tumour vascularization since blood vessels cannot be observed. Finally, the presence of intra spheroid channels of tumour origin was also observed, and the nature and purpose of such structures can be subject of further studies. Nevertheless, this platform can still potentially be used in other purposes, such as, testing of potential anti-angiogenic drugs having tumour size as a readout; and testing of potential Tie2 normalizing drugs having intra-spheroid blood vessel fluorescence as a readout.

2) The aim of establishing a novel *in vivo* longitudinal platform to study NAFLD by combining *in vitro* and *in vivo* NAFLD models could not be achieved within the timeframe of the PhD studies. However, whilst trying to do so, the outcomes of different strategies that attempted to generate liver organoids capable of vascularizing into the host animal iris upon *in vivo* transplantation were tested and reported. In addition, it was showed that co-culturing cells from different species still lead to the formation of liver buds following a previously published approach. Moreover, at least some of those liver buds were capable of vascularizing for long-term ($\geq$ 2 months) upon *in vivo* transplantation into the ACE. However, further experiments are needed to assess whether they are capable of accumulating fat when the host animal is challenged with an HFD.

3) This aim initially sought to use the novel NALFD platform developed in the main project to optimize GCGR agonism, using G108, in the treatment of NAFLD. However, that platform could not be established on time. Nevertheless, using traditional *in vivo* methods, a strategy was still developed where G108 chronic treatment improved hepatic fat steatosis and glycemia whilst completely mitigating previously reported side effects. These results also supported the hypothesis that G108 exerts its effects on hypoaminoacidemia induced lean mass loss, and in glycemia and hepatic steatosis through distinct pathways. Thus, the experiments conducted in this project support the idea that glucagon-based therapy may be an effective treatment for NAFLD, provided that lean mass is monitored and sustained by adequate dietary protein intake.

References

Aboubakr, A., Stroud, A., Kumar, S., & Newberry, C. (2021). Dietary Approaches for Management of Non-Alcoholic Fatty Liver Disease: A Clinician's Guide. *Current Gastroenterology Reports*, *23*(12), 1–8. https://doi.org/10.1007/S11894-021-00827-0/METRICS

Adeva-Andany, M. M., Pérez-Felpete, N., Fernández-Fernández, C., Donapetry-García, C., & Pazos-García, C. (2016). Liver glucose metabolism in humans. *Bioscience Reports*, *36*(6), 416. https://doi.org/10.1042/BSR20160385

Adinolfi, L. E., Rinaldi, L., Guerrera, B., Restivo, L., Marrone, A., Giordano, M., & Zampino, R. (2016). NAFLD and NASH in HCV Infection: Prevalence and Significance in Hepatic and Extrahepatic Manifestations. *International Journal of Molecular Sciences 2016, Vol. 17, Page 803*, *17*(6), 803. https://doi.org/10.3390/IJMS17060803

AHLGREN, M., & BENGTSSON, L. P. (1962). Transplantation of fertilized rabbit eggs to the anterior chamber of the eye. *Journal of Reproduction and Fertility*, *3*, 89–92. https://doi.org/10.1530/JRF.0.0030089

Ajioka, I., Akaike, T., & Watanabe, Y. (1999). Expression of vascular endothelial growth factor promotes colonization, vascularization, and growth of transplanted hepatic tissues in the mouse. *Hepatology (Baltimore, Md.)*, *29*(2), 396–402. https://doi.org/10.1002/HEP.510290233

Akazawa, Y., & Nakao, K. (2016). Lipotoxicity pathways intersect in hepatocytes: Endoplasmic reticulum stress, c-Jun N-terminal kinase-1, and death receptors. *Hepatology Research*, *46*(10), 977–984. https://doi.org/10.1111/HEPR.12658

Akazawa, Y., & Nakao, K. (2018). To die or not to die: death signaling in nonalcoholic fatty liver disease. *Journal of Gastroenterology 2018 53:8*, *53*(8), 893–906. https://doi.org/10.1007/S00535-018-1451-5

Akbari, S., Sevinç, G. G., Ersoy, N., Basak, O., Kaplan, K., Sevinç, K., Ozel, E., Sengun, B., Enustun, E., Ozcimen, B., Bagriyanik, A., Arslan, N., Önder, T. T., & Erdal, E. (2019). Robust, Long-Term Culture of Endoderm-Derived Hepatic Organoids for Disease Modeling. *Stem Cell Reports*, *13*(4), 627. https://doi.org/10.1016/J.STEMCR.2019.08.007

Alexander, S., Koehl, G. E., Hirschberg, M., Geissler, E. K., & Friedl, P. (2008). Dynamic imaging of cancer growth and invasion: A modified skin-fold chamber model. *Histochemistry and Cell Biology*, *130*(6), 1147–1154. https://doi.org/10.1007/S00418-008-0529-1/FIGURES/5

Alieva, M., Ritsma, L., Giedt, R. J., Weissleder, R., & van Rheenen, J. (2014). Imaging windows for long-term intravital imaging: General overview and technical insights. *IntraVital*, *3*(2). https://doi.org/10.4161/INTV.29917

Allen, D. L., McCall, G. E., Loh, A. S., Madden, M. C., & Mehan, R. S. (2010). Acute daily psychological stress causes increased atrophic gene expression and myostatin-dependent muscle atrophy. *American Journal of Physiology - Regulatory Integrative and Comparative Physiology*, *299*(3), 889–898. https://doi.org/10.1152/AJPREGU.00296.2010/SUPPL_FILE/SUPPFIG.PDF

Alzubaidi, A. N., Sekoulopoulos, S., Pham, J., Walter, V., Fuletra, J. G., & Raman, J. D. (2022). Incidence and Distribution of New Renal Cell Carcinoma Cases: 27-Year Trends from a Statewide Cancer Registry. *Journal of Kidney Cancer and VHL*, *9*(2), 7–12. https://doi.org/10.15586/JKCVHL.V9I2.219

Anania, C., Massimo Perla, F., Olivero, F., Pacifico, L., & Chiesa, C. (2018). Mediterranean diet and nonalcoholic fatty liver disease. *World Journal of Gastroenterology*, *24*(19), 2083. https://doi.org/10.3748/WJG.V24.I19.2083

Anderson, N. M., & Simon, M. C. (2020). Tumor Microenvironment. *Current Biology : CB*, *30*(16), R921. https://doi.org/10.1016/J.CUB.2020.06.081

Andonegui-Elguera, M. A., Alfaro-Mora, Y., Cáceres-Gutiérrez, R., Caro-Sánchez, C. H. S., Herrera, L. A., & Díaz-Chávez, J. (2020). An Overview of Vasculogenic Mimicry in Breast Cancer. *Frontiers in Oncology*, *10*, 220. https://doi.org/10.3389/FONC.2020.00220

Arai, T., Atsukawa, M., Tsubota, A., Ono, H., Kawano, T., Yoshida, Y., Okubo, T., Hayama, K., Nakagawa-Iwashita, A., Itokawa, N., Kondo, C., Nagao, M., & Iwakiri, K. (2022). Efficacy and

safety of oral semaglutide in patients with non-alcoholic fatty liver disease complicated by type 2 diabetes mellitus: A pilot study. *JGH Open*, *6*(7), 503–511. https://doi.org/10.1002/JGH3.12780

Arguello, G., Balboa, E., Arrese, M., & Zanlungo, S. (2015). Recent insights on the role of cholesterol in non-alcoholic fatty liver disease. *Biochimica et Biophysica Acta (BBA) - Molecular Basis of Disease*, *1852*(9), 1765–1778. https://doi.org/10.1016/J.BBADIS.2015.05.015

Armstrong, M. J., Gaunt, P., Aithal, G. P., Barton, D., Hull, D., Parker, R., Hazlehurst, J. M., Guo, K., Abouda, G., Aldersley, M. A., Stocken, D., Gough, S. C., Tomlinson, J. W., Brown, R. M., Hübscher, S. G., & Newsome, P. N. (2016). Liraglutide safety and efficacy in patients with non-alcoholic steatohepatitis (LEAN): a multicentre, double-blind, randomised, placebo-controlled phase 2 study. *The Lancet*, *387*(10019), 679–690. https://doi.org/10.1016/S0140-6736(15)00803-X

Aron-Wisnewsky, J., Vigliotti, C., Witjes, J., Le, P., Holleboom, A. G., Verheij, J., Nieuwdorp, M., & Clément, K. (2020). Gut microbiota and human NAFLD: disentangling microbial signatures from metabolic disorders. *Nature Reviews Gastroenterology & Hepatology 2020 17:5*, *17*(5), 279–297. https://doi.org/10.1038/s41575-020-0269-9

Attalla, S., Taifour, T., Bui, T., & Muller, W. (2020). Insights from transgenic mouse models of PyMT-induced breast cancer: recapitulating human breast cancer progression in vivo. *Oncogene 2020 40:3*, *40*(3), 475–491. https://doi.org/10.1038/s41388-020-01560-0

Auf, G., Jabouille, A., Guérit, S., Pineau, R., Delugin, M., Bouchecareilh, M., Magnin, N., Favereaux, A., Maitre, M., Gaiser, T., von Deimling, A., Czabanka, M., Vajkoczy, P., Chevet, E., Bikfalvi, A., & Moenner, M. (2010). Inositol-requiring enzyme 1α is a key regulator of angiogenesis and invasion in malignant glioma. *Proceedings of the National Academy of Sciences of the United States of America*, *107*(35), 15553–15558. https://doi.org/10.1073/PNAS.0914072107/-/DCSUPPLEMENTAL

Badea, M. A., Balas, M., Hermenean, A., Ciceu, A., Herman, H., Ionita, D., & Dinischiotu, A. (2019). Influence of Matrigel on Single- and Multiple-Spheroid Cultures in Breast Cancer Research. *SLAS Discovery : Advancing Life Sciences R & D*, *24*(5), 563–578. https://doi.org/10.1177/2472555219834698

Balan, M., Trusohamn, M., Ning, F. C., Jacob, S., Pietras, K., Eriksson, U., Berggren, P. O., & Nyqvist, D. (2019). Noninvasive intravital high-resolution imaging of pancreatic neuroendocrine tumours. *Scientific Reports 2019 9:1*, *9*(1), 1–11. https://doi.org/10.1038/s41598-019-51093-0

Baptista, I. L., Leal, M. L., Artioli, G. G., Aoki, M. S., Fiamoncini, J., Turri, A. O., Curi, R., Miyabara, E. H., & Moriscot, A. S. (2010). Leucine attenuates skeletal muscle wasting via inhibition of ubiquitin ligases. *Muscle & Nerve*, *41*(6), 800–808. https://doi.org/10.1002/MUS.21578

Bar, J., & Goss, G. D. (2012). Tumor vasculature as a therapeutic target in non-small cell lung cancer. *Journal of Thoracic Oncology : Official Publication of the International Association for the Study of Lung Cancer*, *7*(3), 609–620. https://doi.org/10.1097/JTO.0B013E3182435F3E

Barazzoni, R., Zanetti, M., Tiengo, A., & Tessari, P. (1999). Protein metabolism in glucagonoma. *Diabetologia*, *42*(3), 326–329. https://doi.org/10.1007/S001250051158/METRICS

Baze, A., Parmentier, C., Hendriks, D. F. G., Hurrell, T., Heyd, B., Bachellier, P., Schuster, C., Ingelman-Sundberg, M., & Richert, L. (2018). Three-Dimensional Spheroid Primary Human Hepatocytes in Monoculture and Coculture with Nonparenchymal Cells. *Https://Home.Liebertpub.Com/Tec*, *24*(9), 534–545. https://doi.org/10.1089/TEN.TEC.2018.0134

Belew, G. D., & Jones, J. G. (2022). De novo lipogenesis in non-alcoholic fatty liver disease: Quantification with stable isotope tracers. *European Journal of Clinical Investigation*, *52*(3), e13733. https://doi.org/10.1111/ECI.13733

Belotti, D., Pinessi, D., & Taraboletti, G. (2021). Alternative Vascularization Mechanisms in Tumor Resistance to Therapy. *Cancers 2021, Vol. 13, Page 1912*, *13*(8), 1912. https://doi.org/10.3390/CANCERS13081912

Bentolila, N. Y., Barnhill, R. L., Lugassy, C., & Bentolila, L. A. (2018a). Intravital Imaging of Human Melanoma Cells in the Mouse Ear Skin by Two-Photon Excitation Microscopy. *Methods in Molecular Biology (Clifton, N.J.)*, *1755*, 223–232. https://doi.org/10.1007/978-1-4939-7724-6_15

Bentolila, N. Y., Barnhill, R. L., Lugassy, C., & Bentolila, L. A. (2018b). Intravital Imaging of Human Melanoma Cells in the Mouse Ear Skin by Two-Photon Excitation Microscopy. *Methods in Molecular Biology (Clifton, N.J.)*, *1755*, 223. https://doi.org/10.1007/978-1-4939-7724-6_15

Berná, G., & Romero-Gomez, M. (2020). The role of nutrition in non-alcoholic fatty liver disease: Pathophysiology and management. *Liver International*, *40*(S1), 102–108. https://doi.org/10.1111/LIV.14360

Bhagavan, N. V., & Ha, C.-E. (2015). Protein and Amino Acid Metabolism. *Essentials of Medical Biochemistry*, 227–268. https://doi.org/10.1016/B978-0-12-416687-5.00015-4

Birgersdotter, A., Sandberg, R., & Ernberg, I. (2005). Gene expression perturbation in vitro—A growing case for three-dimensional (3D) culture systems. *Seminars in Cancer Biology*, *15*(5), 405–412. https://doi.org/10.1016/J.SEMCANCER.2005.06.009

Birkenfeld, A. L., & Shulman, G. I. (2014). Non Alcoholic Fatty Liver Disease, Hepatic Insulin Resistance and Type 2 Diabetes. *Hepatology (Baltimore, Md.)*, *59*(2), 713. https://doi.org/10.1002/HEP.26672

Bochner, F., Mohan, V., Zinger, A., Golani, O., Schroeder, A., Sagi, I., & Neeman, M. (2020). Intravital imaging of vascular anomalies and extracellular matrix remodeling in orthotopic pancreatic tumors. *International Journal of Cancer*, *146*(8), 2209–2217. https://doi.org/10.1002/IJC.32759

Böck, J., & Popper, H. (1937). Über Lebertransplantation in die Vorderkammer des Auges. *Virchows Archiv Für Pathologische Anatomie Und Physiologie Und Für Klinische Medizin*, *299*(1–2), 219–234. https://doi.org/10.1007/BF02084471/METRICS

Boden, G., Master, R. W., Rezvani, I. J., Palmer, J. P., Lobe, T. E., & Owen, O. E. (1980). Glucagon deficiency and hyperaminoacidemia after total pancreatectomy. *Journal of Clinical Investigation*, *65*(3), 706. https://doi.org/10.1172/JCI109717

Boutari, C., Pappas, P. D., Anastasilakis, D., & Mantzoros, C. S. (2022). Statins' efficacy in non-alcoholic fatty liver disease: A systematic review and meta-analysis. *Clinical Nutrition*, *41*(10), 2195–2206. https://doi.org/10.1016/J.CLNU.2022.08.001

Brassard-Jollive, N., Monnot, C., Muller, L., & Germain, S. (2020). In vitro 3D Systems to Model Tumor Angiogenesis and Interactions With Stromal Cells. *Frontiers in Cell and Developmental Biology*, *8*. https://doi.org/10.3389/FCELL.2020.594903

Bridgeman, V. L., Vermeulen, P. B., Foo, S., Bilecz, A., Daley, F., Kostaras, E., Nathan, M. R., Wan, E., Frentzas, S., Schweiger, T., Hegedus, B., Hoetzenecker, K., Renyi-Vamos, F., Kuczynski, E. A., Vasudev, N. S., Larkin, J., Gore, M., Dvorak, H. F., Paku, S., … Reynolds, A. R. (2017a). Vessel co-option is common in human lung metastases and mediates resistance to anti-angiogenic therapy in preclinical lung metastasis models. *The Journal of Pathology*, *241*(3), 362–374. https://doi.org/10.1002/PATH.4845

Bridgeman, V. L., Vermeulen, P. B., Foo, S., Bilecz, A., Daley, F., Kostaras, E., Nathan, M. R., Wan, E., Frentzas, S., Schweiger, T., Hegedus, B., Hoetzenecker, K., Renyi-Vamos, F., Kuczynski, E. A., Vasudev, N. S., Larkin, J., Gore, M., Dvorak, H. F., Paku, S., … Reynolds, A. R. (2017b). Vessel co-option is common in human lung metastases and mediates resistance to anti-angiogenic therapy in preclinical lung metastasis models. *The Journal of Pathology*, *241*(3), 362–374. https://doi.org/10.1002/PATH.4845

Bridgeman, V. L., Vermeulen, P. B., Foo, S., Bilecz, A., Daley, F., Kostaras, E., Nathan, M. R., Wan, E., Frentzas, S., Schweiger, T., Hegedus, B., Hoetzenecker, K., Renyi-Vamos, F., Kuczynski, E. A., Vasudev, N. S., Larkin, J., Gore, M., Dvorak, H. F., Paku, S., … Reynolds, A. R. (2017c). Vessel co-option is common in human lung metastases and mediates resistance to anti-angiogenic therapy in preclinical lung metastasis models. *The Journal of Pathology*, *241*(3), 362. https://doi.org/10.1002/PATH.4845

Broekhuyse, R. M. (1971). The Lipid Composition of Aging Sclera and Cornea. In *Netherl. Ophthal. Soc* (Vol. 171).

Broekhuyse, R. M. (1972). Lipids in tissues of the eye: VII. Changes in concentration and composition of sphingomyelins, cholesterol esters and other lipids in aging sclera. *Biochimica et Biophysica Acta (BBA) - Lipids and Lipid Metabolism*, *280*(4), 637–645. https://doi.org/10.1016/0005-2760(72)90143-9

Bromer, W. W., & Chance, R. E. (1969). Zinc glucagon depression of blood amino acids in rabbits. *Diabetes*, *18*(11), 748–754. https://doi.org/10.2337/DIAB.18.11.748

Brumbaugh, D. E., Tearse, P., Cree-Green, M., Fenton, L. Z., Brown, M., Scherzinger, A., Reynolds, R., Alston, M., Hoffman, C., Pan, Z., Friedman, J. E., & Barbour, L. A. (2013). Intrahepatic Fat is Increased in Neonatal Offspring of Obese Women with Gestational Diabetes. *The Journal of Pediatrics*, *162*(5), 930. https://doi.org/10.1016/J.JPEDS.2012.11.017

Bullock, A. J., Zhang, L., O'Neill, A. M., Percy, A., Sukhatme, V., Mier, J. W., Atkins, M. B., & Bhatt, R. S. (2010). Plasma angiopoietin-2 (ANG2) as an angiogenic biomarker in renal cell carcinoma (RCC). *Https://Doi.Org/10.1200/Jco.2010.28.15_suppl.4630*, *28*(15_suppl), 4630–4630. https://doi.org/10.1200/JCO.2010.28.15_SUPPL.4630

Caballero, F., Fernández, A., Matías, N., Martínez, L., Fucho, R., Elena, M., Caballeria, J., Morales, A., Fernández-Checa, J. C., & García-Ruiz, C. (2010). Specific Contribution of Methionine and Choline in Nutritional Nonalcoholic Steatohepatitis: IMPACT ON MITOCHONDRIAL S-ADENOSYL-l-METHIONINE AND GLUTATHIONE*. *The Journal of Biological Chemistry*, *285*(24), 18528. https://doi.org/10.1074/JBC.M109.099333

Cancer - NHS. (n.d.). Retrieved February 14, 2023, from https://www.nhs.uk/conditions/cancer/

Capozzi, M. E., D'Alessio, D. A., & Campbell, J. E. (2022). The past, present, and future physiology and pharmacology of glucagon. *Cell Metabolism*, *34*(11), 1654–1674. https://doi.org/10.1016/J.CMET.2022.10.001

Carbone, J. W., & Pasiakos, S. M. (2019). Dietary Protein and Muscle Mass: Translating Science to Application and Health Benefit. *Nutrients*, *11*(5). https://doi.org/10.3390/NU11051136

Carbonell, W. S., Ansorga, O., Sibson, N., & Muschel, R. (2009). The Vascular Basement Membrane as "Soil" in Brain Metastasis. *PLoS ONE*, *4*(6), 5857. https://doi.org/10.1371/JOURNAL.PONE.0005857

Cataldo, I., Sarcognato, S., Sacchi, D., Cacciatore, M., Baciorri, F., Mangia, A., Cazzagon, N., & Guido, M. (2021). Pathology of non-alcoholic fatty liver disease. *Pathologica*, *113*(3), 194. https://doi.org/10.32074/1591-951X-242

Cernaianu, G., Frank, S., Erbstößer, K., Leonhardt, S., Cross, M., McIvor, Z., Scholz, G., Dansranjavin, T., Celik, I., Tannapfel, A., Wittekind, C., Troebs, R. B., Rothe, K., Bennek, J., Hauss, J., & Witzigmann, H. (2006). TNP-470 fails to block the onset of angiogenesis and early tumor establishment in an intravital minimal disease model. *International Journal of Colorectal Disease*, *21*(2), 143–154. https://doi.org/10.1007/S00384-005-0751-4/FIGURES/7

Chandel, N. S. (2021). Amino Acid Metabolism. *Cold Spring Harbor Perspectives in Biology*, *13*(4). https://doi.org/10.1101/CSHPERSPECT.A040584

Chandler-Laney, P. C., Morrison, S. A., Goree, L. L. T., Ellis, A. C., Casazza, K., Desmond, R., & Gower, B. A. (2014). Return of hunger following a relatively high carbohydrate breakfast is associated with earlier recorded glucose peak and nadir. *Appetite*, *80*, 236. https://doi.org/10.1016/J.APPET.2014.04.031

Chang, H. F., Wirkner, M. L., Krause, E., & Rettig, J. (2020). Investigation of Cytotoxic T Lymphocyte Function during Allorejection in the Anterior Chamber of the Eye. *International Journal of Molecular Sciences*, *21*(13), 1–12. https://doi.org/10.3390/IJMS21134660

Charbonneau, A., Unson, C. G., & Lavoie, J. M. (2007). High-fat diet-induced hepatic steatosis reduces glucagon receptor content in rat hepatocytes: potential interaction with acute exercise. *The Journal of Physiology*, *579*(Pt 1), 255–267. https://doi.org/10.1113/JPHYSIOL.2006.121954

Charidemou, E., Ashmore, T., Li, X., McNally, B. D., West, J. A., Liggi, S., Harvey, M., Orford, E., & Griffin, J. L. (2019a). A randomized 3-way crossover study indicates that high-protein feeding induces de novo lipogenesis in healthy humans. *JCI Insight*, *4*(12). https://doi.org/10.1172/JCI.INSIGHT.124819

Charidemou, E., Ashmore, T., Li, X., McNally, B. D., West, J. A., Liggi, S., Harvey, M., Orford, E., & Griffin, J. L. (2019b). A randomized 3-way crossover study indicates that high-protein feeding induces de novo lipogenesis in healthy humans. *JCI Insight*, *4*(12). https://doi.org/10.1172/JCI.INSIGHT.124819

Chen, C., Soto-Gutierrez, A., Baptista, P. M., & Spee, B. (2018). Biotechnology Challenges to In Vitro Maturation of Hepatic Stem Cells. *Gastroenterology*, *154*(5), 1258. https://doi.org/10.1053/J.GASTRO.2018.01.066

Chen, J., Liao, S., Xiao, Z., Pan, Q., Wang, X., Shen, K., Wang, S., Yang, L., Guo, F., Liu, H. F., & Pan, Q. (2022). The development and improvement of immunodeficient mice and humanized

immune system mouse models. *Frontiers in Immunology*, *13*, 1007579. https://doi.org/10.3389/FIMMU.2022.1007579/BIBTEX

Chen, L., Li, J., Wang, F., Dai, C., Wu, F., Liu, X., Li, T., Glauben, R., Zhang, Y., Nie, G., He, Y., & Qin, Z. (2016). Tie2 expression on macrophages is required for blood vessel reconstruction and tumor relapse after chemotherapy. *Cancer Research*, *76*(23), 6828–6838. https://doi.org/10.1158/0008-5472.CAN-16-1114/652497/AM/TIE2-EXPRESSION-ON-MACROPHAGES-IS-REQUIRED-FOR

Chi, K. Y., & Kim, J.-H. (2022). Recent advances in liver organoids and their use in in vitro modeling of non-alcoholic fatty liver disease. *Organoid*, *2*, e6. https://doi.org/10.51335/ORGANOID.2022.2.E6

Choi, J. Il, Jang, S. I., Hong, J., Kim, C. H., Kwon, S. S., Park, J. S., & Lim, J. B. (2021). Cancer-initiating cells in human pancreatic cancer organoids are maintained by interactions with endothelial cells. *Cancer Letters*, *498*, 42–53. https://doi.org/10.1016/J.CANLET.2020.10.012

Christiansen, A., & Detmar, M. (2011). Lymphangiogenesis and Cancer. *Genes & Cancer*, *2*(12), 1146. https://doi.org/10.1177/1947601911423028

Chu, P. Y., Koh, A. P. F., Antony, J., & Huang, R. Y. J. (2022). Applications of the Chick Chorioallantoic Membrane as an Alternative Model for Cancer Studies. *Cells, Tissues, Organs*, *211*(2), 222. https://doi.org/10.1159/000513039

Cigrovski Berkovic, M., Bilic-Curcic, I., Mrzljak, A., & Cigrovski, V. (2021). NAFLD and Physical Exercise: Ready, Steady, Go! *Frontiers in Nutrition*, *8*, 734859. https://doi.org/10.3389/FNUT.2021.734859

Clarijs, R., Otte-Höller, I., Ruiter, D. J., & de Waal, R. M. W. (2002). Presence of a fluid-conducting meshwork in xenografted cutaneous and primary human uveal melanoma. *Investigative Ophthalmology & Visual Science*, *43*(4), 912–918. http://intl.iovs.org/cgi/content/full/43/4/912

Cooper, A. D. (1997). Hepatic uptake of chylomicron remnants. *Journal of Lipid Research*, *38*(11), 2173–2192. https://doi.org/10.1016/S0022-2275(20)34932-4

Coste, A., Oktay, M. H., Condeelis, J. S., & Entenberg, D. (2020). Intravital Imaging Techniques for Biomedical and Clinical Research. *Cytometry Part A*, *97*(5), 448–457. https://doi.org/10.1002/CYTO.A.23963

Cristante, J., Tubbs, E., Benhamou, P.-Y., & Lablanche, S. (2021). Oxygenation and vascularization of pancreatic islet graft: An overview. *Trends in Transplantation*, *14*(4). https://doi.org/10.15761/TIT.1000307

Cross, E., Dearlove, D. J., & Hodson, L. (2023). Nutritional regulation of hepatic de novo lipogenesis in humans. *Current Opinion in Clinical Nutrition and Metabolic Care*, *26*(2), 65–71. https://doi.org/10.1097/MCO.0000000000000914

Cruz-Ramón, V., Chinchilla-López, P., Ramírez-Pérez, O., & Méndez-Sánchez, N. (2017). Bile Acids in Nonalcoholic Fatty Liver Disease: New Concepts and therapeutic advances. *Annals of Hepatology*, *16*(Suppl. 1: s3-105.), S58–S67. https://doi.org/10.5604/01.3001.0010.5498

Cui, S. (2017). Immunogenic Chemotherapy Sensitizes Renal Cancer to Immune Checkpoint Blockade Therapy in Preclinical Models. *Medical Science Monitor : International Medical Journal of Experimental and Clinical Research*, *23*, 3360. https://doi.org/10.12659/MSM.902426

Currie, M. J., Gunningham, S. P., Tumer, K., Han, C., Scott, P. A. E., Robinson, B. A., Chong, W., Harris, A. L., & Fox, S. B. (2002). Expression of the angiopoietins and their receptor Tie2 in human renal clear cell carcinomas; regulation by the von Hippel-Lindau gene and hypoxia. *The Journal of Pathology*, *198*(4), 502–510. https://doi.org/10.1002/PATH.1228

Cusi, K., Orsak, B., Bril, F., Lomonaco, R., Hecht, J., Ortiz-Lopez, C., Tio, F., Hardies, J., Darland, C., Musi, N., Webb, A., & Portillo-Sanchez, P. (2016). Long-Term Pioglitazone Treatment for Patients With Nonalcoholic Steatohepatitis and Prediabetes or Type 2 Diabetes Mellitus: A Randomized Trial. *Annals of Internal Medicine*, *165*(5), 305–315. https://doi.org/10.7326/M15-1774

Cuypers, A., Truong, A. C. K., Becker, L. M., Saavedra-García, P., & Carmeliet, P. (2022). Tumor vessel co-option: The past & the future. *Frontiers in Oncology*, *12*, 4471. https://doi.org/10.3389/FONC.2022.965277/BIBTEX

Daghlas, S. A., & Mohiuddin, S. S. (2023). Biochemistry, Glycogen. *StatPearls*. https://www.ncbi.nlm.nih.gov/books/NBK539802/

Daniel, E., & Cleaver, O. (2019). Vascularizing organogenesis: Lessons from developmental biology and implications for regenerative medicine. *Current Topics in Developmental Biology*, *132*, 177–220. https://doi.org/10.1016/BS.CTDB.2018.12.012

DAVIDSON., I. W. F., SALTER, J. M., & BEST, C. H. (1960). The Effect of Glucagon on the Metabolic Rate of Rats. *The American Journal of Clinical Nutrition*, *8*(5), 540–546. https://doi.org/10.1093/AJCN/8.5.540

Davis, R. P., Surewaard, B. G. J., Turk, M., Carestia, A., Lee, W. Y., Petri, B., Urbanski, S. J., Coffin, C. S., & Jenne, C. N. (2020). Optimization of In vivo Imaging Provides a First Look at Mouse Model of Non-Alcoholic Fatty Liver Disease (NAFLD) Using Intravital Microscopy. *Frontiers in Immunology*, *10*, 482686. https://doi.org/10.3389/FIMMU.2019.02988/BIBTEX

Day, J. W., Gelfanov, V., Smiley, D., Carrington, P. E., Eiermann, G., Chicchi, G., Erion, M. D., Gidda, J., Thornberry, N. A., Tschöp, M. H., Marsh, D. J., SinhaRoy, R., DiMarchi, R., & Pocai, A. (2012). Optimization of co-agonism at GLP-1 and glucagon receptors to safely maximize weight reduction in DIO-rodents. *Biopolymers*, *98*(5), 443–450. https://doi.org/10.1002/BIP.22072

De Chiara, F., Checcllo, C. U., & Azcón, J. R. (2019). High Protein Diet and Metabolic Plasticity in Non-Alcoholic Fatty Liver Disease: Myths and Truths. *Nutrients*, *11*(12). https://doi.org/10.3390/NU11122985

de Palma, M., Murdoch, C., Venneri, M. A., Naldini, L., & Lewis, C. E. (2007). Tie2-expressing monocytes: regulation of tumor angiogenesis and therapeutic implications. *Trends in Immunology*, *28*(12), 519–524. https://doi.org/10.1016/J.IT.2007.09.004

Debiński, P., Dembowski, J., Kowal, P., Szydełko, T., Kołodziej, A., Małkiewicz, B., Tupikowski, K., & Zdrojowy, R. (2013a). The clinical significance of lymphangiogenesis in renal cell carcinoma. *Medical Science Monitor : International Medical Journal of Experimental and Clinical Research*, *19*(1), 606. https://doi.org/10.12659/MSM.883981

Debiński, P., Dembowski, J., Kowal, P., Szydełko, T., Kołodziej, A., Małkiewicz, B., Tupikowski, K., & Zdrojowy, R. (2013b). The clinical significance of lymphangiogenesis in renal cell carcinoma. *Medical Science Monitor : International Medical Journal of Experimental and Clinical Research*, *19*(1), 606. https://doi.org/10.12659/MSM.883981

DeLeve, L. D., & Maretti-Mira, A. C. (2017). Liver Sinusoidal Endothelial Cell: An Update. *Seminars in Liver Disease*, *37*(4), 377. https://doi.org/10.1055/S-0037-1617455

Deng, D., Dai, B., Wei, J., Yuan, X., Yang, X., Qi, S., & Zhang, Z. (2021). A drawer-type abdominal window with an acrylic/resin coverslip enables long-term intravital fluorescence/photoacoustic imaging of the liver. *Nanophotonics*, *10*(12), 3369–3381. https://doi.org/10.1515/NANOPH-2021-0281/ASSET/GRAPHIC/J_NANOPH-2021-0281_FIG_005.JPG

Dhamija, E., Paul, S., & Kedia, S. (2019). Non-alcoholic fatty liver disease associated with hepatocellular carcinoma: An increasing concern. *The Indian Journal of Medical Research*, *149*(1), 9. https://doi.org/10.4103/IJMR.IJMR_1456_17

Dissanayaka, W. L., Zhu, L., Hargreaves, K. M., Jin, L., & Zhang, C. (2014). Scaffold-free Prevascularized Microtissue Spheroids for Pulp Regeneration. *Journal of Dental Research*, *93*(12), 1296. https://doi.org/10.1177/0022034514550040

Donnelly, K. L., Smith, C. I., Schwarzenberg, S. J., Jessurun, J., Boldt, M. D., & Parks, E. J. (2005a). Sources of fatty acids stored in liver and secreted via lipoproteins in patients with nonalcoholic fatty liver disease. *The Journal of Clinical Investigation*, *115*(5), 1343–1351. https://doi.org/10.1172/JCI23621

Donnelly, K. L., Smith, C. I., Schwarzenberg, S. J., Jessurun, J., Boldt, M. D., & Parks, E. J. (2005b). Sources of fatty acids stored in liver and secreted via lipoproteins in patients with nonalcoholic fatty liver disease. *Journal of Clinical Investigation*, *115*(5), 1343. https://doi.org/10.1172/JCI23621

Donnem, T., Hu, J., Ferguson, M., Adighibe, O., Snell, C., Harris, A. L., Gatter, K. C., & Pezzella, F. (2013). Vessel co-option in primary human tumors and metastases: an obstacle to effective anti-angiogenic treatment? *Cancer Medicine*, *2*(4), 427. https://doi.org/10.1002/CAM4.105

Dossou, A. S., & Basu, A. (2019). The Emerging Roles of mTORC1 in Macromanaging Autophagy. *Cancers*, *11*(10). https://doi.org/10.3390/CANCERS11101422

Drummen, X. M., Dorenbos, E., Vreugdenhil, A. C. E., Raben, A., Fogelholm, M., Westerterp-Plantenga, M. S., & Adam, T. C. (2018). Long-term effects of increased protein intake after weight

loss on intrahepatic lipid content and implications for insulin sensitivity: a PREVIEW study. *Https://Doi.Org/10.1152/Ajpendo.00162.2018*, *315*(5), E885–E891. https://doi.org/10.1152/AJPENDO.00162.2018

du Cheyne, C., Smeets, M., & de Spiegelaere, W. (2021). Techniques used to assess intussusceptive angiogenesis: A systematic review. *Developmental Dynamics*, *250*(12), 1704–1716. https://doi.org/10.1002/DVDY.382

Du, J., Ma, Y. Y., Yu, C. H., & Li, Y. M. (2014). Effects of pentoxifylline on nonalcoholic fatty liver disease: A meta-analysis. *World Journal of Gastroenterology : WJG*, *20*(2), 569. https://doi.org/10.3748/WJG.V20.I2.569

Duan, J. L., Ruan, B., Yan, X. C., Liang, L., Song, P., Yang, Z. Y., Liu, Y., Dou, K. F., Han, H., & Wang, L. (2018). Endothelial Notch activation reshapes the angiocrine of sinusoidal endothelia to aggravate liver fibrosis and blunt regeneration in mice. *Hepatology*, *68*(2), 677–690. https://doi.org/10.1002/HEP.29834/SUPPINFO

Duarte, D., Hawkins, E. D., Akinduro, O., Ang, H., de Filippo, K., Kong, I. Y., Haltalli, M., Ruivo, N., Straszkowski, L., Vervoort, S. J., McLean, C., Weber, T. S., Khorshed, R., Pirillo, C., Wei, A., Ramasamy, S. K., Kusumbe, A. P., Duffy, K., Adams, R. H., … lo Celso, C. (2018). Inhibition of Endosteal Vascular Niche Remodeling Rescues Hematopoietic Stem Cell Loss in AML. *Cell Stem Cell*, *22*(1), 64. https://doi.org/10.1016/J.STEM.2017.11.006

Duarte, S. M. B., Stefano, J. T., Vanni, D. S., Carrilho, F. J., & De Oliveira, C. P. M. S. (2019). IMPACT OF CURRENT DIET AT THE RISK OF NON-ALCOHOLIC FATTY LIVER DISEASE (NAFLD). *Arquivos de Gastroenterologia*, *56*(4), 431–439. https://doi.org/10.1590/S0004-2803.201900000-67

Duncan, R. E., Ahmadian, M., Jaworski, K., Sarkadi-Nagy, E., & Sul, H. S. (2007). Regulation of Lipolysis in Adipocytes. *Annual Review of Nutrition*, *27*, 79. https://doi.org/10.1146/ANNUREV.NUTR.27.061406.093734

Duran, C. L., Borriello, L., Karagiannis, G. S., Entenberg, D., Oktay, M. H., & Condeelis, J. S. (2021a). Targeting Tie2 in the Tumor Microenvironment: From Angiogenesis to Dissemination. *Cancers*, *13*(22). https://doi.org/10.3390/CANCERS13225730

Duran, C. L., Borriello, L., Karagiannis, G. S., Entenberg, D., Oktay, M. H., & Condeelis, J. S. (2021b). Targeting Tie2 in the Tumor Microenvironment: From Angiogenesis to Dissemination. *Cancers*, *13*(22). https://doi.org/10.3390/CANCERS13225730

Ebbeling, C. B., Feldman, H. A., Klein, G. L., Wong, J. M. W., Bielak, L., Steltz, S. K., Luoto, P. K., Wolfe, R. R., Wong, W. W., & Ludwig, D. S. (2018). Effects of a low carbohydrate diet on energy expenditure during weight loss maintenance: randomized trial. *BMJ*, *363*, 4583. https://doi.org/10.1136/BMJ.K4583

Eckrich, J., Kugler, P., Buhr, C. R., Ernst, B. P., Mendler, S., Baumgart, J., Brieger, J., & Wiesmann, N. (2020). Monitoring of tumor growth and vascularization with repetitive ultrasonography in the chicken chorioallantoic-membrane-assay. *Scientific Reports 2020 10:1*, *10*(1), 1–14. https://doi.org/10.1038/s41598-020-75660-y

Eichhorn, M. E., Strieth, S., Luedemann, S., Kleespies, A., Nöth, U., Passon, A., Brix, G., Jauch, K. W., Bruns, C. J., & Dellian, M. (2008). Contrast enhanced MRI and intravital fluorescence microscopy indicate improved tumor microcirculation in highly vascularized melanomas upon short-term anti-VEGFR treatment. *Cancer Biology & Therapy*, *7*(7), 1006–1013. https://doi.org/10.4161/CBT.7.7.5997

El-Deen, R. M., Heeba, G. H., Abdel-latif, R. G., & Khalifa, M. M. A. (2020). Comparative effectiveness of phosphodiesterase 3, 4, and 5 inhibitors in amelioration of high-fat diet-induced nonalcoholic fatty liver in rats. *Fundamental & Clinical Pharmacology*, *34*(3), 353–364. https://doi.org/10.1111/FCP.12530

Enjoji, M., Kohjima, M., & Nakamuta, M. (2016). Lipid metabolism and the liver. *The Liver in Systemic Diseases*, 105–122. https://doi.org/10.1007/978-4-431-55790-6_6/FIGURES/3

Entenberg, D., Voiculescu, S., Guo, P., Borriello, L., Wang, Y., Karagiannis, G. S., Jones, J., Baccay, F., Oktay, M., & Condeelis, J. (2018). A permanent window for the murine lung enables high-resolution imaging of cancer metastasis. *Nature Methods*, *15*(1), 73. https://doi.org/10.1038/NMETH.4511

Eriksen, P. L., Vilstrup, H., Rigbolt, K., Suppli, M. P., Sørensen, M., Heebøll, S., Veidal, S. S., Knop, F. K., & Thomsen, K. L. (2019). Non-alcoholic fatty liver disease alters expression of genes governing hepatic nitrogen conversion. *Liver International*, *39*(11), 2094–2101. https://doi.org/10.1111/LIV.14205

Eslam, M., Newsome, P. N., Sarin, S. K., Anstee, Q. M., Targher, G., Romero-Gomez, M., Zelber-Sagi, S., Wai-Sun Wong, V., Dufour, J. F., Schattenberg, J. M., Kawaguchi, T., Arrese, M., Valenti, L., Shiha, G., Tiribelli, C., Yki-Järvinen, H., Fan, J. G., Grønbæk, H., Yilmaz, Y., … George, J. (2020). A new definition for metabolic dysfunction-associated fatty liver disease: An international expert consensus statement. *Journal of Hepatology*, *73*(1), 202–209. https://doi.org/10.1016/J.JHEP.2020.03.039

Fabbrini, E., Sullivan, S., & Klein, S. (2010). Obesity and Nonalcoholic Fatty Liver Disease: Biochemical, Metabolic and Clinical Implications. *Hepatology (Baltimore, Md.)*, *51*(2), 679. https://doi.org/10.1002/HEP.23280

Fernández, M., Semela, D., Bruix, J., Colle, I., Pinzani, M., & Bosch, J. (2009). Angiogenesis in liver disease. *Journal of Hepatology*, *50*(3), 604–620. https://doi.org/10.1016/J.JHEP.2008.12.011

Fernández-Cortés, M., Delgado-Bellido, D., & Javier Oliver, F. (2019). Vasculogenic mimicry: Become an endothelial cell "But not so much." *Frontiers in Oncology*, *9*(AUG), 803. https://doi.org/10.3389/FONC.2019.00803/BIBTEX

Fernández-Domínguez, I., Echevarria-Uraga, J. J., Gómez, N., Luka, Z., Wagner, C., Lu, S. C., Mato, J. M., Martínez-Chantar, M. L., & Rodríguez-Cuesta, J. (2011). High-frequency ultrasound imaging for longitudinal evaluation of non-alcoholic fatty liver disease progression in mice. *Ultrasound in Medicine & Biology*, *37*(7), 1161. https://doi.org/10.1016/J.ULTRASMEDBIO.2011.04.012

Fernando, D. H., Forbes, J. M., Angus, P. W., & Herath, C. B. (2019). Development and Progression of Non-Alcoholic Fatty Liver Disease: The Role of Advanced Glycation End Products. *International Journal of Molecular Sciences*, *20*(20). https://doi.org/10.3390/IJMS20205037

Fisher-Wellman, K. H., Ryan, T. E., Smith, C. D., Gilliam, L. A. A., Lin, C. Te, Reese, L. R., Torres, M. J., & Neufer, P. D. (2016). A Direct Comparison of Metabolic Responses to High-Fat Diet in C57BL/6J and C57BL/6NJ Mice. *Diabetes*, *65*(11), 3249. https://doi.org/10.2337/DB16-0291

Flessa, C. M., Nasiri-Ansari, N., Kyrou, I., Leca, B. M., Lianou, M., Chatzigeorgiou, A., Kaltsas, G., Kassi, E., & Randeva, H. S. (2022). Genetic and Diet-Induced Animal Models for Non-Alcoholic Fatty Liver Disease (NAFLD) Research. *International Journal of Molecular Sciences 2022, Vol. 23, Page 15791*, *23*(24), 15791. https://doi.org/10.3390/IJMS232415791

Folberg, R., & Maniotis, A. J. (2004). Vasculogenic mimicry. *APMIS*, *112*(7–8), 508–525. https://doi.org/10.1111/J.1600-0463.2004.APM11207-0810.X

Foley, P. J. (2021). Effect of low carbohydrate diets on insulin resistance and the metabolic syndrome. *Current Opinion in Endocrinology, Diabetes, and Obesity*, *28*(5), 463–468. https://doi.org/10.1097/MED.0000000000000659

Fontoura, J. C., Viezzer, C., dos Santos, F. G., Ligabue, R. A., Weinlich, R., Puga, R. D., Antonow, D., Severino, P., & Bonorino, C. (2020). Comparison of 2D and 3D cell culture models for cell growth, gene expression and drug resistance. *Materials Science and Engineering: C*, *107*, 110264. https://doi.org/10.1016/J.MSEC.2019.110264

Francque, S. M., Bedossa, P., Ratziu, V., Anstee, Q. M., Bugianesi, E., Sanyal, A. J., Loomba, R., Harrison, S. A., Balabanska, R., Mateva, L., Lanthier, N., Alkhouri, N., Moreno, C., Schattenberg, J. M., Stefanova-Petrova, D., Vonghia, L., Rouzier, R., Guillaume, M., Hodge, A., … Abdelmalek, M. F. (2021). A Randomized, Controlled Trial of the Pan-PPAR Agonist Lanifibranor in NASH. *The New England Journal of Medicine*, *385*(17), 1547–1558. https://doi.org/10.1056/NEJMOA2036205

Fraunfelder, F. T., Garner, A., & Barras, T. C. (1976). Subconjunctival and episcleral lipid deposits. *The British Journal of Ophthalmology*, *60*(7), 532. https://doi.org/10.1136/BJO.60.7.532

French, W. W., Dridi, S., Shouse, S. A., Wu, H., Hawley, A., Lee, S. O., Gu, X., & Baum, J. I. (2017). A High-Protein Diet Reduces Weight Gain, Decreases Food Intake, Decreases Liver Fat Deposition, and Improves Markers of Muscle Metabolism in Obese Zucker Rats. *Nutrients*, *9*(6). https://doi.org/10.3390/NU9060587

Fu, Z.-D., Cai, X.-L., Yang, W.-J., Zhao, M.-M., Li, R., & Li, Y.-F. (2021). Novel glucose-lowering drugs for non-alcoholic fatty liver disease. *World Journal of Diabetes*, *12*(1), 84. https://doi.org/10.4239/WJD.V12.I1.84

Fushimi, S., Nohno, T., & Katsuyama, H. (2023). Chronic Stress Induces Type 2b Skeletal Muscle Atrophy via the Inhibition of mTORC1 Signaling in Mice. *Medical Sciences (Basel, Switzerland)*, *11*(1), 19. https://doi.org/10.3390/MEDSCI11010019/S1

Galsgaard, K. D. (2020). The Vicious Circle of Hepatic Glucagon Resistance in Non-Alcoholic Fatty Liver Disease. *Journal of Clinical Medicine*, *9*(12), 1–11. https://doi.org/10.3390/JCM9124049

Galsgaard, K. D., Pedersen, J., Knop, F. K., Holst, J. J., & Albrechtsen, N. J. W. (2019). Glucagon Receptor Signaling and Lipid Metabolism. *Frontiers in Physiology*, *10*(APR). https://doi.org/10.3389/FPHYS.2019.00413

Gannon, M. C., Nuttall, F. Q., Saeed, A., Jordan, K., & Hoover, H. (2003). An increase in dietary protein improves the blood glucose response in persons with type 2 diabetes. *The American Journal of Clinical Nutrition*, *78*(4), 734–741. https://doi.org/10.1093/AJCN/78.4.734

Geiselman, P. J., & Novin, D. (1982). The Role of Carbohydrates in Appetite, Hunger and Obesity. *Appetite*, *3*(3), 203–223. https://doi.org/10.1016/S0195-6663(82)80017-2

Geng, Y., Faber, K. N., de Meijer, V. E., Blokzijl, H., & Moshage, H. (2021). How does hepatic lipid accumulation lead to lipotoxicity in non-alcoholic fatty liver disease? *Hepatology International 2021 15:1*, *15*(1), 21–35. https://doi.org/10.1007/S12072-020-10121-2

Godoy-Matos, A. F., Silva Júnior, W. S., & Valerio, C. M. (2020). NAFLD as a continuum: From obesity to metabolic syndrome and diabetes. *Diabetology and Metabolic Syndrome*, *12*(1), 1–20. https://doi.org/10.1186/S13098-020-00570-Y/TABLES/5

Goldberg, I. J., Eckel, R. H., & Abumrad, N. A. (2009). Regulation of fatty acid uptake into tissues: lipoprotein lipase- and CD36-mediated pathways. *Journal of Lipid Research*, *50 Suppl*(Suppl). https://doi.org/10.1194/JLR.R800085-JLR200

Gravholt, C. H., Møller, N., Jensen, M. D., Christiansen, J. S., & Schmitz, O. (2001). Physiological levels of glucagon do not influence lipolysis in abdominal adipose tissue as assessed by microdialysis. *The Journal of Clinical Endocrinology and Metabolism*, *86*(5), 2085–2089. https://doi.org/10.1210/JCEM.86.5.7460

Gromova, L. V., Fetissov, S. O., & Gruzdkov, A. A. (2021). Mechanisms of Glucose Absorption in the Small Intestine in Health and Metabolic Diseases and Their Role in Appetite Regulation. *Nutrients*, *13*(7). https://doi.org/10.3390/NU13072474

Gunn, N. T. (2021). Lean Nonalcoholic Steatohepatitis and Nonalcoholic Fatty Liver Disease. *Gastroenterology & Hepatology*, *17*(4), 184. /pmc/articles/PMC8132629/

Gunti, S., Hoke, A. T. K., Vu, K. P., & London, N. R. (2021). Organoid and Spheroid Tumor Models: Techniques and Applications. *Cancers*, *13*(4), 1–18. https://doi.org/10.3390/CANCERS13040874

Guo, H., Deng, N., Dou, L., Ding, H., Criswell, T., Atala, A., Furdui, C. M., & Zhang, Y. (2020). 3-D Human Renal Tubular Organoids Generated from Urine-Derived Stem Cells for Nephrotoxicity Screening. *ACS Biomaterials Science and Engineering*, *6*(12), 6701–6709. https://doi.org/10.1021/ACSBIOMATERIALS.0C01468/SUPPL_FILE/AB0C01468_SI_001.PDF

Gupta, S., & Chowdhury, J. R. (1992). Hepatocyte transplantation: back to the future. *Hepatology (Baltimore, Md.)*, *15*(1), 156–162. https://doi.org/10.1002/HEP.1840150126

Habegger, K. M., Stemmer, K., Cheng, C., Müller, T. D., Heppner, K. M., Ottaway, N., Holland, J., Hembree, J. L., Smiley, D., Gelfanov, V., Krishna, R., Arafat, A. M., Konkar, A., Belli, S., Kapps, M., Woods, S. C., Hofmann, S. M., D'Alessio, D., Pfluger, P. T., … Tschöp, M. H. (2013). Fibroblast growth factor 21 mediates specific glucagon actions. *Diabetes*, *62*(5), 1453–1463. https://doi.org/10.2337/DB12-1116/-/DC1

Hædersdal, S., Lund, A., Knop, F. K., & Vilsbøll, T. (2018). The Role of Glucagon in the Pathophysiology and Treatment of Type 2 Diabetes. *Mayo Clinic Proceedings*, *93*(2), 217–239. https://doi.org/10.1016/J.MAYOCP.2017.12.003

HAGEN, J. H. (1961). Effect of glucagon on the metabolism of adipose tissue. *The Journal of Biological Chemistry*, *236*, 1023–1027. https://doi.org/10.1016/S0021-9258(18)64236-X

Hagström, H., Simon, T. G., Roelstraete, B., Stephansson, O., Söderling, J., & Ludvigsson, J. F. (2021). Maternal obesity increases the risk and severity of NAFLD in offspring. *Journal of Hepatology*, *75*(5), 1042–1048. https://doi.org/10.1016/J.JHEP.2021.06.045

Haibe, Y., Kreidieh, M., el Hajj, H., Khalifeh, I., Mukherji, D., Temraz, S., & Shamseddine, A. (2020). Resistance Mechanisms to Anti-angiogenic Therapies in Cancer. *Frontiers in Oncology*, *10*, 221. https://doi.org/10.3389/FONC.2020.00221/BIBTEX

Hall, M. G. N., Moshirfar, M., Amin-Javaheri, A., Ouano, D. P., Ronquillo, Y., & Hoopes, P. C. (2020). Lipid Keratopathy: A Review of Pathophysiology, Differential Diagnosis, and Management. *Ophthalmology and Therapy*, *9*(4), 833. https://doi.org/10.1007/S40123-020-00309-Y

Han, H. S., Kang, G., Kim, J. S., Choi, B. H., & Koo, S. H. (2016). Regulation of glucose metabolism from a liver-centric perspective. *Experimental & Molecular Medicine*, *48*(3), e218. https://doi.org/10.1038/EMM.2015.122

Hasek, B. E., Stewart, L. K., Henagan, T. M., Boudreau, A., Lenard, N. R., Black, C., Shin, J., Huypens, P., Malloy, V. L., Plaisance, E. P., Krajcik, R. A., Orentreich, N., & Gettys, T. W. (2010). Dietary methionine restriction enhances metabolic flexibility and increases uncoupled respiration in both fed and fasted states. *American Journal of Physiology - Regulatory, Integrative and Comparative Physiology*, *299*(3), R728. https://doi.org/10.1152/AJPREGU.00837.2009

Hashemi, G., Dight, J., Khosrotehrani, K., & Sormani, L. (2022). Melanoma Tumour Vascularization and Tissue-Resident Endothelial Progenitor Cells. *Cancers*, *14*(17). https://doi.org/10.3390/CANCERS14174216

Hashida, R., Kawaguchi, T., Bekki, M., Omoto, M., Matsuse, H., Nago, T., Takano, Y., Ueno, T., Koga, H., George, J., Shiba, N., & Torimura, T. (2017). Aerobic vs. resistance exercise in non-alcoholic fatty liver disease: A systematic review. *Journal of Hepatology*, *66*(1), 142–152. https://doi.org/10.1016/J.JHEP.2016.08.023

Hayashi, Y. (2021). Glucagon regulates lipolysis and fatty acid oxidation through inositol triphosphate receptor 1 in the liver. *Journal of Diabetes Investigation*, *12*(1), 32. https://doi.org/10.1111/JDI.13315

Hayashi, Y., & Seino, Y. (2018). Regulation of amino acid metabolism and α-cell proliferation by glucagon. *Journal of Diabetes Investigation*, *9*(3), 464. https://doi.org/10.1111/JDI.12797

He, X., Lee, B., & Jiang, Y. (2016). Cell-ECM interactions in tumor invasion. *Advances in Experimental Medicine and Biology*, *936*, 73–91. https://doi.org/10.1007/978-3-319-42023-3_4/FIGURES/6

Hendriks, D., Brouwers, J. F., Hamer, K., Geurts, M. H., Luciana, L., Massalini, S., López-Iglesias, C., Peters, P. J., Rodríguez-Colman, M. J., Chuva de Sousa Lopes, S., Artegiani, B., & Clevers, H. (2023). Engineered human hepatocyte organoids enable CRISPR-based target discovery and drug screening for steatosis. *Nature Biotechnology 2023*, 1–15. https://doi.org/10.1038/s41587-023-01680-4

Henry, Z., Meadows, V., & Guo, G. L. (2023). FXR and NASH: an avenue for tissue-specific regulation. *Hepatology Communications*, *7*(5). https://doi.org/10.1097/HC9.0000000000000127

Hills, A. P., Mokhtar, N., & Byrne, N. M. (2014). Assessment of Physical Activity and Energy Expenditure: An Overview of Objective Measures. *Frontiers in Nutrition*, *1*. https://doi.org/10.3389/FNUT.2014.00005

Hirayama, Y., Gi, M., Yamano, S., Tachibana, H., Okuno, T., Tamada, S., Nakatani, T., & Wanibuchi, H. (2016). Anti-PD-L1 treatment enhances antitumor effect of everolimus in a mouse model of renal cell carcinoma. *Cancer Science*, *107*(12), 1736–1744. https://doi.org/10.1111/CAS.13099

Hirsova, P., & Gores, G. J. (2015). Death Receptor-Mediated Cell Death and Proinflammatory Signaling in Nonalcoholic Steatohepatitis. *Cellular and Molecular Gastroenterology and Hepatology*, *1*(1), 17–27. https://doi.org/10.1016/J.JCMGH.2014.11.005

Holash, J., Wiegand, S. J., & Yancopoulos, G. D. (1999). New model of tumor angiogenesis: dynamic balance between vessel regression and growth mediated by angiopoietins and VEGF. *Oncogene 1999 18:38*, *18*(38), 5356–5362. https://doi.org/10.1038/sj.onc.1203035

Holst, J. J. (2022). Glucagon and other proglucagon-derived peptides in the pathogenesis of obesity. *Frontiers in Nutrition*, *9*, 964406. https://doi.org/10.3389/FNUT.2022.964406/BIBTEX

Honma, M., Sawada, S., Ueno, Y., Murakami, K., Yamada, T., Gao, J., Kodama, S., Izumi, T., Takahashi, K., Tsukita, S., Uno, K., Imai, J., Kakazu, E., Kondo, Y., Mizuno, K., Kawagishi, N.,

Shimosegawa, T., & Katagiri, H. (2018). Selective insulin resistance with differential expressions of IRS-1 and IRS-2 in human NAFLD livers. *International Journal of Obesity (2005)*, *42*(9), 1544–1555. https://doi.org/10.1038/S41366-018-0062-9

Hope, D. C. D. (2022). *Glucagon analogue therapy for obesity and metabolic disease; Implications of amino acid metabolism Digestion and Reproduction Imperial College London*.

Hope, D. C. D., Hinds, C. E., Lopes, T., Vincent, M. L., Shrewsbury, J. V., Yu, A. T. C., Davies, I., Scott, R., Jones, B., Murphy, K. G., Minnion, J. S., Sardini, A., Carling, D., Lutz, T. A., Bloom, S. R., Tan, T. M. M., & Owen, B. M. (2022). Hypoaminoacidemia underpins glucagon-mediated energy expenditure and weight loss. *Cell Reports. Medicine*, *3*(11). https://doi.org/10.1016/J.XCRM.2022.100810

Houttu, V., Csader, S., Nieuwdorp, M., Holleboom, A. G., & Schwab, U. (2021). Dietary Interventions in Patients With Non-alcoholic Fatty Liver Disease: A Systematic Review and Meta-Analysis. *Frontiers in Nutrition*, *8*, 716783. https://doi.org/10.3389/FNUT.2021.716783/BIBTEX

Hristov, M., Erl, W., & Weber, P. C. (2003). Endothelial Progenitor Cells. *Arteriosclerosis, Thrombosis, and Vascular Biology*, *23*(7), 1185–1189. https://doi.org/10.1161/01.ATV.0000073832.49290.B5

Hsu, M. J., Christ, M., & Christ, B. (2021). Co-Culture of Human Mesenchymal Stromal Cells and Primary Mouse Hepatocytes. *Methods in Molecular Biology*, *2269*, 151–165. https://doi.org/10.1007/978-1-0716-1225-5_11

Hu, H., Gehart, H., Artegiani, B., Peters, P. J., De Jong, Y. P., & Clevers Correspondence, H. (2018). Long-Term Expansion of Functional Mouse and Human Hepatocytes as 3D Organoids. *Cell*, *175*. https://doi.org/10.1016/j.cell.2018.11.013

Huang, X., Liu, G., Guo, J., & Su, Z. Q. (2018). The PI3K/AKT pathway in obesity and type 2 diabetes. *International Journal of Biological Sciences*, *14*(11), 1483. https://doi.org/10.7150/IJBS.27173

Huch, M., & Dollé, L. (2016). The plastic cellular states of liver cells: Are EpCAM and Lgr5 fit for purpose? *Hepatology (Baltimore, Md.)*, *64*(2), 652. https://doi.org/10.1002/HEP.28469

Huch, M., Dorrell, C., Boj, S. F., Van Es, J. H., Li, V. S. W., Van De Wetering, M., Sato, T., Hamer, K., Sasaki, N., Finegold, M. J., Haft, A., Vries, R. G., Grompe, M., & Clevers, H. (2013). In vitro expansion of single Lgr5+ liver stem cells induced by Wnt-driven regeneration. *Nature*, *494*(7436), 247. https://doi.org/10.1038/NATURE11826

Huh, Y., Cho, Y. J., & Nam, G. E. (2022). Recent Epidemiology and Risk Factors of Nonalcoholic Fatty Liver Disease. *Journal of Obesity & Metabolic Syndrome*, *31*(1), 17. https://doi.org/10.7570/JOMES22021

Hyogo, H., Tazuma, S., Arihiro, K., Iwamoto, K., Nabeshima, Y., Inoue, M., Ishitobi, T., Nonaka, M., & Chayama, K. (2008). Efficacy of atorvastatin for the treatment of nonalcoholic steatohepatitis with dyslipidemia. *Metabolism: Clinical and Experimental*, *57*(12), 1711–1718. https://doi.org/10.1016/J.METABOL.2008.07.030

Ibrahim, S. H., Kohli, R., & Gores, G. J. (2011). Mechanisms of Lipotoxicity in NAFLD and Clinical Implications. *Journal of Pediatric Gastroenterology and Nutrition*, *53*(2), 131. https://doi.org/10.1097/MPG.0B013E31822578DB

Idowu, T. O., Etzrodt, V., Pape, T., Heineke, J., Stahl, K., Haller, H., & David, S. (2021). Flow-dependent regulation of endothelial Tie2 by GATA3 in vivo. *Intensive Care Medicine Experimental* , *9*(1), 1–14. https://doi.org/10.1186/S40635-021-00402-X/FIGURES/6

Ilegems, E., & Berggren, P. O. (2021). The Eye as a Transplantation Site to Monitor Pancreatic Islet Cell Plasticity. *Frontiers in Endocrinology*, *12*, 379. https://doi.org/10.3389/FENDO.2021.652853/BIBTEX

Inagaki, E., Arai, E., Hatou, S., Sayano, T., Taniguchi, H., Negishi, K., Kanai, Y., Sato, Y., Okano, H., Tsubota, K., & Shimmura, S. (2022). The Anterior Eye Chamber as a Visible Medium for In Vivo Tumorigenicity Tests. *Stem Cells Translational Medicine*, *11*(8), 841. https://doi.org/10.1093/STCLTM/SZAC036

Ipsen, D. H., Lykkesfeldt, J., & Tveden-Nyborg, P. (2018). Molecular mechanisms of hepatic lipid accumulation in non-alcoholic fatty liver disease. *Cellular and Molecular Life Sciences*, *75*(18), 3313. https://doi.org/10.1007/S00018-018-2860-6

Ivascu, A., & Kubbies, M. (2006). Rapid generation of single-tumor spheroids for high-throughput cell function and toxicity analysis. *Journal of Biomolecular Screening*, *11*(8), 922–932. https://doi.org/10.1177/1087057106292763

Jain, R. K., Martin, J. D., & Stylianopoulos, T. (2014). The role of mechanical forces in tumor growth and therapy. *Annual Review of Biomedical Engineering*, *16*, 321–346. https://doi.org/10.1146/ANNUREV-BIOENG-071813-105259

Javed, S., Soukhtehzari, S., Fernandes, N., & Williams, K. C. (2022). Longitudinal bioluminescence imaging to monitor breast tumor growth and treatment response using the chick chorioallantoic membrane model. *Scientific Reports 2022 12:1*, *12*(1), 1–10. https://doi.org/10.1038/s41598-022-20854-9

Jeyakumar, S. M., & Vajreswari, A. (2022). Stearoyl-CoA desaturase 1: A potential target for non-alcoholic fatty liver disease?-perspective on emerging experimental evidence. *World Journal of Hepatology*, *14*(1), 168. https://doi.org/10.4254/WJH.V14.I1.168

Ji, J., Zhang, G., Sun, B., Yuan, H., Huang, Y., Zhang, J., Wei, X., Zhang, X., & Hou, J. (2013). The frequency of tumor-infiltrating Tie-2-expressing monocytes in renal cell carcinoma: its relationship to angiogenesis and progression. *Urology*, *82*(4), 974.e9-974.e13. https://doi.org/10.1016/J.UROLOGY.2013.05.026

Johnson, K. E., & Wilgus, T. A. (2014). Vascular Endothelial Growth Factor and Angiogenesis in the Regulation of Cutaneous Wound Repair. *Advances in Wound Care*, *3*(10), 647. https://doi.org/10.1089/WOUND.2013.0517

Joo, C.-K., Lee, J. Y., Mok, J., SHAWL, A. I., & Paik, D. W. (2018). The anterior chamber of the eye as a clinical transplantation site of pancreatic islets for the treatment of diabetes: a study in a rat model of diabetes. *Investigative Ophthalmology & Visual Science*, *59*(9), 3578–3578.

Juo, Y. Y., & Livingston, E. H. (2019). Testing for Nonalcoholic Fatty Liver Disease. *JAMA*, *322*(18), 1836–1836. https://doi.org/10.1001/JAMA.2019.10696

Kalra, A., Yetiskul, E., Wehrle, C. J., & Tuma, F. (2023). Physiology, Liver. *StatPearls*. https://www.ncbi.nlm.nih.gov/books/NBK535438/

Kanabekova, P., Kadyrova, A., & Kulsharova, G. (2022). Microfluidic Organ-on-a-Chip Devices for Liver Disease Modeling In Vitro. *Micromachines*, *13*(3). https://doi.org/10.3390/MI13030428

Kang, S. M., Kim, D., Lee, J. H., Takayama, S., & Park, J. Y. (2021). Engineered Microsystems for Spheroid and Organoid Studies. *Advanced Healthcare Materials*, *10*(2), 2001284. https://doi.org/10.1002/ADHM.202001284

Kang, S., Park, H. S., Jo, A., Hong, S. H., Lee, H. N., Lee, Y. Y., Park, J. S., Jung, H. S., Chung, S. S., & Park, K. S. (2012). Endothelial progenitor cell cotransplantation enhances islet engraftment by rapid revascularization. *Diabetes*, *61*(4), 866–876. https://doi.org/10.2337/DB10-1492/-/DC1

Karashima, T., Udaka, K., Niimura, M., Suzuki, K., Osakabe, H., Shimamoto, T., Fukata, S., Inoue, K., Kuroda, N., Seiki, M., & Shuin, T. (2017). Therapy with transcutaneous administration of imiquimod combined with oral administration of sorafenib suppresses renal cell carcinoma growing in an orthotopic mouse model. *Oncology Letters*, *14*(1), 1162–1166. https://doi.org/10.3892/OL.2017.6235

Karinen, S., Juurikka, K., Hujanen, R., Wahbi, W., Hadler-Olsen, E., Svineng, G., Eklund, K. K., Salo, T., Åström, P., & Salem, A. (2021a). Tumour cells express functional lymphatic endothelium-specific hyaluronan receptor in vitro and in vivo: Lymphatic mimicry promotes oral oncogenesis? *Oncogenesis 2021 10:3*, *10*(3), 1–11. https://doi.org/10.1038/s41389-021-00312-3

Karinen, S., Juurikka, K., Hujanen, R., Wahbi, W., Hadler-Olsen, E., Svineng, G., Eklund, K. K., Salo, T., Åström, P., & Salem, A. (2021b). Tumour cells express functional lymphatic endothelium-specific hyaluronan receptor in vitro and in vivo: Lymphatic mimicry promotes oral oncogenesis? *Oncogenesis 2021 10:3*, *10*(3), 1–11. https://doi.org/10.1038/s41389-021-00312-3

Kartsoli, S., Kostara, C. E., Tsimihodimos, V., Bairaktari, E. T., & Christodoulou, D. K. (2020). Lipidomics in non-alcoholic fatty liver disease. *World Journal of Hepatology*, *12*(8), 436. https://doi.org/10.4254/WJH.V12.I8.436

Kaser-Eichberger, A., Schrödl, F., Trost, A., Strohmaier, C., Bogner, B., Runge, C., Motloch, K., Bruckner, D., Laimer, M., Schlereth, S. L., Heindl, L. M., & Reitsamer, H. A. (2015). Topography of Lymphatic Markers in Human Iris and Ciliary Body. *Investigative Ophthalmology & Visual Science*, *56*(8), 4943–4953. https://doi.org/10.1167/IOVS.15-16573

Kedrin, D., Gligorijevic, B., Wyckoff, J., Verkhusha, V. v, Condeelis, J., Segall, J. E., & van Rheenen, J. (2008). Intravital imaging of metastatic behavior through a mammary imaging window. *Nature Methods*, *5*(12), 1019–1021. https://doi.org/10.1038/NMETH.1269

Khalid, W. B., Farhat, N., Lavery, L., Jarnagin, J., Delany, J. P., & Kim, K. (2021). Noninvasive assessment of liver fat in ob/ob mice using ultrasound-induced thermal strain imaging and its correlation with hepatic triglyceride content. *Ultrasound in Medicine & Biology*, *47*(4), 1067. https://doi.org/10.1016/J.ULTRASMEDBIO.2020.12.014

Khalil, M., Shariat-Panahi, A., Tootle, R., Ryder, T., McCloskey, P., Roberts, E., Hodgson, H., & Selden, C. (2001). Human hepatocyte cell lines proliferating as cohesive spheroid colonies in alginate markedly upregulate both synthetic and detoxificatory liver function. *Journal of Hepatology*, *34*(1), 68–77. https://doi.org/10.1016/S0168-8278(00)00080-5

Khambu, B., Yan, S., Huda, N., Liu, G., & Yin, X. M. (2018). Autophagy in non-alcoholic fatty liver disease and alcoholic liver disease. *Liver Research*, *2*(3), 112–119. https://doi.org/10.1016/J.LIVRES.2018.09.004

Khazaei, Y., Dehghanseresht, N., Mousavi, S. E., Nazari, M., Salamat, S., Asbaghi, O., & Mansoori, A. (2023). Association Between Protein Intake From Different Animal and Plant Origins and the Risk of Non-Alcoholic Fatty Liver Disease: A Case-Control Study. *Clinical Nutrition Research*, *12*(1), 29. https://doi.org/10.7762/CNR.2023.12.1.29

Kim, H.-S., Park, E.-J., & Lee, C.-W. (2019). Implication of hepatocyte dedifferentiation in pathogenesis and treatment of hepatocellular carcinoma. *Precision and Future Medicine*, *3*(2), 37–42. https://doi.org/10.23838/PFM.2018.00135

Kim, T., Holleman, C. L., Nason, S., Arble, D. M., Ottaway, N., Chabenne, J., Loyd, C., Kim, J. A., Sandoval, D., Drucker, D. J., DiMarchi, R., Perez-Tilve, D., & Habegger, K. M. (2018). Hepatic glucagon receptor signaling enhances insulin-stimulated glucose disposal in rodents. *Diabetes*, *67*(11), 2157–2166. https://doi.org/10.2337/DB18-0068/-/DC1

Kim, T., Nason, S., Holleman, C., Pepin, M., Wilson, L., Berryhill, T. F., Wende, A. R., Steele, C., Young, M. E., Barnes, S., Drucker, D. J., Finan, B., DiMarchi, R., Perez-Tilve, D., Tschöp, M., & Habegger, K. M. (2018). Glucagon Receptor Signaling Regulates Energy Metabolism via Hepatic Farnesoid X Receptor and Fibroblast Growth Factor 21. *Diabetes*, *67*(9), 1773–1782. https://doi.org/10.2337/DB17-1502

Kistler, A. D., Caicedo, A., Abdulreda, M. H., Faul, C., Kerjaschki, D., Berggren, P. O., Reiser, J., & Fornoni, A. (2014). In vivo imaging of kidney glomeruli transplanted into the anterior chamber of the mouse eye. *Scientific Reports*, *4*. https://doi.org/10.1038/SREP03872

Kleinert, M., Sachs, S., Habegger, K. M., Hofmann, S. M., & Müller, T. D. (2019). Glucagon Regulation of Energy Expenditure. *International Journal of Molecular Sciences*, *20*(21). https://doi.org/10.3390/IJMS20215407

Kneeman, J. M., Misdraji, J., & Corey, K. E. (2012). Secondary causes of nonalcoholic fatty liver disease. *Therapeutic Advances in Gastroenterology*, *5*(3), 199. https://doi.org/10.1177/1756283X11430859

Koehl, G. E., Gaumann, A., & Geissler, E. K. (2009). Intravital microscopy of tumor angiogenesis and regression in the dorsal skin fold chamber: Mechanistic insights and preclinical testing of therapeutic strategies. *Clinical and Experimental Metastasis*, *26*(4), 329–344. https://doi.org/10.1007/S10585-008-9234-7/FIGURES/6

Koike, N., Fukumura, D., Gralla, O., Au, P., Schechner, J. S., & Jain, R. K. (2004). Creation of long-lasting blood vessels. *Nature 2004 428:6979*, *428*(6979), 138–139. https://doi.org/10.1038/428138a

Kolaric, T. O., Nincevic, V., Kuna, L., Duspara, K., Bojanic, K., Vukadin, S., Raguz-Lucic, N., Wu, G. Y., & Smolic, M. (2021). Drug-induced Fatty Liver Disease: Pathogenesis and Treatment. *Journal of Clinical and Translational Hepatology*, *9*(5), 731. https://doi.org/10.14218/JCTH.2020.00091

Korhonen, E. A., Murtomaki, A., Jha, S. K., Anisimov, A., Pink, A., Zhang, Y., Stritt, S., Liaqat, I., Stanczuk, L., Alderfer, L., Sun, Z., Kapiainen, E., Singh, A., Sultan, I., Lantta, A., Leppanen, V. M., Eklund, L., He, Y., Augustin, H. G., … Alitalo, K. (2022). Lymphangiogenesis requires Ang2/Tie/PI3K signaling for VEGFR3 cell-surface expression. *The Journal of Clinical Investigation*, *132*(15). https://doi.org/10.1172/JCI155478

Kozyra, M., Johansson, I., Nordling, Å., Ullah, S., Lauschke, V. M., & Ingelman-Sundberg, M. (2018). Human hepatic 3D spheroids as a model for steatosis and insulin resistance. *Scientific Reports 2018 8:1*, *8*(1), 1–12. https://doi.org/10.1038/s41598-018-32722-6

Kuchay, M. S., Martínez-Montoro, J. I., Choudhary, N. S., Fernández-García, J. C., & Ramos-Molina, B. (2021). Non-Alcoholic Fatty Liver Disease in Lean and Non-Obese Individuals: Current and Future Challenges. *Biomedicines*, *9*(10). https://doi.org/10.3390/BIOMEDICINES9101346

Kuczynski, E. A., & Reynolds, A. R. (2019). Vessel co-option and resistance to anti-angiogenic therapy. *Angiogenesis 2019 23:1*, *23*(1), 55–74. https://doi.org/10.1007/S10456-019-09698-6

Kuczynski, E. A., Vermeulen, P. B., Pezzella, F., Kerbel, R. S., & Reynolds, A. R. (2019a). Vessel co-option in cancer. *Nature Reviews Clinical Oncology 2019 16:8*, *16*(8), 469–493. https://doi.org/10.1038/s41571-019-0181-9

Kuczynski, E. A., Vermeulen, P. B., Pezzella, F., Kerbel, R. S., & Reynolds, A. R. (2019b). Vessel co-option in cancer. *Nature Reviews Clinical Oncology 2019 16:8*, *16*(8), 469–493. https://doi.org/10.1038/s41571-019-0181-9

Kuczynski, E. A., Yin, M., Bar-Zion, A., Lee, C. R., Butz, H., Man, S., Daley, F., Vermeulen, P. B., Yousef, G. M., Foster, F. S., Reynolds, A. R., & Kerbel, R. S. (2016). Co-option of Liver Vessels and Not Sprouting Angiogenesis Drives Acquired Sorafenib Resistance in Hepatocellular Carcinoma. *JNCI Journal of the National Cancer Institute*, *108*(8). https://doi.org/10.1093/JNCI/DJW030

Kulkeaw, K., Tubsuwan, A., Tongkrajang, N., & Whangviboonkij, N. (2020). Generation of human liver organoids from pluripotent stem cell-derived hepatic endoderms. *PeerJ*, *8*. https://doi.org/10.7717/PEERJ.9968/SUPP-12

Labelle, P. (2017). The Eye. *Pathologic Basis of Veterinary Disease Expert Consult*, 1265-1318.e1. https://doi.org/10.1016/B978-0-323-35775-3.00021-7

Lang, S., Martin, A., Farowski, F., Wisplinghoff, H., Vehreschild, M. J. G. T., Liu, J., Krawczyk, M., Nowag, A., Kretzschmar, A., Herweg, J., Schnabl, B., Tu, X. M., Lammert, F., Goeser, T., Tacke, F., Heinzer, K., Kasper, P., Steffen, H. M., & Demir, M. (2020). High Protein Intake Is Associated With Histological Disease Activity in Patients With NAFLD. *Hepatology Communications*, *4*(5), 681–695. https://doi.org/10.1002/HEP4.1509

Lange, N. F., Graf, V., Caussy, C., & Dufour, J. F. (2022). PPAR-Targeted Therapies in the Treatment of Non-Alcoholic Fatty Liver Disease in Diabetic Patients. *International Journal of Molecular Sciences*, *23*(8). https://doi.org/10.3390/IJMS23084305

Lebeaupin, C., Vallée, D., Hazari, Y., Hetz, C., Chevet, E., & Bailly-Maitre, B. (2018). Endoplasmic reticulum stress signalling and the pathogenesis of non-alcoholic fatty liver disease. *Journal of Hepatology*, *69*(4), 927–947. https://doi.org/10.1016/J.JHEP.2018.06.008/ATTACHMENT/5BB1F3E9-F0F7-4992-B24C-D683BC5EBCE8/DISCLOSURES.PDF

Lee, C., Kim, J., Han, J., Oh, D., Kim, M., Jeong, H., Kim, T. J., Kim, S. W., Kim, J. N., Seo, Y. S., Suzuki, A., Kim, J. H., & Jung, Y. (2022). Formyl peptide receptor 2 determines sex-specific differences in the progression of nonalcoholic fatty liver disease and steatohepatitis. *Nature Communications*, *13*(1). https://doi.org/10.1038/S41467-022-28138-6

Lee, D. H., Yoon, H. H., Lee, J. H., Lee, K. W., Lee, S. K., Kim, S. K., Choi, J. E., Kim, Y. J., & Park, J. K. (2004). Enhanced liver-specific functions of endothelial cell-covered hepatocyte hetero-spheroids. *Biochemical Engineering Journal*, *20*(2–3), 181–187. https://doi.org/10.1016/J.BEJ.2003.07.005

Lees, E. K., Banks, R., Cook, C., Hill, S., Morrice, N., Grant, L., Mody, N., & Delibegovic, M. (2017). Direct comparison of methionine restriction with leucine restriction on the metabolic health of C57BL/6J mice. *Scientific Reports*, *7*(1). https://doi.org/10.1038/S41598-017-10381-3

Leibiger, I. B., & Berggren, P. O. (2017). Intraocular in vivo imaging of pancreatic islet cell physiology/pathology. *Molecular Metabolism*, *6*(9), 1002–1009. https://doi.org/10.1016/J.MOLMET.2017.03.014

Leow, W. Q., Chan, A. W. H., Mendoza, P. G. L., Lo, R., Yap, K., & Kim, H. (2022). Non-alcoholic fatty liver disease: the pathologist's perspective. *Clinical and Molecular Hepatology*, *29*(Suppl), S302–S318. https://doi.org/10.3350/CMH.2022.0329

Leunig, M., Yuan, F., Menger, M., Boucher, Y., Goetz, A., Messmer, K., & Jain, R. (1992). Angiogenesis, microvascular architecture, microhemodynamics, and interstitial fluid pressure during early growth of human adenocarcinoma LS174T in SCID mice. *Cancer Research*.

Li, H., Gao, L., Du, J., Ma, T., Ye, Z., & Li, Z. (2021). To Better Generate Organoids, What Can We Learn From Teratomas? *Frontiers in Cell and Developmental Biology*, *9*. https://doi.org/10.3389/FCELL.2021.700482

Li, J., Xing, F., Chen, F., He, L., So, K. F., Liu, Y., & Xiao, J. (2019a). Functional 3D Human Liver Bud Assembled from MSC-Derived Multiple Liver Cell Lineages. *Cell Transplantation*, *28*(5), 510. https://doi.org/10.1177/0963689718780332

Li, J., Xing, F., Chen, F., He, L., So, K. F., Liu, Y., & Xiao, J. (2019b). Functional 3D Human Liver Bud Assembled from MSC-Derived Multiple Liver Cell Lineages. *Cell Transplantation*, *28*(5), 510. https://doi.org/10.1177/0963689718780332

Li, L., Martin-Levilain, J., Jiménez-Sánchez, C., Karaca, M., Foti, M., Martinou, J. C., & Maechler, P. (2019). In vivo stabilization of OPA1 in hepatocytes potentiates mitochondrial respiration and gluconeogenesis in a prohibitin-dependent way. *Journal of Biological Chemistry*, *294*(34), 12581–12598. https://doi.org/10.1074/JBC.RA119.007601/ATTACHMENT/657FFD88-1396-4C95-8AF0-63FCFB3D183D/MMC3.PDF

Li, W., Kirchner, T., Ho, G., Bonilla, F., D'Aquino, K., Littrell, J., Zhang, R., Jian, W., Qiu, X., Zheng, S., Gao, B., Wong, P., Leonard, J. N., & Camacho, R. C. (2020). Amino acids are sensitive glucagon receptor-specific biomarkers for glucagon-like peptide-1 receptor/glucagon receptor dual agonists. *Diabetes, Obesity & Metabolism*, *22*(12), 2437–2450. https://doi.org/10.1111/DOM.14173

Liang, K., & Dai, J. Y. (2022). Progress of potential drugs targeted in lipid metabolism research. *Frontiers in Pharmacology*, *13*. https://doi.org/10.3389/FPHAR.2022.1067652

Liangpunsakul, S., & Chalasani, N. (2019). Lipid mediators of liver injury in nonalcoholic fatty liver disease. *American Journal of Physiology - Gastrointestinal and Liver Physiology*, *316*(1), G75–G81. https://doi.org/10.1152/AJPGI.00170.2018/ASSET/IMAGES/LARGE/ZH30011975410001.JPEG

Lokmic, Z., & Mitchell, G. M. (2008). Engineering the Microcirculation. *Https://Home.Liebertpub.Com/Teb*, *14*(1), 87–103. https://doi.org/10.1089/TEB.2007.0299

Loomba, R., Abdelmalek, M. F., Armstrong, M. J., Jara, M., Kjær, M. S., Krarup, N., Lawitz, E., Ratziu, V., Sanyal, A. J., Schattenberg, J. M., & Newsome, P. N. (2023). Semaglutide 2·4 mg once weekly in patients with non-alcoholic steatohepatitis-related cirrhosis: a randomised, placebo-controlled phase 2 trial. *The Lancet Gastroenterology and Hepatology*, *8*(6), 511–522. https://doi.org/10.1016/S2468-1253(23)00068-7

Loomba, R., Sirlin, C. B., Ang, B., Bettencourt, R., Jain, R., Salotti, J., Soaft, L., Hooker, J., Kono, Y., Bhatt, A., Hernandez, L., Nguyen, P., Noureddin, M., Haufe, W., Hooker, C., Yin, M., Ehman, R., Lin, G. Y., Valasek, M. A., … Richards, L. (2015). Ezetimibe for the treatment of nonalcoholic steatohepatitis: Assessment by novel magnetic resonance imaging and magnetic resonance elastography in a randomized trial (MOZART trial). *Hepatology*, *61*(4), 1239–1250. https://doi.org/10.1002/HEP.27647/SUPPINFO

Lopez, M. J., & Mohiuddin, S. S. (2023). Biochemistry, Essential Amino Acids. *StatPearls*. https://www.ncbi.nlm.nih.gov/books/NBK557845/

Lotfy, M., Kalasz, H., Szalai, G., Singh, J., & Adeghate, E. (2014). Recent Progress in the Use of Glucagon and Glucagon Receptor Antago-nists in the Treatment of Diabetes Mellitus. *The Open Medicinal Chemistry Journal*, *8*(1), 28. https://doi.org/10.2174/1874104501408010028

Low-carb diets position statement (May 2021) | Diabetes UK. (n.d.). Retrieved May 7, 2023, from https://www.diabetes.org.uk/professionals/position-statements-reports/food-nutrition-lifestyle/low-carb-diets-for-people-with-diabetes

Lugano, R., Ramachandran, M., & Dimberg, A. (2020a). Tumor angiogenesis: causes, consequences, challenges and opportunities. *Cellular and Molecular Life Sciences*, *77*(9), 1745–1770. https://doi.org/10.1007/S00018-019-03351-7/FIGURES/3

Lugano, R., Ramachandran, M., & Dimberg, A. (2020b). Tumor angiogenesis: causes, consequences, challenges and opportunities. *Cellular and Molecular Life Sciences*, *77*(9), 1745. https://doi.org/10.1007/S00018-019-03351-7

Lund, A., Bagger, J. I., Albrechtsen, N. J. W., Christensen, M., Grøndahl, M., Hartmann, B., Mathiesen, E. R., Hansen, C. P., Storkholm, J. H., Van Hall, G., Rehfeld, J. F., Hornburg, D., Meissner, F., Mann, M., Larsen, S., Holst, J. J., Vilsbøll, T., & Knop, F. K. (2016). Evidence of Extrapancreatic Glucagon Secretion in Man. *Diabetes*, *65*(3), 585–597. https://doi.org/10.2337/DB15-1541

Luo, Q., Wang, J., Zhao, W., Peng, Z., Liu, X., Li, B., Zhang, H., Shan, B., Zhang, C., & Duan, C. (2020). Vasculogenic mimicry in carcinogenesis and clinical applications. *Journal of Hematology & Oncology 2020 13:1*, *13*(1), 1–15. https://doi.org/10.1186/S13045-020-00858-6

Luo, Y., & Lin, H. (2021). Inflammation initiates a vicious cycle between obesity and nonalcoholic fatty liver disease. *Immunity, Inflammation and Disease*, *9*(1), 59. https://doi.org/10.1002/IID3.391

Lupp, A., Danz, M., & Müller, D. (2003). Evaluation of 2-year-old intrasplenic fetal liver tissue transplants in rats. *Cell Transplantation*, *12*(4), 423–438. https://doi.org/10.3727/000000003108746858

Lupp, A., Lucas, N., Lindstrom-Seppa, P., Koponen, K., Hänninen, O., Danz, M., & Klinger, W. (1998). Transplantation of fetal liver tissue suspension into the spleens ofadult syngenic rats: Effects of β-naphthoflavone, Phenobarbital and dexamethasone on cytochrome P450 isoforms expression and on glycogen storage. *Experimental and Toxicologic Pathology*, *50*(3), 173–183. https://doi.org/10.1016/S0940-2993(98)80079-1

Lynch, J. P., Metz, D. C., & Lemaigre, F. P. (2009). Mechanisms of Liver Development: Concepts for Understanding Liver Disorders and Design of Novel Therapies. *Gastroenterology*, *137*(1), 62–79. https://doi.org/10.1053/J.GASTRO.2009.03.035

Ma, X. M., & Blenis, J. (2009). Molecular mechanisms of mTOR-mediated translational control. *Nature Reviews Molecular Cell Biology 2009 10:5*, *10*(5), 307–318. https://doi.org/10.1038/nrm2672

Magnusson, I., Rothman, D. L., Gerard, D. P., Katz, L. D., & Shulman, G. I. (1995). Contribution of Hepatic Glycogenolysis to Glucose Production in Humans in Response to a Physiological Increase in Plasma Glucagon Concentration. *Diabetes*, *44*(2), 185–189. https://doi.org/10.2337/DIAB.44.2.185

Malhotra, P., Gill, R. K., Saksena, S., & Alrefai, W. A. (2020). Disturbances in Cholesterol Homeostasis and Non-alcoholic Fatty Liver Diseases. *Frontiers in Medicine*, *7*, 569021. https://doi.org/10.3389/FMED.2020.00467/BIBTEX

Malloy, V. L., Krajcik, R. A., Bailey, S. J., Hristopoulos, G., Plummer, J. D., & Orentreich, N. (2006). Methionine restriction decreases visceral fat mass and preserves insulin action in aging male Fischer 344 rats independent of energy restriction. *Aging Cell*, *5*(4), 305–314. https://doi.org/10.1111/J.1474-9726.2006.00220.X

Maniotis, A. J., Folberg, R., Hess, A., Seftor, E. A., Gardner, L. M. G., Pe'er, J., Trent, J. M., Meltzer, P. S., & Hendrix, M. J. C. (1999). Vascular channel formation by human melanoma cells in vivo and in vitro: vasculogenic mimicry. *The American Journal of Pathology*, *155*(3), 739–752. https://doi.org/10.1016/S0002-9440(10)65173-5

Mantovani, A., & Dalbeni, A. (2021). Treatments for NAFLD: State of Art. *International Journal of Molecular Sciences*, *22*(5), 1–27. https://doi.org/10.3390/IJMS22052350

Marçola, M., & Rodrigues, C. E. (2015). Endothelial progenitor cells in tumor angiogenesis: Another brick in the wall. *Stem Cells International*, *2015*. https://doi.org/10.1155/2015/832649

Marelli-Berg, F. M., Peek, E., Lidington, E. A., Stauss, H. J., & Lechler, R. I. (2000). Isolation of endothelial cells from murine tissue. *Journal of Immunological Methods*, *244*(1–2), 205–215. https://doi.org/10.1016/S0022-1759(00)00258-1

Margolis, L. M., Rivas, D. A., Ezzyat, Y., Gaffney-Stomberg, E., Young, A. J., McClung, J. P., Fielding, R. A., & Pasiakos, S. M. (2016). Calorie Restricted High Protein Diets Downregulate Lipogenesis and Lower Intrahepatic Triglyceride Concentrations in Male Rats. *Nutrients*, *8*(9). https://doi.org/10.3390/NU8090571

Marra, F., & Svegliati-Baroni, G. (2018). Lipotoxicity and the gut-liver axis in NASH pathogenesis. *Journal of Hepatology*, *68*(2), 280–295. https://doi.org/10.1016/J.JHEP.2017.11.014

Mashek, D. G., Cui, W., Shang, L., & Najt, C. P. (2020). Hepatic Lipid Droplets in Liver Function and Disease. *The Liver: Biology and Pathobiology*, 245–254. https://doi.org/10.1002/9781119436812.CH21

Mazzieri, R., Pucci, F., Moi, D., Zonari, E., Ranghetti, A., Berti, A., Politi, L. S., Gentner, B., Brown, J. L., Naldini, L., & de Palma, M. (2011). Targeting the ANG2/TIE2 Axis Inhibits Tumor Growth and Metastasis by Impairing Angiogenesis and Disabling Rebounds of Proangiogenic Myeloid Cells. *Cancer Cell*, *19*(4), 512–526. https://doi.org/10.1016/j.ccr.2011.02.005

McGarry, J. D., Mannaerts, G. P., & Foster, D. W. (1977). A possible role for malonyl-CoA in the regulation of hepatic fatty acid oxidation and ketogenesis. *The Journal of Clinical Investigation*, *60*(1), 265–270. https://doi.org/10.1172/JCI108764

McMahan, R. H., Porsche, C. E., Edwards, M. G., & Rosen, H. R. (2016). Free Fatty Acids Differentially Downregulate Chemokines in Liver Sinusoidal Endothelial Cells: Insights into Non-Alcoholic Fatty Liver Disease. *PLoS ONE*, *11*(7). https://doi.org/10.1371/JOURNAL.PONE.0159217

Melchiorri, A. J., Nguyen, B. N. B., & Fisher, J. P. (2014). Mesenchymal Stem Cells: Roles and Relationships in Vascularization. *Tissue Engineering. Part B, Reviews*, *20*(3), 218. https://doi.org/10.1089/TEN.TEB.2013.0541

Miao, K. Z., Kim, G. Y., Meara, G. K., Qin, X., & Feng, H. (2021). Tipping the Scales With Zebrafish to Understand Adaptive Tumor Immunity. *Frontiers in Cell and Developmental Biology*, *9*. https://doi.org/10.3389/FCELL.2021.660969

Miller, R. A., & Birnbaum, M. J. (2016). Glucagon: acute actions on hepatic metabolism. *Diabetologia*, *59*(7), 1376–1381. https://doi.org/10.1007/S00125-016-3955-Y/FIGURES/1

Mito, M., Ebata, H., Kusano, M., Onishi, T., Saito, T., & Sakamoto, S. (1979). Morphology and function of isolated hepatocytes transplanted into rat spleen. *Transplantation*, *28*(6), 499–505. https://doi.org/10.1097/00007890-197912000-00013

Montemagno, C., & Pagès, G. (2020). Resistance to Anti-angiogenic Therapies: A Mechanism Depending on the Time of Exposure to the Drugs. *Frontiers in Cell and Developmental Biology*, *8*, 584. https://doi.org/10.3389/FCELL.2020.00584/BIBTEX

Montezano, A. C., Neves, K. B., Lopes, R. A. M., & Rios, F. (2017). Isolation and culture of endothelial cells from large vessels. *Methods in Molecular Biology*, *1527*, 345–348. https://doi.org/10.1007/978-1-4939-6625-7_26/COVER

Moon, J., Kong, E., Lee, J., Jung, J., Kim, E., Park, S. B., & Kim, P. (2020). Intravital longitudinal imaging of hepatic lipid droplet accumulation in a murine model for nonalcoholic fatty liver disease. *Biomedical Optics Express*, *11*(9), 5132. https://doi.org/10.1364/BOE.395890

Moore, M. C., Coate, K. C., Winnick, J. J., An, Z., & Cherrington, A. D. (2012). Regulation of Hepatic Glucose Uptake and Storage In Vivo. *Advances in Nutrition*, *3*(3), 286. https://doi.org/10.3945/AN.112.002089

Morell, P., & Fiszman, S. (2017). Revisiting the role of protein-induced satiation and satiety. *Food Hydrocolloids*, *68*, 199–210. https://doi.org/10.1016/J.FOODHYD.2016.08.003

Morita, Y., Ohno, H., Kobuke, K., Oki, K., & Yoneda, M. (2021). Variation in plasma glucagon levels according to obesity status in Japanese Americans with normal glucose tolerance. *Endocrine Journal*, *68*(1), 95–102. https://doi.org/10.1507/ENDOCRJ.EJ20-0366

Morris, C. H., & Baker, J. (2023). Glucagon. *Handbook of Hormones: Comparative Endocrinology for Basic and Clinical Research*, 129,e17A-2-131,e17A-4. https://doi.org/10.1016/B978-0-12-801028-0.00138-0

Motoike, T., Loughna, S., Perens, E., Roman, B. L., Liao, W., Chau, T. C., Richardson, C. D., Kawate, T., Kuno, J., Weinstein, B. M., Stainier, D. Y. R., & Sato, T. N. (2000). *Universal GFP Reporter for the Study of Vascular Development*. https://doi.org/10.1002/1526-968X(200010)28:2

Mu, W., Xuefang, C., Liu, Y., Qianzhou, L., Gaolin, L., Jigang, Z., & Xiaoyu, L. (2019). Potential nexus of non-alcoholic fatty liver disease and type 2 diabetes mellitus: Insulin resistance between hepatic and peripheral tissues. *Frontiers in Pharmacology*, *9*(JAN), 430129. https://doi.org/10.3389/FPHAR.2018.01566/BIBTEX

Muller, S., Ader, I., Creff, J., Leménager, H., Achard, P., Casteilla, L., Sensebé, L., Carrière, A., & Deschaseaux, F. (2019). Human adipose stromal-vascular fraction self-organizes to form

vascularized adipose tissue in 3D cultures. *Scientific Reports 2019 9:1*, *9*(1), 1–10. https://doi.org/10.1038/s41598-019-43624-6

Müller, T. D., Finan, B., Clemmensen, C., Di Marchi, R. D., & Tschöp, M. H. (2017). The new biology and pharmacology of glucagon. *Physiological Reviews*, *97*(2), 721–766. https://doi.org/10.1152/PHYSREV.00025.2016/ASSET/IMAGES/LARGE/Z9J0021728000010.JPEG

Muñoz-Sánchez, J., & Chánez-Cárdenas, M. E. (2019). The use of cobalt chloride as a chemical hypoxia model. *Journal of Applied Toxicology : JAT*, *39*(4), 556–570. https://doi.org/10.1002/JAT.3749

Murphy, K. A., James, B. R., Wilber, A., & Griffith, T. S. (2017). A Syngeneic Mouse Model of Metastatic Renal Cell Carcinoma for Quantitative and Longitudinal Assessment of Preclinical Therapies. *Journal of Visualized Experiments : JoVE*, *2017*(122), 55080. https://doi.org/10.3791/55080

Nakahara, T., Hyogo, H., Kimura, Y., Ishitobi, T., Arihiro, K., Aikata, H., Takahashi, S., & Chayama, K. (2012). Efficacy of rosuvastatin for the treatment of non-alcoholic steatohepatitis with dyslipidemia: An open-label, pilot study. *Hepatology Research*, *42*(11), 1065–1072. https://doi.org/10.1111/J.1872-034X.2012.01034.X

Nakao, S., Hafezi-Moghadam, A., & Ishibashi, T. (2012). Lymphatics and Lymphangiogenesis in the Eye. *Journal of Ophthalmology*, *2012*, 11. https://doi.org/10.1155/2012/783163

Nalbach, L., Roma, L. P., Schmitt, B. M., Becker, V., Körbel, C., Wrublewsky, S., Pack, M., Später, T., Metzger, W., Menger, M. M., Frueh, F. S., Götz, C., Lin, H., Manning Fox, J. E., MacDonald, P. E., Menger, M. D., Laschke, M. W., & Ampofo, E. (2021). Improvement of islet transplantation by the fusion of islet cells with functional blood vessels. *EMBO Molecular Medicine*, *13*(1). https://doi.org/10.15252/EMMM.202012616

Nevola, R., Epifani, R., Imbriani, S., Tortorella, G., Aprea, C., Galiero, R., Rinaldi, L., Marfella, R., & Sasso, F. C. (2023). GLP-1 Receptor Agonists in Non-Alcoholic Fatty Liver Disease: Current Evidence and Future Perspectives. *International Journal of Molecular Sciences*, *24*(2), 24. https://doi.org/10.3390/IJMS24021703

Newsome, P. N., Buchholtz, K., Cusi, K., Linder, M., Okanoue, T., Ratziu, V., Sanyal, A. J., Sejling, A.-S., & Harrison, S. A. (2021). A Placebo-Controlled Trial of Subcutaneous Semaglutide in Nonalcoholic Steatohepatitis. *The New England Journal of Medicine*, *384*(12), 1113–1124. https://doi.org/10.1056/NEJMOA2028395

Nolan, D. J., Ciarrocchi, A., Mellick, A. S., Jaggi, J. S., Bambino, K., Gupta, S., Heikamp, E., McDevitt, M. R., Scheinberg, D. A., Benezra, R., & Mittal, V. (2007). Bone marrow-derived endothelial progenitor cells are a major determinant of nascent tumor neovascularization. *Genes & Development*, *21*(12), 1546. https://doi.org/10.1101/GAD.436307

Null, M., & Agarwal, M. (2022). Anatomy, Lymphatic System. *StatPearls*. https://www.ncbi.nlm.nih.gov/books/NBK513247/

Nunes, S. S., Maijub, J. G., Krishnan, L., Ramakrishnan, V. M., Clayton, L. R., Williams, S. K., Hoying, J. B., & Boyd, N. L. (2013). Generation of a functional liver tissue mimic using adipose stromal vascular fraction cell-derived vasculatures. *Scientific Reports*, *3*. https://doi.org/10.1038/SREP02141

Obesity. (n.d.). Retrieved July 14, 2023, from https://www.who.int/health-topics/obesity#tab=tab_1

Obi, S., Masuda, H., Shizuno, T., Sato, A., Yamamoto, K., Ando, J., Abe, Y., & Asahara, T. (2012). Fluid shear stress induces differentiation of circulating phenotype endothelial progenitor cells. *American Journal of Physiology - Cell Physiology*, *303*(6), 595–606. https://doi.org/10.1152/AJPCELL.00133.2012/ASSET/IMAGES/LARGE/ZH00181270410008.JPEG

Ok, D. P., Ko, K., & Bae, J. Y. (2018). Exercise without dietary changes alleviates nonalcoholic fatty liver disease without weight loss benefits. *Lipids in Health and Disease*, *17*(1). https://doi.org/10.1186/s12944-018-0852-z

Okun, J. G., Rusu, P. M., Chan, A. Y., Wu, Y., Yap, Y. W., Sharkie, T., Schumacher, J., Schmidt, K. V., Roberts-Thomson, K. M., Russell, R. D., Zota, A., Hille, S., Jungmann, A., Maggi, L., Lee, Y., Blüher, M., Herzig, S., Keske, M. A., Heikenwalder, M., … Rose, A. J. (2021). Liver alanine catabolism promotes skeletal muscle atrophy and hyperglycaemia in type 2 diabetes. *Nature Metabolism 2021 3:3*, *3*(3), 394–409. https://doi.org/10.1038/s42255-021-00369-9

Osaki, T., Sivathanu, V., & Kamm, R. D. (2018). Engineered 3D vascular and neuronal networks in a microfluidic platform. *Scientific Reports*, *8*(1), 5168. https://doi.org/10.1038/S41598-018-23512-1

Osipova, D., Kokoreva, K., Lazebnik, L., Golovanova, E., Pavlov, C., Dukhanin, A., Orlova, S., & Starostin, K. (2022). Regression of Liver Steatosis Following Phosphatidylcholine Administration: A Review of Molecular and Metabolic Pathways Involved. *Frontiers in Pharmacology*, *13*, 797923. https://doi.org/10.3389/FPHAR.2022.797923/BIBTEX

Ouchi, R., Togo, S., Kimura, M., Shinozawa, T., Koido, M., Koike, H., Thompson, W., Karns, R. A., Mayhew, C. N., McGrath, P. S., McCauley, H. A., Zhang, R. R., Lewis, K., Hakozaki, S., Ferguson, A., Saiki, N., Yoneyama, Y., Takeuchi, I., Mabuchi, Y., … Takebe, T. (2019). Modeling Steatohepatitis in Humans with Pluripotent Stem Cell-Derived Organoids. *Cell Metabolism*, *30*(2), 374-384.e6. https://doi.org/10.1016/J.CMET.2019.05.007

OZARDILI, I., GULDUR, M.-E., CIFTCI, H., BITIREN, M., & ALTUNKOL, A. (2012). Correlation between lymphangiogenesis and clinicopathological parameters in renal cell carcinoma. *Singapore Medical Journal*, 332–335. http://dx.doi.org/

Ozdowski, L., & Gupta, V. (2022). Physiology, Lymphatic System. *StatPearls*. https://www.ncbi.nlm.nih.gov/books/NBK557833/

Pacy, P. J., Cheng, K. N., Ford, G. C., & Halliday, D. (2005). Influence of glucagon on protein and leucine metabolism: A study in fasting man with induced insuiin resistance. *British Journal of Surgery*, *77*(7), 791–794. https://doi.org/10.1002/BJS.1800770723

Paddon-Jones, D., Westman, E., Mattes, R. D., Wolfe, R. R., Astrup, A., & Westerterp-Plantenga, M. (2008). Protein, weight management, and satiety. *The American Journal of Clinical Nutrition*, *87*(5), 1558S-1561S. https://doi.org/10.1093/AJCN/87.5.1558S

Pancreatic Islet Transplantation Into the Anterior Chamber of the Eye - Full Text View - ClinicalTrials.gov. (n.d.). Retrieved February 14, 2023, from https://clinicaltrials.gov/ct2/show/NCT02846571

Park, J. S., Kim, I. K., Han, S., Park, I., Kim, C., Bae, J., Oh, S. J., Lee, S., Kim, J. H., Woo, D. C., He, Y., Augustin, H. G., Kim, I., Lee, D., & Koh, G. Y. (2016). Normalization of Tumor Vessels by Tie2 Activation and Ang2 Inhibition Enhances Drug Delivery and Produces a Favorable Tumor Microenvironment. *Cancer Cell*, *30*(6), 953–967. https://doi.org/10.1016/J.CCELL.2016.10.018

Patel, V., Joharapurkar, A., Kshirsagar, S., Sutariya, B., Patel, M., Patel, H., Pandey, D., Patel, D., Ranvir, R., Kadam, S., Bahekar, R., & Jain, M. (2018). Coagonist of GLP-1 and Glucagon Receptor Ameliorates Development of Non-Alcoholic Fatty Liver Disease. *Cardiovascular & Hematological Agents in Medicinal Chemistry*, *16*(1), 35–43. https://doi.org/10.2174/1871525716666180118152158

Paulusma, C. C., Lamers, W. H., Broer, S., & van de Graaf, S. F. J. (2022). Amino acid metabolism, transport and signalling in the liver revisited. *Biochemical Pharmacology*, *201*, 115074. https://doi.org/10.1016/J.BCP.2022.115074

Pavlidou, E., Papadopoulou, S. K., Fasoulas, A., Mantzorou, M., & Giaginis, C. (2023). Clinical Evidence of Low-Carbohydrate Diets against Obesity and Diabetes Mellitus. *Metabolites*, *13*(2). https://doi.org/10.3390/METABO13020240

Pedersen, J. S., Rygg, M. O., Kristiansen, V. B., Olsen, B. H., Serizawa, R. R., Holst, J. J., Madsbad, S., Gluud, L. L., Bendtsen, F., & Wewer Albrechtsen, N. J. (2020). Nonalcoholic Fatty Liver Disease Impairs the Liver-Alpha Cell Axis Independent of Hepatic Inflammation and Fibrosis. *Hepatology Communications*, *4*(11), 1610–1623. https://doi.org/10.1002/HEP4.1562

Pei, K., Gui, T., Kan, D., Feng, H., Jin, Y., Yang, Y., Zhang, Q., Du, Z., Gai, Z., Wu, J., & Li, Y. (2020). An Overview of Lipid Metabolism and Nonalcoholic Fatty Liver Disease. *BioMed Research International*, *2020*. https://doi.org/10.1155/2020/4020249

Peng, W. C., Kraaier, L. J., & Kluiver, T. A. (2021). Hepatocyte organoids and cell transplantation: What the future holds. *Experimental & Molecular Medicine 2021 53:10*, *53*(10), 1512–1528. https://doi.org/10.1038/s12276-021-00579-x

Peng, W. C., Logan, C. Y., Fish, M., Anbarchian, T., Aguisanda, F., Álvarez-Varela, A., Wu, P., Jin, Y., Zhu, J., Li, B., Grompe, M., Wang, B., & Nusse, R. (2018). Tissue Repair Signals and In Vitro Culture: Inflammatory Cytokine TNFα Promotes the Expansion of Primary Hepatocytes in 3D Culture. *Cell*, *175*(6), 1607. https://doi.org/10.1016/J.CELL.2018.11.012

Perry, R. J., Zhang, D., Guerra, M. T., Brill, A. L., Goedeke, L., Nasiri, A. R., Rabin-Court, A., Wang, Y., Peng, L., Dufour, S., Zhang, Y., Zhang, X. M., Butrico, G. M., Toussaint, K., Nozaki, Y., Cline, G. W., Petersen, K. F., Nathanson, M. H., Ehrlich, B. E., & Shulman, G. I. (2020). Glucagon stimulates gluconeogenesis by InsP3R-I mediated hepatic lipolysis. *Nature*, *579*(7798), 279. https://doi.org/10.1038/S41586-020-2074-6

Petrova, V., Annicchiarico-Petruzzelli, M., Melino, G., & Amelio, I. (2018). The hypoxic tumour microenvironment. *Oncogenesis 2018 7:1*, *7*(1), 1–13. https://doi.org/10.1038/s41389-017-0011-9

Pettinato, G., Lehoux, S., Ramanathan, R., Salem, M. M., He, L. X., Muse, O., Flaumenhaft, R., Thompson, M. T., Rouse, E. A., Cummings, R. D., Wen, X., & Fisher, R. A. (2019). Generation of fully functional hepatocyte-like organoids from human induced pluripotent stem cells mixed with Endothelial Cells. *Scientific Reports 2019 9:1*, *9*(1), 1–21. https://doi.org/10.1038/s41598-019-45514-3

Pezeshki, A., & Chelikani, P. K. (2021). Low Protein Diets and Energy Balance: Mechanisms of Action on Energy Intake and Expenditure. *Frontiers in Nutrition*, *8*, 228. https://doi.org/10.3389/FNUT.2021.655833/BIBTEX

Pham, M. T., Pollock, K. M., Rose, M. D., Cary, W. A., Stewart, H. R., Zhou, P., Nolta, J. A., & Waldau, B. (2018). Generation of human vascularized brain organoids. *Neuroreport*, *29*(7), 588. https://doi.org/10.1097/WNR.0000000000001014

Pichon, L., Huneau, J. F., Fromentin, G., & Tomé, D. (2006). A High-Protein, High-Fat, Carbohydrate-Free Diet Reduces Energy Intake, Hepatic Lipogenesis, and Adiposity in Rats. *The Journal of Nutrition*, *136*(5), 1256–1260. https://doi.org/10.1093/JN/136.5.1256

Pickett-Blakely, O., Young, K., & Carr, R. M. (2018). Micronutrients in Nonalcoholic Fatty Liver Disease Pathogenesis. *Cellular and Molecular Gastroenterology and Hepatology*, *6*(4), 451. https://doi.org/10.1016/J.JCMGH.2018.07.004

Pingitore, P., Sasidharan, K., Ekstrand, M., Prill, S., Lindén, D., & Romeo, S. (2019). Human Multilineage 3D Spheroids as a Model of Liver Steatosis and Fibrosis. *International Journal of Molecular Sciences*, *20*(7). https://doi.org/10.3390/IJMS20071629

Polyzos, S. A., Kountouras, J., & Mantzoros, C. S. (2018). *Obesity and nonalcoholic fatty liver disease: From pathophysiology to therapeutics*. https://doi.org/10.1016/j.metabol.2018.11.014

Prior, N., Inacio, P., & Huch, M. (2019). Liver organoids: from basic research to therapeutic applications. *Gut*, *68*(12), 2228–2237. https://doi.org/10.1136/GUTJNL-2019-319256

Qian, C. N. (2013). Hijacking the vasculature in ccRCC--co-option, remodelling and angiogenesis. *Nature Reviews. Urology*, *10*(5), 300–304. https://doi.org/10.1038/NRUROL.2013.26

Rada, P., González-Rodríguez, Á., García-Monzón, C., & Valverde, Á. M. (2020). Understanding lipotoxicity in NAFLD pathogenesis: is CD36 a key driver? *Cell Death & Disease 2020 11:9*, *11*(9), 1–15. https://doi.org/10.1038/s41419-020-03003-w

Rahman, H. S., Tan, B. L., Othman, H. H., Chartrand, M. S., Pathak, Y., Mohan, S., Abdullah, R., & Alitheen, N. B. (2020). An Overview of in Vitro, in Vivo, and Computational Techniques for Cancer-Associated Angiogenesis Studies. *BioMed Research International*, *2020*. https://doi.org/10.1155/2020/8857428

Ramachandran, S. D., Schirmer, K., Münst, B., Heinz, S., Ghafoory, S., Wölfl, S., Simon-Keller, K., Marx, A., Oie, C. I., Ebert, M. P., Walles, H., Braspenning, J., & Breitkopf-Heinlein, K. (2015). In Vitro Generation of Functional Liver Organoid-Like Structures Using Adult Human Cells. *PLoS ONE*, *10*(10). https://doi.org/10.1371/JOURNAL.PONE.0139345

Ramanathan, R. ;, Ali, A. H. ;, Silva, G., Murri, M., Ramanathan, R., Ali, A. H., Ibdah, J. A., & Memorial, H. S. T. (2022). Mitochondrial Dysfunction Plays Central Role in Nonalcoholic Fatty Liver Disease. *International Journal of Molecular Sciences 2022, Vol. 23, Page 7280*, *23*(13), 7280. https://doi.org/10.3390/IJMS23137280

Ramnanan, C. J., Edgerton, D. S., Kraft, G., & Cherrington, A. D. (2011). Physiologic action of glucagon on liver glucose metabolism. *Diabetes, Obesity & Metabolism*, *13*(Suppl 1), 118. https://doi.org/10.1111/J.1463-1326.2011.01454.X

Ramos, M. J., Bandiera, L., Menolascina, F., & Fallowfield, J. A. (2022a). In vitro models for non-alcoholic fatty liver disease: Emerging platforms and their applications. *IScience*, *25*(1). https://doi.org/10.1016/J.ISCI.2021.103549

Ramos, M. J., Bandiera, L., Menolascina, F., & Fallowfield, J. A. (2022b). In vitro models for non-alcoholic fatty liver disease: Emerging platforms and their applications. *IScience*, *25*(1), 103549. https://doi.org/10.1016/J.ISCI.2021.103549

Ran, S., Volk, L., Hall, K., & Flister, M. J. (2010a). Lymphangiogenesis and Lymphatic Metastasis in Breast Cancer. *Pathophysiology : The Official Journal of the International Society for Pathophysiology / ISP*, *17*(4), 229. https://doi.org/10.1016/J.PATHOPHYS.2009.11.003

Ran, S., Volk, L., Hall, K., & Flister, M. J. (2010b). Lymphangiogenesis and Lymphatic Metastasis in Breast Cancer. *Pathophysiology : The Official Journal of the International Society for Pathophysiology / ISP*, *17*(4), 229. https://doi.org/10.1016/J.PATHOPHYS.2009.11.003

Rao, M. S., Thorgeirsson, S., Reddy, M. K., Lalwani, N. D., Evarts, R. E., Usman, M. I., & Singh, B. (1986). Induction of peroxisome proliferation in hepatocytes transplanted into the anterior chamber of the eye. A model system for the evaluation of xenobiotic-induced effects. *The American Journal of Pathology*, *124*(3), 519. /pmc/articles/PMC1888338/?report=abstract

Rashidi, H., Luu, N. T., Alwahsh, S. M., Ginai, M., Alhaque, S., Dong, H., Tomaz, R. A., Vernay, B., Vigneswara, V., Hallett, J. M., Chandrashekran, A., Dhawan, A., Vallier, L., Bradley, M., Callanan, A., Forbes, S. J., Newsome, P. N., & Hay, D. C. (2018). 3D human liver tissue from pluripotent stem cells displays stable phenotype in vitro and supports compromised liver function in vivo. *Archives of Toxicology*, *92*(10), 3117–3129. https://doi.org/10.1007/S00204-018-2280-2/FIGURES/6

Ratziu, V., de Guevara, L., Safadi, R., Poordad, F., Fuster, F., Flores-Figueroa, J., Arrese, M., Fracanzani, A. L., Ben Bashat, D., Lackner, K., Gorfine, T., Kadosh, S., Oren, R., Halperin, M., Hayardeny, L., Loomba, R., Friedman, S., Abdelmalek, M., Angelico, F., … Sanyal, A. J. (2021). Aramchol in patients with nonalcoholic steatohepatitis: a randomized, double-blind, placebo-controlled phase 2b trial. *Nature Medicine 2021 27:10*, *27*(10), 1825–1835. https://doi.org/10.1038/s41591-021-01495-3

Reilly, N. R., Lebwohl, B., Hultcrantz, R., Green, P. H. R., & Ludvigsson, J. F. (2015). Increased Risk of Nonalcoholic Fatty Liver Disease After Diagnosis of Celiac Disease. *Journal of Hepatology*, *62*(6), 1405. https://doi.org/10.1016/J.JHEP.2015.01.013

Resistance to Angiogenesis Inhibitors in Renal Cell Carcinoma – Hematology & Oncology. (n.d.). Retrieved February 14, 2023, from https://www.hematologyandoncology.net/archives/february-2011/resistance-to-angiogenesis-inhibitors-in-renal-cell-carcinoma/

Revskoy, S., Blair, M. E., Powell, S. M., Hausman, E. S., & Blackburn, J. S. (2019). In vivo imaging defines vascular interplay in the development of lymphocytic leukemia in zebrafish models. *BioRxiv*, 806562. https://doi.org/10.1101/806562

Ribatti, D., & Crivellato, E. (2009). Immune cells and angiogenesis. *Journal of Cellular and Molecular Medicine*, *13*(9a), 2822. https://doi.org/10.1111/J.1582-4934.2009.00810.X

Rix, I., Nexøe-Larsen, C., Bergmann, N. C., Lund, A., & Knop, F. K. (2019). Glucagon Physiology. *Canadian Journal of Diabetes*, *34*(3), 187–188. https://doi.org/10.1016/S1499-2671(10)43015-4

Robert, B., St. John, P. L., & Abrahamson, D. R. (1998). Direct visualization of renal vascular morphogenesis in Flk1 heterozygous mutant mice. *American Journal of Physiology - Renal Physiology*, *275*(1 44-1). https://doi.org/10.1152/AJPRENAL.1998.275.1.F164/ASSET/IMAGES/LARGE/AFLU20710008X.JPEG

ROBERTSON, D., HANSEN, L., AMBERY, P., ESTERLINE, R. L., JERMUTUS, L., CHANG, Y.-T., PETRONE, M., JOHANSSON, E., JOHANSSON, L., SJÖBERG, F. B., & PARKER, V. (2020). 354-OR: Cotadutide (medi0382), a Dual Receptor Agonist with Glucagon-Like Peptide-1 and Glucagon Activity, Modulates Hepatic Glycogen and Fat Content. *Diabetes*, *69*(Supplement_1). https://doi.org/10.2337/DB20-354-OR

Romero-Gómez, M., Zelber-Sagi, S., & Trenell, M. (2017). Treatment of NAFLD with diet, physical activity and exercise. *Journal of Hepatology*, *67*(4), 829–846. https://doi.org/10.1016/J.JHEP.2017.05.016

Rossi, J. M., Dunn, N. R., Hogan, B. L. M., & Zaret, K. S. (2001). Distinct mesodermal signals, including BMPs from the septum transversum mesenchyme, are required in combination for hepatogenesis from the endoderm. *Genes & Development*, *15*(15), 1998. https://doi.org/10.1101/GAD.904601

Rossi, M., & Blasi, P. (2022). Multicellular Tumor Spheroids in Nanomedicine Research: A Perspective. *Frontiers in Medical Technology*, *4*, 36. https://doi.org/10.3389/FMEDT.2022.909943

Ruan, B., Duan, J. L., Xu, H., Tao, K. S., Han, H., Dou, G. R., & Wang, L. (2021). Capillarized Liver Sinusoidal Endothelial Cells Undergo Partial Endothelial-Mesenchymal Transition to Actively Deposit Sinusoidal ECM in Liver Fibrosis. *Frontiers in Cell and Developmental Biology*, *9*. https://doi.org/10.3389/FCELL.2021.671081/FULL

Ryu, J. E., Jo, W., Choi, H. J., Jang, S., Lee, H. J., Woo, D. C., Kim, J. K., Kim, K. W., Yu, E. S., & Son, W. C. (2015). Evaluation of Nonalcoholic Fatty Liver Disease in C57BL/6J Mice by Using MRI and Histopathologic Analyses. *Comparative Medicine*, *65*(5), 409. /pmc/articles/PMC4617331/

Saad, R. S., Kordunsky, L., Liu, Y. L., Denning, K. L., Kandil, H. A., & Silverman, J. F. (2006). Lymphatic microvessel density as prognostic marker in colorectal cancer. *Modern Pathology*, *19*(10), 1317–1323. https://doi.org/10.1038/MODPATHOL.3800651

Salem, V., Silva, L. D., Suba, K., Georgiadou, E., Neda Mousavy Gharavy, S., Akhtar, N., Martin-Alonso, A., Gaboriau, D. C. A., Rothery, S. M., Stylianides, T., Carrat, G., Pullen, T. J., Singh, S. P., Hodson, D. J., Leclerc, I., Shapiro, A. M. J., Marchetti, P., Briant, L. J. B., Distaso, W., … Rutter, G. A. (2019a). Leader β-cells coordinate Ca2+ dynamics across pancreatic islets in vivo. *Nature Metabolism*, *1*(6), 615–629. https://doi.org/10.1038/S42255-019-0075-2

Salem, V., Silva, L. D., Suba, K., Georgiadou, E., Neda Mousavy Gharavy, S., Akhtar, N., Martin-Alonso, A., Gaboriau, D. C. A., Rothery, S. M., Stylianides, T., Carrat, G., Pullen, T. J., Singh, S. P., Hodson, D. J., Leclerc, I., Shapiro, A. M. J., Marchetti, P., Briant, L. J. B., Distaso, W., … Rutter, G. A. (2019b). Leader β-cells coordinate Ca2+ dynamics across pancreatic islets in vivo. *Nature Metabolism 2019 1:6*, *1*(6), 615–629. https://doi.org/10.1038/s42255-019-0075-2

Salumbides, B. C., Lehet, K. M., Ndikuyeze, G., & Pili, R. (2009). Pre-clinical models of renal carcinoma and their utility in drug development. *Current Protocols in Pharmacology*, *Chapter 14*(SUPPL.47). https://doi.org/10.1002/0471141755.PH1413S47

Sanders, F. W. B., Acharjee, A., Walker, C., Marney, L., Roberts, L. D., Imamura, F., Jenkins, B., Case, J., Ray, S., Virtue, S., Vidal-Puig, A., Kuh, D., Hardy, R., Allison, M., Forouhi, N., Murray, A. J., Wareham, N., Vacca, M., Koulman, A., & Griffin, J. L. (2018). Hepatic steatosis risk is partly driven by increased de novo lipogenesis following carbohydrate consumption. *Genome Biology*, *19*(1), 1–15. https://doi.org/10.1186/S13059-018-1439-8/TABLES/3

Sanders, F. W. B., & Griffin, J. L. (2016). De novo lipogenesis in the liver in health and disease: more than just a shunting yard for glucose. *Biological Reviews of the Cambridge Philosophical Society*, *91*(2), 452. https://doi.org/10.1111/BRV.12178

Sanders, L. M. (2016). Carbohydrate: Digestion, Absorption and Metabolism. *Encyclopedia of Food and Health*, 643–650. https://doi.org/10.1016/B978-0-12-384947-2.00114-8

Sandri, M. (2013). Protein breakdown in muscle wasting: Role of autophagy-lysosome and ubiquitin-proteasome. *The International Journal of Biochemistry & Cell Biology*, *45*(10), 2121–2129. https://doi.org/10.1016/J.BIOCEL.2013.04.023

Saxena, R., Nassiri, M., Yin, X. M., & Morral, N. (2022). Insights from a high-fat diet fed mouse model with a humanized liver. *PLoS ONE*, *17*(5). https://doi.org/10.1371/JOURNAL.PONE.0268260

Schwarz, J., Tomé, D., Baars, A., Hooiveld, G. J. E. J., & Müller, M. (2012). Dietary Protein Affects Gene Expression and Prevents Lipid Accumulation in the Liver in Mice. *PLOS ONE*, *7*(10), e47303. https://doi.org/10.1371/JOURNAL.PONE.0047303

Secondi, R., Sánchez España, J. C., Castellar Cerpa, J., & Ibáñez Flores, N. (2019). Subconjunctival Orbital Fat Prolapse: An Update on Diagnosis and Management. *Seminars in Ophthalmology*, *34*(2), 69–73. https://doi.org/10.1080/08820538.2019.1576743

Seftor, R. E. B., Hess, A. R., Seftor, E. A., Kirschmann, D. A., Hardy, K. M., Margaryan, N. v., & Hendrix, M. J. C. (2012). Tumor Cell Vasculogenic Mimicry: From Controversy to Therapeutic Promise. *The American Journal of Pathology*, *181*(4), 1115. https://doi.org/10.1016/J.AJPATH.2012.07.013

Seino, Y., Ikeda, M., Nakane, K., Nakahara, H., Seino, S., & Imura, H. (1977). Amino acid modulation of glucose-induced insulin and glucagon release in diabetic patients. *Metabolism*, *26*(8), 911–919. https://doi.org/10.1016/0026-0495(77)90010-5

Sengupta, S., Johnson, B., Seirup, M., Ardalani, H., Duffin, B., Barrett-Wilt, G. A., Stewart, R., & Thomson, J. A. (2020). Co-culture with mouse embryonic fibroblasts improves maintenance of metabolic function of human small hepatocyte progenitor cells. *Current Research in Toxicology*, *1*, 70. https://doi.org/10.1016/J.CRTOX.2020.08.001

Serova, M., Tijeras-Raballand, A., Santos, C. dos, Martinet, M., Neuzillet, C., Lopez, A., Mitchell, D. C., Bryan, B. A., Gapihan, G., Janin, A., Bousquet, G., Riveiro, M. E., Bieche, I., Faivre, S., Raymond, E., & de Gramont, A. (2016). Everolimus affects vasculogenic mimicry in renal carcinoma resistant to sunitinib. *Oncotarget*, *7*(25), 38467. https://doi.org/10.18632/ONCOTARGET.9542

Shan, S., Sorg, B., & Dewhirst, M. W. (2003). A novel rodent mammary window of orthotopic breast cancer for intravital microscopy. *Microvascular Research*, *65*(2), 109–117. https://doi.org/10.1016/S0026-2862(02)00017-1

Sharmin, S., Taguchi, A., Kaku, Y., Yoshimura, Y., Ohmori, T., Sakuma, T., Mukoyama, M., Yamamoto, T., Kurihara, H., & Nishinakamura, R. (2016). Human induced pluripotent stem cell-derived podocytes mature into vascularized glomeruli upon experimental transplantation. *Journal of the American Society of Nephrology*, *27*(6), 1778–1791. https://doi.org/10.1681/ASN.2015010096/-/DCSUPPLEMENTAL

Sherriff, J. L., O'Sullivan, T. A., Properzi, C., Oddo, J. L., & Adams, L. A. (2016). Choline, Its Potential Role in Nonalcoholic Fatty Liver Disease, and the Case for Human and Bacterial Genes. *Advances in Nutrition*, *7*(1), 5. https://doi.org/10.3945/AN.114.007955

Shi, Y., Sun, L., Wang, M., Liu, J., Zhong, S., Li, R., Li, P., Guo, L., Fang, A., Chen, R., Ge, W. P., Wu, Q., & Wang, X. (2020). Vascularized human cortical organoids (vOrganoids) model cortical development in vivo. *PLoS Biology*, *18*(5). https://doi.org/10.1371/JOURNAL.PBIO.3000705

Shimizu, H., Miyazaki, M., Wakabayashi, Y., Mitsuhashi, N., Kato, A., Ito, H., Nakagawa, K., Yoshidome, H., Kataoka, M., & Nakajima, N. (2001). Vascular endothelial growth factor secreted by replicating hepatocytes induces sinusoidal endothelial cell proliferation during regeneration after partial hepatectomy in rats. *Journal of Hepatology*, *34*(5), 683–689. https://doi.org/10.1016/S0168-8278(00)00055-6

Sibulesky, L. (2013). Normal liver anatomy. *Clinical Liver Disease*, *2*(Suppl 1), S1. https://doi.org/10.1002/CLD.124

Siemann, D. W. (2011). The Unique Characteristics of Tumor Vasculature and Preclinical Evidence for its Selective Disruption by Tumor-Vascular Disrupting Agents. *Cancer Treatment Reviews*, *37*(1), 63. https://doi.org/10.1016/J.CTRV.2010.05.001

Simões, I. C. M., Fontes, A., Pinton, P., Zischka, H., & Wieckowski, M. R. (2018). Mitochondria in non-alcoholic fatty liver disease. *The International Journal of Biochemistry & Cell Biology*, *95*, 93–99. https://doi.org/10.1016/J.BIOCEL.2017.12.019

Sjøberg, K. A., Schmoll, D., Piper, M. D. W., Kiens, B., & Rose, A. J. (2020). Effects of Short-Term Dietary Protein Restriction on Blood Amino Acid Levels in Young Men. *Nutrients*, *12*(8), 1–9. https://doi.org/10.3390/NU12082195

Song, T., Jia, Y., Li, Z., Wang, F., Ren, L., & Chen, S. (2021). Effects of Liraglutide on Nonalcoholic Fatty Liver Disease in Patients with Type 2 Diabetes Mellitus: A Systematic Review and Meta-Analysis. *Diabetes Therapy*, *12*(6), 1735. https://doi.org/10.1007/S13300-021-01072-4

Song, Z., Xiaoli, A. M., & Yang, F. (2018). Regulation and Metabolic Significance of De Novo Lipogenesis in Adipose Tissues. *Nutrients*, *10*(10). https://doi.org/10.3390/NU10101383

Sookoian, S., & Pirola, C. J. (2017). Genetic predisposition in nonalcoholic fatty liver disease. *Clinical and Molecular Hepatology*, *23*(1), 1. https://doi.org/10.3350/CMH.2016.0109

Soret, P. A., Magusto, J., Housset, C., & Gautheron, J. (2020). In Vitro and In Vivo Models of Non-Alcoholic Fatty Liver Disease: A Critical Appraisal. *Journal of Clinical Medicine 2021, Vol. 10, Page 36*, *10*(1), 36. https://doi.org/10.3390/JCM10010036

Southgate, D. A. T. (1995). Digestion and metabolism of sugars. *The American Journal of Clinical Nutrition*, *62*(1 Suppl). https://doi.org/10.1093/AJCN/62.1.203S

Speier, S., Nyqvist, D., Köhler, M., Caicedo, A., Leibiger, I. B., & Berggren, P. O. (2008). Noninvasive high-resolution in vivo imaging of cell biology in the anterior chamber of the mouse eye. *Nature Protocols*, *3*(8), 1278–1286. https://doi.org/10.1038/NPROT.2008.118

St Croix, C. M., Shand, S. H., & Watkins, S. C. (2005). Confocal microscopy: comparisons, applications, and problems. *BioTechniques*, *39*(6 Suppl). https://doi.org/10.2144/000112089/ASSET/IMAGES/LARGE/FIGURE4.JPEG

Štampar, M., Tomc, J., Filipič, M., & Žegura, B. (2019). Development of in vitro 3D cell model from hepatocellular carcinoma (HepG2) cell line and its application for genotoxicity testing. *Archives of Toxicology*, *93*(11), 3321–3333. https://doi.org/10.1007/S00204-019-02576-6/FIGURES/6

Stentz, F. B., Brewer, A., Wan, J., Garber, C., Daniels, B., Sands, C., & Kitabchi, A. E. (2016). Remission of pre-diabetes to normal glucose tolerance in obese adults with high protein versus high carbohydrate diet: randomized control trial. *BMJ Open Diabetes Research and Care*, *4*(1), e000258. https://doi.org/10.1136/BMJDRC-2016-000258

Stephenson, K., Kennedy, L., Hargrove, L., Demieville, J., Thomson, J., Alpini, G., & Francis, H. (2018). Updates on Dietary Models of Nonalcoholic Fatty Liver Disease: Current Studies and Insights. *Gene Expression*, *18*(1), 5. https://doi.org/10.3727/105221617X15093707969658

Stern, J. H., Smith, G. I., Chen, S., Unger, R. H., Klein, S., & Scherer, P. E. (2019). Obesity dysregulates fasting-induced changes in glucagon secretion. *The Journal of Endocrinology*, *243*(2), 149. https://doi.org/10.1530/JOE-19-0201

Strobel, H. A., Gerton, T., & Hoying, J. B. (2021). Vascularized adipocyte organoid model using isolated human microvessel fragments. *Biofabrication*, *13*(3), 035022. https://doi.org/10.1088/1758-5090/ABE187

Strobel, H. A., Moss, S. M., & Hoying, J. B. (2023). Vascularized Tissue Organoids. *Bioengineering*, *10*(2). https://doi.org/10.3390/BIOENGINEERING10020124

Subclavian Vein: Location, Anatomy and Function. (n.d.). Retrieved September 1, 2022, from https://my.clevelandclinic.org/health/body/23941-subclavian-vein

Subramanian, K., Owens, D. J., Raju, R., Firpo, M., O'Brien, T. D., Verfaillie, C. M., & Hu, W. S. (2014). Spheroid culture for enhanced differentiation of human embryonic stem cells to hepatocyte-like cells. *Stem Cells and Development*, *23*(2), 124–131. https://doi.org/10.1089/SCD.2013.0097

Sun, J. G., Wang, Y., Chen, Z. T., Zhuo, W. L., Zhu, B., Liao, R. X., & Zhang, S. X. (2009). Detection of lymphangiogenesis in non-small cell lung cancer and its prognostic value. *Journal of Experimental and Clinical Cancer Research*, *28*(1), 1–10. https://doi.org/10.1186/1756-9966-28-21/FIGURES/5

Sun, X., & Harris, E. N. (2020). New aspects of hepatic endothelial cells in physiology and nonalcoholic fatty liver disease. *American Journal of Physiology - Cell Physiology*, *318*(6), C1200. https://doi.org/10.1152/AJPCELL.00062.2020

Sunny, N. E., Bril, F., & Cusi, K. (2016). *Mitochondrial Adaptation in Nonalcoholic Fatty Liver Disease: Novel Mechanisms and Treatment Strategies*. https://doi.org/10.1016/j.tem.2016.11.006

Svoboda, M., Tastenoy, M., Vertongen, P., & Robberecht, P. (1994). Relative quantitative analysis of glucagon receptor mRNA in rat tissues. *Molecular and Cellular Endocrinology*, *105*(2), 131–137. https://doi.org/10.1016/0303-7207(94)90162-7

Tabibian, J. H., Masyuk, A. I., Masyuk, T. V., O'Hara, S. P., & LaRusso, N. F. (2013). Physiology of Cholangiocytes. *Comprehensive Physiology*, *3*(1), 541–565. https://doi.org/10.1002/CPHY.C120019

Takebe, T., Koike, N., Sekine, K., Enomura, M., Chiba, Y., Ueno, Y., Zheng, Y. W., & Taniguchi, H. (2012). Generation of Functional Human Vascular Network. *Transplantation Proceedings*, *44*(4), 1130–1133. https://doi.org/10.1016/J.TRANSPROCEED.2012.03.039

Takebe, T., Sekine, K., Enomura, M., Koike, H., Kimura, M., Ogaeri, T., Zhang, R. R., Ueno, Y., Zheng, Y. W., Koike, N., Aoyama, S., Adachi, Y., & Taniguchi, H. (2013a). Vascularized and functional human liver from an iPSC-derived organ bud transplant. *Nature 2013 499:7459*, *499*(7459), 481–484. https://doi.org/10.1038/nature12271

Takebe, T., Sekine, K., Enomura, M., Koike, H., Kimura, M., Ogaeri, T., Zhang, R. R., Ueno, Y., Zheng, Y. W., Koike, N., Aoyama, S., Adachi, Y., & Taniguchi, H. (2013b). Vascularized and functional human liver from an iPSC-derived organ bud transplant. *Nature 2013 499:7459*, *499*(7459), 481–484. https://doi.org/10.1038/nature12271

Takebe, T., Sekine, K., Kimura, M., Yoshizawa, E., Ayano, S., Koido, M., Funayama, S., Nakanishi, N., Hisai, T., Kobayashi, T., Kasai, T., Kitada, R., Mori, A., Ayabe, H., Ejiri, Y., Amimoto, N.,

Yamazaki, Y., Ogawa, S., Ishikawa, M., … Taniguchi, H. (2017). Massive and Reproducible Production of Liver Buds Entirely from Human Pluripotent Stem Cells. *Cell Reports*, *21*(10), 2661–2670. https://doi.org/10.1016/J.CELREP.2017.11.005

Takebe, T., Zhang, R. R., Koike, H., Kimura, M., Yoshizawa, E., Enomura, M., Koike, N., Sekine, K., & Taniguchi, H. (2014). Generation of a vascularized and functional human liver from an iPSC-derived organ bud transplant. *Nature Protocols*, *9*(2), 396–409. https://doi.org/10.1038/NPROT.2014.020

Tanaka, K., Morimoto, Y., Toiyama, Y., Matsushita, K., Kawamura, M., Koike, Y., Okugawa, Y., Inoue, Y., Uchida, K., Araki, T., Mizoguchi, A., & Kusunoki, M. (2012). In vivo time-course imaging of tumor angiogenesis in colorectal liver metastases in the same living mice using two-photon laser scanning microscopy. *Journal of Oncology*. https://doi.org/10.1155/2012/265487

Tappy, L., & Le, K. A. (2010). Metabolic effects of fructose and the worldwide increase in obesity. *Physiological Reviews*, *90*(1), 23–46. https://doi.org/10.1152/PHYSREV.00019.2009

Teichert-Kuliszewska, K., Maisonpierre, P. C., Jones, N., Campbell, A. I. M., Master, Z., Bendeck, M. P., Alitalo, K., Dumont, D. J., Yancopoulos, G. D., & Stewart, D. J. (2001). Biological action of angiopoietin-2 in a fibrin matrix model of angiogenesis is associated with activation of Tie2. *Cardiovascular Research*, *49*(3), 659–670. https://doi.org/10.1016/S0008-6363(00)00231-5

Ter Horst, K. W., Vatner, D. F., Zhang, D., Cline, G. W., Ackermans, M. T., Nederveen, A. J., Verheij, J., Demirkiran, A., van Wagensveld, B. A., Dallinga-Thie, G. M., Nieuwdorp, M., Romijn, J. A., Shulman, G. I., & Serlie, M. J. (2021). Hepatic Insulin Resistance Is Not Pathway Selective in Humans With Nonalcoholic Fatty Liver Disease. *Diabetes Care*, *44*(2), 489. https://doi.org/10.2337/DC20-1644

Timmins, N. E., & Nielsen, L. K. (2007). Generation of multicellular tumor spheroids by the hanging-drop method. *Methods in Molecular Medicine*, *140*, 141–151. https://doi.org/10.1007/978-1-59745-443-8_8

Toyoda, Y., Takada, T., Umezawa, M., Tomura, F., Yamanashi, Y., Takeda, K., & Suzuki, H. (2019). Identification of hepatic NPC1L1 as an NAFLD risk factor evidenced by ezetimibe-mediated steatosis prevention and recovery. *FASEB BioAdvances*, *1*(5), 283. https://doi.org/10.1096/FBA.2018-00044

Trefts, E., Gannon, M., & Wasserman, D. H. (2017). The liver. *Current Biology : CB*, *27*(21), R1147. https://doi.org/10.1016/J.CUB.2017.09.019

Tsai, S. Y., Rodriguez, A. A., Dastidar, S. G., Del Greco, E., Carr, K. L., Sitzmann, J. M., Academia, E. C., Viray, C. M., Martinez, L. L., Kaplowitz, B. S., Ashe, T. D., La Spada, A. R., & Kennedy, B. K. (2016). Increased 4E-BP1 expression protects against diet-induced obesity and insulin resistance in male mice. *Cell Reports*, *16*(7), 1903. https://doi.org/10.1016/J.CELREP.2016.07.029

Tsuji, S., Koyama, S., Taniguchi, R., Fujiwara, T., Fujiwara, H., & Sato, Y. (2019). Association of Serum Amino Acid Concentration With Loss of Skeletal Muscle Mass After 1 Year in Cardiac Rehabilitation Center Patients. *Circulation Reports*, *1*(10), 456. https://doi.org/10.1253/CIRCREP.CR-19-0053

Tsukada, Y., Muramatsu, F., Hayashi, Y., Inagaki, C., Su, H., Iba, T., Kidoya, H., & Takakura, N. (2021). An in vivo model allowing continuous observation of human vascular formation in the same animal over time. *Scientific Reports 2021 11:1*, *11*(1), 1–9. https://doi.org/10.1038/s41598-020-80497-6

Tucker, W. D., Arora, Y., & Mahajan, K. (2022). Anatomy, Blood Vessels. *StatPearls*. https://www.ncbi.nlm.nih.gov/books/NBK470401/

Tun, S. B. B., Chua, M., Tan, G. S. W., Leibiger, I., Ali, Y., Barathi, V. A., & Berggren, P. O. (2022). Local Dexamethasone Administration Delays Allogeneic Islet Graft Rejection in the Anterior Chamber of the Eye of Non-Human Primates. *Cell Transplantation*, *31*, 1–11. https://doi.org/10.1177/09636897221098038

Turrini, R., Pabois, A., Xenarios, I., Coukos, G., Delaloye, J. F., & Doucey, M. A. (2017). TIE-2 expressing monocytes in human cancers. *Oncoimmunology*, *6*(4). https://doi.org/10.1080/2162402X.2017.1303585

Tzanaki, I., Agouridis, A. P., & Kostapanos, M. S. (2022). Is there a role of lipid-lowering therapies in the management of fatty liver disease? *World Journal of Hepatology*, *14*(1), 119. https://doi.org/10.4254/WJH.V14.I1.119

Vaja, R., & Rana, M. (2020). Drugs and the liver. *Anaesthesia and Intensive Care Medicine*, *21*(10), 517. https://doi.org/10.1016/J.MPAIC.2020.07.001

Valentin, J. E., Donnenberg, A., Marra, K. G., & Rubin, J. P. (2016). Adipose Tissue as a Plentiful Source of Stem Cells for Regenerative Medicine Therapies. *Translating Regenerative Medicine to the Clinic*, 241–250. https://doi.org/10.1016/B978-0-12-800548-4.00016-4

Van Herck, M. A., Vonghia, L., & Francque, S. M. (2017). Animal Models of Nonalcoholic Fatty Liver Disease—A Starter's Guide. *Nutrients*, *9*(10). https://doi.org/10.3390/NU9101072

van Os, E. A., Cools, L., Eysackers, N., Szafranska, K., Smout, A., Verhulst, S., Reynaert, H., McCourt, P., Mannaerts, I., & van Grunsven, L. A. (2022). Modelling fatty liver disease with mouse liver-derived multicellular spheroids. *Biomaterials*, *290*, 121817. https://doi.org/10.1016/J.BIOMATERIALS.2022.121817

Vasileva, A., Marx, T., Beaudry, J. L., & Stern, J. H. (2022a). Glucagon receptor signaling at white adipose tissue does not regulate lipolysis. *American Journal of Physiology - Endocrinology and Metabolism*, *323*(4), E389–E401. https://doi.org/10.1152/AJPENDO.00078.2022/ASSET/IMAGES/LARGE/AJPENDO.00078.2022_F005.JPEG

Vasileva, A., Marx, T., Beaudry, J. L., & Stern, J. H. (2022b). GPCR-Mediated Regulation of Fuel and Energy Metabolism in Peripheral Tissues: Glucagon receptor signaling at white adipose tissue does not regulate lipolysis. *American Journal of Physiology - Endocrinology and Metabolism*, *323*(4), E389. https://doi.org/10.1152/AJPENDO.00078.2022

Verseijden, F., Posthumus-van Sluijs, S. J., Farrell, E., Van Neck, J. W., Hovius, S. E. R., Hofer, S. O. P., & Van Osch, G. J. V. M. (2010). Prevascular structures promote vascularization in engineered human adipose tissue constructs upon implantation. *Cell Transplantation*, *19*(8), 1007–1020. https://doi.org/10.3727/096368910X492571

Vilar-Gomez, E., Martinez-Perez, Y., Calzadilla-Bertot, L., Torres-Gonzalez, A., Gra-Oramas, B., Gonzalez-Fabian, L., Friedman, S. L., Diago, M., & Romero-Gomez, M. (2015). Weight Loss Through Lifestyle Modification Significantly Reduces Features of Nonalcoholic Steatohepatitis. *Gastroenterology*, *149*(2), 367-378.e5. https://doi.org/10.1053/J.GASTRO.2015.04.005

Virtue, S., & Vidal-Puig, A. (2021). GTTs and ITTs in mice: simple tests, complex answers. *Nature Metabolism 2021 3:7*, *3*(7), 883–886. https://doi.org/10.1038/s42255-021-00414-7

Volpe, S., Lisco, G., Fanelli, M., Racaniello, D., Colaianni, V., Triggiani, D., Donghia, R., Crudele, L., Rinaldi, R., Sabbà, C., Triggiani, V., De Pergola, G., & Piazzolla, G. (2022). Once-Weekly Subcutaneous Semaglutide Improves Fatty Liver Disease in Patients with Type 2 Diabetes: A 52-Week Prospective Real-Life Study. *Nutrients*, *14*(21). https://doi.org/10.3390/NU14214673

Vu, J. P., Luong, L., Parsons, W. F., Oh, S., Sanford, D., Gabalski, A., Lighton, J. R. B., Pisegna, J. R., & Germano, P. M. (2017). Long-Term Intake of a High-Protein Diet Affects Body Phenotype, Metabolism, and Plasma Hormones in Mice. *The Journal of Nutrition*, *147*(12), 2243. https://doi.org/10.3945/JN.117.257873

Waghorn, P. A., Ferreira, D. S., Erstad, D. J., Rotile, N. J., Masia, R., Jones, C. M., Tu, C., Sojoodi, M., Chen, Y. ching I., Schlerman, F., Wellen, J., Martinez, R. V. P., Tanabe, K. K., Fuchs, B. C., & Caravan, P. (2021). Quantitative, noninvasive MRI characterization of disease progression in a mouse model of non-alcoholic steatohepatitis. *Scientific Reports 2021 11:1*, *11*(1), 1–12. https://doi.org/10.1038/s41598-021-85679-4

Wang, C., & Chu, M. (2021). Advances in Drugs Targeting Lymphangiogenesis for Preventing Tumor Progression and Metastasis. *Frontiers in Oncology*, *11*. https://doi.org/10.3389/FONC.2021.783309

Wang, Q. S., He, R., Yang, F., Kang, L. J., Li, X. Q., Fu, L., Sun, B., & Feng, Y. M. (2018). FOXF2 deficiency permits basal-like breast cancer cells to form lymphangiogenic mimicry by enhancing the response of VEGF-C/VEGFR3 signaling pathway. *Cancer Letters*, *420*, 116–126. https://doi.org/10.1016/J.CANLET.2018.01.069

Wang, S., Wang, X., Tan, Z., Su, Y., Liu, J., Chang, M., Yan, F., Chen, J., Chen, T., Li, C., Hu, J., & Wang, Y. (2019). Human ESC-derived expandable hepatic organoids enable therapeutic liver

repopulation and pathophysiological modeling of alcoholic liver injury. *Cell Research 2019 29:12*, *29*(12), 1009–1026. https://doi.org/10.1038/s41422-019-0242-8

Wang, X., Bullock, A. J., Zhang, L., Wei, L., Yu, D., Mahagaokar, K., Alsop, D. C., Mier, J. W., Atkins, M. B., Coxon, A., Oliner, J., & Bhatt, R. S. (2014). The Role of Angiopoietins as Potential Therapeutic Targets in Renal Cell Carcinoma. *Translational Oncology*, *7*(2), 188. https://doi.org/10.1016/J.TRANON.2014.02.003

Wasilewska, N., & Lebensztejn, D. M. (2021). Non-alcoholic fatty liver disease and lipotoxicity. *Clinical and Experimental Hepatology*, *7*(1), 1. https://doi.org/10.5114/CEH.2021.104441

Wewer Albrechtsen, N. J., Pedersen, J., Galsgaard, K. D., Winther-Sørensen, M., Suppli, M. P., Janah, L., Gromada, J., Vilstrup, H., Knop, F. K., & Holst, J. J. (2019). The Liver–α-Cell Axis and Type 2 Diabetes. *Endocrine Reviews*, *40*(5), 1353–1366. https://doi.org/10.1210/ER.2018-00251

Wiering, L., & Tacke, F. (2023). Treating inflammation to combat non-alcoholic fatty liver disease. *Journal of Endocrinology*, *256*(1). https://doi.org/10.1530/JOE-22-0194

Williamson, S. C., Metcalf, R. L., Trapani, F., Mohan, S., Antonello, J., Abbott, B., Leong, H. S., Chester, C. P. E., Simms, N., Polanski, R., Nonaka, D., Priest, L., Fusi, A., Carlsson, F., Carlsson, A., Hendrix, M. J. C., Seftor, R. E. B., Seftor, E. A., Rothwell, D. G., … Dive, C. (2016). Vasculogenic mimicry in small cell lung cancer. *Nature Communications 2016 7:1*, *7*(1), 1–14. https://doi.org/10.1038/ncomms13322

Winkler, J., Abisoye-Ogunniyan, A., Metcalf, K. J., & Werb, Z. (2020). Concepts of extracellular matrix remodelling in tumour progression and metastasis. *Nature Communications 2020 11:1*, *11*(1), 1–19. https://doi.org/10.1038/s41467-020-18794-x

Wolfe, R. R. (2006). The underappreciated role of muscle in health and disease1–3. *The American Journal of Clinical Nutrition*, *84*(3), 475–482. https://doi.org/10.1093/AJCN/84.3.475

Wu, F., Wu, D., Ren, Y., Huang, Y., Feng, B., Zhao, N., Zhang, T., Chen, X., Chen, S., & Xu, A. (2019). Generation of hepatobiliary organoids from human induced pluripotent stem cells. *Journal of Hepatology*, *70*(6), 1145–1158. https://doi.org/10.1016/J.JHEP.2018.12.028

Xia, Q., Huang, X., Huang, J., Zheng, Y., March, M. E., Li, J., & Wei, Y. (2021). The Role of Autophagy in Skeletal Muscle Diseases. *Frontiers in Physiology*, *12*, 638983. https://doi.org/10.3389/FPHYS.2021.638983

Xiong, Y., Scerbo, M. J., Seelig, A., Volta, F., O'brien, N., Dicker, A., Padula, D., Lickert, H., Gerdes, J. M., & Berggren, P. O. (2020). Islet vascularization is regulated by primary endothelial cilia via VEGF-A-dependent signaling. *ELife*, *9*, 1–27. https://doi.org/10.7554/ELIFE.56914

Xu, C., Li, X., Liu, P., Li, M., & Luo, F. (2019). Patient-derived xenograft mouse models: A high fidelity tool for individualized medicine. *Oncology Letters*, *17*(1), 3–10. https://doi.org/10.3892/OL.2018.9583

Xu, C., Markova, M., Seebeck, N., Loft, A., Hornemann, S., Gantert, T., Kabisch, S., Herz, K., Loske, J., Ost, M., Coleman, V., Klauschen, F., Rosenthal, A., Lange, V., Machann, J., Klaus, S., Grune, T., Herzig, S., Pivovarova-Ramich, O., & Pfeiffer, A. F. H. (2020). High-protein diet more effectively reduces hepatic fat than low-protein diet despite lower autophagy and FGF21 levels. *Liver International : Official Journal of the International Association for the Study of the Liver*, *40*(12), 2982–2997. https://doi.org/10.1111/LIV.14596

Y, D., Z, F., Y, L., & K, T. (2022). *Possible-sarcopenic Screening with Disturbed Plasma Amino Acid Profile in the Elderly*. https://doi.org/10.21203/RS.3.RS-2149153/V1

Yadav, L., Puri, N., Rastogi, V., Satpute, P., & Sharma, V. (2015). Tumour Angiogenesis and Angiogenic Inhibitors: A Review. *Journal of Clinical and Diagnostic Research : JCDR*, *9*(6), XE01. https://doi.org/10.7860/JCDR/2015/12016.6135

Yamada, M., Kimura, Y., Ishiyama, D., Nishio, N., Tanaka, T., Ohji, S., Otobe, Y., Koyama, S., Sato, A., Suzuki, M., Ogawa, H., Ichikawa, T., Ito, D., & Arai, H. (2018). Plasma Amino Acid Concentrations Are Associated with Muscle Function in Older Japanese Women. *The Journal of Nutrition, Health & Aging*, *22*(7), 819–823. https://doi.org/10.1007/S12603-018-1014-8

Yamakawa, M., Liu, L. X., Belanger, A. J., Date, T., Kuriyama, T., Goldberg, M. A., Cheng, S. H., Gregory, R. J., & Jiang, C. (2004). Expression of angiopoietins in renal epithelial and clear cell carcinoma cells: Regulation by hypoxia and participation in angiogenesis. *American Journal of Physiology - Renal Physiology*, *287*(4 56-4), 649–657.

https://doi.org/10.1152/AJPRENAL.00028.2004/ASSET/IMAGES/LARGE/ZH2010041676100 7.JPEG
Yanagisawa, K., Konno, M., Liu, H., Irie, S., Mizushima, T., Mori, M., Doki, Y., Eguchi, H., Matsusaki, M., & Ishii, H. (2020). A Four-Dimensional Organoid System to Visualize Cancer Cell Vascular Invasion. *Biology*, *9*(11), 1–14. https://doi.org/10.3390/BIOLOGY9110361
Yanagisawa, Y. (2023). How dietary amino acids and high protein diets influence insulin secretion. *Physiological Reports*, *11*(2), e15577. https://doi.org/10.14814/PHY2.15577
Yang, B., Gu, W., Peng, B., Xu, Y., Liu, M., Che, J., Geng, J., & Zheng, J. (2012). High level of circulating endothelial progenitor cells positively correlates with serum vascular endothelial growth factor in patients with renal cell carcinoma. *The Journal of Urology*, *188*(6), 2055–2062. https://doi.org/10.1016/J.JURO.2012.08.039
Yang, M., Baranov, E., Li, X. M., Wang, J. W., Jiang, P., Li, N., Moossa, A. R., Penman, S., & Hoffman, R. M. (2001). Whole-body and intravital optical imaging of angiogenesis in orthotopically implanted tumors. *Proceedings of the National Academy of Sciences of the United States of America*, *98*(5), 2616–2621. https://doi.org/10.1073/PNAS.051626698/ASSET/05432A14-E0A8-4F9D-BEB9-FD857EDAFAD7/ASSETS/GRAPHIC/PQ0516266004.JPEG
Yang, S. N., & Berggren, P. O. (2019). The eye as a novel imaging site in diabetes research. *Pharmacology & Therapeutics*, *197*, 103. https://doi.org/10.1016/J.PHARMTHERA.2019.01.005
Ying Tsang, H., Hau Yi Lo, P., Ka Ho Lee, K., & Kenneth Lee, P. (2021). Generation of liver organoids from human induced pluripotent stem cells as liver fibrosis and steatosis models. *BioRxiv*, 2021.06.29.450347. https://doi.org/10.1101/2021.06.29.450347
You, B., Sun, Y., Luo, J., Wang, K., Liu, Q., Fang, R., Liu, B., Chou, F., Wang, R., Meng, J., Huang, C. P., Yeh, S., Chang, C., & Xu, W. (2021). Androgen receptor promotes renal cell carcinoma (RCC) vasculogenic mimicry (VM) via altering TWIST1 nonsense-mediated decay through lncRNA-TANAR. *Oncogene*, *40*(9), 1674. https://doi.org/10.1038/S41388-020-01616-1
Younossi, Z. M., Golabi, P., de Avila, L., Paik, J. M., Srishord, M., Fukui, N., Qiu, Y., Burns, L., Afendy, A., & Nader, F. (2019). The global epidemiology of NAFLD and NASH in patients with type 2 diabetes: A systematic review and meta-analysis. *Journal of Hepatology*, *71*(4), 793–801. https://doi.org/10.1016/J.JHEP.2019.06.021
Younossi, Z. M., Ratziu, V., Loomba, R., Rinella, M., Anstee, Q. M., Goodman, Z., Bedossa, P., Geier, A., Beckebaum, S., Newsome, P., Sheridan, D., Sheikh, M. Y., Trotter, J., Knapple, W., Lawitz, E., Abdelmalek, M. F., Kowdley, K. V., Montano-Loza, A. J., Boursier, J., … Zuin, M. (2019a). Obeticholic acid for the treatment of non-alcoholic steatohepatitis: interim analysis from a multicentre, randomised, placebo-controlled phase 3 trial. *Lancet (London, England)*, *394*(10215), 2184–2196. https://doi.org/10.1016/S0140-6736(19)33041-7
Younossi, Z. M., Ratziu, V., Loomba, R., Rinella, M., Anstee, Q. M., Goodman, Z., Bedossa, P., Geier, A., Beckebaum, S., Newsome, P., Sheridan, D., Sheikh, M. Y., Trotter, J., Knapple, W., Lawitz, E., Abdelmalek, M. F., Kowdley, K. V., Montano-Loza, A. J., Boursier, J., … Zuin, M. (2019b). Obeticholic acid for the treatment of non-alcoholic steatohepatitis: interim analysis from a multicentre, randomised, placebo-controlled phase 3 trial. *Lancet (London, England)*, *394*(10215), 2184–2196. https://doi.org/10.1016/S0140-6736(19)33041-7
Younossi, Z. M., Stepanova, M., Nader, F., Loomba, R., Anstee, Q. M., Ratziu, V., Harrison, S., Sanyal, A. J., Schattenberg, J. M., Barritt, A. S., Noureddin, M., Bonacci, M., Cawkwell, G., Wong, B., & Rinella, M. (2022). Obeticholic Acid Impact on Quality of Life in Patients With Nonalcoholic Steatohepatitis: REGENERATE 18-Month Interim Analysis. *Clinical Gastroenterology and Hepatology : The Official Clinical Practice Journal of the American Gastroenterological Association*, *20*(9), 2050-2058.e12. https://doi.org/10.1016/J.CGH.2021.07.020
Zarychta, E., & Ruszkowska-Ciastek, B. (2022). Cooperation between Angiogenesis, Vasculogenesis, Chemotaxis, and Coagulation in Breast Cancer Metastases Development: Pathophysiological Point of View. *Biomedicines 2022, Vol. 10, Page 300*, *10*(2), 300. https://doi.org/10.3390/BIOMEDICINES10020300
Zeigerer, A., Sekar, R., Kleinert, M., Nason, S., Habegger, K. M., & Müller, T. D. (2021). Glucagon's Metabolic Action in Health and Disease. *Comprehensive Physiology*, *11*(2), 1759. https://doi.org/10.1002/CPHY.C200013

Zhang, J., Pivovarova-Ramich, O., Kabisch, S., Markova, M., Hornemann, S., Sucher, S., Rohn, S., Machann, J., & Pfeiffer, A. F. H. (2022). High Protein Diets Improve Liver Fat and Insulin Sensitivity by Prandial but Not Fasting Glucagon Secretion in Type 2 Diabetes. *Frontiers in Nutrition*, *9*, 1069. https://doi.org/10.3389/FNUT.2022.808346/BIBTEX

Zhang, R., Liu, W., Zeng, J., Meng, J., Jiang, H., Wang, J., & Xing, D. (2022). Niemann-Pick C1-Like 1 inhibitors for reducing cholesterol absorption. *European Journal of Medicinal Chemistry*, *230*. https://doi.org/10.1016/J.EJMECH.2022.114111

Zhang, X., Deng, R., Zhang, X., & Deng, R. (2018). Dysregulation of Bile Acids in Patients with NAFLD. *Nonalcoholic Fatty Liver Disease - An Update*. https://doi.org/10.5772/INTECHOPEN.81474

Zhang, Z., Dales, N. A., & Winther, M. D. (2014). Opportunities and challenges in developing stearoyl-coenzyme A desaturase-1 inhibitors as novel therapeutics for human disease. *Journal of Medicinal Chemistry*, *57*(12), 5039–5056. https://doi.org/10.1021/JM401516C/ASSET/IMAGES/MEDIUM/JM-2013-01516C_0024.GIF

Zhang, Z., Imani, S., Shasaltaneh, M. D., Hosseinifard, H., Zou, L., Fan, Y., & Wen, Q. (2019). The role of vascular mimicry as a biomarker in malignant melanoma: A systematic review and meta-analysis. *BMC Cancer*, *19*(1), 1–12. https://doi.org/10.1186/S12885-019-6350-5/FIGURES/6

Zorn. (2008). x. *StemBook*. https://doi.org/10.3824/STEMBOOK.1.25.1